Regulation of self-renewal in colorectal cancer cell models

Regulación de la auto-renovación en modelos celulares de cáncer colorrectal

Oscar Meca-Cortés

UNIVERSITAT DE BARCELONA

FACULTAT DE FARMÀCIA

DEPARTAMENT
Bioquímica i Biologia Molecular

Regulation of self-renewal in colorectal cancer cell models

Regulación de la auto-renovación en modelos celulares de cáncer colorrectal

Oscar Meca-Cortés – 2014

UNIVERSITAT DE BARCELONA

FACULTAT DE FARMÀCIA

DEPARTAMENT
Bioquímica
i
Biologia Molecular

PROGRAMA DE
DOCTORAT EN BIOMEDICINA

Regulation of self-renewal in colorectal cancer cell models

Regulación de la auto-renovación en modelos celulares de cáncer colorrectal

Memoria presentada por Oscar Meca-Cortés para optar al título de Doctor por la Universitat de Barcelona

Este trabajo ha sido realizado en el departamento de Biología Celular del Instituto de Biología Molecular de Barcelona (IBMB), Consejo Superior de Investigaciones Científicas (CSIC), bajo la dirección del Dr.Timothy M.Thomson

Director: Timothy Thomson Okatsu

Doctorando: Oscar Meca-Cortés

A mis buenos compañeros de laboratorio y a Tim.

A mi madre y Alonso, hermano y abuelas.

A Virginia…

También a la memoria de mi amigo M.A. Pastor.

Gracias

Index

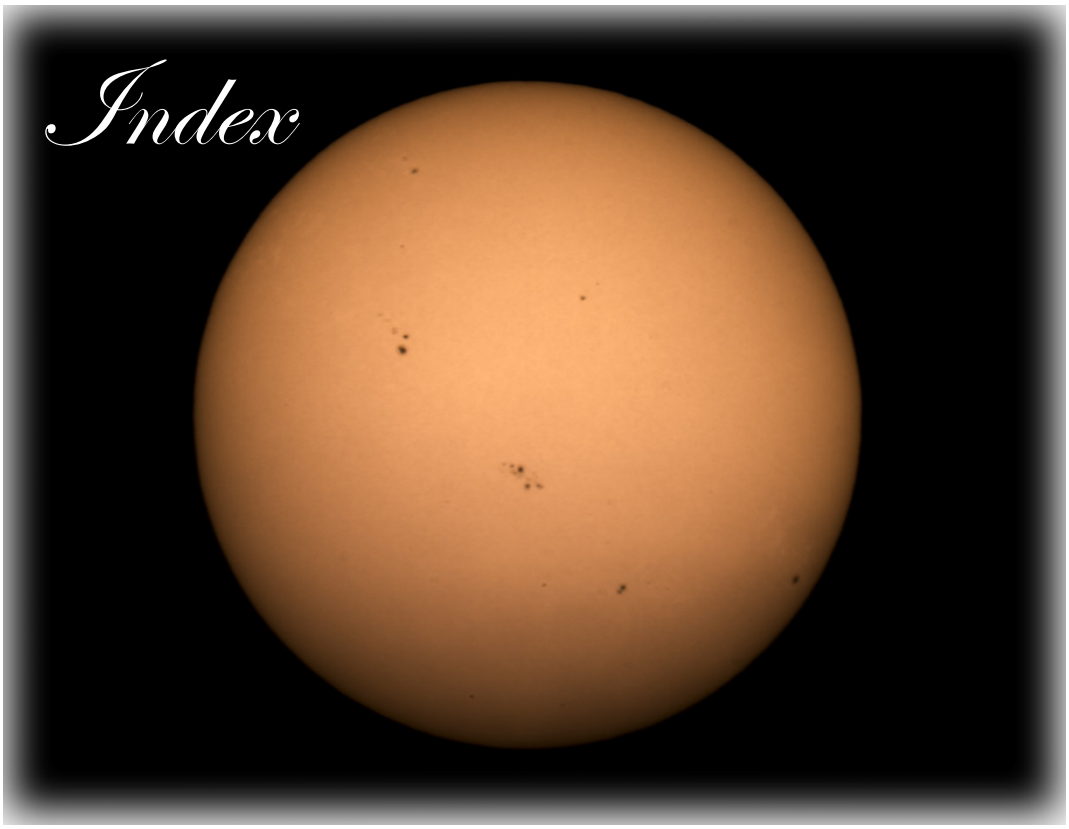

The Sun

The Sun fuels the life on Earth. It was formed about 4.567 billion years ago. The Sun is a G-type main-sequence star (G2V) based on spectral class and it is informally designated as a yellow dwarf. It is almost perfectly spherical and consists of hot plasma interwoven with magnetic fields. It has a diameter of about 1,392,684 km, around 109 times that of Earth, and its mass (approximately 330,000 times the mass of our planet), which is formed from hydrogen (75%), helium (24%) and other elements such as oxygen, carbon, neon and iron, accounts for about 99.86% of the total mass of the Solar System. The distance between the Earth and the Sun is $1.5x10^8$ Km, or in other words, 8 light-minutes…


Introduction

Jupiter

At about 42 light-minutes on average from the Earth, Jupiter is the fifth planet from the Sun and the largest planet in the Solar System. It is a gas giant with mass one-thousandth of that of the Sun but is two and a half times the mass of all the other planets in the Solar System combined. Jupiter is primarily composed of hydrogen with a quarter of its mass being helium. It may also have a rocky core of heavier elements, but like the other gas giants, Jupiter lacks a well-defined solid surface. Because of its rapid rotation, the planet's shape is that of an oblate spheroid. A prominent result is the Great Red Spot, a giant storm large enough to contain two or three Earths, which is known to have existed since at least the 17th century when it was first seen by Gian Domenico Cassini. Surrounding Jupiter is a faint planetary ring system and a powerful magnetosphere. It also possesses at least 67 moons, including the four large satellites called the Galilean moons (Io, Europa, Ganymede and Callisto) that were first seen by Galileo Galilei in 1610…

1. INTRODUCTION TO CANCER PROGRESSION

The progression of cancer to a deadly disease is a consequence of the acquisition of different biological capabilities by tumor cells. In 2000, Doug Hanahan and Robert Weinberg proposed six hallmarks of cancer [1]: sustaining proliferative signaling, evading growth suppressors, resisting cell death, enabling replicative immortality, inducing angiogenesis and activating invasion and metastasis (Figure 1A). Recently, the authors included two additional hallmarks, which have emerged from evidences accumulated over the last decade [2]: reprogramming of energy metabolism and evading immune destruction. Moreover, two enabling characteristics underlie and allow the acquisition of these hallmarks: genome instability, which generates genetic diversity, and inflammation, which foster multiple functional hallmark functions (Figure 1B). All of this needs to be considered in a context where tumor microenvironment (TME) plays a key role; tumors are composed of a mixture of populations of neoplastic and non-neoplastic cells, the latter contributing to the acquisition of cancer hallmarks [3].

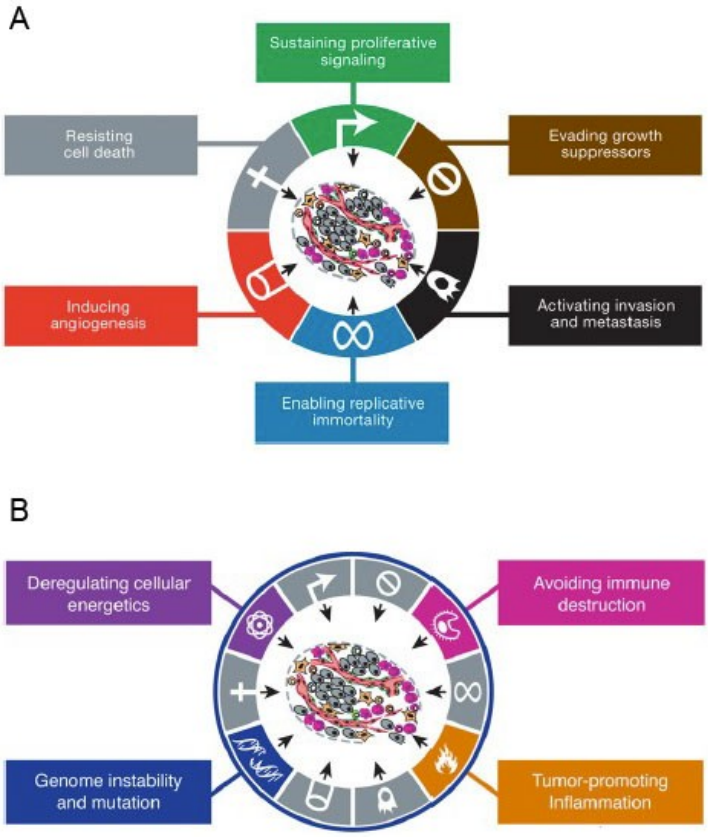

Figure 1. *Hallmarks of Cancer*. (**A**) Six biological capabilities for cancer progression established in 2000 by Hanahan and Weinberg. (**B**) New hallmarks for cancer progression, added as a consequence of their biological importance reported by the new studies during the last decade. *Hanahan & Weinberg 2011*.

2. MODELS FOR TUMOR PROPAGATION AND HETEROGENEITY

A tumor can be understood as a complex ecosystem in which interactions between neoplastic cells and the TME can influence the function of the tumor as a whole. TME can, for instance, foster metabolic changes (e.g. hypoxic environment and nutrient fluctuations) which contribute to heterogeneity in the function of malignant cells and thus contribute to therapeutic failure [4]. In addition to these non-cell autonomous effects, individual malignant cells within a tumor can display variation in other hallmarks of cancer, a fact known as intratumoral heterogeneity, and whose driving mechanisms and their role in therapy resistance, tumor progression and recurrence are being unmasked in recent years.

Intratumoral heterogeneity has been shown in a number of studies over the past decades and is now being addressed through the application of high-throughput sequencing of tumor samples or single cells, demonstrating, among other facts, that a given tumor within a single patient is indeed a heterogeneous mixture of genetically different subclones that are generated by branching evolution [5], [6]. Further evidence of contribution to functional heterogeneity comes from studies of the so-called non-genetic determinants, which are tightly related to developmental pathways and epigenetic modifications (DNA methylation, histone modification, chromatin remodeling, microRNAs, and other noncoding RNAs) [7]–[9].

2.1 Accounting for intratumoral heterogeneity in tumors: the unified model of clonal evolution and cancer stem cells

Several models have attempted to account for the heterogeneity and inherent differences in tumor-regenerating capacity of neoplastic cells within a given tumor. In 1976, Nowell proposed the clonal evolution model [10], which states that tumor initiation and progression result from multiple and sequential acquisition of genetic mutations in a random single cell that contribute to subsequent clonal expansions; over time and following the Darwinian model of evolution, those new mutations conferring growth advantages (e.g. resistance to apoptosis, uncontrolled proliferation, etc.) are selected and new progenies become dominant while less fit subclones disappear or remain forming

reservoirs from which evolution can continue. In either case, several subpopulations coexist within the tumor resulting in tumor heterogeneity [11]–[16].

However, epigenetics and the influence of TME are also likely to play important roles in tumor heterogeneity. In addition, the dependence of the establishment of a stable malignant phenotype on the accumulation of a series of in principle, rare events or mutations, makes unlikely that this process can occur within the number of cell divisions that are required to produce differentiated, non-dividing progeny from most normal adult stem cells found in several human tissues [17]–[20]. In contrast, adult stem cells constitute a life-long reservoir of cells with active mechanisms for self-renewal. These considerations make stem cells (or more differentiated progenitors) obvious candidates for accumulating the events that can generate a fully malignant cell population, and are the basis of the cancer stem cell (CSCs) model of carcinogenesis.

By definition, CSCs represent a subset of tumor cells capable of driving tumor initiation, progression and recurrence, which can be isolated from the bulk of tumor cells and show clonal long-term repopulation (differentiation) and self-renewal capacities [9], [21]. Their self-renewal and differentiation capacities lead to the production of all cell types of a tumor, thereby generating tumor heterogeneity [22], [23]. Simultaneously, the other cells in a tumor do not have unlimited self-renewal capacity and cannot differentiate to produce all tumor cell types. Therefore, this model implies that tumors are hierarchically arranged, with CSCs lying at the apex of the hierarchy. Evidence of hierarchical organization of tumors and that only a subset of cells can initiate and maintain the disease have been convincingly demonstrated by xenotransplant experiments in immunodeficient mice, in both leukemias [24] and solid tumors [25]–[34].

Notably, the CSC model proposes that CSCs are responsible for metastatic spread (called metastatic CSCs or mCSCs) [35]–[37], therapy failure and recurrence [38]–[41].

Research in stem cell biology has focused on determining the molecular mechanisms controlling the homeostasis of normal tissues as well as how these mechanisms are deregulated and involved in disease and particularly in cancer.

Normal stem cells and cancer stem cells are regulated by epigenetic mechanisms and microenvironmental influences [42][3]. Important signaling pathways in stem cell biology are involved in cancer, including Wnt, Hedgehog or Notch [43], [44]. In general, many key processes in cancer are reminiscent of molecular programs that govern and maintain the stem cell state (collectively known as *stemness programs*), as has been highlighted by common genetic signatures [45], [46].

The main limitation of the CSC/hierarchical model is that it views the tumor as genetically homogeneous and static, and does not reflect the existence of genetically distinct subclones; however, CSCs can undergo clonal evolution and thus, both models of carcinogenesis can be coupled and account for experimental evidences (Figure 2). Both models postulate that the origin of a tumor is a single cell that has acquired mutations and gained unlimited proliferative potential. In both cases, microenvironmental factors may influence tumor progression and furthermore, in both cases the presence of stem-like properties would confer a selective growth advantage over the rest of the tumor cell population.

For instance, evidence for this unified model of tumorigenesis comes from recent studies in different regions of a primary tumor and their metastases in pancreatic and kidney cancers that have been sequenced, revealing an unexpected degree of intratumoral heterogeneity [12], [47], [48], perhaps reflecting the fact that CSCs are genetically unstable. Indeed, in colorectal cancer, such genetic instability has been reported, leading to the formation of new CSC clones deriving from an initial parental CSC clone [49]. In this situation, it is explainable why tumors in general become resistant to conventional and targeted therapies, since after successfully eliminating sensitive CSC clones, pre-existent resistant clones may take over, mimicking an acquisition of resistance to the applied treatment. As a result, tumors might not be represented by single-headed hierarchical structures but rather resemble more oligarchic structures. Thus, dynamic hierarchies might exist within a single CSC clone and its non-CSC progeny (known as intra-CSC clone hierarchy), but also between different genetically diverse CSC clones that compete with each other (known as inter-CSC clone hierarchy), leading to the selection of those clones with high self-renewal activity and simultaneous loss of differentiation

capacity. Nonetheless, it is far from being established whether the latter cells are the only CSCs driving tumor evolution or they do so together with the earlier generation of CSCs. Some authors consider a second possibility and suggest an alternative stochastic model of tumor evolution oscillating between CSC and non-CSC states [50]. In addition, it is also possible that mutations or microenvironmental cues in non-CSCs confer them with self-renewal capacity and convert them into CSCs (a process called phenotypic plasticity) [51]. A relevant consequence of this model in prognosis and therapy based on CSC biomarkers is that these might be unstable for a given tumor stage [52]–[56], needing further validation in each case in conjunction with functional analyses.

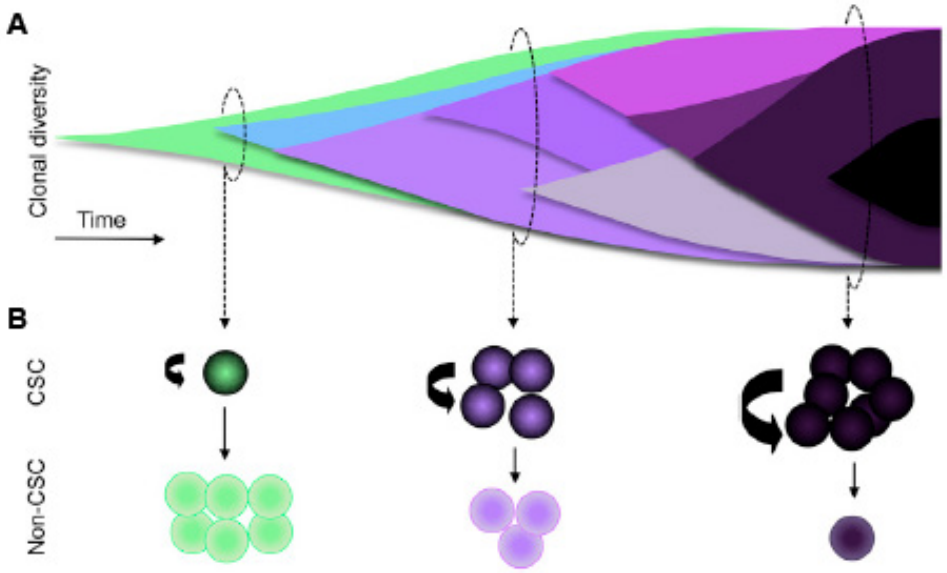

Figure 2. *Unified Model of Clonal Evolution and Cancer Stem Cells.* (**A**) Clonal expansion can occur when the founder cell acquires favorable mutations. In parallel, a new subclone may arise after the occurrence of a different mutation in a different cell. Over time, distinct subclones evolve in parallel due to the accumulation of genetic mutations. (**B**) It is likely that CSCs are not static and can evolve over the lifetime of a given cancer as genetic changes can influence CSC frequency. Some subclones may contain a steep developmental hierarchy (in green), where only few self-renewing CSCs exist among a large number of non-CSCs. Other subclones (in lilac and violet) may contain an intermediate hierarchy, where the number of CSCs is relatively high but a hierarchy still exists. Some subclones may have the genetic alterations that confer high self-renewal potential, where most cells are tumorigenic. *Kreso & Dicke, 2014.*

2.2 Interactions between tumor cells and their microenvironment

Adult stem cells reside in a specific microenvironment (or niche) that regulates their self-renewal and differentiation. The location and constitution of stem cell niches have been defined in various tissues, including the intestinal epithelium, hematopoietic bone marrow, epidermis, and brain [57]–[60]. A similar niche concept has been extrapolated to cancer in which

microenvironmental cues regulate CSC fate during tumor development [61]. This phenotypic plasticity of CSCs due to microenvironmental signals can give rise to distinct and functionally diverse tumor populations, converting epithelial tumor cells into mesenchymal-like invasive cells or transdifferentiate them into non-tumoral-collaborative cells, as has been shown to occur for instance in glioblastoma [62].

The tumor microenvironment consists of an extra-cellular matrix (ECM) and multiple cell types. The tumor ECM mainly results from the extravasation of plasma proteins and dense deposits of collagen and other ECM proteins delivered by the fibrotic component. The cellular components include substantial inflammatory infiltrates (e.g. macrophages, dendritic or T-cells), cancer-associated fibroblasts (CAFs), vascular cells, and local or recruited progenitors (bone marrow-derived mesenchymal stem cells or MSCs, as well as endothelial progenitors) [2] (Figure 3).

Endothelial quiescent cells can be activated by an *angiogenic switch,* causing them to enter into a cell program that allows them to construct new blood vessels. Networks of interconnected signals modulate endothelial tumor-associated phenotypes, including Notch, Neuropilin, ROBO, ephrin, vascular endothelial growth factor (VEGF), angiopoetin and fibroblast growth factor (FGF) signals [2]. Bidirectional crosstalk between CSCs and vascular cells has been demonstrated in the perivascular niche of highly vascularized tumors (e.g. in glioblastoma). Local endothelial cells support the retention of the stem cell phenotype and tumorigenicity of CSCs [63]; for instance, glioma CSCs closely promote local angiogenesis through the release of VEGF and stromal-derived factor 1 (SDF1) [63]–[67]. Particularly, glioma CSCs´ self-renewal has been shown to be mediated by activation of the Notch pathway following the release of nitric oxide by endothelial cells [68] and furthermore, they do not only promote recruitment and expansion of the local vascular network by releasing VEGF [64], [69], but also protect vascular cells from hypoxia and irradiation-induced apoptosis [70], [71]. Skin carcinoma CSCs have also been shown to populate a vascular niche [72]. Both niches seem to revolve around an autocrine VEGF loop that regulates both CSC and niche self-renewal [72]. Therefore, understanding the conversion of normal to tumor-associated endothelial cells could be important for developing novel therapies. While within

the tumors the lymphatic vessels are collapsed, tumor-associated endothelial cells engage lymphangiogenesis at the periphery of the tumors, facilitating the channeling out of tumor cells, leading to cancer cell dissemination.

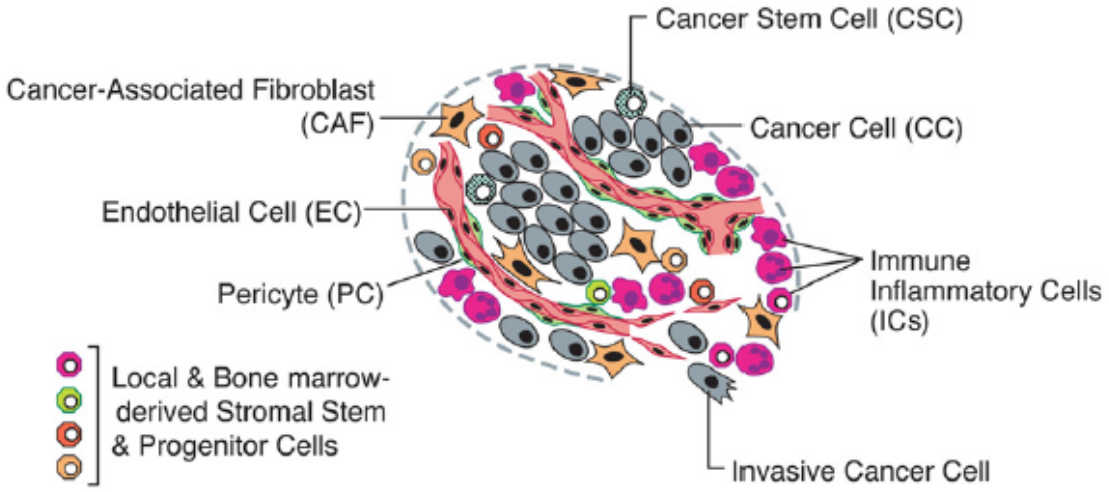

Figure 3. *Neoplastic and tumor microenvironment cells*. Both the parenchyma and stroma of tumors contain distinct cell types and subtypes that collectively enable tumor growth and progression. ECM components are not depicted. *Hanahan & Weinberg, 2011.*

Immune inflammatory cells were evidenced in the tumors in the 90s and over the years they have been shown to play diverse and critical roles in fostering tumorigenesis. Influx of proinflammatory cytokines, including tumor necrosis factor alpha (TNF-α) and transforming growth factor beta (TGF-β), as well as cytotoxic mediators, proteases, matrix metalloproteinases (MMPs), interleukins and interferons, produce potent lymphangiogenic and angiogenic growth factors (FGF2, VEGF) allowing tumor growth and metastatic spread to the lymph nodes. Tumor cells themselves produce cytokines which attract neutrophils, macrophages, lymphocytes and dendritic cells, all contributing to tumorigenic growth and metastatic potential [73]. Infiltrating immune cells also exert control over the CSC pool. The secretion of interleukin-6 (IL-6) by innate immune cells stimulates the proliferation of colon CSCs [74]. In addition, IL-6 has been also found to enhance the conversion of breast cancer progenitors to a CSC phenotype through a positive feedback loop involving NF-κB, Lin28, and Let7 miRNA [75], and has been identified as an inducer of tumor-initiating capacity and chemotherapy resistance in colon and lung cancer cells [76].

Tumor-associated macrophages (TAMs) often accumulate in hypoxic areas and can support angiogenesis through the release of proangiogenic

factors sequestered in the ECM (e.g. VEGF), or can facilitate revascularization through the release of MMPs [77]. TAMs have been shown to interact with CSCs in several cancers, including breast, hepatocellular and colon carcinomas and gliomas [76], [78], [79]. Under hypoxic conditions, glioma CSCs can inhibit TAM-phagocytosis, as well as T-cell proliferation and activation via STAT3 signaling [80]. Although the tumor microenvironment is often considered to promote tumorigenicity by inhibition of the innate and adaptive responses [81], including dendritic cell maturation and subsequent antigen presentation [82], immune cells such as follicular dendritic cells can directly support the maintenance of the tumorigenic CSC state.

In this regard, Hedgehog (HH) signaling seems to be essential for the maintenance of leukemia–CSCs [83], [84], possibly involving the activation of β-catenin signaling. Recently, stromal cells have been shown to modulate HH signaling and proliferation in myeloid neoplasms via expression of the HH-interacting protein [85]. Induction of HH signaling in epithelial cancers upon interaction with TAMs has also been reported [76].

Cancer-associated fibroblasts (CAFs) are a subpopulation of activated fibroblasts. Numerous growth factors such as TGF-β, chemokines such as monocyte chemotactic protein 1 (MCP1), and ECM-degrading proteases, have been shown to mediate the activation of stromal fibroblasts [86]. Activated CAFs secrete a battery of growth factors and cytokines at the tumor primary site to support both cancer cell proliferation and survival. CAFs not only directly regulate tumor growth, but can also support local angiogenesis through the recruitment of endothelial progenitors [87]. In addition, CAFs can also induce a CSC phenotype in non-CSCs through reactivation of the Wnt pathway and hepatocyte growth factor (HGF) signaling [88]. Wnt signaling has also been proposed to be essential for the maintenance of a CSC phenotype in epidermal tumors [89]. In fact, Wnt activation by the surrounding microenvironment and HGF signaling appear to be redundant mechanisms to promote tumor activation [88], [90], [91]. Another type of CAFs, the tumor associated myofibroblasts, may act by remodeling the ECM and facilitating the path for tumor populations to reach the bloodstream and subsequent dissemination [92].

Large numbers of bone marrow-derived mesesenchymal stem cells (MSCs) can be mobilized and recruited to the local microenvironment through

the release of endocrine and paracrine signals during tumor development. MSCs interact with other stromal–resident populations. They can replenish CAFs via differentiation, regulate local angiogenesis and modulate innate immunity through interactions with macrophages [93]. Several studies have suggested that MSCs can contribute to the acquisition of a CSC phenotype by non-CSCs or promote local invasion and metastatic spread of tumor populations [94]. Cancer-associated MSCs have been shown to rely on altered bone morphogenetic proteins (BMPs) production to regulate ovarian CSCs and their tumorigenesis [95]. Similarly, pancreatic stromal cells can enhance the CSC phenotype in pancreatic cancer cells and promote their self-renewal and invasiveness [96]. MSC-secreted factors include cytokines such as platelet-derived growth factor (PDGF), CCL2, and IL-6, and have already been implicated in the acquisition of CSC features. For example, CCL2 has been shown to mediate crosstalk between cancer cells and stromal fibroblasts that augments the CSC phenotype and self-renewal of breast cancer cell lines [97]. MSCs secretion of IL-6 has also been suggested to modulate the CSC content of breast cancer [98].

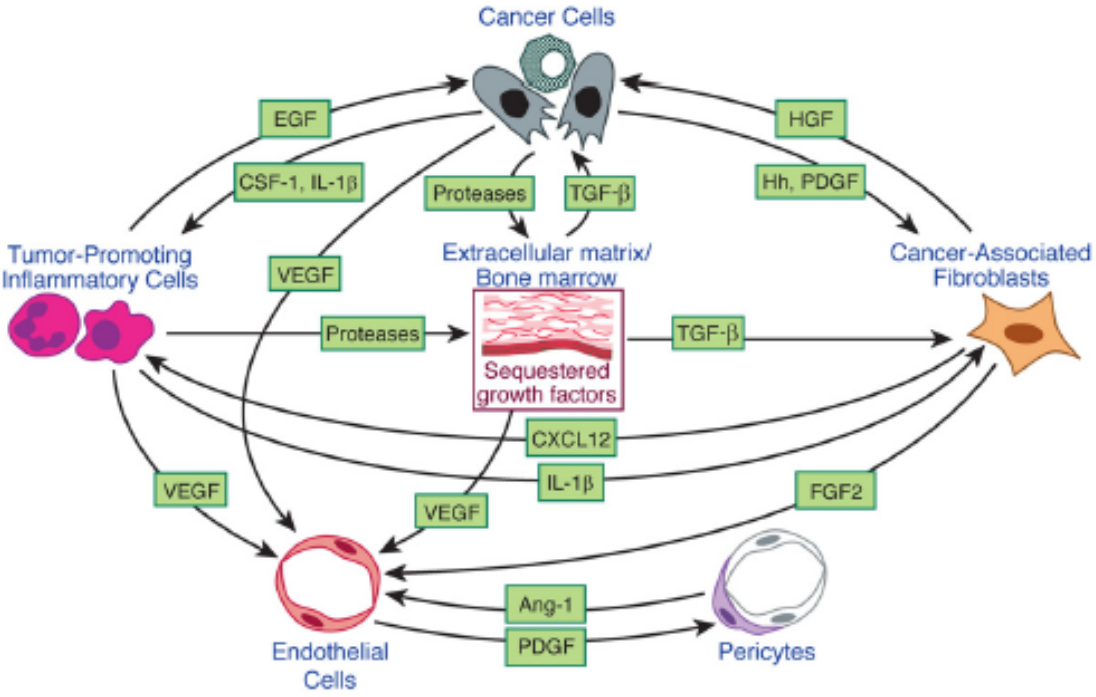

Figure 4. *Interactions in the tumor microenvironment***.** The assembly and collective contributions of the assorted cell types constituting the tumor microenvironment are orchestrated and maintained by reciprocal heterotypic signaling interactions (only few of them are represented). *Hanahan & Weinberg, 2011*.

2.3 The Epithelial-to-mesenchymal transition (EMT) program

A developmental regulatory program, known as epithelial-to-mesenchymal transition (EMT), has become prominently implicated in the acquisition of an invasive phenotype by transformed epithelial cells, as well as enhanced apoptosis resistance and dissemination [53], [99]–[101]. The EMT program is involved in various steps of embryonic morphogenesis and wound healing but it is also recapitulated in some pathological situations such as cancer or fibrosis. The EMT program can be activated transiently or stably (and to different degrees) by tumor cells during the course of invasion and metastasis. A set of miRNAs [102], [103], and transcription factors, such as members of the SNAI, TWIST and ZEB families, (reviewed in [104]) (Figure 5), have been shown to orchestrate the EMT program and related migratory processes during embryogenesis; in fact, most of them were initially identified by developmental genetics [94].

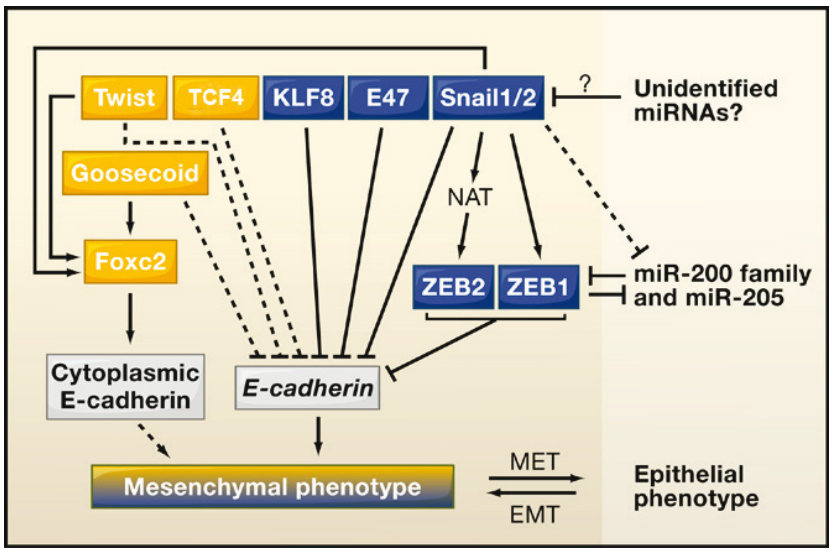

Figure 5. *E-cadherin transcriptional repressors***.** SNAIs, ZEBs, E47, and KLF8 directly repress E-cadherin transcription whereas TWIST, Goosecoid, TCF4, and FOXC2 are indirect E-cadherin repressors. SNAI1 activates the expression of the ZEB genes by different mechanisms, including the induction of a natural antisense transcript for ZEB2 (NAT). The miR-200 family and in some cases also miR-205, represses the transcription of ZEB genes preventing EMT. A loop of miRNAs and ZEB crossregulation plus the cooperation of several EMT inducers reinforces the control of the EMT process. There is evidence that indicates that SNAI1 may also repress the expression of the miR-200 family. Whether miRNAs can also control SNAI1 expression awaits further investigation. EMT, epithelial-to-mesenchymal transition; MET, mesenchymal-to-epithelial transition. *Thiery et al., 2009.*

These transcriptional regulators are expressed in several combinations in a number of malignant tumor types, and have been shown in experimental

models of carcinoma formation to be important for promoting local invasion; furthermore, some have been found to promote metastasis when ectopically overexpressed [94], [105], [106]. The phenotypic traits of cells that have undergone EMT include loss of adherens junctions and conversion from a polygonal/epithelial to a fibroblastic morphology, expression of ECM-degrading enzymes, increased motility and/or resistance to apoptosis. However, the main molecular trait common to EMT transcription factors or inducers is that they can directly repress E-cadherin gene expression, thereby promoting increase in cell motility and invasiveness [107]. Evidence from developmental genetics indicates that microenvironmental signals received from neighboring cells in the embryo are involved in triggering expression of these transcription factors in those cells destined to undergo an EMT [108]; in parallel, increasing evidence indicates that interactions of cancer cells with adjacent tumor-associated stromal cells can induce the expression of the malignant cell phenotypes that are known to be mediated by one or more of these transcriptional regulators [109], [110]. Moreover, cancer cells at the invasive margins of certain carcinomas can be seen to have undergone an EMT, suggesting that these cancer cells are subject to microenvironmental cues distinct from those received by cancer cells located at the cores of these lesions [111]. Although the evidence is still incomplete, it would appear that EMT-inducing transcription factors are able to orchestrate most steps of the invasion-metastasis cascade except the final step of colonization. However, little is known about the several manifestations and temporal stability of the mesenchymal state produced by an EMT. In addition, it remains to be determined whether invasive carcinoma cells necessarily acquire their capability through activation of parts of the EMT program, or whether alternative regulatory programs can also enable this capability.

The fact that microenvironmental signals can induce an invasive growth capability implies that this process may be reversible. In other words, those tumor cells that have spread and abandoned the primary tumor focus to secondary or metastatic sites may no longer be exposed to factors from activated stroma-EMT or invasion-inducing cues so that they may revert in a noninvasive phenotype. Thus, carcinoma cells that have undergone an EMT during initial invasion and metastatic dissemination may pass through the

reverse process, termed the mesenchymal-to-epithelial transition (MET), since metastasis of epithelial tumors display an epithelial cytology, not mesenchymal [112]. Moreover, the fact that cancer cells routinely pass through a complete EMT program is probably rather simplistic and it is likely that cancer cells may undergo a partial EMT program, thus showing mixed mesenchymal and epithelial properties.

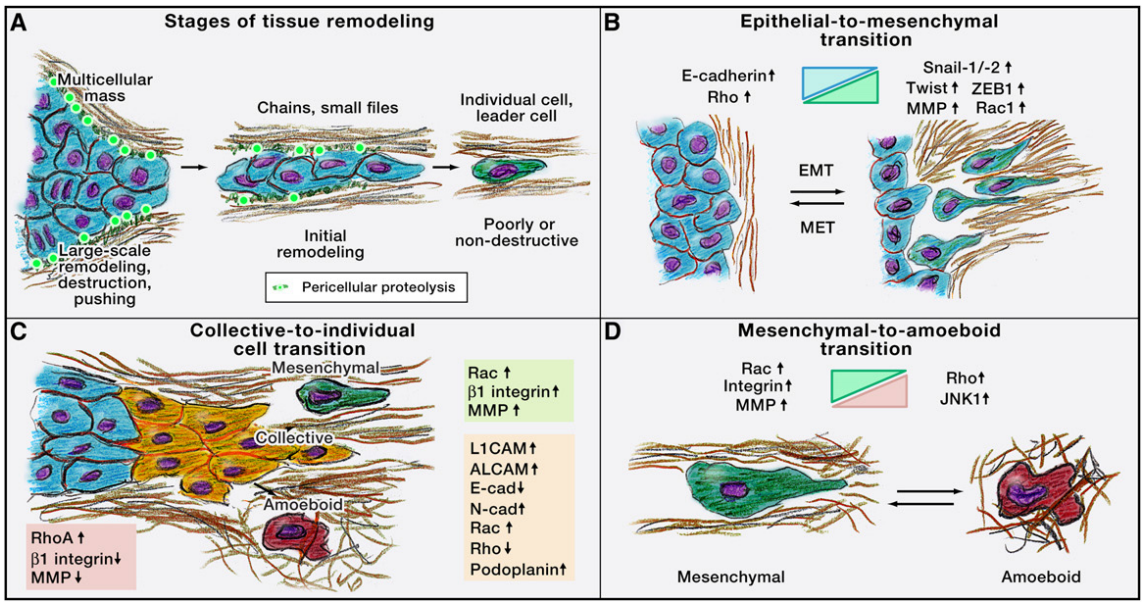

Figure 6. *Plasticity of invasion mechanisms.* (**A**) Migrating cells transition from an initial nondestructive dissemination to migration that involves small and large-scale tissue remodeling. The pre-existing space available to invading cells governs the caliber of individual and multicellular invasion and becomes widened by pericellular proteolysis. (**B**) EMT of a stable epithelium facilitates single-cell detachment. (**C & D**) Invasion programs display plasticity, or adaptability, including transition from collective cell migration to individual cell migration and mesenchymal-to-amoeboid transition. *Friedl & Alexander, 2011*.

The EMT program regulates a particular type of invasiveness that has been termed *mesenchymal*. In addition, distinct modes of invasion have been identified and implicated in cancer cell invasion [113], [114] (Figure 6). For instance, *collective invasion* involves bulges of cancer cells advancing into adjacent tissues and is characteristic of, for example, squamous cell carcinomas. Less clear is the prevalence of an *amoeboid* form of invasion [115], [116], in which individual cancer cells show morphological plasticity, enabling them to slip through existing interstices in the ECM rather than forming a path, as occurs in both the mesenchymal and collective forms of invasion. It is currently unresolved whether cancer cells in the collective and amoeboid forms

of invasion use components of the EMT program or whether entirely different cell programs are responsible for alternating these invasion modes. Another emerging concept, noted above, involves the facilitation of cancer cell invasion by inflammatory cells that assemble at the boundaries of tumors, producing extracellular matrix-degrading enzymes and other factors that enable invasive growth [117]–[119]; these functions may obviate the need by cancer cells to produce these proteins through activation of EMT programs. Thus, cancer cells may secrete the chemoattractants that recruit proinvasive inflammatory cells rather than producing the matrix-degrading enzymes themselves.

2.4 Regulation of local invasion and EMT by the tumor microenvironment

It is increasingly apparent that crosstalk between cancer cells and cells of the tumor stroma can promote tumor invasion, growth and metastasis [118]–[120]. More examples of interactions that can lead to the acquisition of an invasive phenotype in tumor cells (in addition to some commented above), can be the secretion of CCL5 from MSCs present in the tumor stroma in response to signals released by cancer cells, that in turn, stimulates their invasive behavior [121] or TAMs located at the tumor periphery that stimulate invasion of tumor cells by supplying matrix-degrading enzymes such as MMPs and cysteine cathepsin proteases [117], [119], [122], [123]. Moreover, in one model system, the invasion-promoting macrophages are activated by IL-4 produced by the cancer cells [124]. Another example is provided by a model of metastatic breast cancer, in which TAMs supply EGF to breast cancer cells, while the cancer cells stimulate the macrophages with colony stimulating factor 1 (CSF-1); as a result of this reciprocal interaction, intravasation into the circulatory system and metastatic dissemination of the cancer cells is achieved [118], [125].

To sum up, the acquisition of an invasive or EMT phenotype in tumor cells can be triggered by a number of factors secreted by tumor-stromal cells, including among others, VEGF, HGF, EGF (via tyrosine kinase receptors or RTKs) or TGF-β (via TGF-β family receptors) [104]. The pathways known to be involved in EMT induction are depicted in Figure 7.

A critical hallmark of solid tumors is low oxygen tension, because the vasculature cannot sustain the demands of the cancer cells after a certain tumor mass is attained. Hypoxia may play a dual role in tumorigenesis;

insufficient oxygen levels limits tumor cell division while simultaneously selects more malignant cells and induces cell adaptations that allow a more invasive behavior. Hypoxia-inducible factor 1 (HIF-1) can control the expression of specific EMT inducers (SNAI1, TCF3, ZEB1, and ZEB2) likely by direct binding of HIF-1α to the HIF-responsive elements on the SNAI1 and ZEB2 promoters, or indirectly by upregulating TGF-β or β1-integrin [126], [127]. SNAI1 and TWIST1 collaborate with other EMT transcription factors induced by hypoxia and also with lysil oxidase-like 2 (LOXL2), which clinically correlates with hypoxia, playing an important role in EMT induction [128]. Other EMT-related pathways induced by HIF-1α are the activation of Wnt/β-catenin signaling, the activation of urokinase-type plasminogen activator (uP), its receptor (uPAR), MMP2 or MMP9 [129]. Thus, hypoxia can engage an EMT program to eventually transform cells into malignancy, invasion and dissemination of the tumor.

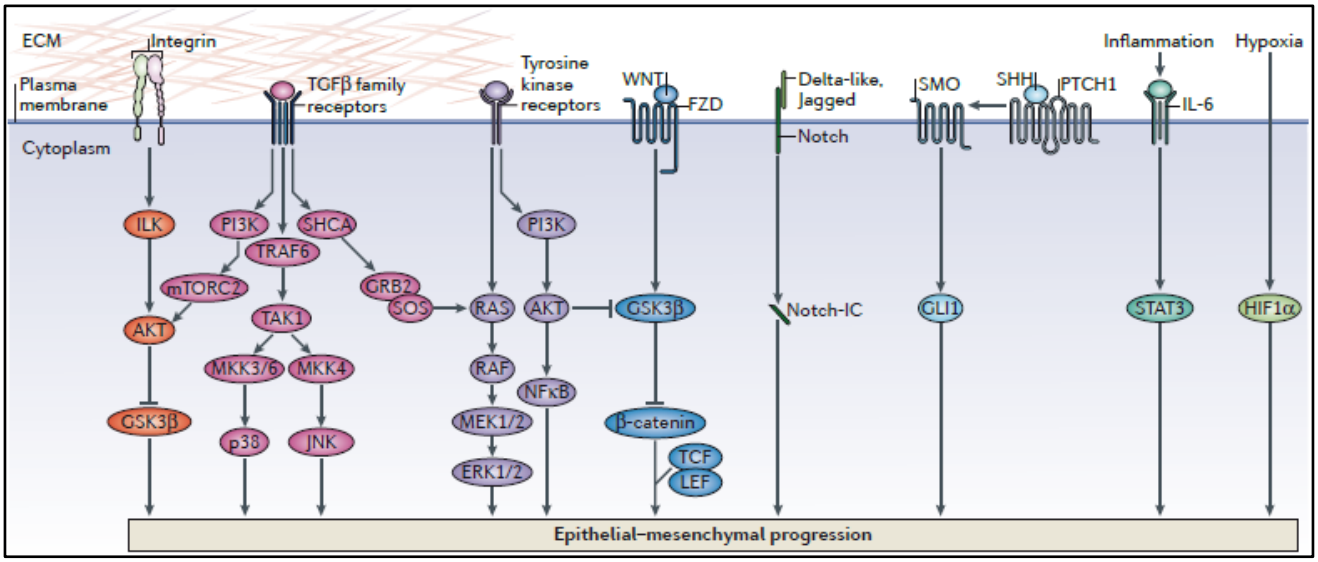

Figure 7. *Overview of signaling pathways involved in EMT*. TGF-β can activate the expression of EMT inducers such as SNAI1 or ZEB1 through SMAD transcription factors (not depicted) and activate the PI3K–AKT, ERK MAPK, p38 MAPK and JUN N-terminal kinase (JNK) pathways. The MAPK signaling cascade represents a major pathway activated by RTKs in response to growth factors. Once activated, ERK1 and ERK2 MAPK can facilitate EMT by increasing the expression of EMT transcription factors (e.g. SNAI1 and 2) and regulators of cell motility and invasion (Rho-like GTPases). Wnt and integrins signaling promotes EMT by inhibiting glycogen synthase kinase-3β (GSK3β) to stabilize SNAI1 and β-catenin, which translocates to the nucleus and engages a gene expression program that favors EMT. In Hedgehog (HH) signaling, glioma 1 (GLI1) can induce SNAI1 expression, and the intracellular domain of Notch (Notch-IC) can activate SNAI2 expression. Inflammation can induce the expression of SNAI1 via STAT3. Hypoxia can activate the expression of EMT inducers via HIF-1α. EMT responses can be increased through crosstalk and cooperation between distinct pathways. *Lamouille et al., 2014.*

Specific interactions that may promote metastasis within the tumor microenvironment as well as the establishment of a metastatic niche in distant organs will be discussed below.

2.5 Interactions between subpopulations of tumor cells

Undeniably, the intense research focused on elucidating how interactions between tumor cells and their microenvironment play key roles in tumorigenesis and tumor progression, has greatly increased our knowledge of these processes and provided new therapeutic approaches. However, comparatively, little is known about the biological significance of the heterogeneity within neoplastic cells and interactions among cancer cells subpopulations in the aforementioned processes. Recently, we and others have reported that distinct tumor subpopulations displaying specialized phenotypes, can interact and cooperate to boost tumor progression and metastasis [130], [131].

In recent years, whether EMT and CSC correspond to mutually exclusive or overlapping gene programs has been matter of debate [132]. Many labs have reported that EMT-undergoing cells show enriched CSC functions compared to cells not undergoing EMT [52], [54]–[56]. Nevertheless, these studies have been performed using cell lines harboring highly heterogeneous populations and rely on the use of biomarkers that may not allow the isolation or identification of pure populations of CSCs. In contrast, our study was based on different clones of prostate and bladder cancer cell lines obtained by their enhanced metastatic potential after serial transplantation in mice and isolated by limiting dilution cloning. After phenotypic characterization of such cell lines, we have demonstrated that the CSC phenotype displayed by metastatic clones is associated with an epithelial program, and that it can be abrogated by the strong EMT induced by overexpression of Snai1; thus concluding that these programs are mutually exclusive in our cell models. In turn, non-metastatic clones displayed traits of having undergone a complete EMT; in *in vitro* assays (among others), they showed a high capacity to invade, in striking distinction from their metastatic-epithelial counterparts. In addition to demonstrating that these clones can coexist in the parental cell line of origin, when metastatic epithelial clones and non-metastatic mesenchymal-like clones were differentially labeled and ortothopically co-injected into mice, the metastatic spread of the epithelial clones was potentiated by the presence of the mesenchymal cell line, and only epithelial-CSC clones were found in metastatic sites. Based on these

observations, we have hypothesized that given their specialized and complementary phenotypes, different subpopulations within a tumor can cooperate for a successful tumor progression. Then in these cell models, we have found evidence that neoplastic cells displaying a strong EMT phenotype are responsible for local invasion while cells displaying epithelial-CSC traits drive the metastatic colonization of distant organs.

3. IDENTIFYING THE CELL OF ORIGIN OF CANCER

The identification of the oncogenic alterations that underlie the malignant transformation of cells that lead to the acquisition of different *hallmarks of cancer* [133] as well as the cells in which they accumulate, are under intense and continuous study.

Lineage tracing experiments in mice models with conditional expression of a reporter gene (β-galactosidase or fluorescent protein/s) in identified adult multipotent/unipotent stem cells or their committed progeny, have allowed to understand the cellular hierarchy of normal tissues [134]. By combining lineage tracing approach with conditional expression of oncogenes, or deletion of tumor suppressor genes through targeted activation of Cre recombinase expression in different epithelial populations (including adult stem cells in several tissues), it has been possible to track the cellular origin in mice of some of the most frequent solid tumors in humans (Figure 8).

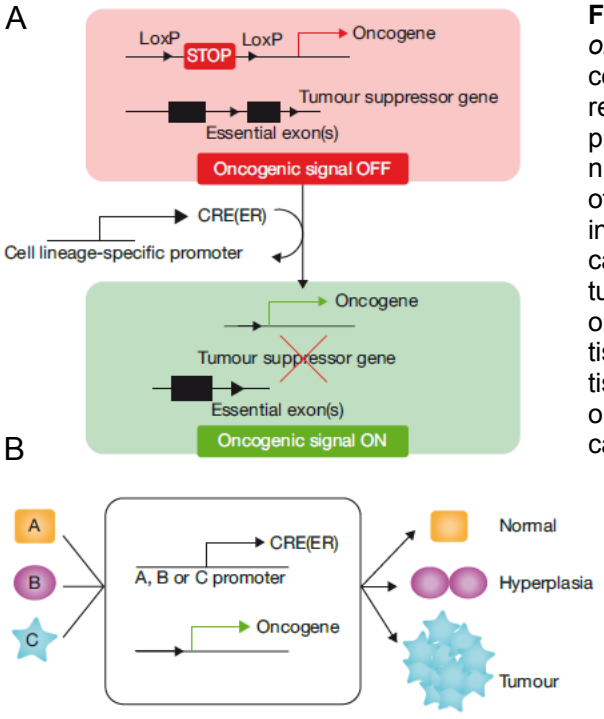

Figure 8. *Genetic approach to determine the cellular origin of epithelial cancers*. (**A**) Mice co-express a conditional oncogene or tumor suppressor and CRE recombinase, under the control of a specific cell- lineage promoter. After administration of a drug that induces nuclear translocation of CRE (e.g tamoxifen in the case of CREER) or spontaneously in the case of a non-inducible CRE, CRE recombinase excises the stop cassette preceding an oncogene or essential exon in a tumor suppressor gene, inducing the activation of the oncogenic program in one of the cell lineages of a given tissue. (**B**) Being A, B or C different cell lines of a given tissue, the oncogene is only expressed specifically in only one cell lineage (leading to tumor formation in this case, in type C cells). *Blanpain, 2014.*

3.1 Skin squamous cell carcinoma has distinct cells of origin

The interfollicular epidermis (IFE) forms the skin barrier and epidermal appendages (hair follicles, sebaceous and sweat glands). Lineage tracing experiments in homeostasis have revealed that different compartments of the epidermis are maintained by their own resident stem cell, defined by the expression of different markers including different types of keratins (Figure 9).

Squamous cell carcinoma (SCC) is the second most frequent skin cancer after basal cell carcinoma and is also the predominant cancer in locations such as the oral cavity, head, neck and oesophagus [135]. The most used mouse model for skin SCC is a multistage, chemically-induced carcinogenesis model [136], [137], in which benign tumors (papillomas) first appear and later some progress to invasive SCC. This model selects cells with an activate Ras pathway [138]; in most papillomas, the most common mutation affects the HRas gene although mutations in KRas have been also reported in mouse and human skin SCC. SCC often shows signs of squamous differentiation, suggesting that they may derive from cells undergoing this process, such as IFE cells [139]. However, when these cells are removed by dermoabrasion, followed by repair of the epidermis by hair follicle stem cells, tumor formation decreases but does not disappear, indicating that different cell lineages, including IFE progenitors and bulge stem cells bearing oncogenic forms of Ras, can form papillomas that may develop into SCC [140]–[144]. These studies have also highlight that the expression of differentiation markers can also be misleading in extrapolating the cellular origin of papillomas.

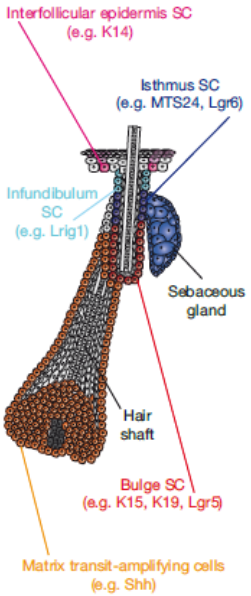

Figure 9. *Multiple cells of origin in skin squamous cancer.* Schematic representation of the different epidermal stem cells and their lineages. Typical molecular markers of each cell type are indicated. (SC, stem cell, K, Keratins). *Blanpain, 2014.*

3.2 Different progenitors can give rise to medulloblastoma

These tumors form in the cerebellum and constitute a heterogeneous disease which can be classified into distinct histological subgroups that show different clinical prognoses [145]. These subgroups arise from distinct types of progenitors and from the activation of different oncogenic pathways [146]–[151].

The first subtype (30% of cases) displays a marked Hedgehog (HH) pathway activation signature and possesses a good-intermediate prognosis. It arises from mutations that constitutively activate HH signaling (Smoothened (Smo) and Patched (Ptch) gain of function or Sufu loss of function) [145]. Smo2 or Ptch1 induced-expression in brain stem cells (using glial fibrilar acid protein (GFAP)-Cre) or Gli-Cre (and others) in cerebral granule neuronal precursors (CGNPs), produce a similar type of medulloblastoma [146], [147]. The effect of constitutive HH activation is tumorigenic only in these stem or progenitor cells, as no tumors are formed in terminal differentiated cells, such as astrocytes, oligondendrocytes or non-granular neurons expressing GFAP [146], [147].

The second subtype (10% of cases) shows Wnt pathway activation and has good prognosis. Conditional expression of β-catenin in CGNPs does not display tumorigenic effect, but it induces hyperproliferation and medulloblastoma formation when expressed in dorsal brain stem progenitors when p53 was also deleted [148].

The third group (25% of cases) shows a Myc signature and has poor prognosis [145]. Forced c-Myc expression in p53 deficient CGNPs transplanted in the cerebellar cortex of immunodeficient mice gives rise to medulloblastomas that molecularly resemble the Myc subgroup [149], [150].

Collectively, these data indicate that although both HH and Myc subtypes are formed from CGNPs, other oncogenic stimuli are capable of inducing different medulloblastoma classes in these cells.

The last medulloblastoma subtype presents similar histological traits to the Wnt subtype but has worse prognosis [145].

3.3 Luminal origin of basal-like breast and prostate cancers

3.3.1 Breast cancer

Breast cancer is the most frequent malignant tumor type in women. It is a heterogeneous disease and is classified into distinct immunohistological and molecular subclasses presenting distinct clinical prognoses [152]. To date, it is unknown whether this heterogeneity is related to the different cellular origins of its distinct subtypes. The mammary gland is constituted by basal and luminal cells that include ductal and alveolar cells [134], [153]. Recent work indicates that epithelial expansion occurring in a variety of physiological contexts (e.g. puberty, pregnancy or lactancy) is sustained by unipotent basal and luminal stem cells [154]. However, using lineage tracing labeling, the same study showed that unipotent basal cells transplanted into the cleared mammary fat pad of immunodeficient mice is able to repopulate the gland including basal and luminal lineages, demonstrating that in these conditions, the restricted differentiation potential of basal stem cells could be expanded.

The diverse cellular origin of breast cancer could explain its observed heterogeneity; this is basal-like tumors originating from basal stem cells and luminal tumors from luminal stem cells. Nonetheless, this proposal may be too simplistic. Women with BRCA1 mutations normally develop basal-like breast cancer [155], although conditional deletion of Brca1 and p53 in both basal and luminal cells using K14-Cre mice (K14 marks embryonic progenitors and all adult mammary epithelium) induce preferentially basal-like adenocarcinomas [156]. Other experiments comparing tumors from $Brca1^{fl/fl}$ $p53^{fl/+}$ mice using specific Cre transgenes (Blg-Cre for luminal progenitor and K14-Cre targeting all mammary epithelium), found that Brca1/p53 deletion using Blg-Cre led to basal-like breast cancer, indicating that luminal progenitors can initiate this type of cancer [157]. In addition, it was found that carriers for Brca1 mutation show an expansion of luminal progenitor cells and that these cells express high levels of basal markers [158] and importantly, that human basal-like breast cancers present a molecular signature more similar to luminal progenitors than that of mature luminal cells and myoepithelial lineage, which include basal stem cells [159]. All these observations suggest that tumor differentiation should not be used to deduce the cellular origin of a cancer [143], [160]. Eventually, the

generation of new CREER mice with more specific markers of basal and luminal stem cells at distinct stages of development, could clarify the cellular origin of other types of breast cancers, including the very common ER^+ luminal subtype.

3.3.2 Prostate cancer

Prostate cancer is the second most frequent cancer in men [135]. Some of the known genetic abnormalities occurring in this cancer include PTEN and TP53 deletions, downregulation of NKX3.1 and gene translocations, such as TMPRSS2-ERG [161]. The prostate epithelium is formed by three distinct lineages, including basal, luminal and neuroendocrine cells [161].

Recent lineage tracing approaches of basal or luminal progenitors after androgen-mediated prostate regeneration after castration have indicated that regeneration can be mediated by basal and luminal unipotent progenitors [162]–[164], suggesting in one study, the existence in the latter of a multipotent rare population [162]. However, there is evidence that both lineages can initiate prostate cancer. Transplantation experiments have shown that basal cells carrying oncogenic mutations can induce cancer formation [165]–[167], and experiments using conditional deletion of Pten in mice expressing Cre (under control of probasin or PSA promoter, which is preferentially expressed in luminal cells), also lead to prostate cancer formation [168]–[170]. Other experiments in castration-resistant luminal cells with deleted Pten and expressing Nkx3.1, also induce cancer formation [162].

Recent studies using lineage tracing approaches have compared the frequency and timing of prostate tumor initiation in Pten deletion in both basal (using K14-CREER) and luminal progenitors (using K8-CREER) [164]. The results showed that luminal progenitors give rise to prostate tumors in all the animals in two months, while basal cells produce hyperplasia of the gland only in few mice that progress in some cases to cancer in six to eight months, and thus suggesting that basal cells are more resistant to oncogenic transformation than luminal cells.

3.4 Stem cell origin of intestinal cancers

The small and large intestines form the gut. Both present a similar anatomical and proliferative unit called crypt of Lieberkühn. The main difference

in their structures is that in the small intestine, the crypts have protrusions to the lumen of the digestive tract (villi), while in the large intestine (colon and rectum), these protrusions are not present and the crypts are longer than those in the small intestine. The composition and abundance of differentiated cells are also different [171].

In both small and large intestine, multipotent stem cells have been identified, characterized by the expression of the seven-transmembrane protein Lgr5, a putative member of the G protein-coupled receptor family. These cells reside at the bottom of the crypts (at positions +1 to +3 from the crypt base), and generate progenitors (transient amplifying cells, located higher up along the crypt) that in turn, give rise to the rest of the differentiated cells in the intestinal epithelium [20]. In the small intestine, a second stem cell population has also been identified expressing high levels of Bmi1, mTERT or Hopx [172]–[174], and located at position +4. These cells are in equilibrium with $Lgr5^+$ stem cells and are able to replace them upon removal [175]. It is unknown whether these cells are different populations of stem cells or derive from the $Lgr5^+$ subpopulation [176], [177] (Figure 10 left).

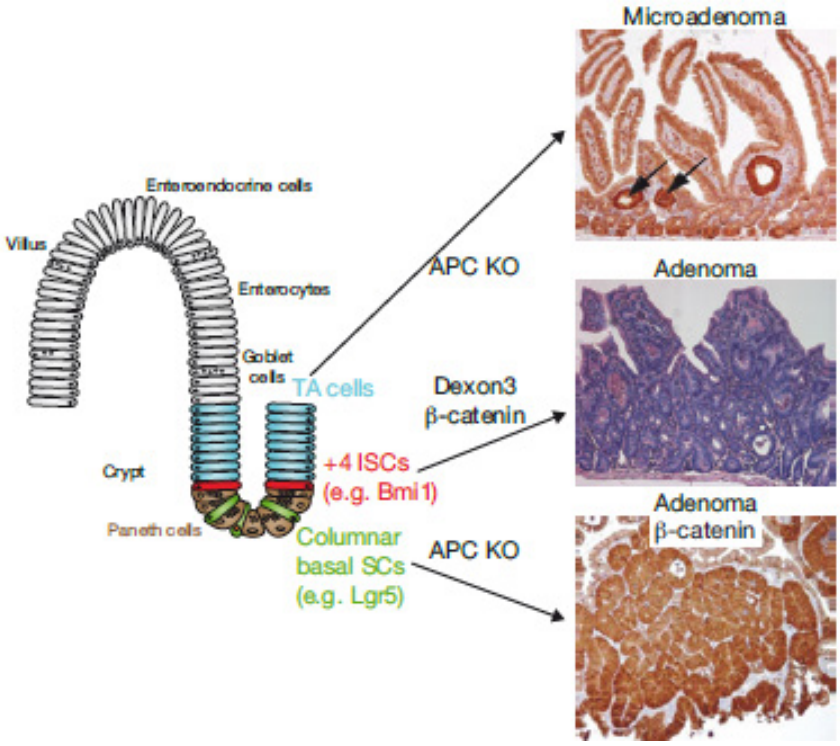

Figure 10. *Cells of origin in intestinal cancers.* Schematic representation of the intestinal crypt with their stem cell populations, transient amplifying (TA) cells and the different epithelial lineages. Constitutive activation of the Wnt/β-catenin signaling in intestinal basal columnar stem cell via Apc deletion or in +4 intestinal stem cell (ISC) via stabilized β-catenin expression, leads to intestinal adenoma within a month, while Apc deletion in TA cells only induces microadenoma in the same period of time. *Blanpain, 2014.*

Cancer of the digestive tract occurs preferentially in colon and rectum, perhaps due to anatomical and physiological differences with the small intestine

(pH, different rate of epithelium turnover or presence of bacteria). However, most of the knowledge of crypt homeostasis and tumorigenesis comes from studies in small intestine crypts in mice.

Colorectal cancer (CRC) represents the third most common cancer in men and the second in women [178]. Mutations known to lead to CRC affect oncogenes such as KRAS and β-catenin (CTNNB1), and (or) tumor suppressor genes (TP53 or adenomatous polyposis coli, APC) [179]; among them, the most frequently found mutations in CRC involve APC deletion or stabilized β-catenin expression that lead to a constitutive activation of the Wnt pathway [180].

In mouse models, the stem cell origin of intestinal cancer has been demonstrated through lineage tracing experiments in basal columnar stem cells in which Apc deletion was forced using a Lgr5 or prominin-CREER system or through the constitutive activation of the Wnt pathway in +4 $Bmi1^{+}$ intestinal stem cells, which leads to adenoma formation. In contrast, deletion of Apc in committed progenitors or transient amplifying cells only produced slow growing benign tumors (Figure 10 right) [172], [181], [182].

3.5 Tracking the cell of origin in other types of cancers and implications of the technique

In addition to the examples described above, similar approaches have allowed to identify the cell/s endowed with intrinsic tumorigenic potential in other mouse models of human cancers. For example, as described above for squamous cell carcinoma, interfollicular epidermis and bulge stem cells have the potential to form basal cell carcinomas (the most frequent skin cancer in humans), dependent on the constitutive activation of Hedgehog signaling [183], [184]. In small cell lung cancers (SCLC), where p53 and Rb mutations are the key features in most cases, it has been demonstrated that cancer mainly arises from neuroendocrine-lineage alveolar type II cells [185]. Another example is bladder cancer, where it has been shown that basal stem cells constitutively expressing Hedgehog signaling can initiate the disease [186].

However, in almost all cases, the fact that oncogenes (or deletions in tumor suppressors) induced the transformation of only certain types of cells, which did not necessarily correlate with their proliferation potential, indicates that epigenetic or transcriptional status of target cells is relevant for tumor

initiation. Preventing tumor initiation or blocking tumor progression could rely on the study of the underlying mechanisms of sensitiveness or resistance to oncogenic stimuli in different types of cells.

As noted above, lineage tracing experiments have highlighted that tumor differentiation does not necessarily reflect their cellular origin; for instance, basal-like breast cancer potentially originates from luminal cells that normally do not express markers observed in tumors. In addition, this approach also allows the isolation of tumor-initiating cells at different time points and thus the characterization of the relevant molecular events associated to each step of tumor progression, or marking individual tumor cells for evaluating their contribution to tumor growth or recurrence. Representative examples of the latter are recent studies that have demonstrated that a small subset of cells displaying a CSC phenotype promote tumor growth in glioblastoma, benign skin and intestine tumors [187]–[189], or are responsible for relapse after chemotherapy in a glioblastoma mouse model [190]. Therefore, lineage tracing approaches have also greatly reinforced the foundations of the CSC hypothesis.

4. METASTASIS: DISSECTING A MULTI-STEP PROCESS

There is a growing body of evidence that suggests that metastasis, which accounts for the vast majority of cancer-related deaths, develops when distant organs are seeded with CSCs that arise from a primary tumor (called metastatic cancer stem cells or mCSCs) [191].

Metastasis, however, is a complex process that implies that tumor cells must overcome a number of physiological barriers. It involves invasion of surrounding tissue and intravasation of cancer cells from the primary focus, dissemination and survival through the circulation, extravasation in homing organ/s, survival on arrival, dormancy or latency, reactivation, colonization and capacity to grow a new tumor (Figure 11).

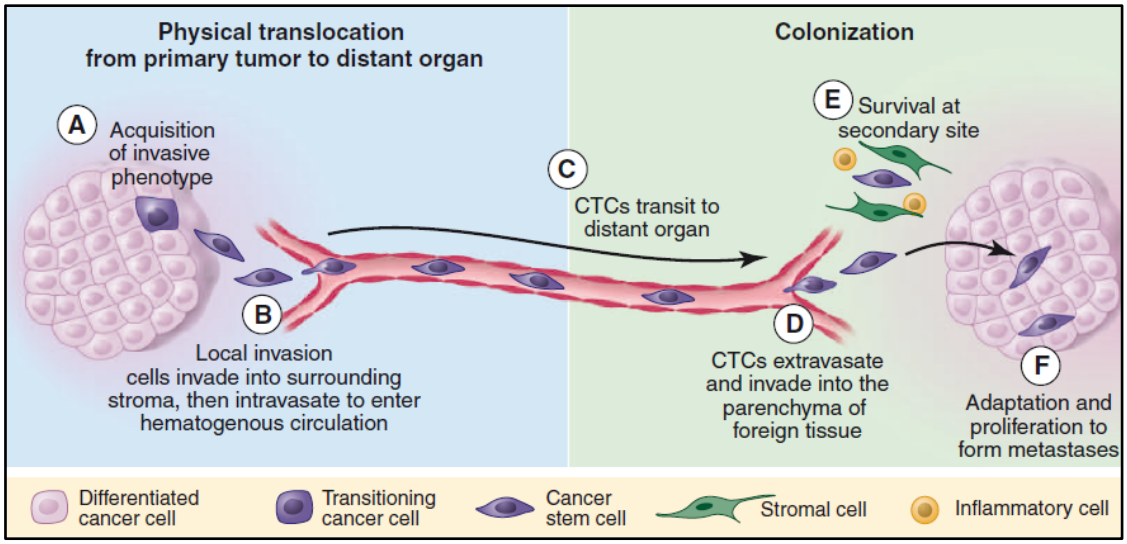

Figure 11. *Overview of the metastatic process*. Metastasis can be split into different phases, one phase of physical translocation from the primary tumor to a distant organ, and a second phase related to colonization of the distant organ and growing a new tumor. (**A**) The first step involves local invasion of the surrounding tissue, by means for instance, of the acquisition of an invasive phenotype (e.g. EMT phenotype). (**B**) Tumor cells reach the circulation and intravasate. (**C**) Most disseminating or circulating tumor cells (CTC) die but some present anchorage-independent survival properties (mCSCs). (**D**) At distant organs, CTCs extravasate and invade the foreign tissue. (**E**) Cancer cells must be capable of evading the immune system response. As single cells or as clusters, they may follow a period of dormancy or latency. (**F**) After reactivation, mCSC must be able to adapt to the new microenvironment and proliferate, forming a new macroscopic tumor. The process can then be repeated. *Chaffer & Weinberg, 2011.*

4.1 Definition and origin of mCSCs

A mCSC can be defined as any disseminating or circulating tumor cell (CTC) that is able to grow a macroscopic tumor in a distant organ. Regarding their origin, there are different possibilities; these cells may already exist in the primary tumor or may be originated by microenvironmental cues in other populations of non-CSCs within the primary tumor (due to phenotypic plasticity), or even from CTCs that acquire the competence to initiate tumor grow after a period of latency.

Evidence for the intrinsic existence of mCSCs in primary tumors derive from studies demonstrating the CSC-unified model of cell heterogeneity due to hierarchical organization in tumors (discussed above), supported by recent lineage tracing experiments in mouse models of brain, colon, and skin cancers [181], [188]–[190]. The capacity to self-renew and produce short-lived progeny in primary tumors (including transient amplifying and more differentiated cells), suggests that mCSCs may be in origin CSCs that resume their regenerative potential in metastatic sites. Additional evidence comes from studies showing a

correlation between high levels of expression of adult stem cell markers in primary tumors and poor prognosis or metastatic recurrence [45], [46], [192], also from studies of isolation of CTCs expressing stem cell markers in the blood of breast cancer patients that form metastases when inoculated into mice [193], or from studies of clonal analysis in human colorectal samples that have demonstrated that metastases arise from tumor cells in the primary focus that show self-renewal capacity, quiescence and resistance to chemotherapy [194], [195].

On the other hand, the generation of mCSCs may be based on regaining tumor-initiating capacity through phenotypic plasticity. As discussed above, an assortment of molecules secreted by tumor-stromal cells (certain cytokines, or growth factors) can enhance CSC features in both CSCs and non-CSCs. EMT induction by microenvironmental cues can provide the migratory and invasive phenotype that enable tumor cells to clear a path and surpass local barriers. As also discussed above, while some studies have demonstrated that EMT is a program not compatible with CSC phenotype [130] and interferes with initiation of metastatic outgrowth [196]–[198], there are studies that have found that EMT provides a gain in stem-like features [8], [53], [199], [200]. Indeed, there is evidence that CSCs exist in both epithelial and mesenchymal states [201]. Histopathological observations suggest that, if mCSCs undergo an EMT at the tumor primary sites, they must reacquire an epithelial phenotype through MET at metastatic sites in order to initiate tumor growth (discussed below).

4.2 Sources of metastatic traits

Regardless of their origin, there is evidence that the CSC phenotype requires additional traits to fully display metastasis-initiating potential. However, a number of studies indicate that, during tumor initiation and progression, mutations or epigenetic modifications affect mainly key genes controlling proliferation, survival or self-renewal, which are known collectively as tumor drivers [202], rather than in *metastasis genes* [48], [203]; a concept referred to genes that confer advantages to tumor cells for overcoming one or more barriers to progress through the metastatic cascade (Figure 12).

In contrast, mutations in epigenetic regulators or in metabolic pathways that support their function could underlie the acquisition of metastatic

capabilities in tumor cells probably due to their pleiotropic effects on transcriptomic output [204], thereby producing imbalances in processes such as cell growth, invasiveness or self-renewal. One example is provided by renal adenocarcinoma driven by the Von Hippel-Lindau (VHL)-HIF2α pathway, where alterations in the methylation status of histone H3K27 enhance the expression of CXCR4 and CYTIP, which are HIF2α target genes and are not required for tumor initiation but enhance metastasis [205]. Another example is provided by non-small cell lung carcinoma, where probably due to epigenetic suppression of the expression of certain differentiation factors (Nkx2-1, GATA6, and HOPX), potentiates metastasis [206], [207]. Finally, there is also evidence for induction of metastatic traits by alterations in mRNA processing, non-coding RNAs or in the translational machinery [208]–[212].

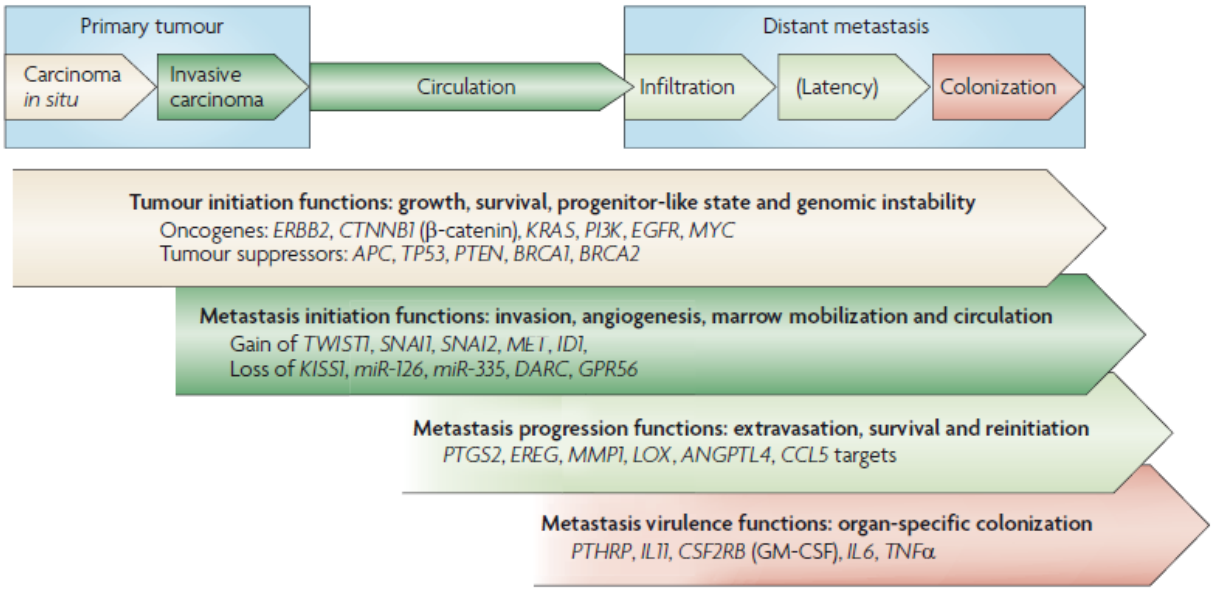

Figure 12. *Examples of putative classes of metastasis genes***.** In addition to the tumor-initiating events that produce an incipient carcinoma (only some examples are listed), metastasis requires functionally distinct classes of genes that provide metastasis initiation, progression and virulence functions. These functions might collectively endow circulating cancer cells with the competence to infiltrate, survive in latency and colonize distant organs. ANGPTL4, angiopoietin-like 4;DARC, Duffy antigen chemokine receptor; EREG, epiregulin; GM-CSF, granulocyte–macrophage colony stimulating factor; GPR56, G protein-coupled receptor 56; ID1, inhibitor of differentiation 1; KISS1, kisspeptin 1; PTGS2, prostaglandin G/H synthase 2; PTHRP, parathyroid hormone-related protein. *Nguyen et al., 2009.*

4.3 Metastatic selection in primary tumors

Several studies have identified metastasis-promoting genes among gene expression signatures in primary tumors that predict relapse, suggesting that acquisition of these traits by tumor cells takes place before dissemination from

the primary focus [205], [206], [209], [213]–[219]. Within the primary focus, tumor cells located at the invasive front are more likely to be selected for their metastatic traits, given their direct exposure to microenvironmental cues (including hypoxia, immune surveillance and cytokines secreted by the reactive stroma). This selection may be not only for general metastasis-supporting traits but also for organ-specific traits; for instance, recent studies in breast cancer metastatic to the bone have shown that stromal CAFs in breast tumors secrete CXCL12/SDF1 and IGF1, which select for Src-hyperactive cancer clones that present a highly activated PI3K-AKT survival pathway; once in the bone marrow, these clones demonstrate to possess a high chance of survival by responding to local sources of these factors [220].

Other studies have proposed that tumor cells that leave early the primary focus could evolve in parallel after a period of latency in a distant organ and be responsible for metastatic relapse [221]. However, large-scale genome sequencing studies have shown that primary tumors and their metastases are highly similar, indicating that most of the genetic alterations for establishing metastases occur in the primary focus [48].

4.4 Metastasis: patterns and probabilities

The type of cancer determines the tropism for certain organs and the latency period between diagnosis and relapse [222], [223]. Some cancers can relapse in multiple organs such as bones, lungs, liver or brain (e.g. breast or lung cancer) or mainly in one organ (e.g. prostate cancer in bone). In turn, the latency period of metastasis can be long (e.g. melanoma, prostate cancer and luminal breast cancer) or relatively short (e.g. lung and basal breast cancer).

A number of studies have focused on the variables affecting the accomplishment of the metastatic process. Indeed, dissemination of cancer cells is affected by circulation patterns (as it is manifest in colorectal cancers, whose metastases occur primarily in the liver via mesenteric circulation), or by cancer cell-autonomous functions (e.g. invadipodia formation), paracrine factors, proteases, recruitment of stromal components and interactions with platelets. Although these mediators of tumor cell dissemination have not been studied in the context of CSCs, it is known that their expression in primary tumors predict their metastatic recurrence, thus presumably affecting the

dissemination of the mCSCs. The organ tropism of these cells depends not only on the probability of reaching these distant organs but also on their overall survival. It is thought that this probability is very low due to the cellular composition, vascularity, immune surveillance and inflammatory status of the infiltrated tissues, that largely differ from organ to organ and from those present in the primary tumor. Experimental evidence and clinical observation indicate that CTCs suffer a dramatic reduction in viability upon infiltrating distant tissues [224]–[226], that mostly tumor cells undergo apoptosis within two days after intravenous injection into mice [227], or more specifically that only a small fraction of melanoma cells are able to form liver metastases when injected intraportally [228], [229]. In fact, CTCs are more capable of reinfiltrating the tumor of origin than metastatic sites (known as tumor self-seeding) [230].

Little is known of the mechanisms underlying the death of cancer cells upon infiltrating distant organs, but it is likely that these mechanisms are related to the lack of a supportive stroma or elimination by the innate immune system [224]–[226], [231], which is present in all organs, being especially acute in the brain [232]–[234]. A recent work in models of brain metastases from breast and lung cancers has demonstrated that tumor cells extravasating from brain capillaries, face reactive astrocytes that generate plasmin that cleaves membrane bound FasL and induce Fas-mediated apoptosis in cancer cells; in turn, a small fraction of cells (about 1%), are able to override this mechanism by producing serpin inhibitors of plasmin generation [235].

4.5 Metastatic niches

As it occurs with cancer cells in the primary tumor, finding supportive sites or niches is thought to be crucial for survival and fitness of CTCs and for establishing metastases in distant organs. Three distinct sources of metastatic niches are possible; mCSCs may usurp native stem cells in distant organs, niche functions might be provided by stromal cells not belonging to stem cell niches, or mCSCs may produce stem cells niches components themselves (Figure 13).

In general terms, stem cell niches provide developmental and self-renewal signals, including Wnt, Notch, TGF-β family components, CXCL12/SDF1, and Hedgehog signals [57]–[60], and in fact, gene expression

profiles of both metastatic samples and adult stem cells show activation of these pathways [236]. For example, in the bone marrow, mesenchymal stem cells generate CXCL12/SDF1 for hematopoetic stem cells, and their receptor CXCR4 is often found overexpressed in bone metastatic cells [237], [238]. While the metastatic lesion grows, mCSCs recruit stromal cells (including TAMs, myeloid precursors and mesenchymal cells), and a paracrine loop is established that eventually provides survival and self-renewal cues, thereby resembling the primary tumor niche [88], [119], [214], [239].

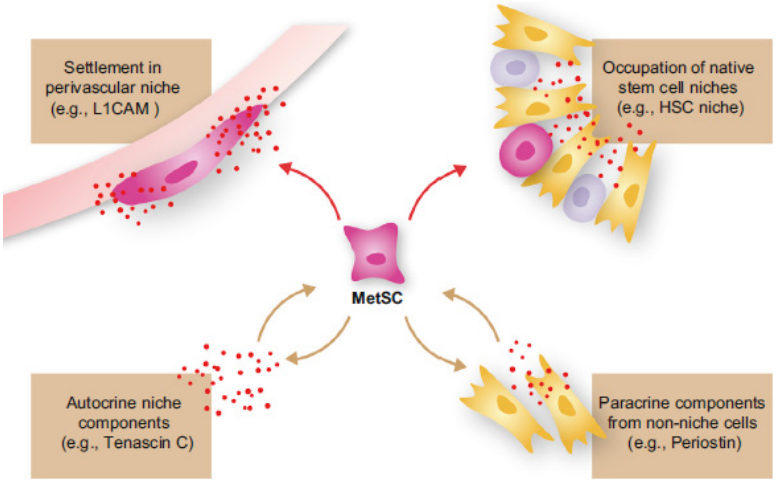

Figure 13. *Three possible sources of metastatic niche support*. mCSCs can find stem cell niche support by occupying native stem cell niches (including perivascular sites), by recruiting stromal cells that produce stem cell niche-like components or by producing niche components themselves. *Oskarsson et al., 2014.*

Blood capillaries (constituting the perivascular niche) have been shown to be a location where CTCs are bound to initiate metastatic outgrowth in a variety of cancer cells, including glioma, melanoma, breast and lung cancer cells [232], [240]–[242]. Recent studies have demonstrated that brain metastasis-initiating cells express the adhesion molecule L1CAM that is used to stretch and surround the perivascular basal lamina [235]. This adhesion molecule is also expressed in other types of cancers and is associated with poor prognosis [243], [244], suggesting that expression of L1CAM may be relevant to initiate metastasis in other organs through this mechanism.

Perivascular niches are thought to support mCSCs by providing attachment, oxygen, nutrients and paracrine factors from the recruited endothelium [245], as has been shown in colorectal cancer, where expression of Jagged1 from endothelial cells promotes a CSC phenotype in tumor cells [246]. In addition, endothelial cells express ECM components that promote metastatic functions in tissue culture [247].

Furthermore, it is also known that primary tumors can influence the microenvironment of distant organs (particularly the lung) through systemic secretion of a battery of cytokines to establish a premetastatic niche [248], as it has been shown in mouse models of breast, lung, stomach and intestinal tumors, which secrete systemic inflammatory cytokines and ECM-remodeling enzymes that facilitate the initiation of metastasis by CTCs in the lung parenchyma [248], [249].

In addition to the interactions between cancer cells and tumor-stromal cells, interactions between neoplastic cells and ECM components also seem to play an important role in the homeostasis of both primary tumor and metastatic niche. Some components of the ECM that have been shown to be relevant in the metastatic niche in mouse models are tenascin C (TNC) and periostin.

TNC is a glycoprotein present in stem cell niches that supports their functions by regulating Notch and Wnt signaling (Figure 14). In xenotransplants, it has been demonstrated that cells expressing high levels of TNC are more likely to invade and grow metastasis in the lung [250].

Periostin is also present in stem cells niches and promotes the initiation of lung metastasis in breast cancer cells in mice [251]. In response to TGF-β secreted by cancer cells, myofibrobalsts of the niche produce periostin, which binds Wnt stromal ligands and stimulates this signaling pathway in tumor cells. Like TNC, periostin enhances Wnt and Notch signaling (Figure 14), which in mCSCs facilitates the colonization of distant organs. Both proteins are known to bind to each other and to cell surface integrins [252].

Other ECM components such as the glycosaminoglycan hyaluronan, the glycoprotein osteopontin (both interact with CD44 in cancer cells), or hyaluronan synthase-2 (HAS2), have been shown to inhibit apoptosis in breast cancer cells during lung colonization, as well as to enhance aggressiveness of glioma cells in the perivascular niche, or to induce metastasis in mouse models of breast cancer, respectively [253]–[255].

As discussed above, most CTCs die when they infiltrate a distant tissue. The survival of tumor cells upon arrival to a distant organ depends on the balance of lethal inputs from the reactive stroma and upregulation of mechanisms that engage cell survival and evasion of apoptosis. The PI3K-AKT pathway plays an important role in engaging cell survival in CTCs and several

mechanisms can amplify its effects. Src kinase activity amplifies PI3K-AKT signaling in response of breast cancer cells to stromal CXCL12/SDF1 and IGF1 in the bone marrow (Figure 14) [256]. The endothelial adhesion molecule VCAM1 also amplifies PI3K-AKT signaling in breast cancer cells upon interaction with α4-integrins on pulmonary macrophages in the lung [257]. In fact, Src activity in human breast tumor samples has been associated with bone relapse and VCAM1 expression with lung recurrence [216], [256], [257].

Other interactions and pathways can enhance metastatic abilities in CTCs. Some examples are the interactions between EGFR and Met with ECM binding integrins that promote colonization in model systems [258], the role of NF-κB signaling in metastasis of colon, lung and breast cancers in mouse models [259]–[261], or the JAK-STAT signaling in mediating metastasis in melanoma, breast and pancreatic carcinomas [262]–[265]. It has also been described that upon infiltration of mCSCs in liver or lungs, mCSCs generate TGF-β that induce IL11 production in resident fibroblasts; IL11 then activates prosurvival signaling via GP130/STAT3 in tumor cells that promote metastasis initiation in these organs (Figure 14) [214].

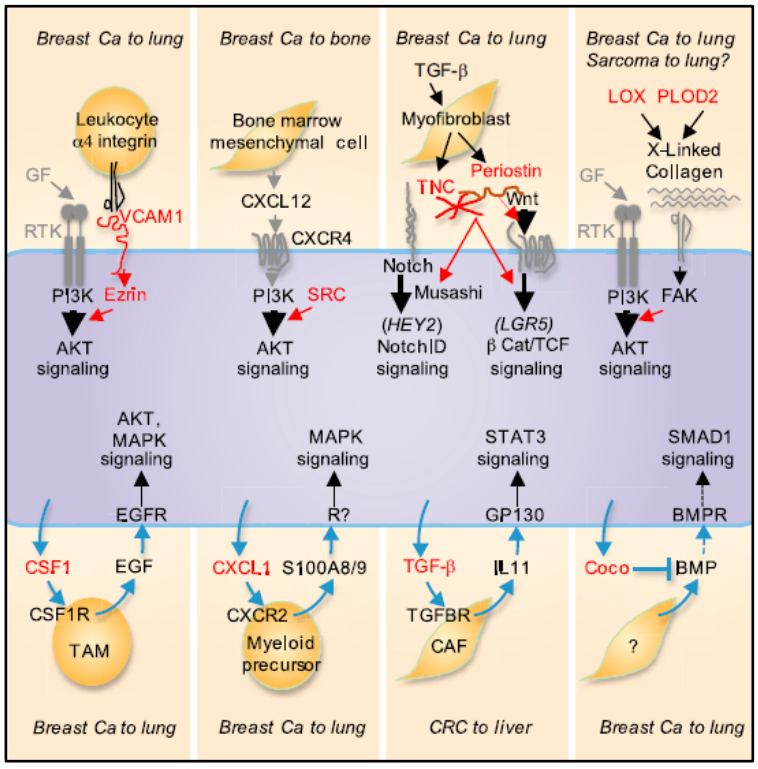

Figure 14. *Pathway amplifiers and paracrine loops for mCSCs support.* Metastatic dissemination is mediated by gene products (in red) that are expressed by tumor cells to amplify their own responsiveness to prosurvival signals. These activating cues include RTKs growth factor ligands (GF), chemokines (e.g. CXCL12), Wnt or Notch ligands. Amplifiers include adhesion receptors like VCAM1-Ezrin complex that is engaged by tumor leukocyte integrins; Src that amplifies PI3K-AKT activation by CXCR4 (or IGF1R); the ECM components TNC and periostin that enhance Wnt and/or Notch pathways and are secreted by tumor cells or myofibrobalsts; the collagen crosslinking enzymes LOX and PLOD2 that stiffen the ECM for integrins or FAK-mediated amplification of RTK signaling. Several cytokines secreted by cancer cells (bottom, red) promote stromal cells recruitment. Stromal cells provide additional support by producing activators of AKT, MAPK, and STAT3 in incipient metastatic lesions. mCSCs-derived BMP inhibitors like Coco, protect self-renewal by inhibiting Smad1 signaling. *Oskarsson et al., 2014.*

As important as survival cues, maintaining the self-renewal capacity of cancer cells is a key feature provided by the metastatic niche. It is known that Notch and Wnt signaling promote self-renewal in several stem cell niches, including the bone marrow and the gut crypts [57], [59], and presumably have the same role in metastatic niches. ECM components like TNC or periostin (among others mechanisms) may act as amplifiers for the ability of mCSC to respond to relative low levels of Wnt and Notch ligands secreted by stromal tumor cells.

4.6 Reversing EMT

As commented above, if mCSCs have undergone an EMT at the primary tumor, they must revert to an epithelial phenotype (via MET) as supported by the epithelial cytology displayed by carcinoma metastases.

Evidence for this has been found in a model of squamous cell carcinoma, where expression of the EMT master regulator Twist, enhanced cancer cell dissemination but their metastases required the downregulation of this transcription factor and reacquisition of an epithelial phenotype [198]. In another study, expression of the EMT inducer Prrx-1 promoted dissemination of breast cancer cells but metastatic colonization was facilitated upon MET induced by loss of Prrx-1 expression [196]. Id1 is a transcription factor that meditates metastatic colonization of breast cancer cells [266], and acts downstream of TGF-β to downregulate Twist expression and mediate MET in basal breast cancer cells that invade the lung [197]. Strikingly, TGF-β signaling promotes EMT in the primary tumor and dissemination of cancer cells [267]; the duality in its functions may rely on microenvironmental cues but these are unknown.

4.7 Entering and exiting dormancy

Clinical evidence indicates that metastasis can remain latent years after removal of a tumor. However, the nature of most mice models limits the study of the determinants that may induce latency in CTCs in distant organs and the mechanisms that lead to an exit from this state. For this reason, the role of the above described pathways and interactions between stromal cells and cancer cells are largely unclear before, during and after passage of mCSCs through a period of quiescence.

The majority of CTCs detected in bone marrow are in a dormant state [268]. It is thought that latency may be a defense mechanism of tumor cells under adverse conditions [269], [270]. The few available models have demonstrated the implication of several cues and pathways in the balance between latency and active proliferation of tumor cells. p38 and ERK MAPKs seem to control the switch of CTCs between these two states [271]. In addition, BMP signaling has been proposed to promote latency in breast cancer cells in the lung parenchyma by suppressing self-renewal and inducing differentiation, with subsequent metastatic colonization being triggered by Coco, an inhibitor of BMP signaling (Figure 14) [272].

It is likely that in locations other than bone marrow and resembling what occurs in adult stem cells, CTCs may be constantly entering and leaving the latency state and evolving during active periods to eventually awake their potential of initiating a metastasis in a distant organ.

4.8 Engaging colonization

There are few models available that have described the molecular mechanisms underlying the overt metastatic colonization of a given organ by cancer cells. Perhaps the best characterized example is the osteolytic bone metastasis occurring in advanced breast cancer. After secretion of a battery of molecules by mCSCs (including IL11, TNF-α, parathyroid hormone-related protein (PTHrP), MMP1, VCAM1 and Jagged1), osteoclasts differentiate and activate, and start to resorb bone matrix clearing the path for tumor growth. Moreover, osteolysis provides matrix-stored factors such as TGF-β (and other growth factors), that in turn stimulates the production of more osteoclast-activating molecules by cancer cells, and establishing a positive feedback loop that potentiates the destruction of the tissue and tumor expansion [273]. Evidence from experimental models suggests that the acquisition of the ability to stimulate osteoclast activation occurs after dormancy of mCSCs for months, followed by reactivation and formation of micrometastases in the bone marrow [274]. One interpretation could be that organ colonization may involve the acquisition of a final set of metastatic traits by the progeny of mCSCs that originally arrived and survived in the metastatic host tissue.

5. PLURIPOTENCY GENES AS ONCOGENES

5.1 Overview of the transcriptional regulatory circuitry controlling pluripotency in embryonic stem cells (ESCs)

ESCs derived from the inner cell mass of the blastocyst-stage embryos give rise to the three germ layers and eventually to all differentiated cells of an organism. In contrast to adult stem cells, ESCs do not need a niche to maintain their undifferentiated open state but do need to be protected from differentiating agents.

In ESCs, the intricate interplay between transcription factors and their targets on the genomic template serves as building blocks for the transcriptional network that governs self-renewal and pluripotency. At the core of this complex network is the transcription factor trio, OCT4, SOX2 and NANOG, which constitute the ESC transcriptional core, with feedforward and feedback loops of regulation (Figure 15A) [275]. Regulatory mechanisms such as autoregulatory and feedforward loops support the ESC transcriptional framework and act as homeostatic control for ESC maintenance. In addition, genome-wide studies have further revealed additional players involved in pluripotency and the interconnectivity within the complex ESC transcriptional circuitry in concert with epigenetic regulators (such as members of the Polycomb complex) that maintain the homeostasis of ESCs [275].

OCT4 (or POU5F1), a key octamer transcription factor in ESCs, is downregulated upon differentiation and cells tend to lose their self-renewing state. For instance, in ESCs, OCT4 acts repressing the differentiation specific-lineage gene CDX2. Thus, it is crucial for ESCs to maintain OCT4 at the appropriate levels in order to maintain the pluripotency, because increased or decreased levels may lead to differentiation [276].

SOX2, a SRY (Sex determining region-Y)-related transcription factor, a high mobility group box (HMGB) DNA-binding domain, can preserve ESCs stability maintaining OCT4 expression at correct levels. In addition, OCT4 is a partner of heterodimerization with SOX2 and OCT4/SOX2 dimers regulate many ESC-specific genes, including themselves. The cis-regulatory element to which SOX2/OCT4 complex binds consist of neighboring sox (5'-CATTGTA-3') and oct (5'-ATGCAAAT-3') elements [277].

NANOG is a homeodomain transcription factor and functions as a dimer. Its loss of dimerization may compromise the preservation of self-renewal and pluripotency of ESCs. Moreover, dimerization of NANOG is crucial for its interaction with other pluripotency related proteins [278]. NANOG is essential for the establishment of pluripotency but is dispensable for its maintenance, provided that SOX2 and OCT4 are expressed.

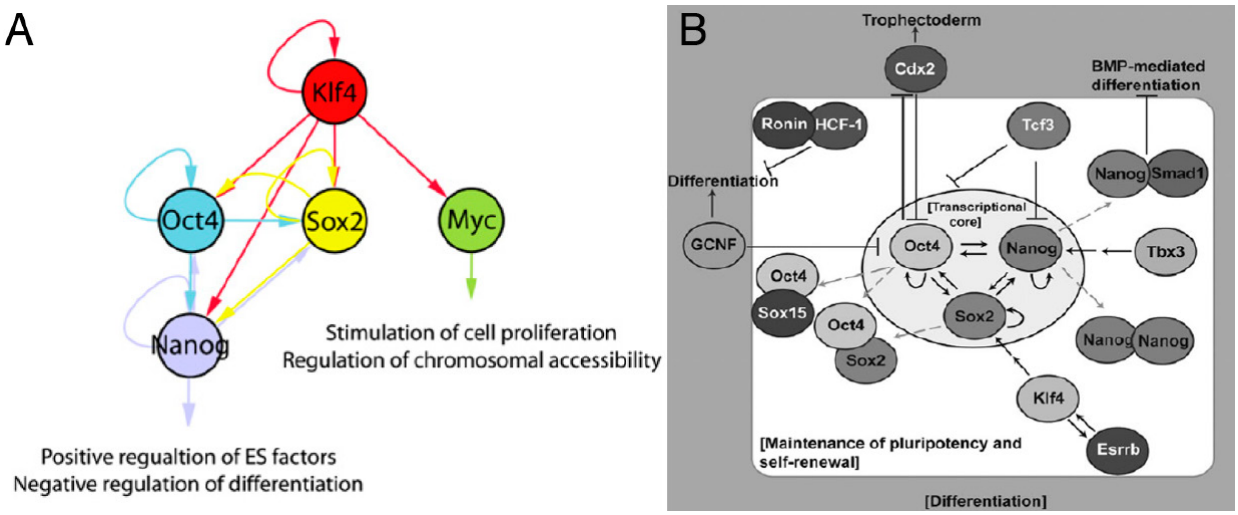

Figure 15. *ESC transcriptional regulatory networks.* (**A**) Regulatory circuit with four somatic regulatory factors and Nanog. *Modified from Kim et al. 2008*. (**B**) Transcriptional core and interplay with other positive or negative ESC-regulating factors. Factors located in the white region are associated with pluripotency and self-renewal, whereas factors located within the grey region are associated with differentiation. *Modified from Heng & Huck-Hui, 2010*.

Other factors relevant for ESCs and pluripotency have been identified. KLF4 is a zinc-finger transcription factor with a defined role in maintaining self-renewal and thus contributing to the pluripotency and self-renewing framework in ESCs [279]. KLF4 also plays important roles in the autoregulatory network of pluripotency in ESCs because it acts upstream of OCT4 and SOX2, and share common downstream targets, such as NANOG, and also occupies the c-MYC promoter.

MYC can support ESCs through functions distinct from those of the mentioned core genes, including positive cell proliferation regulation, negative regulation of differentiation, and regulation of chromosomal accessibility [280].

KLF2, KLF5 and KLF9 play roles in pluripotency [279]. RONIN, another zinc-finger protein, can rescue the phenotype of OCT4 by repressing differentiation genes. RIF1, TCL1, TRIM28, CHD1, HDAC2 and others, also

interact and contribute to the pluripotent state of ESCs [275]. In general terms, the co-occupancy of many different transcription factors on gene promoters determines their state of activation or repression. Genes bound by more than four factors are generally transcriptionally active, whereas those bound by fewer transcription factors can be repressed [280].

The balance between upstream signaling pathways regulating the expression of these factors and other regulators, controls the maintenance of the pluripotent state and self-renewal of ESCs (Figure 15B). These signaling pathways include leukemia inhibitory factor (LIF)-STAT, PI3K-AKT and MAPK pathways, TGF-β, BMP/SMAD or Wnt/β-catenin signaling [280]–[287].

Strikingly, the paradigmatic irreversibility of stem cell differentiation was challenged by virtue of the successful transformation of fully differentiated adult cells into ESCs analogs through the action of a few ESC-transcription factors. In 2006, Yamanaka and colleagues were able to reprogram adult mouse fibroblasts into induced pluripotent stem cells (iPSCs) similar to ESCs, by introducing the transcription factors Sox2, Myc, Klf4 and Oct4 [288]. One year later, human neonate-fibroblasts were reprogrammed using the same or slightly modified combination of genes (OCT4, SOX2, NANOG and LIN28), although in that report, reprogramming was not applied in adult human fibroblast [289]. Later, adult mouse and human fibroblasts were successfully reprogrammed into iPSC state through the introduction of only 3 exogenous factors (SOX2, OCT4, KLF4) [290], even though the study provided evidence that endogenous MYC expression was required for such transformation, suggesting that MYC is still an indispensable factor for induced pluripotency. Thus, SOX2, MYC, KLF4 and OCT4 are considered the four core reprogramming factors for iPSCs. More recently, it has been reported that the epithelial phenotype, and more specifically, E-cadherin expression, is required for reprogramming of fibroblasts into an induced pluripotent state [291].

5.2 CSCs transcriptional gene networks: linking stemness, prognosis and therapy

Modern techniques in stem cell biology in the postgenomic era have led to dramatic advances in our understanding of the molecular underpinnings of both ESCs and cancer. Detailed gene expression maps have now shown the

diversity and distinctiveness in gene expression programs associated with stemness in embryonic and adult stem cells. These maps have further revealed a shared transcriptional program in ESCs and CSCs. Yet, the inability to define a consensus stemness signature in a gene-by-gene analysis may suggest that different types of stem cells utilize distinct mechanisms to achieve self-renewal and pluripotency. Alternatively, the failure to identify a robust signature may be due to technical variations in stem cell isolation, degrees of cell purity including contamination from neighbor populations, microarray platforms, or statistical analysis methods.

Indeed, it has been shown that embryonic and adult stem cells can be distinguished into two predominant groups based on their gene expression, and surprisingly, CSCs may demonstrate gene expression programs more similar to ESCs than adult stem cells [292]. In one study, an *ESC-like gene module* was identified based on genes whose promoters are occupied by regulatory proteins conferring pluripotency such as OCT4, NANOG and Polycomb. Based on the motif module map method [293], the c-MYC binding motif was predicted to be the top driver of the ESC module and it was shown to be sufficient to force activation of an ESC-like gene expression program in adult epithelial cells and moreover, capable of reprogramming them into human epithelial CSCs and thus, endow them with pathological self-renewal and tumor initiating capacity [292].

The ESC-like module is defined by 335 genes and contains many transcriptional regulators, in particular, several associated with pluripotency, including SOX2, c-MYC, DNMT1, CBX3, HDAC1 and YY1. OCT4 and NANOG are not in the ESC-like module because they are specifically expressed in ESCs. This implies that part of the transcriptional program mediated by these key ESC regulators, can be regulated in other stem cells by alternative mechanisms. The ESC-like module is activated in many different human epithelial cancers, including breast, liver, gastric, prostate and lung cancers. The ESC-like transcriptional program is associated with aggressiveness and activated in diverse human epithelial cancers and strongly predicts metastasis and death, particularly in lung and breast cancers, and thus it is clinically relevant [292].

An independent analysis of embryonic stem cell gene signatures by Ben-

Porath and colleagues also observed increased expression of ESC signatures in clinically aggressive epithelial cancers, such as glioblastoma and bladder cancers [294]. Histologically, poorly differentiated tumors show preferential overexpression of genes normally enriched in ESCs, combined with repression of Polycomb regulated genes. Likewise, activation of targets of NANOG, OCT4, SOX2 and c-MYC are more frequently overexpressed in poorly differentiated and aggressive tumors than in well-differentiated and less aggressive tumors [294].

Recently, stemness signatures have been inferred from adult stem cells in solid tissues including the intestine and breast, and have demonstrated to be highly predictive of CSC content and patient outcome [45], [46]. Strong evidence is emerging to support a link between stemness and therapy resistance in glioblastoma, colon cancer, breast cancer, and numerous other tumors, where studies show that CSCs are more resistant to therapy compared to non-CSCs [295]–[300]. Indeed, CSCs display a number of biological properties that distinguish them from the remainder of tumor cells; not only resistance to treatment [38], [295], [301] but also evasion of cell death [302], [303] and dormancy [195]. Collectively, these studies highlight the relationship between genetics and CSC properties that drive clinical parameters such as therapy response and eventually overall survival. The emerging evidence linking stemness to prognosis and therapy failure suggests that therapeutic targeting of determinants of stemness might lead to eliminate CSCs and prevent recurrence.

Although the mechanisms that regulate cancer stemness still remain largely unknown, several regulators including the Polycomb protein Bmi-1 have been strongly linked to self-renewal and have been involved in the maintenance of stem cells in several tissues [304]–[306]. A recent work has found that human colorectal CSCs properties rely on BMI-1. Downregulation of this protein inhibits the self-renewal capacity of colorectal CSCs, resulting in a dramatic reduction of their tumorigenic potential [307]. Moreover, treatment of primary colorectal cancer xenografts with an inhibitor of BMI-1 led to colorectal CSC reduction with long-term and irreversible impairment of tumor growth.

Additional examples are studies from two groups that have found that Sox2-expressing cells act as the founding population that generate tumor

growth, and give rise to differentiated heterogeneous cell progenies in different cancer types. In the first study, rare quiescent Sox2^{+} cells were demonstrated to be responsible for propagating sonic Hedgehog (SHH) subgroup of medulloblastoma using a Ptch1$^{+/-}$ mouse model and lineage tracing approach [308]. These cells generated a rapidly cycling progeny (doublecortin^{+} (DCX^{+}) progenitors) that in turn, generated short-lived differentiated cells (Neuronal nuclei-positive or NeuN^{+}). Exposure to anti-mitotic chemotherapy (cytarabine) or SHH inhibitor (vismodegib), resulted in residual tumors that were enriched for Sox2^{+} cells, indicating their role in tumor relapse. Targeting Sox2^{+} cells with mithramycin abrogated tumor growth (Figure 16 left).

In the second study using Sox2-GFP knock-in mice, it was demonstrated that Sox2-GFP^{+} cells drive the formation of squamous cell carcinoma (SCC), and that its expression is epigenetically activated during tumor initiation. Transplantation of these cells in immunodeficient mice at limiting dilution numbers, resulted in tumors that could be serially transplanted. In contrast, conditional deletion of Sox2 in SCC from the epidermis triggered tumor regression, indicating that rather than being a bystander stemness marker, Sox2 is critical for tumor initiating ability in skin SCCs (Figure 16 right) [309].

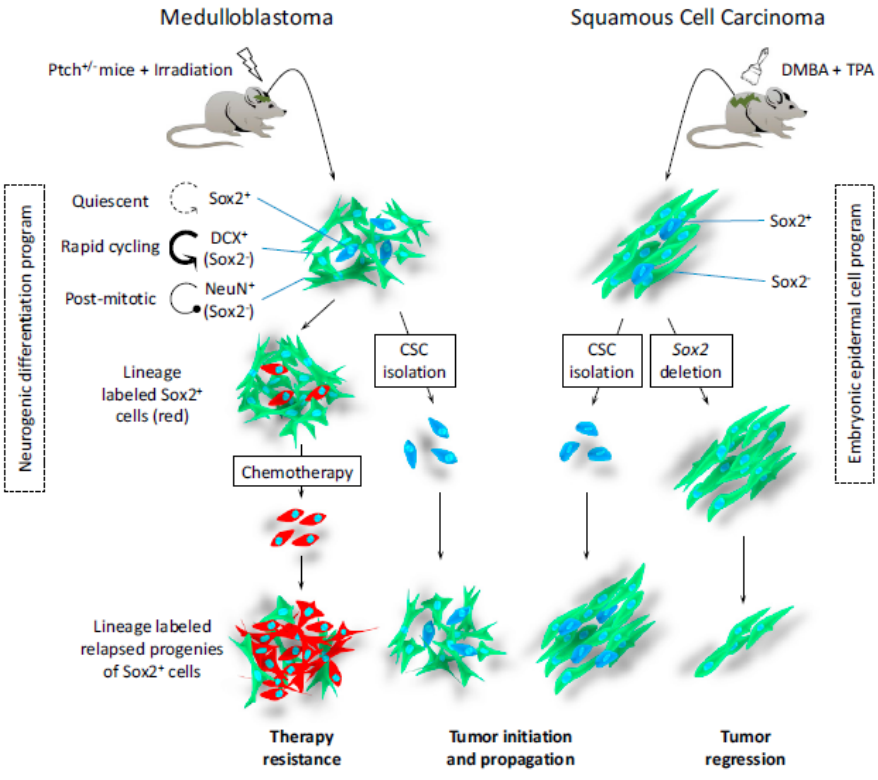

Figure 16. *Sox2 expression underlies CSC function.* In two distinct mouse cancer models, Sox2^{+} cells initiate tumor growth and spawn differentiated cell lineages that recapitulate primary tumor composition. In medulloblastoma, Sox2^{+} cells are quiescent and in lineage tracing experiments, were found to be chemotherapy-resistant, thus promoting tumor recurrence. Conditional deletion of Sox2 from the epidermis in SCC triggers tumor regression, as Sox2^{+} cells are responsible for tumor initiation and growth. Tumor propagation by the founder cells appears to recapitulate embryonic and stem cell differentiation programs that operate within normal tissues. *Tam & Huck-Hui, 2014.*

Other recent study using lineage tracing approaches and GFP-reporters, has identified a quiescent population in primary brain tumors expressing the nuclear receptor tailless (tlx), capable of self-renewing and generating all lineages of tumor cells. Targeting Tlx^+ cells led to loss of self-renewal, induction of cell-cycle arrest, cell death and neural differentiation [187].

Collectively, these studies point to the need for targeting predicted components of the self-renewal machinery. However, due to the fact that stemness-associated factors are likely shared between adult stem cells and CSCs, successful elimination of CSCs will require understanding the differences between them in order to minimize the impact of therapies on adult stem cell functions.

5.3 Oncogenic functions of SOX2: additional experimental evidence

Given the relevance of the SOX2 transcription factor in this thesis, it will be next discussed its importance in tumorigenesis, tumor progression and resistance to therapy, based on experimental data in several models.

First, recurrent amplification of the SOX2 gene (3q26.3 gene locus) has been found in several cancer types including glioblastoma, small-cell lung cancer (SCLC) and several forms of squamous cell carcinoma (SCC) [310]–[315]. Recent works on SOX2 have studied the co-amplification of this transcription factor with other genes; in lung squamous cell carcinoma (LSCC), PRKC1 is co-amplified with SOX2 and cooperate to engage tumorigenesis via activation of HH signaling [316]; in another study in non-small cell lung cancer (NSCLC), FISH analysis from 447 tissue samples showed that SOX2 amplification is associated with an increased gene copy number of the FGFR1 and PI3KCA genes [317].

A number of studies have related SOX2 activity with several hallmarks of cancer. Thus, it has been shown to promote cell proliferation (in breast, pancreatic and prostate cancer cells) [318]–[320], evasion of apoptotic signals (in prostate, gastric cancer cells and NSCLC cells) [320]–[322], and engaging invasion, migration and metastasis (in glioma, breast, prostate and ovarian cancer cells) [311], [323], [324].

SOX2 has been found to be involved in the regulation of cell proliferation in many cell models of different tumor types. In pancreatic cancer cells, SOX2

knock down induced cell cycle arrest, but not apoptosis, through transcriptional induction of $p21^{Cip1}$ and $p27^{Kip1}$, while overexpression promoted cell proliferation via cyclinD3 expression [319]. Similar results were obtained in gastric cancer cells models; decreased endogenous SOX2 transcriptional activity by introduction of a DNA-binding competitive truncated SOX2 protein, led to a decrease of cell proliferation by upregulation of $p21^{Cip1}$ and downregulation of an isoform of p63 (Δp63) [321]. In LSCC, SOX2 silencing impaired cell proliferation through upregulation of BMP4 [325]. Nevertheless, the role of SOX2 in cell proliferation has been controversial in colon and gastric cancer [321], [325], [326], indicating that SOX2 functions may depend on cellular context.

SOX2 has also been associated with evasion from apoptotic signals. In prostate cancer cells, in *in vitro* and also in *in vivo* xenograft experiments, it was shown that DU145 cells overexpressing SOX2 are more resistant to apoptosis by decreasing store-operated Ca^{2+} entry via inhibition of calcium release-activated calcium modulator 1 (ORAI1) expression (Figure 17) [320]. In contrast, SOX2 silencing in NSCLC cell lines increased apoptosis [322]. In gastric cell lines, after 48 h of inhibition of SOX2, caspase 3/7 assay revealed a two-fold increase of apoptotic cells compared to control levels [321].

Some studies have indicated the role of SOX2 as a novel regulator of cell invasion, migration and metastasis. In colorectal cancer cells, SOX2 expression has been involved in cellular migration and invasion *in vitro*, through regulation of MMP2 [327]. Likewise, this invasive phenotype was also observed in glioma cells, where siRNA downregulation of SOX2 produced a decrease in these properties, while overexpression of SOX2 in U87-MG cells promoted migratory and invasive properties [311].

In addition to the recent studies in medulloblastoma and SCC discussed above, evidence for SOX2 function in self-renewal maintenance has been provided in other cancer types, including breast, ovarian and prostate cancers, glioma, osteosarcoma, lung adenocarcinoma and NSCLC [311], [328]–[334]. For instance, in prostate CSCs, activation of EGFR signaling associated with SOX2 upregulation, produced an increase of their capacity to grow spheroids *in vitro* [330]. In NSCLC cells, siRNA-mediated knock down of SOX2 led to a dramatic reduction in spheroid formation, and similar results were obtained

upon inhibition of EGFR or Src kinase, that effectively diminished SOX2 levels in these cells by reduction of AKT signaling (Figure 17) [331]. Studies in melanoma cells have demonstrated that ectopic expression of SOX2 was sufficient to enhance their self-renewal capacity. Moreover, in this system it was shown by chromatin immunoprecipitation (ChIP) that HH signaling regulates SOX2 expression through GLI1 and GLI2, since these transcription factors were found associated with the proximal promoter region of the SOX2 gene in primary melanoma cells (Figure 17) [335].

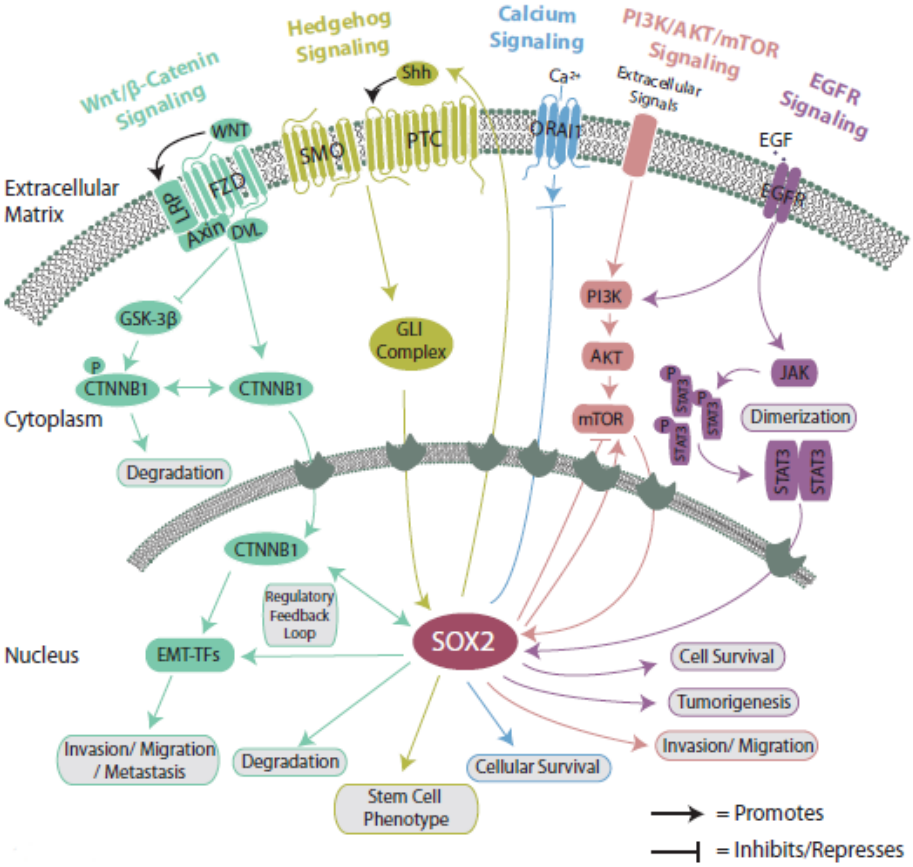

Figure 17. *Possible influence of SOX2 on oncogenic-related processes*. SOX2 seems to be an important regulator of cellular processes related to cancer. Some of these processes may include (but are not limited to) Wnt/β-catenin signaling, EMT and JAK/STAT3 signaling. In most cases, SOX2 functions downstream in the nucleus. SOX2 activity leads to further downstream effects and finally alters cellular properties such as cell proliferation, survival, invasion and/or metastasis. *Weina & Utikal 2014.*

In addition, other works studying Hedgehog acyltransferase (HHAT) in LSCC, have found that not only PRKCI and SOX2 are co-amplified and cooperate but also that SOX2 is phosphorylated by Protein Kinase Cι (PKCι). Phosphorylated SOX2 is then recruited and required for HHAT and thus promote the maintenance of a CSC phenotype in these cells [316].

Finally, since ATP binding cassette (ABC) transporters cause efflux of molecules across the cell membrane by using ATP and are highly expressed in both normal and CSCs [336], SOX2 function has also been related to therapy resistance in several cell models by putative regulation of members of the family

of ABC transporters. For instance, upon reduction of CSC population by SOX2 knock down, sensitivity to tamoxifen was restored in breast cancer cells [337]. In another study using glioma cell lines, it was demonstrated that inhibitor of differentiation 4 (ID4) promotes a CSC phenotype and drug resistance through inhibition of miR-9, a known negative regulator of SOX2. Subsequent increase of SOX2 levels resulted in drug resistance through induction of the ABC transporters ABCC3 and ABCC6 [338].

6. MOLECULAR BASIS OF COLORECTAL CANCER (CRC)

Next, as the bulk of the work in this thesis has been performed with colorectal cancer cell models, a brief discussion is presented about the etiology and the most relevant molecular events and deregulated pathways that drive CRC progression.

6.1 Etiology of CRC

As discussed above, the WHO estimates that CRC is the third most common cancer in men and the second in women, with more than 1,350,000 new cases in both sexes and almost 700,000 related-deaths worldwide in 2012 [178]. The etiological factors and genetic mechanisms underlying CRC development seem to be rather heterogeneous. Known factors that contribute to CRC development include dietary and lifestyle factors and inherited somatic mutations. Among the most relevant dietary and lifestyle risk factors identified, there are a diet rich in unsaturated fats and red meat, elevated energy intake, excessive alcohol consumption, and reduced physical activity [339]. In contrast, nonsteroidal anti-inflammatory drugs, estrogens, calcium, and perhaps some statins, protect against CRC [340].

In the past decades, significant work has been undertaken towards identifying the gene alterations that underlie the inherited predisposition to CRC, as well as the somatic alterations that lead to sporadic CRC [11]. These molecular alterations are basically related to increased or novel functions of oncogenes and loss-of-function of tumor suppressor genes. The former can result from specific point mutations or rearrangements that modify the gene structure and function, or from chromosome rearrangements that disrupt regulated gene expression. Currently, only somatic oncogene mutations have

been recurrently described in CRCs. In turn, tumor suppressor gene inactivation is a consequence of localized mutations, complete loss of the gene, or epigenetic alterations that alter gene expression. Likewise, most of tumor suppressor gene alterations in CRC are also somatic.

A relatively small but significant fraction of CRCs (15-30%), display a major hereditary component and about a quarter of these familial cases present a highly penetrant cancer syndrome that predisposes to CRC [341]. Most of these cases are attributable to the hereditary nonpolyposis colorectal cancer (HNPCC) syndromes, or are associated with familial adenomatous polyposis (FAP) and closely related variant syndromes (Table 1).

Syndrome	Common features	Gene defect(s)
FAP	Multiple adenomatous polyps (>100) and carcinomas of the colon and rectum; duodenal polyps and carcinomas; fundic gland polyps in the stomach; congenital hypertrophy of retinal pigment epithelium	*APC* (>90%)
Gardner syndrome	Same as FAP; also, desmoid tumors and mandibular osteomas	*APC*
Turcot's syndrome	Polyposis and colorectal cancer with brain tumors (medulloblastomas); colorectal cancer and brain tumors (glioblastoma)	*APC*
		MLH1, PMS2
Attenuated adenomatous polyposis coli	Fewer than 100 polyps, although marked variation in polyp number (from ~5 to >1,000 polyps) observed in mutation carriers within a single family	*APC* (predominantly 5′ mutations)
Hereditary nonpolyposis colorectal cancer	Colorectal cancer without extensive polyposis; other cancers include endometrial, ovarian and stomach cancer, and occasionally urothelial, hepatobiliary, and brain tumors	*MSH2*
		MLH1
		PMS2
		GTBP, MSH6
Peutz-Jeghers syndrome	Hamartomatous polyps throughout the GI tract; mucocutaneous pigmentation; increased risk of GI and non-GI cancers	*LKB1, STK11* (30–70%)
Cowden disease	Multiple hamartomas involving breast, thyroid, skin, central nervous system, and GI tract; increased risk of breast, uterus, and thyroid cancers; risk of GI cancer unclear	*PTEN* (85%)
Juvenile polyposis syndrome	Multiple hamartomatous/juvenile polyps with predominance in colon and stomach; variable increase in colorectal and stomach cancer risk; facial changes	*DPC4* (15%)
		BMPR1a (25%)
		PTEN (5%)
MYH-associated polyposis	Multiple adenomatous GI polyps, autosomal recessive basis; colon polyps often have somatic *KRAS* mutations	*MYH*

Table 1. *Genetics of inherited CRC syndromes. Fearon, 2011.*

Despite representing a small fraction of all CRC cases, the study of the molecular basis of these types of cancers has been crucial for understanding the factors and mechanisms that underlie sporadic CRC development. In either case, CRC follows the so-called adenoma-carcinoma sequence [11]; it begins as a benign adenomatous polyp that develops into a high-grade advanced adenoma that eventually progresses to an invasive carcinoma. Invasive carcinoma that remains confined within the colon anatomical structure is curable and classified as tumor-node-metastasis stages I and II. If untreated, it reaches the regional lymph nodes (stage III), and eventually metastasize to distant sites (primarily to the liver) being assigned stage IV [342]. Stages I and II

are curable by surgical removal of affected regions while about 75% of cases of stage III are curable with surgery and adjuvant chemotherapy [343]. Stage IV is usually considered incurable.

6.2 Genomic instability in CRC

6.2.1 Chromosomal instability

Chromosomal instability is the most common type of genomic instability in CRC. It produces a number of changes in chromosomal copy number and structure [344], and may lead to the physical loss of a wild type copy of a tumor suppressor gene, such as APC, TP53, SMAD3 or SMAD4. It has also been reported that there are several rare inactivating mutations of genes involved in chromosomal stability during replication [345]. In contrast to other cancer types, recurrent amplification, gene copy number gains or gene rearrangements are not frequently involved as CRC drivers [346]. Nevertheless, some genes that are found in altered copy number include MYC, HER2 or insulin growth factor 2 (IGF2). Recently, a new recurrent gene rearrangement has been described in CRC involving NAV2 and TCFL7L1 (chromosome 11 and 2, respectively) [347].

6.2.2 DNA-repair defects

A subset of CRC patients present inactivation of genes involved in mismatch-repair genes, most frequently MLH1 and MSH2. The inactivation can be inherited (e.g. in HNPCC) or acquired, as it is found in cancers with methylation-associated silencing of these mismatch-repair genes. In HNPCC patients, germ-line mutations in addition to subsequent somatic mutations in MLH1 and MSH2, lead to a high lifetime risk of development of CRC, with CRC evident by the age of 45 years on average [348]–[350]. Other germ-line mutations in mismatch-repair genes (e.g. MSH6), attenuates the predisposition to familial cancer [351]–[353]. In contrast, somatic inactivation of mismatch-repair genes occur in about 15% of patient with non-familial CRC, and within this group of patients, it has been reported that loss of mismatch-repair response is caused by biallelic methylation of the MLH1 promoter [354]–[356].

Usually, the loss of mismatch-repair response is tightly related to microsatellite instability. Microsatellite instability is produced by the inability to

repair strand slippage within repetitive DNA sequences elements that modify the size of mono or dinucleotide repeats (the so-called microsatellites), which are spread throughout the genome. CRCs characterized by mismatch-repair deficiency mainly arise in the proximal colon and they are associated with older age and female sex [357]. In these cases, there is a high incidence of inactivation of tumor suppressor genes such as TGFBR2 or BCL2-associated X protein (BAX), that harbor functional regions containing microsatellites.

Germ-line mutations in the base-excision repair gene mutY homologue (MYH), can also lead to CRC [352], [358]. Patients carrying two inactive germ-line MYH alleles develop a polyposis phenotype, with a risk of CRC of 100% by the age of 60 years [352].

Aberrant DNA methylation pattern in CpG islands in certain genes is another mechanism that leads to gene inactivation and CRC. It has been reported that somatic epigenetic silencing represses the expression of MLH1 in sporadic CRC with microsatellite instability [359].

It has also been observed that among the loci that can undergo aberrant methylation in CRC, there is a subset that appears to be aberrantly methylated as a group, and it is known as the CpG island methylator phenotype (CIMP) [359]. While the molecular mechanism underlying this phenotype is poorly understood, CIMP is observed in about 15% of CRCs and present in almost all cases with aberrant methylation of MLH1 [359]–[361]. An intermediate level of aberrant methylation in CIMP may define a subtype (CIMP2), which is thought to account for 30% of CIMP cases [362], [363].

6.3 Mutational inactivation of tumor-suppressor genes and associated deregulation of signaling pathways in CRC

6.3.1 Overview of the Wnt pathway. APC and Wnt/β-catenin signaling deregulation

Wnt proteins are secreted glycoproteins that interact with seven-pass transmembrane receptors of the Frizzled (Fzd) family and/or single-pass transmembrane co-receptors, such as lipoprotein receptor-related protein 5/6 (Lrp5/6), Ror2, and Ryk [364], [365]. The interaction between Wnt ligands and their receptors leads to the activation of several intracellular signaling cascades

in which crosstalk exists or act independently from each other. Depending on the activated pathway, Wnt signaling can regulate a variety of diverse processes, including cell proliferation, differentiation, migration, polarity and asymmetric cell division [366]. Wnt pathways can be classified in two distinct groups, namely, canonical and noncanonical Wnt signaling (Figure 18). Canonical Wnt signaling is often referred to as the Wnt/β-catenin pathway, and it involves β-catenin-dependent transcriptional activation. In contrast, noncanonical Wnt pathways, including the Wnt/Ca^{2+} and Wnt/JNK (c-Jun N-terminal kinase) pathways, are β-catenin-independent and usually trigger a variety of different intracellular signaling cascades [365], [367]–[369]. Re-

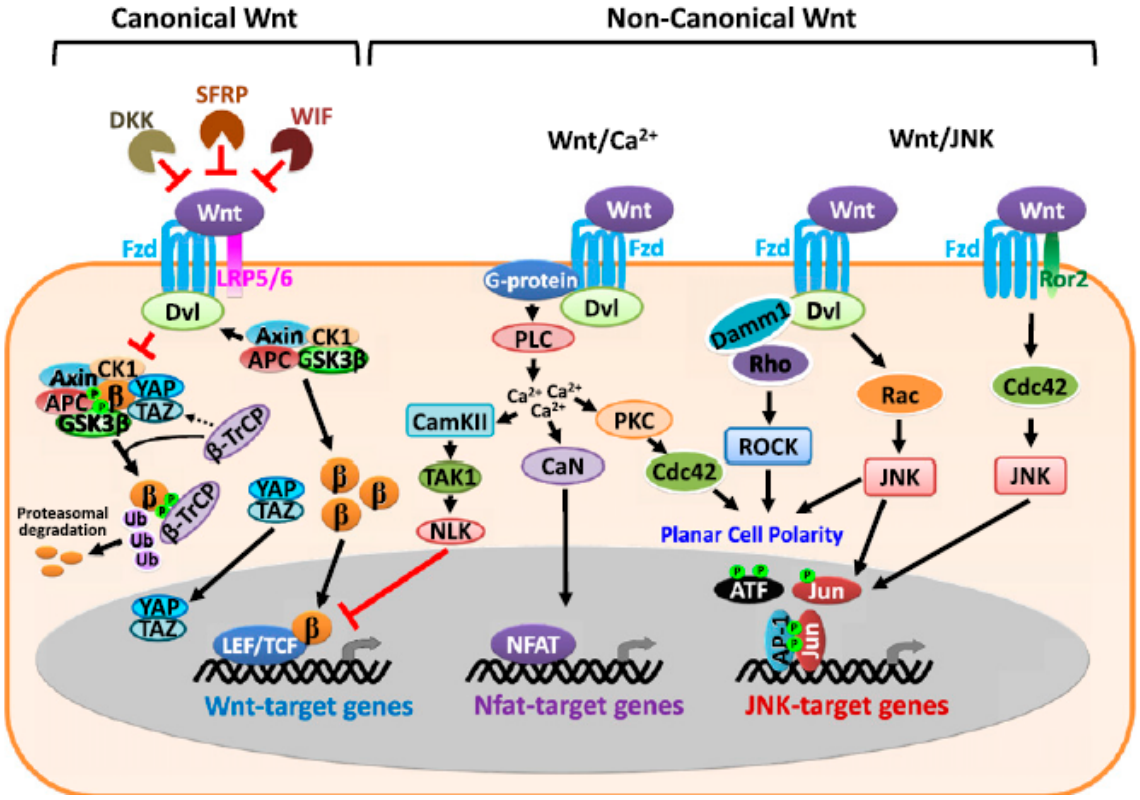

Figure 18. *Overview of the Wnt signaling pathways*. The illustration shows simplified canonical and noncanonical Wnt signaling pathways. In the absence of Wnt ligands, β-catenin is targeted by a destructive complex that phosphorylates it for degradation. This complex is composed of the core proteins Axin, CK1α, APC, and GSK3β. Like β-catenin. YAP/TAZ (regulated by the Hippo pathway) can also associate with this complex, which mediates recruitment of the β-TrCP E3 ubiquitin ligase, which in turn promotes the ubiquination of phosphorylated β-catenin for its degradation. Binding of Wnt ligands to Fzd and LRP5/6 activates the cytosolic protein Dvl, leading to the inhibition of the complex. Accumulation of stabilized β-catenin in the presence of TCF/LEF transcription factors results in their translocation into the nucleus to activate Wnt-responsive genes. This activation can be suppressed by TAK1-NLK, which is activated through noncanonical Wnt pathways. Also shown here are the Wnt/Ca^{2+} and Wnt/JNK pathways, both of which are β-catenin-independent. Binding of Wnt isoforms to either Fzd or other tyrosine kinase-like receptors (e.g. Ror2) can trigger multiple signaling cascades. Some of them result in activation of small GTPases Rho, Rac, and Cdc42, which regulate cytoskeleton rearrangement and planar cell polarity (PCP); some cascades trigger transcriptional events by activating transcription factors (e.g. NFAT or AP-1). *Lien & Fuchs, 2014.*

markably, canonical and noncanonical signaling are generally antagonistic or mutually exclusive.

Playing a central role in the canonical Wnt signaling pathway is the inhibition of glycogen synthase kinase 3β (GSK3β), which, when active, phosphorylates the N-terminus of any free-cytoplasmic β-catenin that does not take part in cell-cell adhesion [370], [371]. GSK3β forms a complex with Axin, a kinase for β-catenin called casein kinase 1α (CK1α) and adenomatous polyposis coli (APC) [372]–[374]; this so-called β-catenin destructive complex is also formed by the β-transducin repeat-containing protein (β-TrCP) E3 ligase, which promotes the ubiquitination of phosphorylated β-catenin and targets it for proteasomal degradation (Figure 18). Upon the interaction of canonical Wnt ligands to its receptors, the complex formed by Fzd and co-receptor LRP5/6, the Dishevelled (Dvl) protein is recruited, the destruction complex is inhibited, and β-catenin is stabilized in the cytoplasm [364], [375], [376].

In CRC, constitutive activation of the canonical Wnt signaling is regarded as a major initiating event and is due mainly to APC inactivation, which in turn, is the most common mutation in CRC. As described above, APC mutations give rise to familial adenomatous polyposis (FAP), an inherited disease in which almost 100% of carriers develop CRC by the age of 40 years. In sporadic CRC, mutations or deletions that inactivate both alleles of APC are present in a high percentage of patients (70-80% of cases) [377]. Mutations that provide resistance to degradation of β-catenin by the destruction complex also lead to constitutive Wnt/β-catenin signaling and form a small subset of CRC cases (5%) with wild-type APC [180], [377], [378]. In addition to these mutations, recently other mutations that may contribute to enhanced Wnt/β-catenin signaling have been described in CRC, such as loss-of-function mutations in AXIN1, AXIN2, SOX9 or FAM123B (negative regulators of Wnt/β-catenin signaling), oncogenic mutation of CDK8 or overexpression of the Wnt receptor gene FZD10 [347].

An intriguing intersection is the pathway involving the YAP/TAZ transcriptional regulators, which govern cell contact-regulated proliferation and organ size [379]. YAP/TAZ can be regulated by mechanosensing, a feature that leads to block the inhibitory kinase Hippo, and allows YAP/TAZ to translocate into the nucleus and function as transcriptional cofactors for the TEAD family of

DNA-binding proteins [374], [380]–[383]. Hippo signaling can also regulate β-catenin, and reciprocally, YAP/TAZ can inhibit Wnt/β-catenin signaling [380]–[382]. Interestingly, Wnt signaling can also induce YAP/TAZ stabilization and nuclear translocation in a manner independent of Hippo signaling. Unexpectedly, YAP/TAZ turns out to be essential for the recruitment of β-TrCP into β-catenin's destruction complex, which is active in the absence of Wnts (Figure 18). Upon Wnt stimulation, YAP/TAZ is released from the destruction complex, and this in turn promotes β-catenin stabilization and activation as well as YAP nuclear translocation [384].

Although β-catenin itself lacks a DNA-binding domain, it can directly promote gene expression upon nuclear translocation and interaction with transcriptional cofactors [385]. The activation of canonical Wnt signaling can be blocked by extracellular proteins, such as Dickkopf (DKK), secreted Frizzled-related protein (SFRP), and Wnt inhibitory factor (WIF); all of them inhibit Wnt ligand-receptor interactions (Figure 18) [386]–[388].

Wnt/β-catenin signaling directs cell fate and proliferation in a variety of cell types [366], [389]. The core of the pathway depends on the stability of β-catenin, a protein that plays a dual role in intercellular junction formation and transcriptional regulation [385], [390], [391]. β-catenin was first characterized as an adherens junction protein, which through its Armadillo repeats, binds to the core transmembrane adhesion protein E-cadherin and through its N-terminal domain, associates with α-catenin, a protein that binds actin and other actin regulators. In addition, stabilized cytoplasmic β-catenin can translocate into the nucleus where it binds to members of the TCF/LEF family of DNA-binding proteins and activate the expression of target genes [385], [392]–[396]. Similar to other high-mobility group (HMG) box-containing proteins, TCF/LEF proteins possess minimal transcriptional activity on their own and affect transcription by recruiting various binding cofactors, which in turn recruit chromatin modifiers to suppress or activate their target genes (Figure 19). The mammalian TCF/LEF family includes LEF1, TCF1, TCF3, and TCF4 proteins. *In vitro* studies with recombinant proteins revealed that these monomers recognize a core consensus sequence, the TCF/LEF DNA-binding motif [397], [398]. Like E-cadherin, TCF/LEFs contain a domain that can interact with Armadillo repeats,

which serve as the platform for β-catenin binding [399], [400]. β-catenin binds to TCF/LEFs through its Armadillo repeats and then uses the C-terminus to interact with other cofactors, including BCL9, the Drosophila Pygopus (Pygo) and chromatin modifiers such as CBP/p300 and BRG1, which ensure the efficient transcription of its target genes (Figure 19) [400]–[402]. In contrast, the ability of TCF/LEFs to repress genes has been attributed to transducin-like enhancer of split (TLE) proteins, which are mammalian homologs of the Drosophila Groucho transcriptional co-repressor [403]. Although TLE proteins are not exclusive of the Wnt pathway, they regulate canonical Wnt transcription by binding to TCF/LEF family members and act as adapters to recruit negative chromatin modifiers (Figure 19) [404]–[406]. It is known that in the absence of Wnt signaling, TCFs interact with a TLE tetramer [405]. In turn, this complex has been shown to recruit histone deacetylases (HDACs) to form a specialized repressive chromatin structure that prevents the inappropriate activation of TCF target genes (Figure 19) [406], [407].

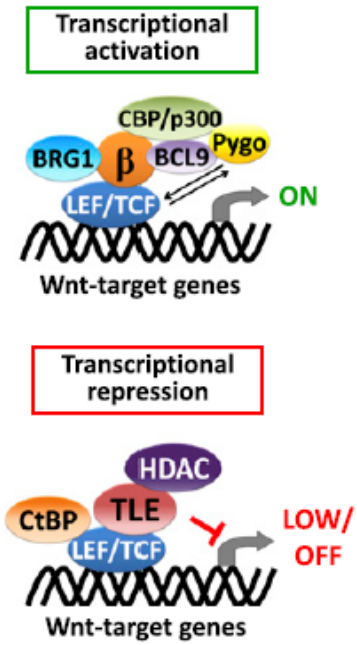

Figure 19. *Transcriptional regulation of canonical Wnt pathway.* The graph describes transcriptional activation or repression complex of TCF/LEF on Wnt target genes. In the activation mode, β-catenin interacts with a member of the TCF/LEF family of DNA-binding proteins. This conformation is thought to recruit histone modifiers CBP/p300 and BRG1 to promote an active chromatin structure for its target genes. Recruitment of BCL9 and Pygo enhance β-catenin transactivator activity, although the mechanism is not entirely known. Conversely, when nuclear β-catenin is absent, TCF3 and/or TCF4 proteins interact with transcriptional repressor Groucho/TLEs and in turn recruit histone deacetylase (HDAC) to yield an inactive chromatin state for the target genes. Another repressor, CtBP, has also been reported to interact with TCF4 for gene silencing. In general, whether TCF/LEF proteins act to activate or repress genes is determined by their binding partners and is dependent on cell context. *Modified from Lien & Fuchs, 2014.*

In APC or β-catenin mutant CRC cells, the abnormal stabilized β-catenin levels lead to inappropriate activation of TCF4 target genes [378], [394], [408]. The Wnt/TCF4-driven genetic program in colon cancer was first determined in 2002 [409], and consists of a core of about 80 TCF4 target genes (e.g. c-MYC, cyclinD1, CD44, c-MYB, BMP4, EphB2, EphB3 or claudin1 genes).

Interestingly, one of these TCF4 target genes is LGR5, which is differentially expressed in multipotent stem cells located at the bottom of the crypt [20], [410], although lineage tracing experiments have also demonstrate its expression in stem cells of other organs or tissues, including the stomach, pancreas, liver, kidney and mammary gland [411]–[416].

In intestinal stem cells, LGR5 is co-expressed with its close homologs LGR6 and LGR4, although the latter is also found in all other crypt cells [417]. These receptors belong to a subgroup of LGR receptors within the superfamily of Rhodopsin GPCRs, and are characterized by seven transmembrane domains connected by a hinge region with a large extracellular domain composed of seventeen leucin-rich repeat units. Their cognate ligands are the R-spondins (Rspo), known agonists of the Wnt pathway that are members of a family of proteins characterized by the presence of thrombospondin repeats. All four R-spondins have been found to bind with high affinity to the three LGRs. In intact cells, this interaction leads to increased phosphorylation of LRP5/6 and stabilization of β-catenin but does not appear to involve G-protein signaling [417], [418]. The proposed model by which LGRs-Rspo interaction enhances canonical Wnt signaling is by tethering and promoting the membrane clearance of two negative regulators of Fzd-LPR5/6 complexes; the Wnt target genes RNF43 and ZNFR3 (Figure 20). These proteins are single-pass transmembrane

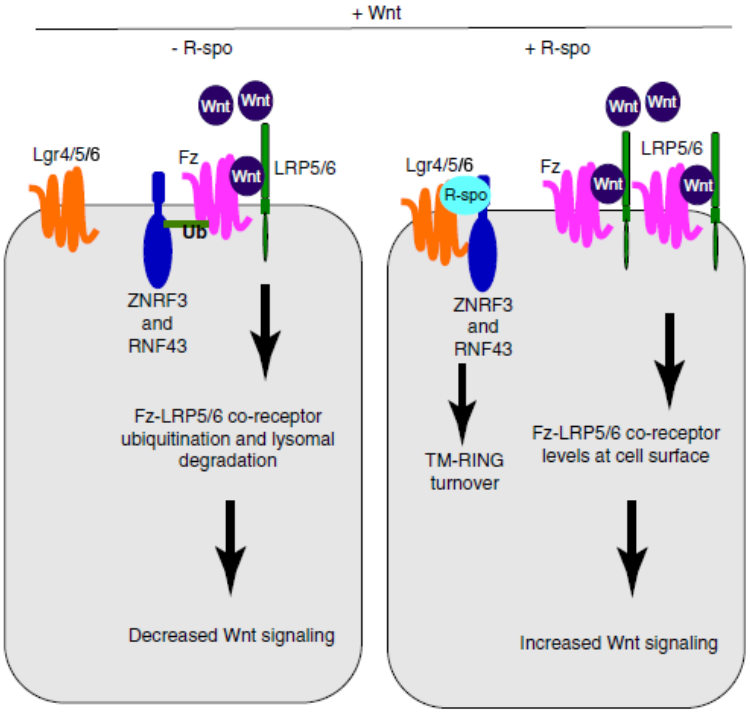

Figure 20. *Proposed model for R-spondin (Rspo), LGR4/5/6, and ZNRF3/RNF43 interactions in the modulation of Wnt/β-catenin signaling.* (Left graph) In the presence of Wnt ligand and the absence of Rspo, the transmembrane E3 ubiquitin ligase proteins RNF43 or ZNFR3 ubiquitinate Fzd-LRP5/6 co-receptor proteins, resulting in internalization and lysosomal degradation of the Fzd-LRP complex. In the presence of Rspo (right graph), RNF43/ZNFR3 proteins and LGRs are brought into a complex by Rspo, and the LGR-Rspo-RNF43/ZNFR3 complex is then targeted for lysosomal degradation in an E3 ligase-dependent manner. This potentiates Wnt/β-catenin signaling by reducing Fzd and LRP turnover. *Fearon & Spence, 2012.*

E3 ligases related to GRAIL (RNF128), and are expressed in $LGR5^+$-intestinal stem cells and enriched in CRC [419], [420]. In the absence of R-spondins, it is thought that RNF43 and ZNFR3 mediate multiubiquitination of Fzd receptors, resulting in the rapid endocytosis of Wnt receptors and their destruction in lysosomes [419], [420]. Since RNF43 and ZNRF3 are encoded by Wnt target genes, they are presumed to function as negative feedback regulators of canonical Wnt signaling (Figure 20).

In contrast to the widely studied canonical Wnt signaling, the knowledge of noncanonical Wnt pathways mainly comes from their ability to interfere with Wnt/β-catenin signaling. Depending on the cellular mediators, the noncanonical Wnt pathways are subdivided into two general groups: the Wnt/Ca^{2+} and JNK pathways (Figure 18). In the Wnt/Ca^{2+} pathway, the interaction of noncanonical Wnt ligands and receptors recruits Dvl and G proteins and leads to the activation of phospholipase C (PLC), thereby triggering intracellular calcium release. Induced calcium ion flux activates second messengers such as protein kinase C (PKC), calcium-calmodulin-dependent kinase II (CamKII), or the calcium-dependent phosphatase calcineurin (CaN) [367], [421]–[424]. An example of how noncanonical Wnt pathways antagonize canonical Wnt pathways can be illustrated by the signaling mediated by intracellular kinases proteins TGFβ-activated kinase 1 (TAK1)-activated and Nemo-like kinase (NLK), which are involved in the repression of activated Wnt/β-catenin signaling by blocking β-catenin-induced transcriptional activity [425]. In addition, CamKII can also antagonize the Wnt/β-catenin pathway [425], while activated CaN can dephosphorylate nuclear factor of activated T-cell (NFAT) transcription factors, which can then enter the nucleus and activate their target genes [426], [427]. In parallel, PKC members can activate the small GTPase Cdc42, which can in turn activate the planar cell polarity (PCP) pathway (Figure 18).

PCP can also be co-regulated by Rho and Rac GTPases, which are activated in Wnt/JNK noncanonical signaling. In contrast to calcium-regulated noncanonical signaling, Wnt/JNK signaling uses Ror2-dependent circuitry to activate downstream effectors of the activating protein-1 (AP-1) family of transcription factors [368], [369]. In intestinal homeostasis and cancer development, JNK/AP-1 has been shown to interplay with the Wnt/β-catenin

pathway through an interaction between c-JUN and TCF4 [428]. Genome-wide chromatin immunoprecipitation (ChIP) analyses for β-catenin in human colon cancer cells further reveal that β-catenin-enriched regions contain both AP-1 and TCF4 consensus motifs [429], highlighting the crosstalk between the Wnt pathways.

6.3.2 TGF-β tumor-suppressor pathway

Another important step in CRC progression is the mutational inactivation of TGF-β signaling and therefore the loss of its growth inhibitory effects (Figure 21). In about 30% of CRCs, somatic mutations inactivate TGFBR2 [430], [431]. In almost all cases of CRC with mismatch-repair defects, TGFBR2 is inactivated by a distinctive frameshift mutation in a polyadenine tract [432]. In about 50% of CRC cases with normal mismatch-repair function, missense mutations affecting the kinase domain of TGFBR2 and inactivating mutations or deletions in chromosome 18q (70% of CRC cases), affect downstream components such as SMAD transcription factor members (SMAD2-4), leading to TGF-β signaling abrogation [346], [430], [432], [433]. Mutations that lead to inactivation of TGF-β pathway overlap with the transition from adenoma to high-grade dysplasia or carcinoma [434].

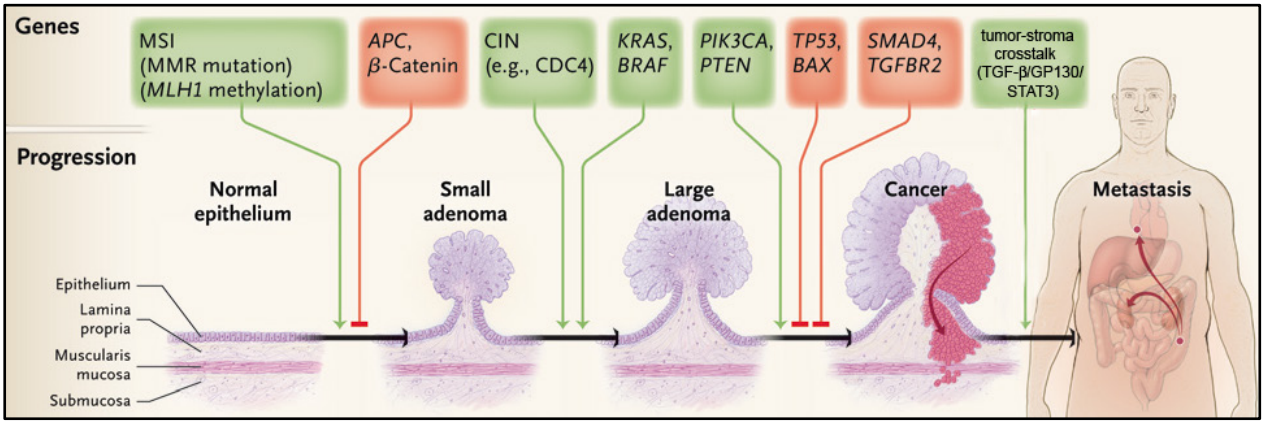

Figure 21. *Overview of the main molecular events that drive CRC progression.* In the progression of CRC, genetic alterations target the genes that are identified at the top of the graph. The microsatellite instability (MSI) pathway is initiated by mismatch-repair (MMR) gene mutation or by aberrant MLH1 methylation and is further associated with downstream mutations in TGFBR2 and BAX. Aberrant MLH1 methylation and BRAF mutation are each associated with the serrated adenoma pathway. A recent mechanism involving TGF-β-driven program in stromal cells (production of IL11) is important for metastasis initiation (activation of GP130/STAT3 signaling in cancer cells). *Modified from Markowitz & Bertagnolli, 2009.*

Paradoxically, despite this inactivation is displayed in most CRC cases, there is an elevated production of TGF-β in tumor cells. In advanced CRC, it has been demonstrated that tumor stromal cells, mainly CAFs, secrete IL11 in response to TGF-β. It has been established that a crosstalk between tumor cells and CAFs takes place, by which cancer cells activate GP130/STAT3 signaling in response to IL11, which in turn confers tumor cells with a survival advantage and promote organ colonization in mice [214]. This is one of the known mechanisms involved in promoting metastasis in CRC (Figure 21).

6.4 Activation of oncogene pathways in CRC

6.4.1 RAS, BRAF and MAPK pathway

Mutations in oncogenes RAS and BRAF activate the MAPK signaling pathway in about 40% and 10% of CRC patients (respectively) [435], [436], and contribute to enhance cell proliferation and survival. PI3K signaling is also regulated by RAS proteins.

The RAS small-G proteins act as molecular switches downstream of growth factor receptors. Its three members, KRAS, HRAS, and NRAS, are common targets of somatic mutations in a number of human cancers [435]. In CRC, RAS mutations affect mainly the KRAS gene and only a small subset of patients present activating mutations in NRAS [431]. In adenomatous polyps, the frequency of KRAS mutations positively correlates with the size and degree of dysplasia of the lesion, indicating that KRAS mutations contribute to colorectal adenoma development but are not required for adenoma initiation (Figure 21) [11]. Mutations and copy number alterations affecting members of the receptor tyrosine kinase family EGFR (e.g. EGFR, HER2 and HER3) are uncommon in CRC (about 5% of cases) [346], [347].

BRAF protein kinase is directly activated by RAS proteins and further activates the MAPK signaling cascade. Mutations in BRAF are found in 5-10% of CRC patients [437]. In contrast to RAS mutations, BRAF mutations are detectable even in small polyps [360], and more commonly in hyperplastic polyps, serrated adenomas and proximal colon cancers, particularly in those that display a CIMP phenotype [361].

6.4.2 Phosphatidylinositol 3-kinase (PI3K)/AKT signaling axis

Phosphatidylinositol-3,4,5-triphosphate (PIP_3) is a key second messenger that regulates several cellular processes (e.g. cell growth, proliferation and/or survival). Formation of PIP_3 from phosphatidylinositol- 4,5-biphosphate (PIP_2) at the cell membrane depends on the activity of the class I PI3Ks that are activated by upstream RTKs [438]. Somatic mutations in the PIK3CA gene which encodes the catalytic subunit (p110α) of PI3K class I or in the regulatory subunit (p85α), lead to aberrant activation of PI3K and are found in about 30% of CRCs (Figure 21) [439]. A less frequent somatic mutation in CRC (about 10% of cases), is the loss of PTEN protein phosphatase that mediates dephosphorylation of PIP_3 to PIP_2. Loss of PTEN is found in both KRAS mutant and wild-type tumors. Similar to PIK3CA activating mutations, PTEN inactivation may act to enhance KRAS downstream effects through activation of AKT by PIP_3 [440]. In turn, AKT acts on downstream antiapoptotic factors and the mTOR pathway, which integrates nutrient availability with cell growth. Other less frequent mutations involved in abnormal activation of PI3K/AKT signaling axis include amplifications of insulin receptor substrate 2 (IRS2), insulin growth factor 2 (IGF2) and co-amplification of downstream effectors such as AKT itself and PAK4 [347], [440].


Objectives

Messier object 20, The Trifid Nebula

The Trifid Nebula is an H II region located in the constellation of Sagittarius at about 5,000 light-years away from Earth. It was discovered by Charles Messier on June 5th of 1764. Its name means 'divided into three lobes'. The object is an unusual combination of an open cluster of stars; an emission nebula (the lower, red portion), a reflection nebula (the upper, blue portion) and a dark nebula (the apparent 'gaps' within the emission nebula that cause the trifurcated appearance). The close-up images show a dense cloud of dust and gas, which is a stellar nursery full of embryonic stars, located 8 light-years away from the nebula's central star…

1. Explore the possible correlation of SOX2 expression with drug resistance in cell lines derived from distinct tumor types.

2. Phenotypic characterization, study of cell signaling involved and impact on self-renewal and tumorigenicity due to modulation of SOX2 levels in a colorectal cancer cell model of divergent tumor aggressiveness.

Material and Methods

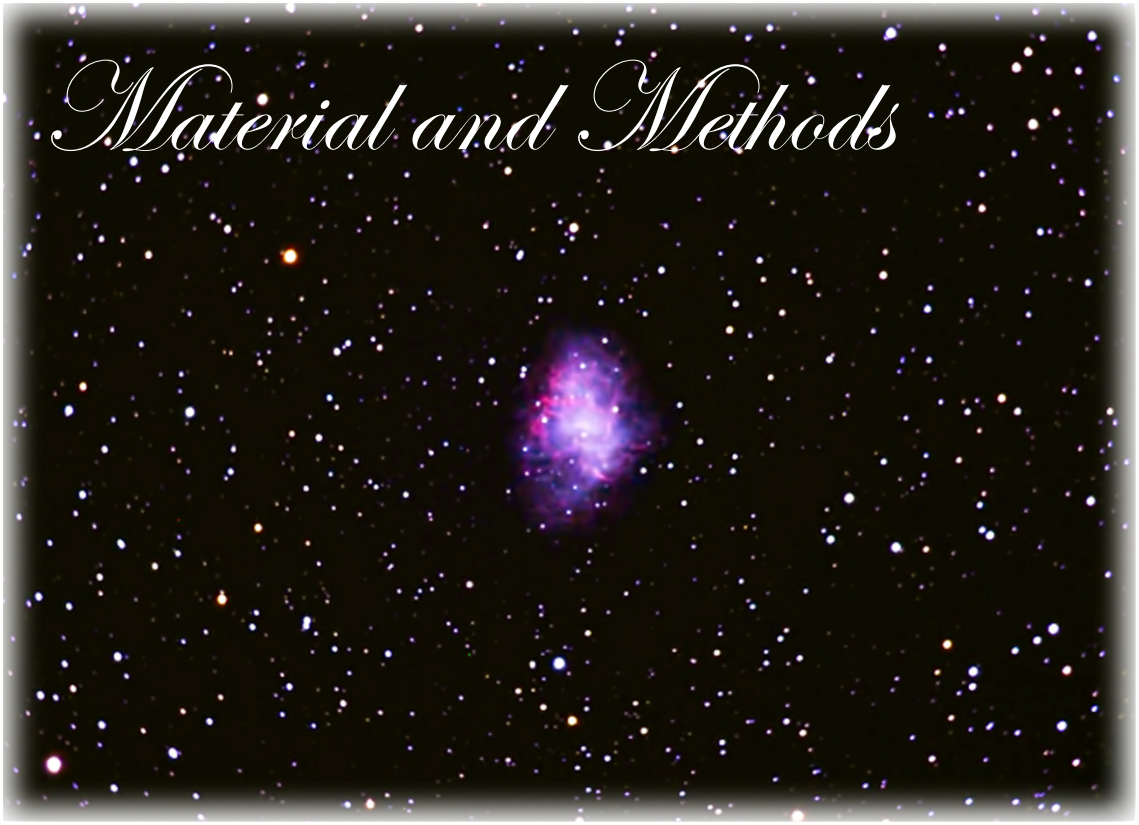

Messier object 1, The Crab Nebula

The Crab Nebula (catalog designations M1 and NGC1952) is a supernova remnant and pulsar wind nebula in the constellation of Taurus. It is located at the Perseus Arm of the Milky Way at about 6,300 light-years away from Earth. Corresponding to a bright supernova recorded by Chinese and Arab astronomers in July 5th of 1054 that was observable around 22 months even in daylight, the nebula was rediscovered in 1731 by John Bevis and soon Charles Messier adopted it as the first celestial noncometary object of his catalog. It has a diameter of 11 light-years and expands at a rate of about 1,500 km/s. At the center of the nebula lies the Crab Pulsar (PSR0531+121), a neutron star 28–30 km across with a spin rate of 30.2 times per second, which emits pulses of radiation…

Cell lines

All cell lines in this study were originally obtained from the ATCC (Manassas, Virginia, USA) and grown at 37°C in a 5% CO_2 atmosphere and humidity to saturation in complete RMPI 1640 or DMEM media (as indicated in Table 1), supplemented with 1x non-essential aminoacids, 2 mM L-glutamine, 100 U/mL penicillin, 100 µg/mL streptomycin, 1 mM sodium pyruvate and 10% fetal bovine serum (FBS). Supplements, medium and FBS were purchased from PAA (Cölbe, Germany).

Table 1. Cell lines used in this study

Name	Origin (human)	Culture medium
HeLa	Cervical Adenocarcinoma	DMEM
HEK293T	Transfromed embrionyc cells from kidney	DMEM
Phoenix	HEK293T transfected to express Moloney Murine Leukemia viral packaging proteins	DMEM
PC-3	Prostate adenocarcinoma, grade IV, derived from bone metastasis	RPMI
PC-3/Mc	Bone metastasis of prostate adenocarcinoma. Clone selected *in vivo* for its high metastatic potential	RPMI
PC-3/S	Bone metastasis of prostate adenocarcinoma. Clone isolated from parental cell line PC-3 by limiting dilution	RPMI
DU-145	Prostate adenocarcinoma isolated from brain metastasis	DMEM
MCF-7	Breast adenocarcinoma isolated from pleural metastasis	DMEM
MCF10CA1A	Mammary gland from fybrocistic disease	DMEM
MCF10CA1H	Mammary gland from fybrocistic disease	DMEM
MDA-MB-231	Breast adenocarcinoma isolated from pleural metastasis	DMEM
MDA-MB-468	Breast adenocarcinoma isolated from pleural metastasis	DMEM
T-47D	Breast adenocarcinoma isolated from pleural metastasis	DMEM
HT29-M6	Colorectal adenocarcinoma	DMEM
HCT116 40.16	Colorectal adenocarcinoma, clone of HCT 116 with p21+/+ & p53+/+	DMEM
HCT116 379.2	Colorectal adenocarcinoma, clone of HCT 116 p21+/+ & p53-/-	DMEM
HCT116 clone 4	Colorectal adenocarcinoma, clone of HCT 116 p53+/+ & p21-/-	DMEM
SW620	Colorectal adenocarcinoma (Dukes' type C) isolated from lymph node metastasis	RPMI
SW480	Colorectal adenocarcinoma (Dukes' type B)	RPMI

CAPAN-1	Pancreatic adenocarcinoma isolated from liver metastasis	DMEM
PANC-1	Invasive pancreatic adenocarcinoma. Metastasis in peripancreatic lymph node.	DMEM
SK-N-SH	Neuroblastoma, isolated from bone marrow metastasis	DMEM
U87-MG	Glioblastoma (astrocytoma), grade IV	DMEM
HAL-8	Lung adenocarcinoma	RPMI
HAL-24	Lung adenocarcinoma	RPMI

Cell proliferation analysis and treatments

Cell proliferation assays were performed in 96-well plates (Corning) by seeding $5x10^3$ cells/well on day 0 in complete medium. Cell numbers were determined daily for up to 6 days. To assess cell proliferation or viability, the MTT colorimetric assay (Sigma-Aldrich) was used. This assay is based on the capacity of NAD(P)H-dependent cellular oxidoreductase enzymes for reducing the tetrazolium dye MTT [3-(4,5-dimethylthiazol-2-yl)-2,5-diphenyltetrazolium bromide] to its insoluble compound formazan, which has a purple color. Absorbance was measured at 570 nm in a microplate spectrophotometer (Biotek Instruments). Cell numbers were extrapolated from standard curves drawn from MTT absorbance values for known numbers of cells, processed in parallel for each cell line tested. All conditions were assayed in sextuplicates.

For cell viability assays, cells were seeded, allowed to attach, and one of the following drugs was added to the wells: 5-fluorouracil, cisplatin, doxorubicin and etoposide (all from Sigma-Aldrich), at the indicated concentrations. Absorbance was measured after 72 h of drug treatment, following the described protocol used for assessing cell proliferation.

Cell cycle analysis

For standard cell cycle analysis, cells ($2x10^5$) were seeded in 6-well plates (triplicates) and allowed to attach and grow for 48 h under standard culture conditions, detached with Trypsin-EDTA-1%BSA, washed twice and resuspended in PBS, then fixed by dropwise addition of cold 70% ethanol and kept at -20ºC for 1 hour. Subsequently, the cell suspension was washed in PBS-1%BSA-EDTA and incubated with RNase A (200 μg/mL, Sigma-Aldrich) and propidium iodide (40 μg/mL, Sigma-Aldrich) in an orbital shaker at 225

r.p.m and RT during 2 h. Cell DNA content was quantified by flow cytometry in a CouLter XL cytometer (Beckman) and cell cycle analysis performed with the Multicycle program coupled to the flow cytometer equipment.

To analyze cell cycle profiles after cell cycle synchronization, cells were seeded and allowed to attach overnight. The double thymidine protocol was used for blocking cells in G1/S. Briefly, cells were incubated for 16 h in complete medium supplemented with 2 mM thymidine (Sigma-Aldrich), the medium was removed and cells were washed with fresh medium and re-incubated with fresh medium supplemented with 24 μM deoxycytidine (Sigma-Aldrich). After 9 h, the medium was removed and replaced with fresh medium supplemented with 2 mM thymidine. Cells were released from the G1/S block by removing the thymidine-supplemented medium, washing with fresh medium and replacing it with fresh medium supplementing with 24 μM deoxycytidine. Samples were collected and analyzed for their cell cycle profiles at 1 h intervals for a total of 11 h. To block cells in mitosis, 24 h after plating in standard culture conditions, cells were treated with 0.2 μg/mL nocodazole (Sigma-Aldrich) in complete medium for 16 h. Subsequently, the cells were collected and analyzed for their cell cycle profiles as described above.

Spheroid growth assay

Cells ($5x10^3$ cells/mL) were seeded in 6 or 24-well ultralow-attachment plates (Corning), in a mixture of 0.22 μm-filtered HAM F-12: DMEM (1:1) medium (PAA) supplemented with 1x non-essential aminoacids, 2 mM L-glutamine, 100 U/mL penicillin, 100 μg/mL strepromycin, 1x B-27 supplement and 20 ng/mL bFGF (Invitrogen, Life Technologies), 20 ng/mL EGF (Sigma-Aldrich), 50 μg/mL insulin (Sigma-Aldrich) and 0.2 % methyl cellulose (Sigma-Aldrich), and allowed to grow for 5-7 days. For serial transfer experiments, spheroids were collected and resuspended in PBS, centrifuged at 600 r.p.m. for 5 min, and the medium replaced. Subsequently, cells were reseeded as described above and allowed to grow for 5-7 days. At the end of the culture period, the plates were scanned (HP scanjet G4010) at 2,500 dpi and the spheroid area measured with the ImageJ software. All experimental conditions were done in triplicate.

In vitro invasiveness assay

Invasiveness assays were performed in 24 or 96-well Boyden chambers (Transwell, Corning) with 8-µm pore diameter membranes. 24 h before seeding the cells, a layer of Matrigel growth factors reduced (BD Biosciences, Clontech) diluted to 410 µg/mL in PBS was added onto the membrane and allowed to polymerize overnight at 37 ºC. Cells were serum-starved 24 h before the assay, detached and resuspended with RMPI 1640, 1%BSA, 0.5% FBS and then seeded onto the upper chamber of Matrigel-coated Transwell membranes ($6.5x10^4$ cells or $1.5x10^5$ cells in each 96 or 24-well Transwell insert, respectively). Lower chambers were filled with growth medium with 0.5% or 10% FBS. After 24 h, cells that had migrated to the lower side of the membrane and to the bottom of the well were collected by detachment with trypsin-EDTA. Collected cells were washed with PBS and propidium iodide added (40 µg/mL). Both living and dead invading cells were scored by means of flow cytometry in a CouLter XL cytometer (Beckman). Each experimental condition was done in quadruplicate.

In vitro cell migration assay

Cell migration assays were performed in 96-well Transwell inserts with 8-µm pore diameter membranes. Cells were serum-starved 24 h before the assay, detached and resuspended in RMPI 1640, 1%BSA, 0.5% FBS and then seeded onto the upper chambers of the Transwell inserts ($6.5x10^4$ cells). Lower chambers were filled with growth medium containing 10% FBS. After 24 h, cells that had migrated to the bottom chambers and the lower side of the membranes were collected by detachment with trypsin-EDTA. Collected cells were washed with PBS and propidium iodide was added (40 µg/mL). Both living and dead migrating cells were scored by means of flow cytometry in a CouLter XL cytometer (Beckman). Each experiment was done in quadruplicate.

Transient transfections and luciferase reporter assays

For β-catenin/TCF/LEF transcriptional activity determination, we performed a reporter assay based on constructs expressing firefly luciferase under the control of three copies of the optimal TCF motif CCTTTGATC repeated in tandem (TOPFlash) or three copies in tandem of the mutant motif

CCTTTGGCC (FOPFlash) [378]. These plasmids and pRL-TK were a gift from Dr. Rosanna Paciucci (VHIR, Barcelona). In addition, for assessing levels of p27 transcription, construct pGL3-p27PF, expressing firefly luciferase under the control of 2.8 kb of the p27 promoter [441], was used. This construct was kindly provided by Dr. Toshiyuki Sakai (KPUM, Kyoto, Japan) (see Table 3). In both determinations, transfections were performed using Metafectene (Biosintex) or XtremeGene9 (Roche) as vehicles in a 3:1 ratio (μL vehicle: μg DNA) according to the manufacturer's instructions. Cells ($2x10^5$) were seeded in 6-well plates and allowed to attach. To determine β-catenin/TCF transcriptional activity, cells were co-transfected overnight with 2 μg of the β-catenin TOPflash or FOPflash reporter constructs together with 0.2 μg of plasmid pRL-TK for the constitutive expression of *Renilla* luciferase. To determine p27 transcriptional activity, the same amount of DNA was co-transfected overnight with pGL3-p27PF or pGL3-basic plasmids, together with pRL-TK. After 24 h, cell lysates were processed for the Dual luciferase assay (Promega) and measured in an OrionII Microplate Luminometer (Berthold Detection Systems). In both series of determinations, *Renilla* luciferase activity was used as a transcription efficiency control and to normalize firefly luciferase activities. In the β-catenin/TCF transcription activity determinations, *Renilla*-normalized values for FOPflash (mutant β-catenin/TCF binding sites) firefly luciferase values were subtracted from normalized TOPflash (wild-type β-catenin/TCF sites) values to yield β-catenin/TCF-specific signals. All experiments were performed in triplicates at least 3 times.

Measurement of intracellular ROS Levels

Quantification of intracellular ROS levels was performed by adapting the protocol described in [442]. Briefly, $1.5x10^5$ cells were seeded in 6-well plates and allowed to grow for 48 h until reaching 70-80% confluence in standard culture conditions. At this point, cells were washed twice with PBS and afterwards, prewarmed (37 ºC) incubation buffer containing 5.5 mM glucose in PBS with 5 μM 2',7'-dichlorodihydrofluorescein diacetate (H_2DCFDA, Sigma-Aldrich) was added to the wells for 15 min and the plates were returned to the incubator. Subsequently, the incubation buffer was removed and replaced with complete medium and cells were incubated again for 15 min at 37 ºC. Finally, cells were rinsed with PBS, trypsinized, and resuspended with PBS containing

H_2DCFDA (50 µM) and propidium iodide (20 µg/mL). Samples were covered with aluminium foil and the green fluorescence intensity of oxidized H_2DCFDA in living cells (gate of $5x10^3$ cells), reflecting ROS generation, was analyzed by FACS using a Cytomics FC500 instrument (Beckamn Coulter). As a positive control, pretreatment for 5 min with 10.1 µM H_2O_2 was done and processed in parallel. Each condition was assayed in triplicate.

Determination of apoptosis by flow cytometry

Cells ($1.5x10^5$) were seeded in each of 6-well plates in triplicate in complete medium. After 48h, cells were trypsinized and resuspended in a buffer containing annexin V-Alexa fluor 488 and propidium iodide for 15 min at room temperature (Annexin V Conjugates for Apoptosis Detection kit, Molecular Probes) following the manufacturer's instructions. After incubation, shifts in fluorescence intensity of dead or permeabilized cells with propidium iodide and apoptotic cells labeled with annexin V-Alexa fluor 488 were analyzed and quantified by flow cytometry and compared to fluorescence levels in control conditions (Gallios instrument, Beckman Coulter).

Immunoblotting

Cell lysates were prepared in 80 mM Tris-HCl pH 6.8, 2% SDS buffer and sonicated (Branson digital sonicator) in two cycles of 20 s and 10% amplitude with a conic tip. Protein from the sonicated samples was quantified by the Lowry method (BioRad) and boiled in Laemmli buffer (60 mM Tris-Cl pH 6.8, 2% SDS, 10% glycerol, 5% β-mercaptoethanol, 0.01% bromophenol blue). Samples (30 to 100 µg) were electrophoresed by SDS-PAGE and transferred to PVDF membranes (Immobilon-FL, Millipore). The efficiency of the electrophoretic transfer was monitored visually by complete transfer of pre-stained protein molecular weight standards (BioRad) electrophoresed in parallel with the samples, and by Ponceau Red protein staining of the membranes after transfer. Membranes were washed briefly with PBS and blocked for 1 h in an orbital shaker at room temperature with either Odyssey blocking buffer (Li-COR Biosciencies) or PBS/5% powder skim milk/0.05% Tween-20 (chemiluminescence blocking buffer) and incubated o/n at 4 ºC with primary antibodies diluted in blocking buffer (see Table 2). After incubations,

membranes were washed 3x with PBS (15 min) and incubated with secondary antibodies diluted in blocking buffer for 1 h. Membranes were washed 3x with PBS and reactions detected either by chemoluminescence or by fluorescence. In the case of chemoluminescence, the detection was done with 1/2000 dilution in blocking buffer of secondary antibodies conjugated with horseradish peroxidase (Pharmacia) and revealed with ECL (Amersham Life Sciences) substrate using X-ray films (Kodak) and the signal was quantified by scanning the film and analyzed with the imageJ software. In the case of fluorescence, the detection was done with 1/10000 dilution in blocking buffer of fluorescent dye-conjugated secondary antibodies and the membranes were scanned with an Odyssey infrared imaging system (Li-COR Biosciences) and quantified with the software provided by the manufacturer. Sample loadings were normalized against actin, tubulin levels or Ponceau-S staining of the membrane.

Table 2. Primary and secondary antibodies used in this study

Primary antibodies				
protein	**source**	**Brand / clone**	**wb**	**ICC**
SOX2	rabbit	Cell Signalling Technologies D6D9 clone	1/500	1/50
β-catenin	mouse	BD Transduction laboratories clone 14	1/500	1/50
E-cadherin	mouse	BD Transduction laboratories clone 36	1/8000	1/500
Fibronectin	goat	Sigma-Aldrich, polyclonal	1/500	-
Cyclin A	rabbit	Santa Cruz Biotechnology H-432 clone	1/500	1/50
Cyclin B1	mouse	BD Transduction laboratories GNS-11	1/250	1/50
Cyclin D1	mouse	Santa Cruz Biotechnology DCS-6 clone	1/250	1/50
Caspase 3	mouse	Cell Signalling Technologies 3G2 clone	1/500	-
cleaved caspase 3	rabbit	Cell Signalling Technologies 5A1E clone	1/500	-
P-H2AX	rabbit	Cell Signalling Technologies 20E3 clone	1/1000	1/200
P-H2AX	mouse	Upstate, clone JBW301	-	1/5000
53BP1	mouse	BD Transduction laboratories clone 19	-	1/5000
p21	mouse	BD Pharmingen SXM30	1/500	1/50
p21	mouse	Millipore EA10 clone	1/500	-
p27	mouse	BD Pharmingen clone 57	1/500	1/50
Actin	goat	Santa Cruz Biotechnology clone I-19	1/2000	1/200
tubulin	mouse	Sigma-Aldrich clone tub 2.1	1/2000	1/200

Secondary antibodies				
name	**source**	**brand**	**wb**	**ICC**
mouse alexa 488	goat	Invitrogen	-	1/600
rabbit alexa 488	goat	Invitrogen	-	1/600
mouse alexa 555	goat	Invitrogen	-	1/600
rabbit alexa 555	goat	Invitrogen	-	1/600
anti mouse (odyssey 800)	goat	Li-COR	1/10000	-
anti rabbit (odyssey 700)	goat	Li-COR	1/10000	-
anti goat (odyssey 700)	donkey	Li-COR	1/10000	-
anti-mouse HRP	goat	Pharmacia	1/2000	-
anti-rabbit HRP	goat	Pharmacia	1/2000	-
anti-goat-HRP	donkey	Pharmacia	1/2000	-

Immunocytochemistry and nuclear fluorescent foci determinations

Sterile coverslips placed at the bottom of 24-well plates were seeded with $8x10^4$ cells, allowed to attach for 48 h, washed with PBS and fixed for 1 h with methanol at -20 ºC. After fixation, samples were rinsed with acetone, then 5 times with PBS, blocked for 30 min with blocking buffer (5% normal goat serum, 0.5% Triton X-100 in PBS) and incubated for 2 h at room temperature with primary antibodies (see Table 2). This step was followed by PBS washes and 1 h incubation with appropriate Alexa-conjugated secondary antibodies (Invitrogen) (Table 2) and DAPI (1/5000, Sigma-Aldrich). After 3 washes with PBS, coverslips were mounted on slides with Mowiol 4-88, images captured with a Zeiss LSM780 confocal microscope and processed with Zen software (black edition 2011, Zeiss). For nuclear foci counting (53BP1 or P-H.2AX foci) as well as determination of levels of fluorescence (p21), the Volocity software (Perkin Elmer Corporation) was used.

Production and transduction of retroviral particles

Construct pRetroSuper-shp21B and control plasmid pRetroSuper-puro were kindly provided by Dr. Javier León (IBBTEC-CSIC, Santander) and pMSVC-Flag-hSOX2 (human) was a gift from Dr. Ángel Raya (IBEC, Barcelona). Control plasmid pMSVC-empty was obtained from the latter after removing the Flag-hSOX2 insert by double digestion with EcoRI and ClaI, followed by Klenow filling and vector religation. The retrovirus packaging cell line Phoenix was co-transfected for 12 h with these DNAs and pVSV-G (Clontech) using Metafectene or XtremeGene-9 as vehicles. Supernatants were

collected during the following 48 h and filtered through 0.45 µm methylcellulose filters (Millipore). Target cells were infected using supernatants (or dilutions with fresh medium) supplemented with 4 µg/mL hexadimethrine bromide (polybrene), at 37 ºC for 24 h. Infected cells were allowed to recover in fresh medium for 24-48 h. If necessary, cells with integrated retroviral sequences were selected for 5 days in medium supplemented with 3 µg/mL puromycin (Biomol).

Production and transduction of lentiviral particles

Table 3 lists the lentiviral constructs for stable gene silencing, overexpression or reporter plasmids used in this thesis. The lentivirus packaging cell line HEK293T was co-transfected for 12 h with these DNAs together with pCMVdeltaR8.91 and pVSV-G using Metafectene or XtremeGene-9 as vehicles. Supernatants were collected for the following 48 h and filtered through 0.45 µm methylcellulose filters. Target cells were infected and selected using supernatants as above.

Table3. Plasmids used in this study

Control plasmids	backbone plasmid / Lenti/Retroviral vector (L/R)	insert
pLK.0-puro SHC002	TRC1/1.5 (L)	CCGG**CAACAAGATGAAGAGCACCAA**CTC GAG**TTGGTGCTCTTCATCTTGTTG**TTTTT
pRetroSuper-puro	pSuperRetro (R)	---
pMSVC-empty	pMSVC (R)	---
Gene overexpression	**retroviral vector**	**insert**
SOX2	pMSVC-flag-hSOX2	mature mRNA + flag (1kb)

Gene knock down	Backbone plasmid + Lenti/Retroviral vector (L/R)	TRC Clone / ID	Target sequence
SOX2	pLK.0 (L)	TRCN0000003252	GAAGAAGGATAAGTACACGCT
		TRCN0000003253	**CTGCCGAGAATCCATGTATAT**
		TRCN0000010772	CAGCTCGCAGACCTACATGAA
LGR5	pLK.0 (L)	TRCN0000011585	CCATCCAATTTGTTGGGAGAT
		TRCN0000011586	**CCATAGCAGTTCTGGCACTTA**
		TRCN0000011587	CCGTCTGCAATCAGTTACCTA

LGR5	pLK.0 (L)	TRCN0000011588	CTTACATTTATCAGTCCTGAA
		TRCN0000011589	GCTCTACTGCAATTTGGACAA
CDKN1B (p27)	pLK.0 (L)	TRCN0000039928	GTAGGATAAGTGAAATGGATA
		TRCN0000039929	CCGACGATTCTTCTACTCAAA
		TRCN0000039930	**GCGCAAGTGGAATTTCGATTT**
		TRCN0000039931	CCTCAGAAGACGTCAAACGTA
		TRCN0000039932	CAGCGCAAGTGGAATTTCGAT
CTNNB1 (β-catenin)	pLK.0 (L)	TRCN0000003843	AGGTGCTATCTGTCTGCTCTA
		TRCN0000003844	**CGCATGGAAGAAATAGTTGAA**
		TRCN0000003845	GCTTGGAATGAGACTGCTGAT
		TRCN0000003846	CCTTTAGCTGTATTGTCTGAA
CDKN1A (p21)	pRetroSuper-puro (R)	shp21B	**AACACCTCCTCATGTACAT**

Reporter plasmids	Stable/transient expression	Insert and / or reporter gene/s
pCMV-GFP/luc	Stable (lentiviral vector)	GFP & firefly luciferase (for *in vivo* experiments)
pL-SIN-EF1α-eGFP	Stable (lentiviral vector)	EF1α promoter / enhanced GFP
pL-SIN-EOS-C3^{+}-eIP	Stable (lentiviral vector)	Early Transposon promoter and OCT-4 and SOX2 enhancers (3 repetitions in tandem) / enhanced GFP
pGL3-basic	Transient expression	firefly luciferase
pGL3-p27PF	Transient expression	p27 promoter (2.8 Kb) / firefly luciferase
FOPflash	Transient expression	mutated TCF binding site / firefly luciferase
TOPflash	Transient expression	TCF binding site / firefly luciferase
pTK-Renilla	Transient expression	renilla luciferase

RNA isolation and Reverse transcription

Cells were lysed when confluence reached approximately 70-80% and RNA was isolated with TRIzol (Invitrogen), Rneasy Kit (Qiagen) or High Pure RNA Isolation Kit (Roche), with an optional genomic DNA removal step with DNase (Qiagen or Roche, respectively). Total RNA quality assessment was determined using a nanodrop instrument (Thermo Scientific). Retro-transcription to cDNA was performed with 1 µg of total RNA with the High-Capacity cDNA Reverse Transcription Kit (Applied Biosystems) using a bench thermocycler (Biorad), following manufacturer's instructions.

Real time-quantitative PCR (RT-qPCR)

Quantitative PCR assays were performed in a LightCycler 480 instrument (Roche Diagnostics) and analyzed with the LightCycler 480 Software release 1.5.0. Either gene-specific TaqMan assays (for RNA18S1 and SOX2) (Life technologies-Gene expression assays, refs.Hs99999901_s1 for RNA18S1 and Hs01053049_s1 for SOX2) or the Universal Probe Library system (UPL, Roche) were used (Table 4), following the specific running conditions recommended in each case. In the case of the UPL system, primer design was performed using the *Universal Probe Library Assay Design Center* (Roche website) selecting all the isoforms available for each gene assayed. The amplification levels of 18S rRNA (18S ribosomal RNA) or HMBS (hydroxymethylbilane synthase) were used as an internal reference to estimate the relative levels of specific transcripts, and relative quantification was determined by the $\Delta\Delta$Cp method. All determinations were done in triplicate.

Table 4. Primers and UPL probes used for RT-qPCR

GENE	UPL PROBE	primer	OLIGONUCLEOTIDES 5'->3'
RNA18S1	#40	FW	ggagagggagcctgagaaac
		REV	tcgggagtgggtaatttgc
HMBS	#26	FW	tgtggtgggaaccagctc
		REV	tgttgaggtttccccgaat
SOX2	#19	FW	atgggttcggtggtcaagt
		REV	ggaggaagaggtaaccacagg
LGR5	#60	FW	cccttcattcagtgcagtgtt
		REV	attctgatcagccagccatc
CDKN1B (p27)	#60	FW	tttgacttgcatgaagagaagc
		REV	agctgtctctgaaagggacatt
CDKN1A (p21)	#1	FW	cctccccccttgtcctttc
		REV	gtgggacaggcacctcag
CDH1	#35	FW	cccgggacaacgtttattac
		REV	gctggctcaagtcaaagtcc
CTNNB1 (β-catenin)	#8	FW	tgttaaattcttggctattacgaca
		REV	ccaccactagccagtatgatga
KLF4	#82	FW	gccgctccattaccaaga
		REV	tcttcccctctttggcttg
MYC	#34	FW	caccagcagcgactctga
		REV	gatccagactctgacctttgc
NANOG	#69	FW	atgcctcacacggagactgt
		REV	agggctgtcctgaataagca
POU5F1 (OCT3/4)	#52	FW	gtgcctgcccttctaggaat
		REV	ggcacaaactccaggttttct

KLF9	#76	FW REV	ctccgaaaagaggcacaagt cgggagaacttttaaggcagt
CD24	#66	FW REV	atgggcagagcaatggtg gaataaatctgcgtgggtagga
POU2F1	#21	FW REV	acaatagcagcaaccccaat caagctgggagtatcaattcg
DSP	#49	FW REV	gaatgtttggggtggatgag ctgaggccaggtccacac
EPCAM	#3	FW REV	ccatgtgctggtgtgtgaa tgtgttttagttcaatgatgatcca
SPARC	#77	FW REV	gtgcagaggaaaccgaagag tgtttgcagtggtggttctg
FN1	#43	FW REV	gaactatgatgccgaccagaa ggttgtgcagatttcctcgt
VIM	#16	FW REV	aaagtgtggctgccaagaac agcctcagagaggtcagcaa
ZEB1	#3	FW REV	gggaggagcagtgaaagaga tttcttgcccttcctttctg
TWIST2	#35	FW REV	aattctgttgaaactggaccaag ggggaggggaaggaactc
SNAI1	#11	FW REV	gctgcaggactctaatccaga atctccggaggtgggatg
SNAI2	#73	FW REV	acagcgaactggacacacat gatggggctgtatgctcct
ZNFR3	#72	FW REV	gctcgagcaaggatccag caaggagaccacgacgaag
RNF43	#22	FW REV	gcaccaaagagcacaatgag gagttcgcttctgagcttgtc
RNF128	#38	FW REV	tacggaatgcaagagctcaa tgtttcagtgtgcgtagttgaa
MDM2	#13	FW REV	agctgtctctgaaagggacatt gctgaagcagaaccacttga
MDM4	#2	FW REV	ctgctcaccgcaacctct cagctatctgggaggctga
NUP188	#18	FW REV	tctgacctcgttggagctg cggccaatacttcacatgc
BBC3 (PUMA)	#1	FW REV	aagagcaaatgagccaaacg caaacgagccccactctc
PMAIP1 (NOXA)	#11	FW REV	ggagatgcctgggaagaag ccaaatctcctgagttgagtagc
GADD45A	#4	FW REV	aaaaggaacaaaaattacaaagaacc ccaaactatggctgcacactt
RRM2B	#3	FW REV	ttggtagtggacttgggaaatc aaagggaaatggtgggaaac

In vivo tumorigenic assays

SW620 cells were transduced with pCMV-GFP/luc for the constitutively expression of the firefly luciferase gene and GFP. GFP^+ cells were selected by fluorescence activated cell sorting (FACS) and luciferase expression was assessed as described in luminometric reporter assays. These cells were then used for generating the control cell lines (transduced for expressing the pLK.0-puro SHC002 plasmid containing a shRNA sequence that should not target any known mammalian gene) and the knock down cell lines (SOX2 or LGR5), after selection with puromycin (2 μg/mL) for 5 days. *In vivo* tumorigenic potential was assessed by intramuscular injection of the generated cell lines in hind legs of immunodeficient (SCID-NOD) mice and monitored by non-invasive bioluminescence. For this, mice were anesthetized with 100 mg/kg ketamine (Merial) and 3.3 mg/kg xilacine (Henry Schein). Previously, cells were detached from plates, washed and resuspended in medium without FBS at $1x10^4$ cells/μL. Fifty μL ($5x10^5$ cells) of cell suspension was injected in each hind limb of 6-week old mice (2 injection sites per mouse). *In vivo* optical imaging of engrafted mice was performed after intraperitoneal injection with 150 mg/kg of D-luciferin (16.7 mg/mL in physiological serum) (Caliper Life Science). Tumor growth was monitored once or twice a week *in vivo* at real time in anesthetized mice and after intraperitoneal injection of D-luciferin. Mice were then placed in the detection chamber of an ORCA-2BT imaging system (Hamamatsu Photonics) provided with a C4742–98-LWG-MOD camera and a 512 x 512 pixel, charge-coupled device (CCD) cooled at -80 ºC at a distance of 200 mm from the camera objective (HFP-Schneider Xenon 0.95/25 mm). Imaging was performed routinely 5 min after substrate injection. Two images were generated from each mouse, one using a light source inside the chamber to register the animal position and a second one, in total darkness, during a 5 min period to acquire photons from the light emitting cells. To increase detection sensitivity the readout noise of the recorded signal was reduced by adding the light events recorded by arrays of 8 x 8 adjacent pixels (binning 8 x 8) in the camera CCD. Mice were monitored during a 4 week period at days 1, 7, 14, 21 and 28. Quantification and analysis of photons recorded in the areas of interest from images were carried out using the Hokawo Imaging Software (Hamamatsu Photonics).

Immunohistochemistry

Two µm thick sections were obtained for immunohistochemistry from formalin-fixed and paraffin-embedded tissue blocks from immunodeficient mouse xenografts. Tissue sections were mounted on xylaned glass slides (DAKO, Glostrup, Denmark) and used for immunohistochemical staining using the Bond Polymer Refine Detection System (Leica, Wetzlar, Germany). Samples were deparaffinized, antigen retrieval performed at pH 6 for 20 minutes and anti-β-catenin primary antibody incubated for 1 h. Images were captured with an Olympus BX-51 microscope equipped with an Olympus DP70 camera.

Statistical analysis

The statistical significance of the variations measured for data of both *in vitro* and *in vivo* assays are represented with * (p value < 0.05), ** (p value < 0.01) or *** (p value < 0.001) after applying a two-tailed Student's t-test or a repeated measures ANOVA analysis, respectively. Deviations are expressed as mean ± SEM, illustrated as error bars.


Results

Messier object 16, The Eagle Nebula

The Eagle Nebula is a young open cluster of stars in the constellation Serpens at about 7,000 light-years away from Earth. It contains several active star-forming gas and dust regions, including the famous "Pillars of Creation". The height of the tallest tower of gas and dust is about 9.5 light-years, the double of the distance from the Sun to Alpha-Centauri, the closest star to our solar system…

OBJECTIVE 1

-Explore the potential correlation of SOX2 expression with drug resistance in cell lines derived from distinct tumor types.

1.1 Survey of SOX2 activity in cell lines from distinct tumor types displaying differential features of tumor aggressiveness

With the purpose of identifying cell models in which SOX2 is differentially expressed and in which previously documented studies indicated differential features of tumor aggressiveness, we performed a screening in a number of cell lines derived from distinct tumor types. The cell lines selected for this survey focused on pairs from given tumor types in which one cell line had been reported to display aggressive traits (e.g. highly metastatic) while a second cell line or matching counterpart was known to display less aggressive traits (e.g. low or nonmetastatic). Additional non-paired cell lines were also included in this survey, including the U87-MG glioblastoma cell line, with known high SOX2 expression and activity levels, or the widely used HeLa cervical cancer cell line.

The method chosen to quantify SOX2 activity in these cells was based on lentiviral GFP reporter constructs under the transcriptional control of the SOX2/OCT3/4 enhancer [443]. The system includes the plasmid pL-SIN-EF1α-eGFP that reflects the transcriptional activity of the ubiquitous EF1α and was used as positive control; while a second plasmid, pL-SIN-EOS-C3^{+}-eIP, directs SOX2/OCT3/4-specific GFP expression since it carries in its promoter tandemly arranged SOX2/OCT3/4 dimer DNA binding motifs. The assay readout consists of flow cytometry quantifications of GFP intensity and proportion of GFP-positive cells within the total cell population. It is important to remark that, originally, these plasmids were generated for improving the efficiency of detection and isolation of mouse and human induced pluripotent stem cells (iPS).

The lentiviral particles carrying these two GFP reporter plasmids were generated in parallel, and, in a preliminary experiment, we determined the minimal volume of lentiviral particle supernatant necessary to transduce close to 100% of cells, using for that purpose only the EF1α positive control GFP-reporter vector and assuming that supernatants for both types of constructs contained similar concentrations of lentiviral particles. Thus, after separate transduction in each cell line with both GFP-reporter systems, we were able to

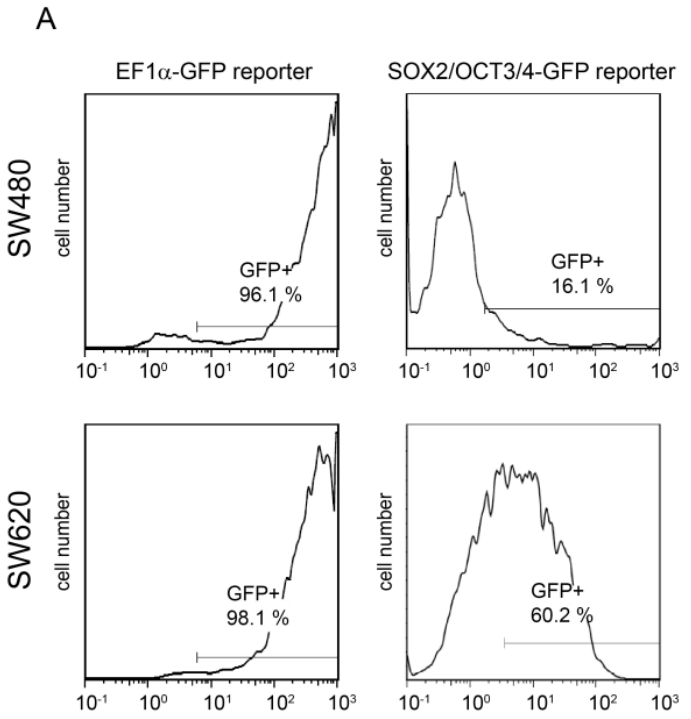

B

origin / cell line	normalized % of positive GFP cells	SEM
prostate cancer		
PC-3	20.8	1.3
PC-3/Mc	81.3	1.8
PC-3/S	18.4	1.0
DU-145	6.1	0.5
breast cancer		
MCF-7	26.2	0.3
MCF10A	45.9	2.5
MCF10H	44.8	0.6
MDA-MB-231	24.5	1.7
MDA-MB-468	63.1	0.7
T-47D	37.4	0.2
colorectal cancer		
HT29-M6	11.3	0.3
HCT116 40.16	65.3	1.0
HCT116 379.2	57.2	0.6
SW620	58.1	1.6
SW480	18.2	0.5
pancreatic cancer		
CAPAN-1	10.6	0.7
PANC-1	77.3	1.0
cervical cancer		
HeLa	22.8	0.9
neuroblastoma		
SK-N-SH	12.2	0.2
glioblastoma		
U87-MG	68.1	1.6
lung cancer		
HAL-8	9.5	0.3
HAL-24	6.1	0.2

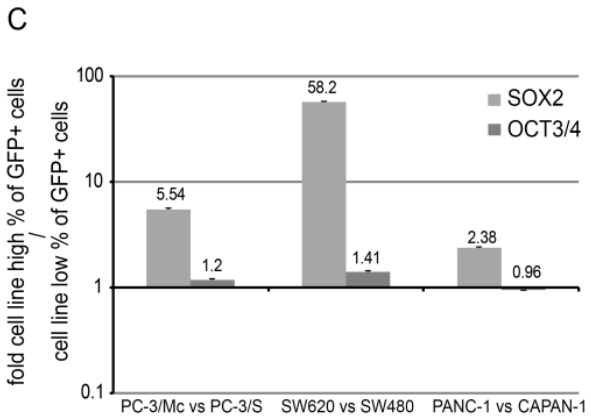

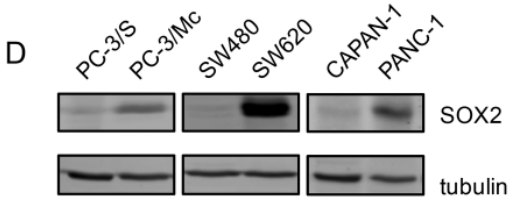

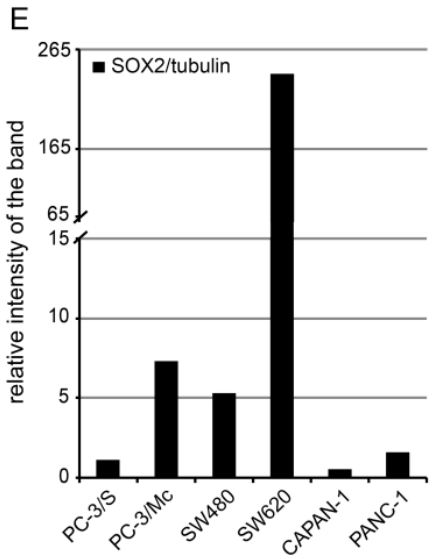

Figure 1. *Screening in different cell lines of distinct tumor types for their high or low transcriptional activity and expression of SOX2*. (**A**) Representative flow cytometry histograms for two cell lines (SW480 and SW620) analyzed and transduced with GFP-reporter plasmids reflecting EF1α and SOX2/OCT3/4 transcription factor activity. (**B**) All cell lines were transduced with GFP-reporter plasmids and analyzed by flow cytometry. Total GFP-positive subpopulations for SOX2/OCT3/4 transcription factor activity were normalized for GFP-reporter transcriptional activity of EF1α, which was transduced and processed in parallel. (**C**) RT-qPCR analysis for SOX2 and OCT3/4 levels in selected pairs of cell lines. (**D**) Western blotting analysis to determine SOX2 protein levels in the indicated cell lines. (**E**) Graphical representation of SOX2 protein levels normalized to tubulin levels, corresponding to the same experiment shown in (**D**).

normalize the data (Figure 1A & B) and compare the SOX2/OCT3/4 transcription factor activities of the different cell lines analyzed; for prostate cancer cell lines, the percentages of normalized GFP-positive cells lines reflecting SOX2/OCT3/4 transcription factor activities were 20.8% for PC-3, 81.3% for PC-3/Mc, 18.4% for PC-3/S and 6.1% for DU-145. In breast cancer cell lines, the percentages were 26.2% for MCF-7, 45.9% for MCF10A, 44.8% for MCF10H, 24.5% for MDA-MB-231, 63.1% for MDA-MB-468 and 37.4% for T-47D. In colorectal cancer cell lines, 11.3% for HT29-M6, 65.3% for HCT116 40.16, 57.2% for HCT116 379.2, 58.1% for SW620 and 18.2% for SW480, whereas in pancreatic cancer cell lines were 10.6% for CAPAN-1 and 77.6% for PANC-1. Cervical cancer, neuroblastoma and glioblastoma cell lines, HeLa, SK-N-SH and U87-MG, displayed respectively 22.8%, 12.2% and 68.1% of GFP-positive cells for SOX2/OCT3/4 transcription factor activity. Finally, lung cancer cells HAL-8 and HAL-24, showed 9.5% and 6.1% of GFP-positive cells, respectively (Figure 1B).

Among the cell lines tested, we preferentially chose pairs of cell lines belonging to the same tumor type and origin (if possible) displaying high *vs.* low SOX2/OCT3/4 transcription factor activities. Based on these criteria, the following pairs of cell lines were selected for further study because of previous evidence of differential features of tumor aggressiveness: PC-3/Mc *vs*. PC-3/S (prostate cancer, derived from the same parental cell line PC-3 [444]), SW620 *vs*. SW480 (colorectal cancer, derived from the same patient [445]), and PANC-1 *vs*. CAPAN-1 (pancreatic cancer [446], [447]).

The PC-3/Mc *vs*. PC-3/S pair was studied previously in our lab [130] as clonal populations derived from the parental PC-3 prostate cancer cell line that display very distinct phenotypes and transcriptional programs. PC-3/Mc cells are poorly autonomously invasive *in vitro*, but display a very high growth rate *in vitro* and *in vivo* and are potently metastatic. In contrast, PC-3/S cells are highly invasive *in vitro*, but grow slowly *in vitro* and *in vivo* and do not form metastases. These phenotypes correlated very well with the SOX2/OCT3/4 transcriptional activities determined here, with PC-3/Mc cells containing 81.3% and PC-3/S cells 18.4% GFP-positive cells. These results are also in excellent agreement with our previous observations of differential SOX2 transcript and protein levels between these two PC-3 subpopulations [130]. This differential

expression was corroborated by real-time qPCR and Western blotting (Figure 1C-E). Therefore, our results confirm that, in this dual-cell model, the more aggressive cells exhibit higher SOX2 transcriptional activity.

The SW620 *vs.* SW480 pair was originally isolated from the same patient suffering from a colon adenocarcinoma [445], SW620 from a lymph node metastasis and SW480 from the primary tumor. Similar to the prostate cancer cell model, SW480 is highly invasive and motile *in vitro*, but grow relatively slow when xenografted and is poorly metastatic in comparison to SW620, which is much less invasive *in vitro* but grow rapidly when xenografted in immunodeficient mice and is highly metastatic. In addition, both cell lines grow with a similar rate *in vitro* [448], [449]. This differential aggressiveness also correlated with the observed differential transcriptional activity of SOX/OCT3/4; SW620 showed 58.1% and SW480 18.2% of GFP-positive cells. As in the case of the prostate cancer pair model, it appears that the differences in the frequency of GFP-positive cells can be attributed to SOX2 rather than OCT3/4, because SOX2 but not POU5F1 (OCT3/4) transcript levels correlated with GFP-positive cells (Figure 1C). At the protein level, SW620 expressed much higher levels of SOX2 than SW480 cells (Figure 1D-E).

In contrast to the other two cell line pairs, the PANC-1 *vs.* CAPAN-1 pair presents similar aggressiveness features but differential transcriptional activities of SOX/OCT3/4 (77.3% of positive cells for PANC-1 and 10.6% positive cells for CAPAN-1). CAPAN-1 was isolated from a liver metastasis of a patient with pancreatic adenocarcinoma [446], while PANC-1 was isolated from an invasive pancreatic adenocarcinoma in which a metastasis was found in one pancreatic lymph node [447]. Both cell lines display similar growth rates and invasiveness *in vitro*, although CAPAN-1 demonstrated to be slightly more tumorigenic when injected ortothopically in immunodeficient mice [450]. However, some studies have shown that despite presenting a similar metastatic potential, histologically, tumors formed in immunodeficient mice by PANC-1 are poorly differentiated as compared to those formed by CAPAN-1 [451]. As in the other prostate and colorectal pairs of cell lines, the differential activity of SOX/OCT3/4 correlated with the SOX2 expression at the transcript and protein levels (Figure 1C-E).

1.2 Experimental manipulation of SOX2 levels in selected pairs of cell lines

In order to address whether high levels of expression of SOX2 are associated with a gain in drug resistance (and vice versa), we proceeded to manipulate SOX2 levels in the selected cell line pairs. With that aim, we forced the overexpression of SOX2 by means of retroviral transduction in cell lines with relative low levels of SOX2 expression (PC-3/S, SW480 and CAPAN-1). The same retroviral construct employed in these experiments is used for the generation of induced pluripotent stem cells from adult cells [452]. The procedure was extremely efficient at inducing very high levels of SOX2 expression in these cells (Figure 2A).

Conversely, we proceeded to knock down SOX2 in counterpart cell lines with relative high endogenous SOX2 expression levels (PC-3/Mc, SW620 and PANC-1) by means of shRNA, in which cells are transduced with lentiviral particles for the expression of mRNA-specific shRNAs against SOX2 and stable lentiviral integration is then selected by puromycin resistance. The resulting SOX2-specific knock down efficiencies varied from 60% in PC-3/Mc and PANC-1 cells to 83% in SW620 cells (Figure 2B).

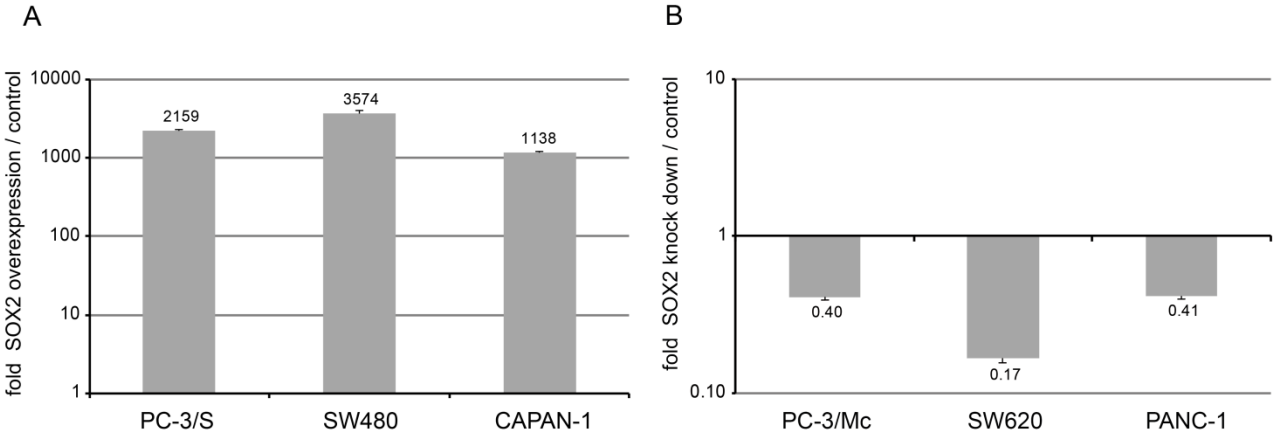

Figure 2. *Manipulation of SOX2 levels in selected pairs of cell lines.* (**A**) Cell lines with low endogenous expression of SOX2 were transduced with retroviral particles for the overexpression of this transcription factor and analyzed by RT-qPCR. (**B**) Cell lines with high endogenous levels of SOX2 were transduced with lentiviral particles for the expression of shRNAs for specific knock down and analyzed by RT-qPCR.

1.3 Assessing the relationship between SOX2 expression levels and drug resistance

We next performed end-point cytotoxicity assays at 72 h of treatment with some of the most common chemotherapeutics agents used in clinical practice, such as cisplatin, 5-fluorouracil (5-FU), etoposide and doxorubicin.

First, we studied the consequences on cytotoxic responses of repressing SOX2 in the relatively high endogenous SOX2-expressing cell line PC-3/Mc. As illustrated in Figure 3, control uninfected cells (left panels) showed relatively high resistance to cisplatin or 5-FU, with no or low effect on growth at the tested concentrations, a dose-dependent response to etoposide, and a high sensitivity to doxorubicin that affected cell viability at relatively low concentrations.

However, contrary to our hypothesis that high levels of SOX2 might confer enhanced drug resistance and thus its knock down might cause drug sensitization, we did not observed a diminished resistance to 5-FU, cisplatin, etoposide or doxorubicin in PC-3/Mc cells in which SOX2 had been knocked down (Figure 3, right panels). In fact, we did not observe significant differences in cytotoxicity at any of the concentrations and drugs tested between control knock down cells in comparison with treated cells, indicating that the mere fact of silencing SOX2 severely impaired not only the normal growth rate of PC-3/Mc cells under standard culturing conditions but also their viability.

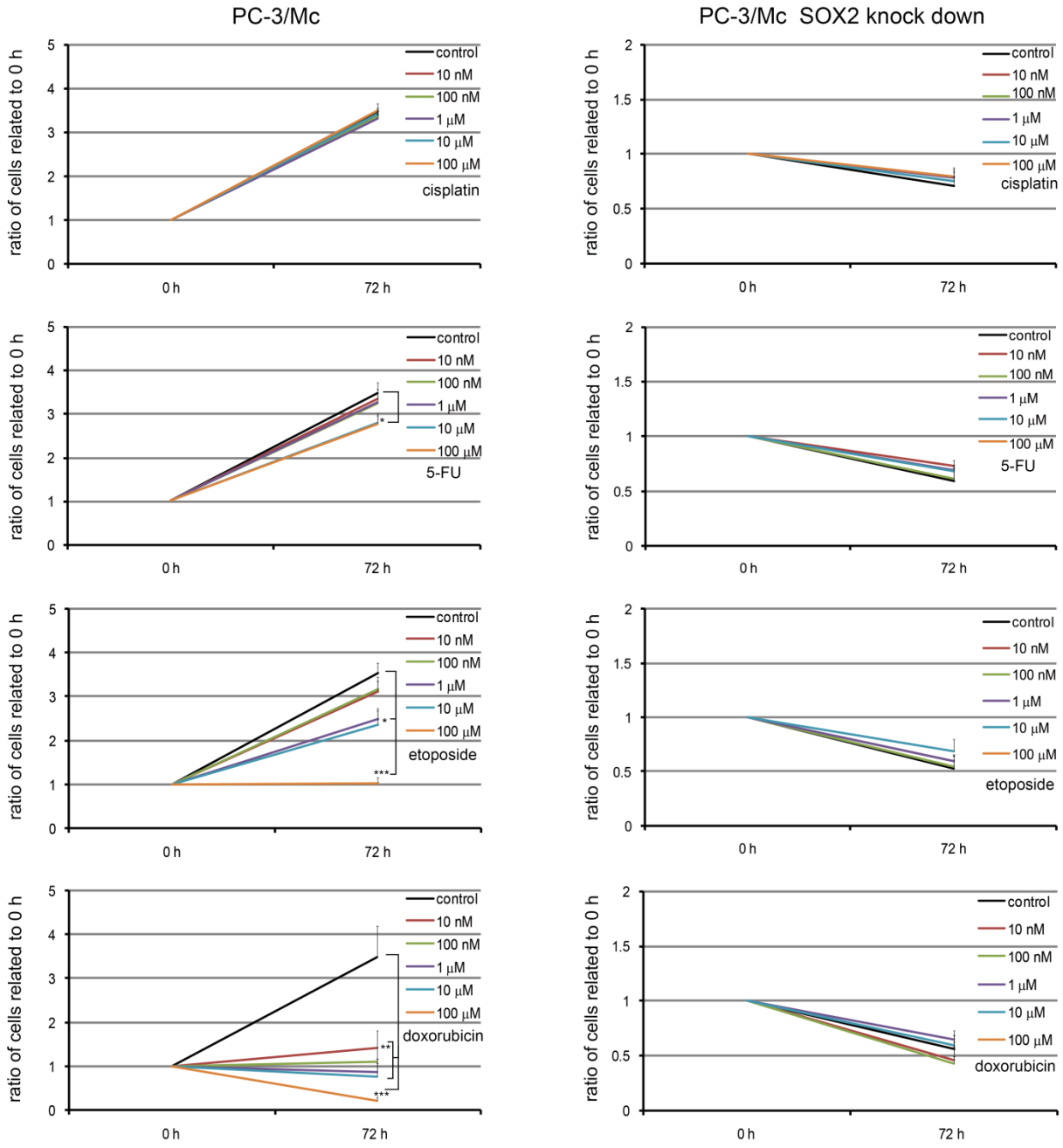

Figure 3. *Drug sensitivity in control and SOX2-knockdown PC-3/Mc prostate cancer cells*. Dose-response viability was assayed in uninfected (left graphs) and SOX2 repressed cells (right graphs) in the presence of cisplatin, 5-fluorouracil (5-FU), etoposide and doxorubicin for 72 h at the indicated concentrations.

In reciprocal experiments, we determined whether overexpression of SOX2 could confer drug resistance to PC-3/S cells, the other member of this first pair of cell lines selected for analysis, with relatively low endogenous expression levels of this transcription factor (Figure 4). For control PC-3/S cells

(left panels), cisplatin exerted a significant growth inhibitory effect only at high concentrations (100 μM), while 5-FU and etoposide showed a growth inhibitory effect in a clear dose-dependent fashion, and doxorubicin, similarly to the response observed for PC-3/Mc cells, had a very potent effect on growth and cell viability even at relatively low concentrations.

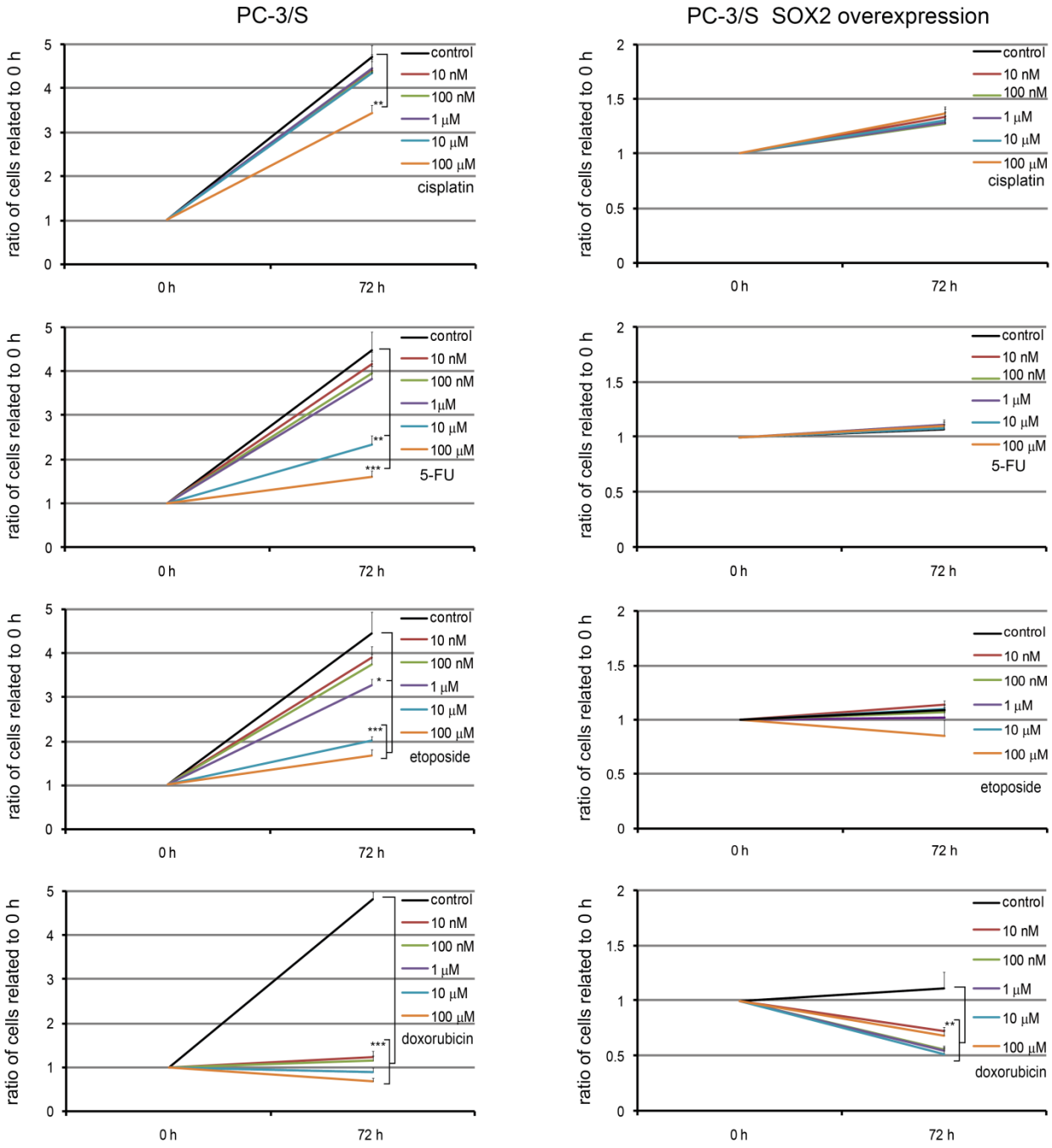

Figure 4. *Drug sensitivity in control and SOX2-overexpressing PC-3/S prostate cancer cells*. Dose-response viability was assayed for uninfected (left graphs) and SOX2-overexpressing (right graphs) cells were performed in the presence of cisplatin, 5-fluorouracil (5-FU), etoposide and doxorubicin for 72 h at the indicated concentrations.

Strikingly, and again contrary to our expectations, overexpression of SOX2 in PC-3/S cells significantly reduced *per se*, almost abolishing, the growth of this cell line *in vitro*, and as a consequence, no enhanced drug resistance was observed to any compound tested as a consequence of SOX2 overexpression (Figure 4, right panels). Moreover, in the case of doxorubicin, the effect on cell viability of the drug was significantly exacerbated relative to the control SOX2-overexpressing PC-3/S cells.

Given these unexpected results, we next extended the analysis to the pair of pancreatic cancer cell lines with differential SOX2 expression levels, in order to determine whether the observed effect of SOX2 manipulation over growth, cell viability and putative relationship with drug tolerance/sensitization, was specific to the selected prostate cancer cell model. Therefore, we proceeded to perform dose-response curves to 5-FU (Figure 5) in the CAPAN-1 and PANC-1 pancreatic cancer cell lines.

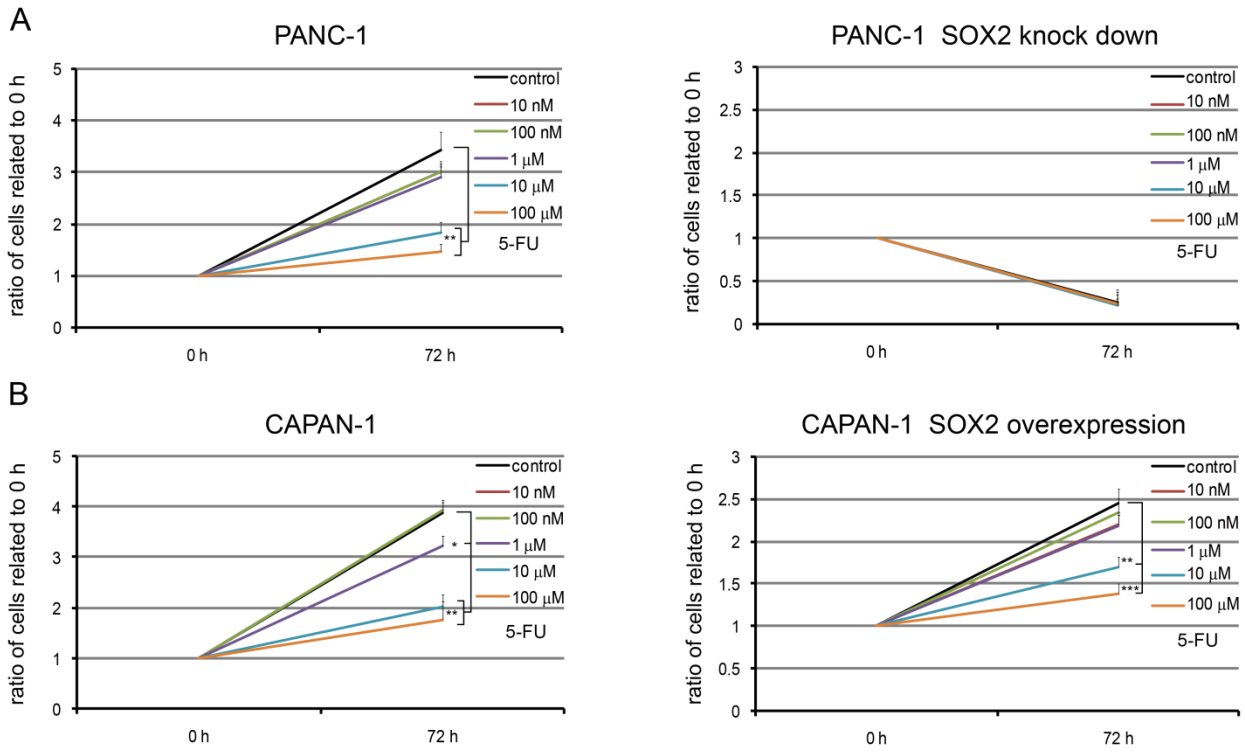

Figure 5. *Drug sensitivity in pancreatic cancer cell lines with manipulated SOX2 levels*. (**A**) PANC-1 cells, with relative high endogenous SOX2 levels, were knocked down for SOX2 and dose-response viability determined in control (left graph) and SOX2-knockdown (right graph) cells after exposure to 5-fluorouracil (5-FU) for 72 h at the indicated concentrations. (**B**) CAPAN-1 cells, with relative low endogenous SOX2 expression, were transduced with retroviral vectors for the overexpression SOX2, and dose-response viability in control (left graph) and SOX2-overexpressing cells (right graph) was determined after exposure to 5-fluorouracil (5-FU) for 72 h at the indicated concentrations.

Firstly, we determined the effect of 5-FU on the viability and growth of control cells and observed that both PANC-1 and CAPAN-1 diminished their growth in a dose-dependent manner in the presence of 5-FU (Figure 5A & B, left panels). In contrast, and similar to the results obtained for PC-3/Mc cells, knock down of SOX2 in PANC-1 cells led to a dramatic reduction in cell growth and viability, and as a result, no differential response to the drug was observed compared to untreated knock down cells (Figure 5A, right panel).

In a reciprocal experiment, overexpression of SOX2 in CAPAN-1 cells diminished *per se* the growth of this cell line and did not confer resistance to 5-FU (Figure 5B, right panel), resembling the results obtained for the overexpression of SOX2 in PC-3/S cells.

We further extended this analysis to the colorectal cancer cell lines SW620 and SW480 (Figures 6 & 7). Unlike the effects observed for PC-3/M and PANC-1, knock down of SOX2 in SW620 cells slightly diminished the growth rate compared to control cells. In these conditions, nM and low μM concentrations had a similar effect in control and knock down cells while a certain degree of gain in drug resistance (rather than sensitization) was observed in all compounds at higher μM concentrations in SW620 SOX2 knock down cells compared to control uninfected cells (in terms of decrease of number of cells respect their untreated control condition). Remarkably, both control (Figure 6, left panels) and SOX2-knockdown SW620 cells (Figure 6, right panels), showed a clear dose-dependent growth inhibitory response to all drugs, particularly to etoposide and doxorubicin.

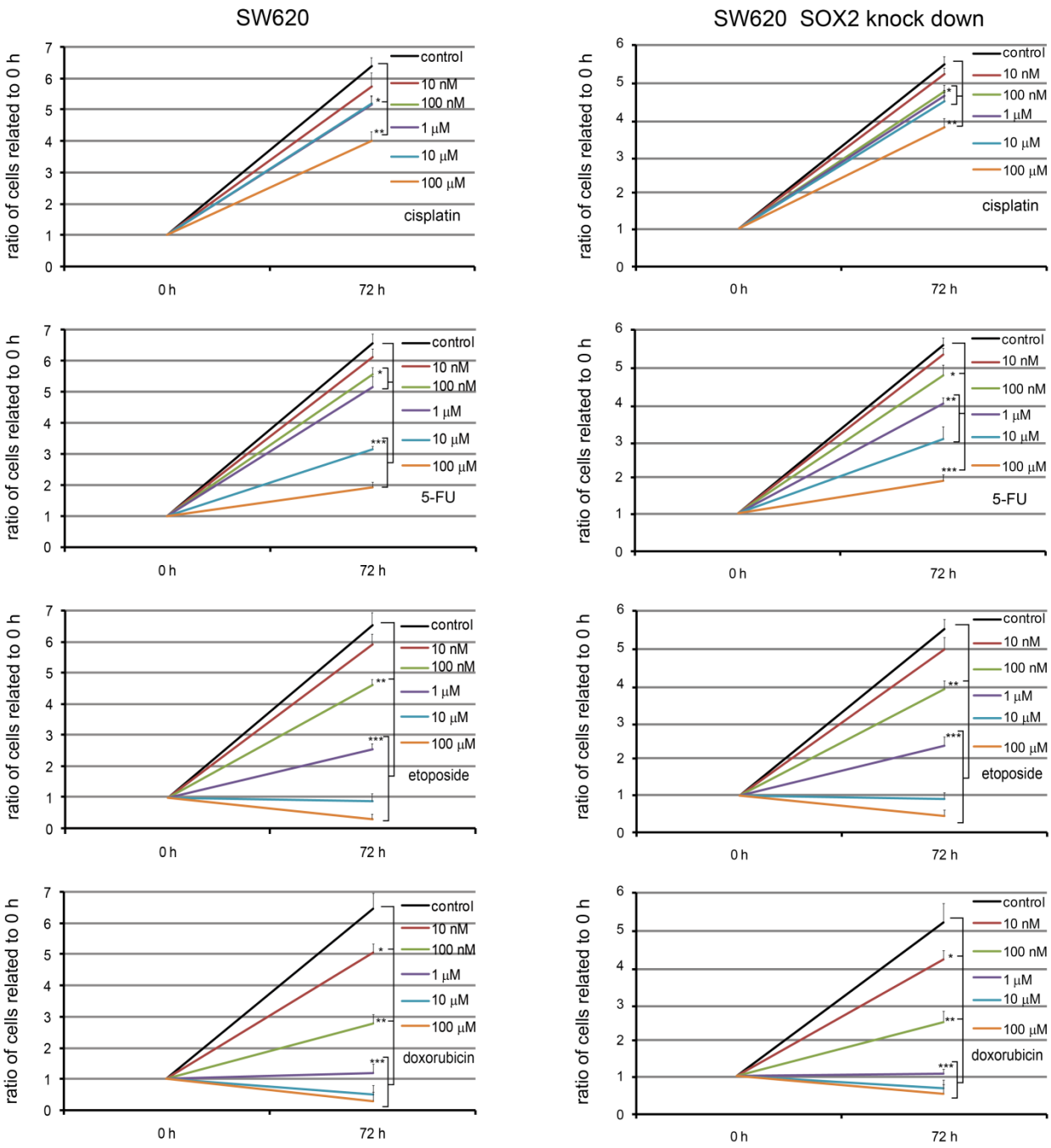

Figure 6. *Drug sensitivity in control and SOX2-knockdown SW620 colorectal cancer cells*. Dose-response viability in control (left graphs) and SOX2-knockdown (right graphs) cells was determined after exposure to cisplatin, 5-fluorouracil (5-FU), etoposide and doxorubicin for 72 h at the indicated concentrations.

Finally, we overexpressed SOX2 in SW480 cells and evaluated their drug sensitivity (Figure 7). Control SW480 cells were relatively resistant to cisplatin and showed cell growth inhibition at μM concentrations for 5-FU and etoposide, being more sensitive to doxorubicin (Figure 7, left panels). However, as observed previously for PC-3/S and CAPAN-1, the growth of SW480 cells was

affected in control SOX2-overexpressing cells compared to control uninfected cells, and drug treatments potentiated the growth inhibition induced by SOX2 overexpression (Figure 7, right panels).

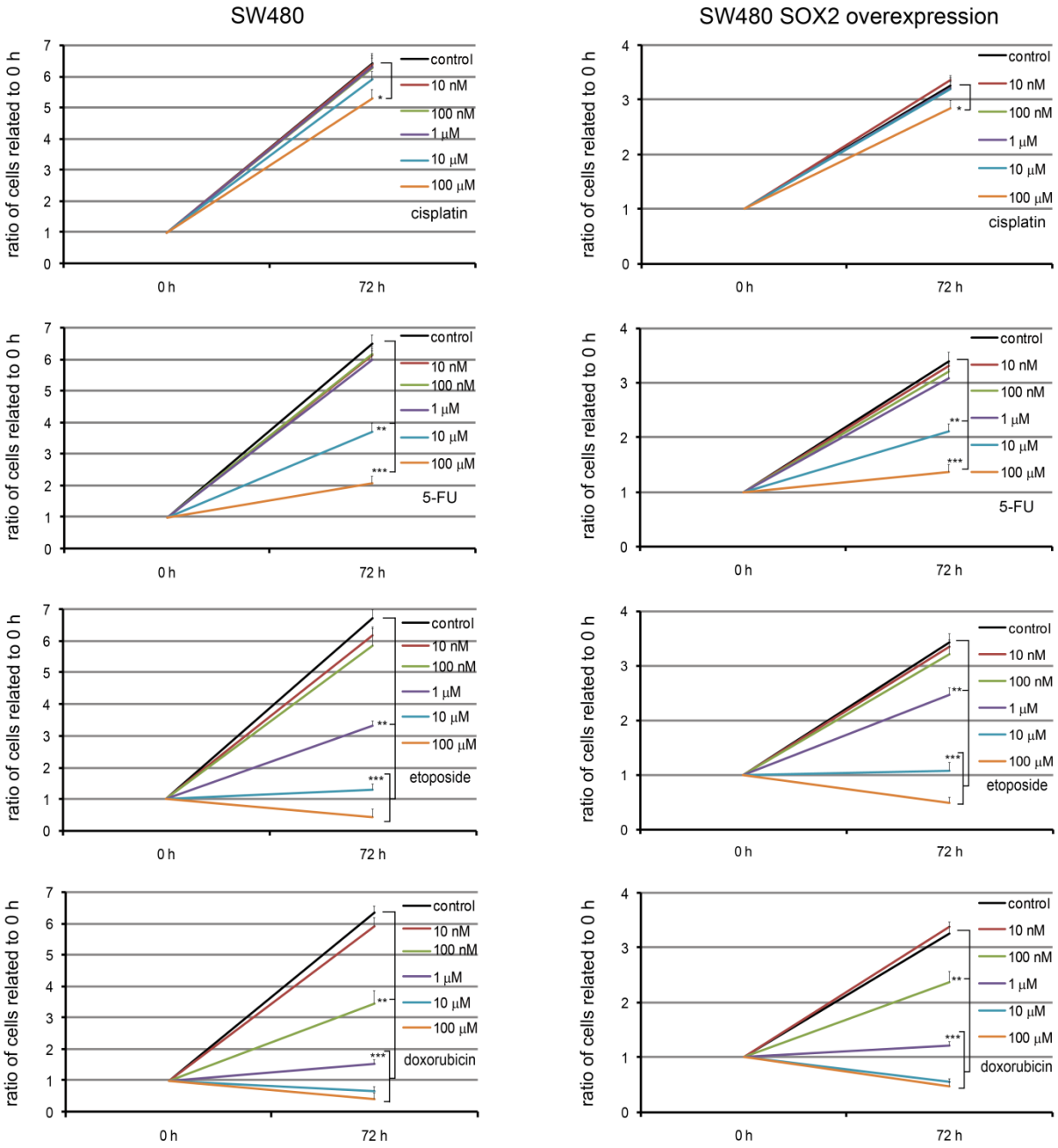

Figure 7. *Drug sensitivity in control and SOX2-overexpressing SW480 colorectal cancer cells*. Dose-response viability in control (left graphs) and SOX2-overexpressing (right graphs) cells was determined after exposure to cisplatin, 5-fluorouracil (5-FU), etoposide and doxorubicin for 72 h at the indicated concentrations.

1.4 SOX2 overexpression and hypothetical gain of drug resistance: a matter of fine-tuning SOX2 levels?

Because the forced overexpression of any gene may cause non-specific effects due to artifacts (including protein aggregation or mislocalization, or quenching or sequestering of other proteins), we wondered to what extent the loss of cell proliferation/viability observed in dose-response curves, was a specific effect exert by high levels of SOX2 or was otherwise related to non-specific effects induced by the mere process of overexpressing an exogenous gene. To approach this issue, we used as a model the SW480 colorectal cancer cells, which express low endogenous levels of SOX2, and transduced them with different SOX2-retroviral loads (different dilutions of HEK293T supernatants containing active retroviral particles) once or several times. The effective expression of SOX2 achieved under these experimental conditions was assessed by determining SOX2 protein levels by means of Western blotting (Figure 8), since the retroviral vectors used bear no selection markers and virus titration was not readily determined. Subsequently, dose-response cytotoxicity analyses were performed after exposure to etoposide and doxorubicin (Figure 9A & B, respectively).

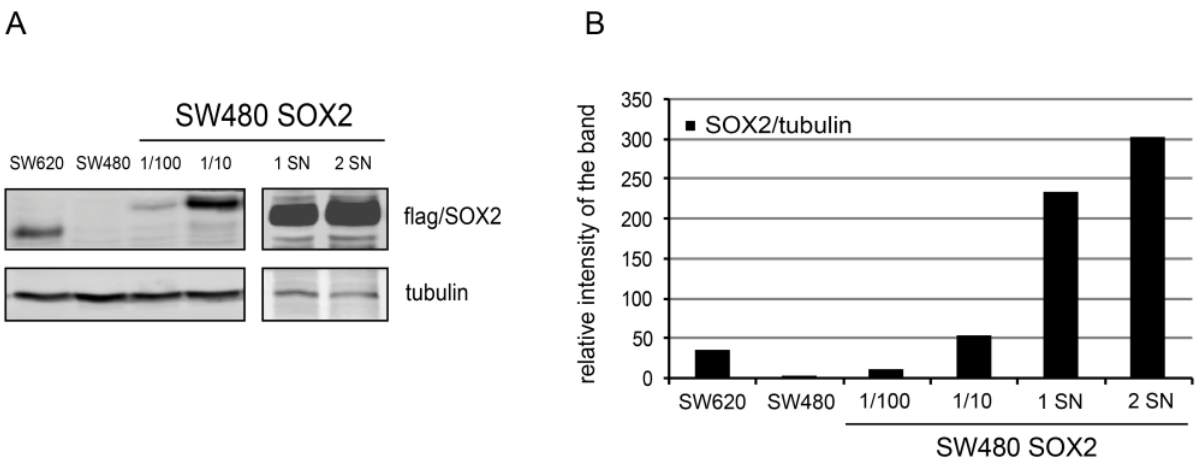

Figure 8. *Different levels of SOX2 overexpression in SW480 cells*. (**A**) Western blot showing different SOX2 protein levels in SW480 cells transduced with 1/100 and 1/10 dilutions of retrovirus supernatants (SN), and 1 or 2 sequential infections (in consecutive days) with undiluted retrovirus supernatants. Endogenous SOX2 level in SW620 is shown for comparison. (**B**) Histogram for quantification of SOX2 levels normalized to tubulin protein levels, corresponding to (**A**).

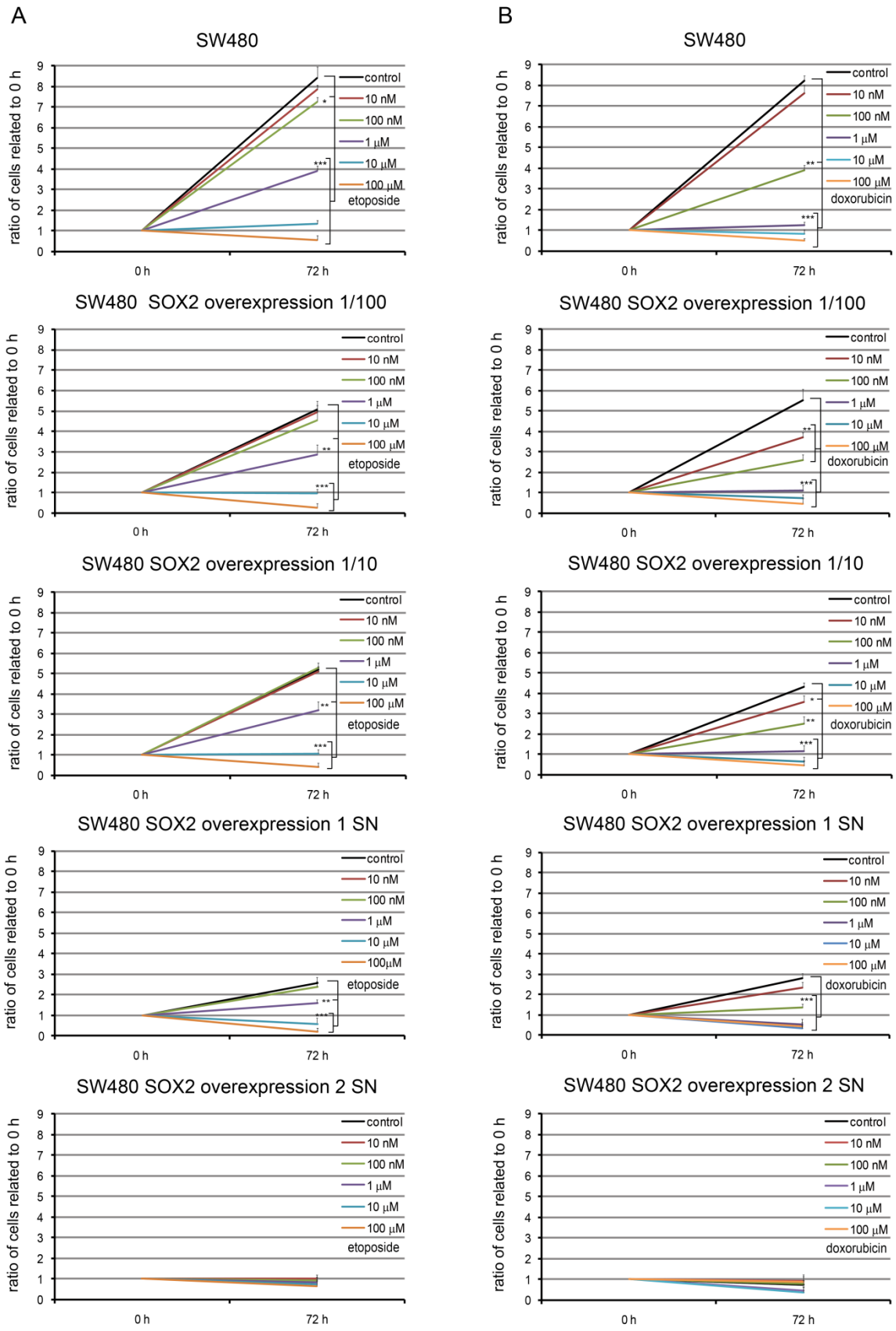

Figure 9. *Drug sensitivity in SW480 cells expressing different levels of retrovirally transduced SOX2*. SW480 was transduced with 1/100 or 1/10 dilutions of retrovirus supernatants (SN) or with 1 or 2 undiluted retrovirus supernatants (in two consecutive days). Dose-response viability in control and infected cells was determined after exposure of cells to etoposide (**A**) or doxorubicin (**B**) for 72 h at the indicated concentrations.

The levels of exogenous SOX2 expression achieved by this approach ranged from significantly less to almost ten-fold SOX2 protein levels higher than the expression levels of endogenous SOX2 in SW620 cells, which express relatively high endogenous levels of this transcription factor (Figure 8B). One condition (transduction with 1/10 dilution of retrovirus supernatant) led to the expression of exogenous SOX2 in SW480 cells at a level range similar to that of the endogenous SOX2 protein levels expressed by SW620 cells (Figure 8B). However, even the lowest load of SOX2-expressing retroviruses caused a growth inhibition of SW480 cells, with a lineal response as a function of retroviral load (control conditions in all graphs of Figure 9A & B). Increasing concentrations of doxorubicin or etoposide had an additive effect to retroviral load in inhibiting the growth of SW480 cells.

From these observations, we can conclude that the overexpression of exogenous SOX2 does not confer drug resistance to the prostate, pancreas or colorectal cancer cells analyzed. On the contrary, it inhibits cell growth in all the cell lines tested and potentiates the growth inhibitory effect of several genotoxic drugs. Given these results, an outstanding issue is by what mechanisms SW620 cells tolerate relatively high endogenous levels of SOX2 while their counterpart SW480 cell line, is inhibited in its growth by high levels of exogenous SOX2.

OBJECTIVE 2

-Phenotypic characterization, study of cell signaling involved and impact on self-renewal and tumorigenicity due to modulation of SOX2 levels in colorectal cancer cell models of divergent aggressiveness.

2.1 Phenotypic characterization of the retroviral transduction of SOX2 in SW480 and SW620 colorectal cancer cells

As an initial approach to better understand possible mechanisms that allow SW620 cells to express endogenous SOX2 at relatively high levels without suffering from the growth inhibitory consequences observed by experimental overexpression of SOX2, we decided to characterize in detail several phenotypic consequences of SOX2 overexpression in both SW620 and SW480 cells. Notably, we first realized that overexpression of exogenous SOX2 by retroviral transduction caused in both cell lines remarkable morphological changes. Both cell types appeared to increase their cell size when compared to control cells, and in the case of SW480, some cells presented marked vacuolization (Figure 10A & B). No evident changes in morphology were observed in cells transduced with retroviral particles carrying an empty expression vector. In striking parallel to the dose-response growth inhibitory effects observed above for SW480, overexpression of SOX2 in SW620 also reduced their capacity to proliferate *in vitro*, proportional to the levels of exogenous SOX2 overexpression (Figure 10C). This suggests that expression of exogenous SOX2 in addition to endogenously expressed SOX2 might surpass a hypothetical limit of tolerance of SW620 cells to high SOX2 levels and, once this has occurred, adverse phenotypic effects are observed. Therefore, in order to observe unequivocal phenotypic effects of SOX2 expression over such a hypothetical tolerance threshold, in subsequent experiments we decided to transduce both cell lines with undiluted retroviral supernatants.

We next determined whether exogenous SOX2 overexpression affected the capacity of SW620 and SW480 cells to grow under anchorage independent conditions (spheroid formation assay). This *in vitro* assay is an indicator of tumor cell self-renewal and is a good predictor of the tumorigenic potential of cells when xenografted in immunodeficient mice. We found that SOX2 overexpression, but not the transduction of control retroviruses, significantly inhibited the capacity of both cell lines to form spheroids (Figure 10D & E).

The observed growth inhibition could be due to increased cell death or cell cycle inhibition. We used several approaches to test if overexpression of

SOX2 induced apoptosis in these colorectal cancer cell lines (Figure 11). The AnnexinV-Alexa 488/propidium iodide staining assay, measured by flow cito-

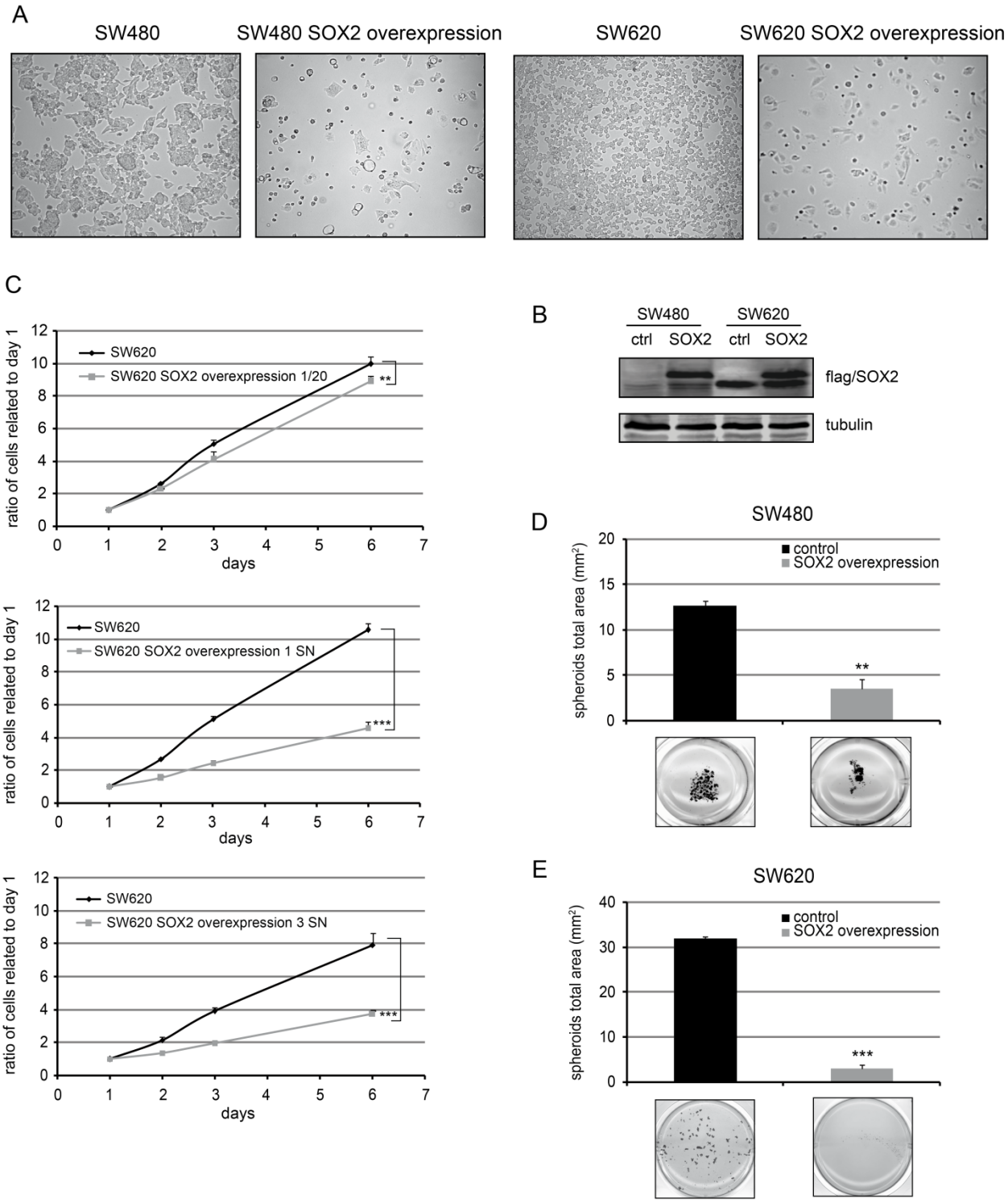

Figure 10. *Consequences on cell growth properties of the transduction of SOX2 in SW480 and SW620 cells*. (**A**) Bright field images of control or SOX2-transduced SW480 and SW620 cells. (**B**) Western blot showing overexpression of SOX2 (flag/SOX2) in SW480 and SW620 cells transduced with undiluted SOX2 retrovirus supernatant once, and endogenous levels of control cells. (**C**) Growth curves for control and SW620 cells transduced with 1/20 dilution or undiluted SOX2 retrovirus supernatant (once or three times in three consecutive days, indicated as 1 SN or 3 SN, respectively). (**D**) Effect of SOX2 transduction on spheroid formation in SW480 cells *vs*. control and (**E**) SW620 cells *vs*. control.

metry, showed that transduction of SOX2 in both cell lines increased the percentage of apoptotic and necrotic cells relative to control levels (Fig. 11A & B). The reduction in cell viability caused by SOX2 overexpression was not equal in the two cell lines, with SW480 cells being markedly more affected by SOX2 overexpression than SW620 cells (decrease of 25% *vs.* 10% in cell viability, respectively) possibly reflecting a greater tolerance of the latter to putative cell death engaged by increased SOX2 levels.

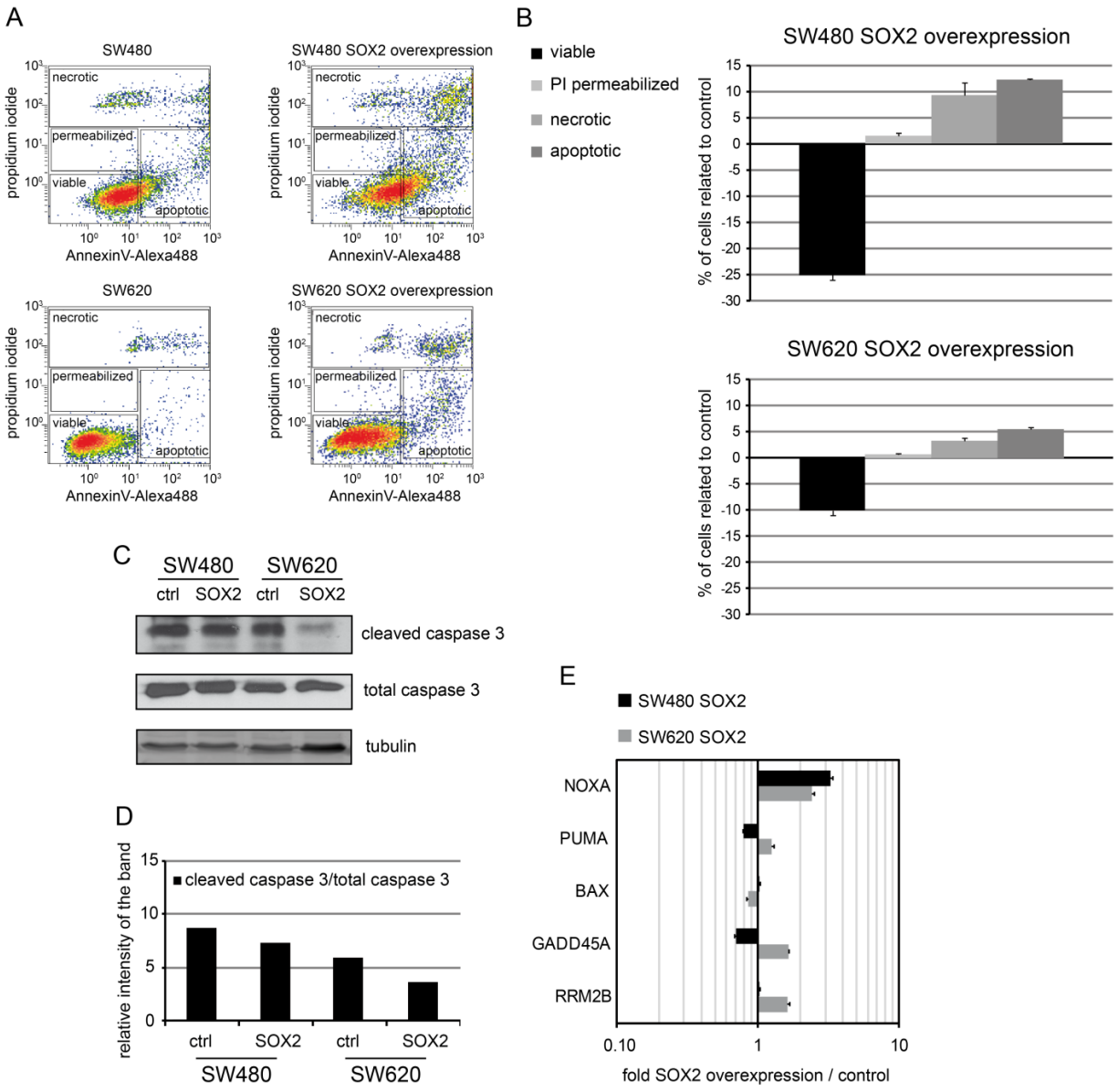

Figure 11. *Effects on cell viability of the transduction of SOX2 in SW480 and SW620 cells*. (**A**) Flow cytometry histograms reflecting apoptosis induced by SOX2 overexpression in SW480 and SW620 cells as compared to control cells, detected by the AnnexinV-Alexa 488 assay. (**B**) Graphs showing the viable, permeabilized for propidium iodide, necrotic (propidium iodide staining) and apoptotic subpopulations in SW480 and SW620 cells transduced with SOX2, relative to control levels. (**C**) Western blot for the detection of caspase 3 in SW480 and SW620 cells overexpressing SOX2 and control cells. (**D**) Graphic representation of cleaved caspase 3 protein levels normalized to tubulin, corresponding to the Western blot in (**C**). (**E**) RT-qPCR quantification for several transcripts involved in apoptotic pathways, in SW480 and SW620 cells transduced with SOX2. Values are normalized to those of control cells.

Consistent with the possible induction of apoptosis, both cell lines displayed sub G1 subpopulations in cell cycle profile determinations, upon forced expression of exogenous SOX2 (Figure 12A) that were proportional to the decline in the proportion of viable cells in apoptosis determination assay. However, neither cell line showed increased levels of the cleaved form of caspase 3 upon SOX2 overexpression, which in fact showed a diminished cleavage in SW620 cells with SOX2 overexpression as compared to control cells (Figure 11C & D). In addition, we assessed by RT-qPCR the expression levels of several known pro-apoptotic (NOXA, PUMA and BAX) and growth arrest-associated (GADD45A and RRM2B) genes. Of these, the only transcript that showed a significant upregulation in both cell lines in response to SOX2 overexpression was NOXA. GADD45A and RRM2B were upregulated in SW620, but not in SW480 cells upon overexpression of SOX2 (Figure 11E).

The latter results suggested that cell cycle dysregulation could be a prominent response that may explain the inhibition of growth as a result of SOX2 overexpression at least in SW620 cells. This was confirmed by cell cycle profiling (Figure 12), which provided another differential trait in the response of SW480 and SW620 cells to SOX2 overexpression, namely that SOX2 overexpression caused a G2/M accumulation in SW480, but not in SW620, whereas SW620 cells, but not SW480 cells, displayed a significant G1/S arrest (Figure 12B).

To assess the robustness of the G1/S arrest observed in SW620 cells after SOX2 overexpression, we resorted to cell cycle analysis after blocking the cell cycle progression in G2/M by incubating the cells overnight with the mitotic poison nocodazole. The rationale behind these experiments is that cells that progress past G1 and S, even in conditions under which they undergo a short delay at these transitions, will all accumulate in G2/M (4n DNA content) in the presence of nocodazole. However, cells with a lasting block at G1/S or S are not expected to progress and accumulate in G2/M during overnight nocodazole treatment. This experimental approach provided unequivocal evidence that SOX2 overexpression produced a strong and lasting arrest at G1/S in SW620 cells but not in SW480 cells (Figure 12C & D).

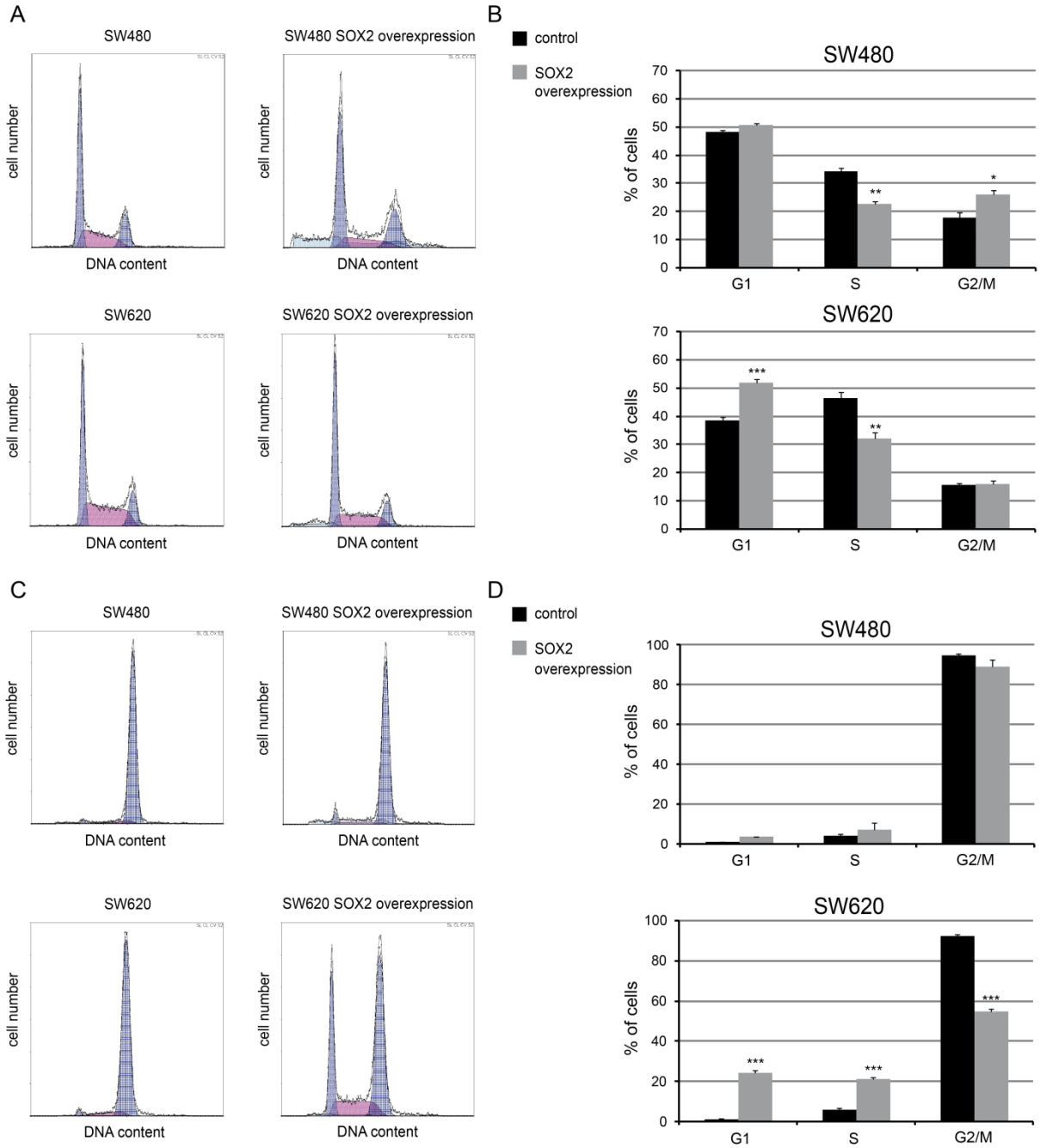

Figure 12. *Cell cycle effects caused by transduction of SOX2 in SW480 and SW620 cells (I)*. (**A**) Flow cytometry histograms corresponding to DNA contents of control and SOX2-transduced SW480 and SW620 cells and (**B**) graphical representantion of the distribution of cells in each phase of the cell cycle. (**C**) Histograms of DNA content in control and SOX2-transduced SW480 and SW620 cells after G2/M block with nocodazole and (**D**) graphical representation of the distribution of cells in each phase of the cell cycle.

Cell synchronization by double thymidine block followed by release and flow cytometry DNA content analysis further indicated that the overexpression of SOX2 in SW620 cells induced a slower passage through G1/S as compared to control cells (Figure 13A & B, shown as kinetics of G2/M entrance).

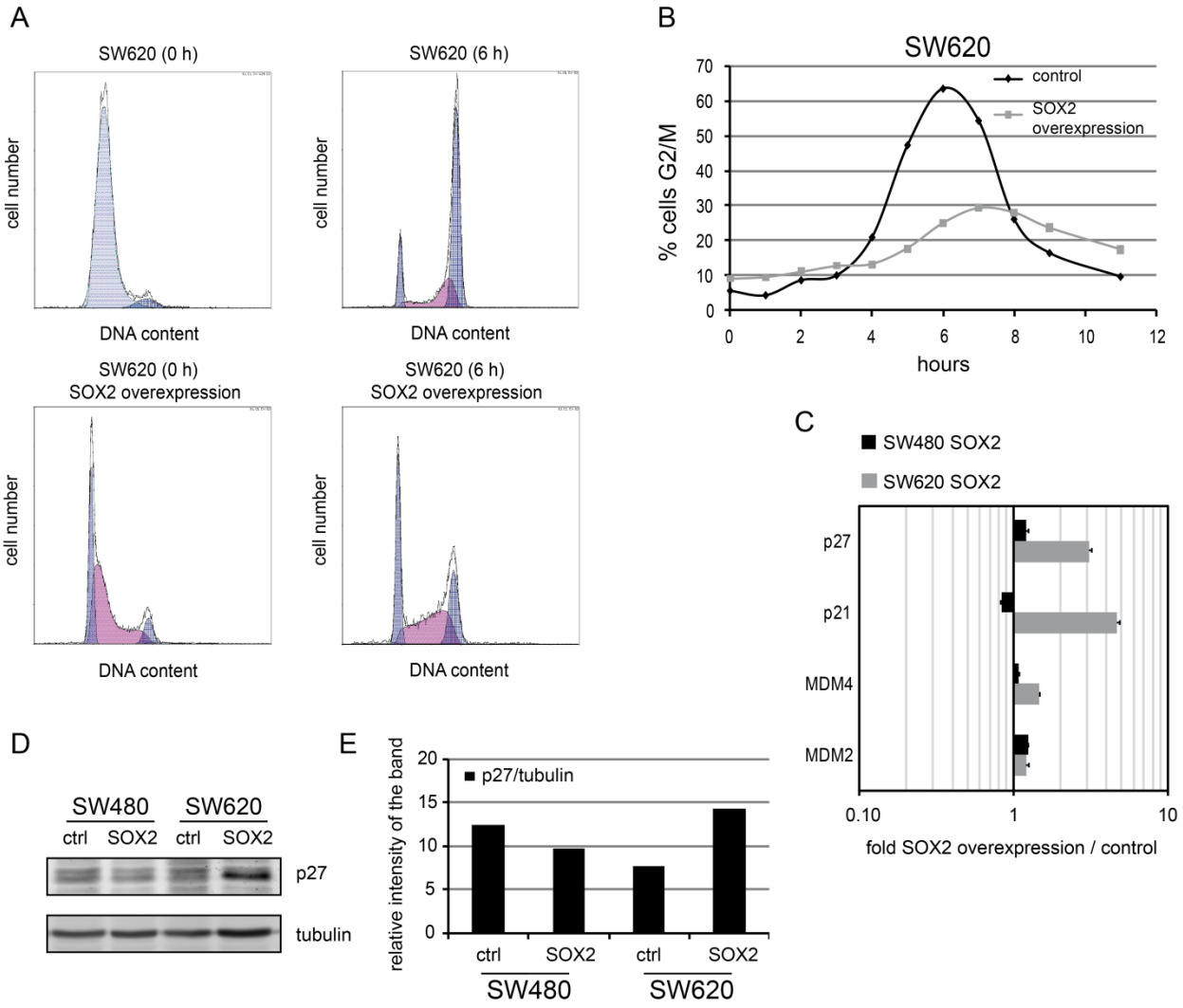

Figure 13. *Cell cycle effects caused by transduction of SOX2 in SW480 and SW620 cells (II)*. (**A**) Representative histograms showing cell cycle progression (at 0 and 6 h) in control *vs.* SOX2-transduced SW620 cells after G1/S double thymidine block and release and (**B**) graphical representation showing quantification of G2/M entry of SW620 cells (from 0 to 11 h after block release). (**C**) RT-qPCR gene expression analysis of selected cell cycle regulators. (**D**) Western blot for p27 in control and SOX2-transduced SW480 and SW620 cells. (**E**) Normalization of p27 protein levels, corresponding to (**D**).

The G1/S arrest induced by SOX2 overexpression in SW620 cells was accompanied with a clear upregulation of the cyclin-dependent kinase inhibitors p27 and p21 (Figure 13C-E & Figure 14). These changes were not as evident in SW480 cells although evidence for p21 upregulation in these cells upon SOX2 overexpression was observed by immunocytochemistry (Figure 14).

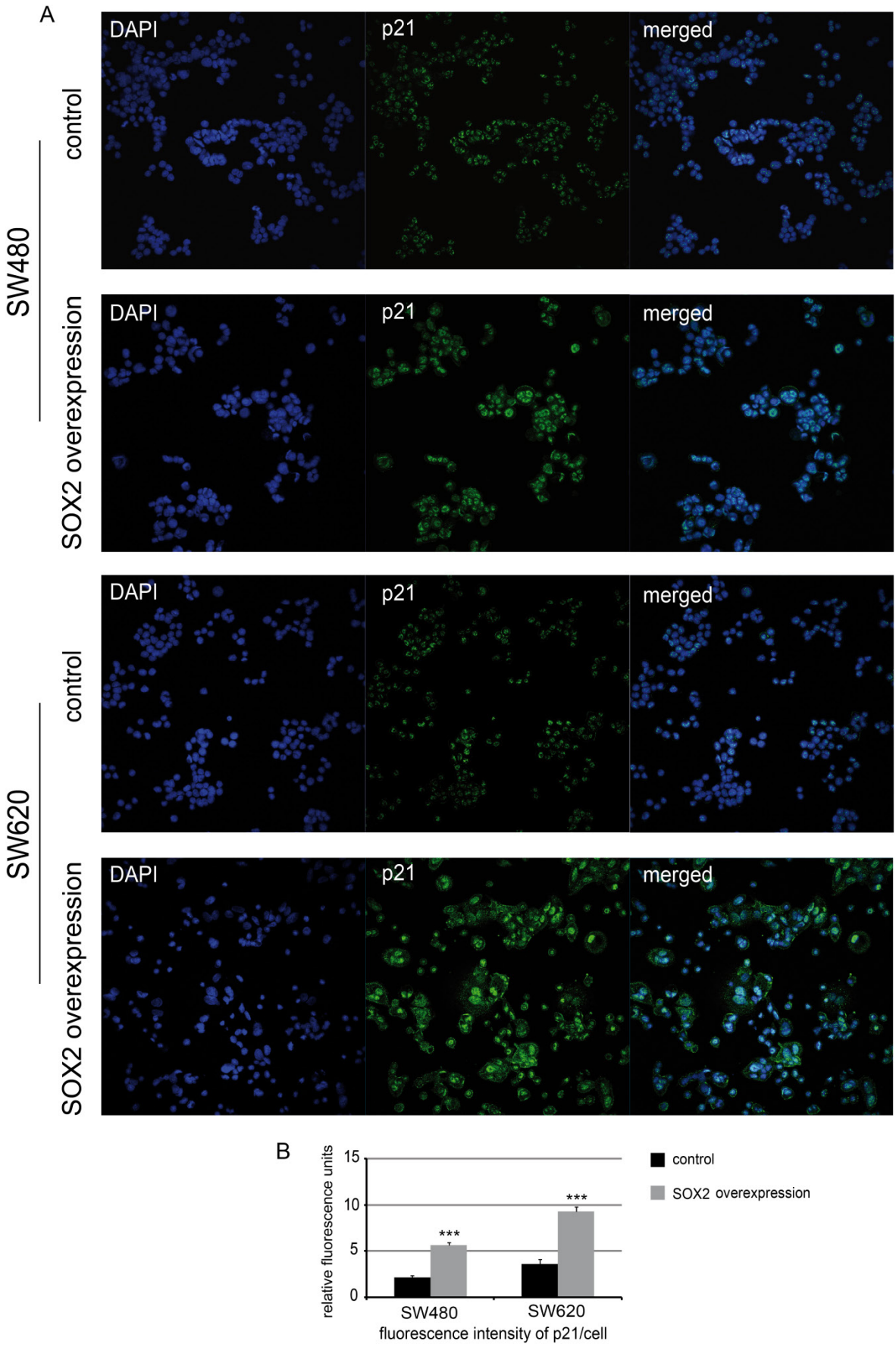

Figure 14. *Immunocytochemical changes in p21 expression caused by SOX2 transduction in SW480 and SW620 cells*. (**A**) Immunocytochemistry for p21 in control SW480 and SW620 *vs* SOX2- overexpressing cells. (**B**) Quantification of fluorescence levels of p21 staining per cell.

2.2 Exploring the p53 and p21 dependence of SOX2-induced cell cycle phenotypes

The above results suggested a link between the induction of a G1/S arrest by the expression of high SOX2 levels in SW620 cells and the upregulation of p27 and p21. While p27 is under complex transcriptional and translational regulation [453]–[457], p21 is a well-known p53 transcriptional target, although it can also be under p53-independent regulation [458], [459]. SW480 and SW620 cells lack functional p53 [460] and as a consequence, we do not expect the observed p21 upregulation to be dependent on p53.

In order to determine if the G1/S arrest induced by SOX2 overexpression is dependent on p21, we transduced SOX2 into clonal variants of the HCT116 colorectal cancer cell line that had been knocked out for p21 [461] and studied their cell cycle profiles compared to a parental cell line with a wild-type p21 gene (Figures 15 & 16). In parallel, we also overexpressed SOX2 in a HCT116 clone knocked out for p53 and its matched parent clone harboring wild-type p53, with the aim to assess SOX2-induced cell cycle effects in a different cell type and their p53 dependence or independence.

After retroviral transduction, exogenous SOX2 expression levels were verified by Western blotting (Figure 15A). Cell cycle analysis showed that SOX2 overexpression induced a significant accumulation of cells in G1 in parental and p53 knockout cells, but not in p21 knockout cells (Figure 15B & C), suggesting that this SOX2-induced effect is p53-independent and p21-dependent in HCT116 cells. Next, SOX2-transduced cells were subjected to mitotic block with nocodazole to determine the proportion of cells with long-lasting G1/S arrest. Under these conditions, SOX2 overexpression caused a significant accumulation of cells in G1 in wild-type (parental), p21 KO and p53 KO variants, with no significant differences observed for this accumulation between the different HCT116 variant clones (Figure 16). These results suggest that transient G1 accumulation induced by high levels of SOX2 is p21-dependent but p53-independent, while long-lasting G1/S arrest is independent of both p21 and p53.

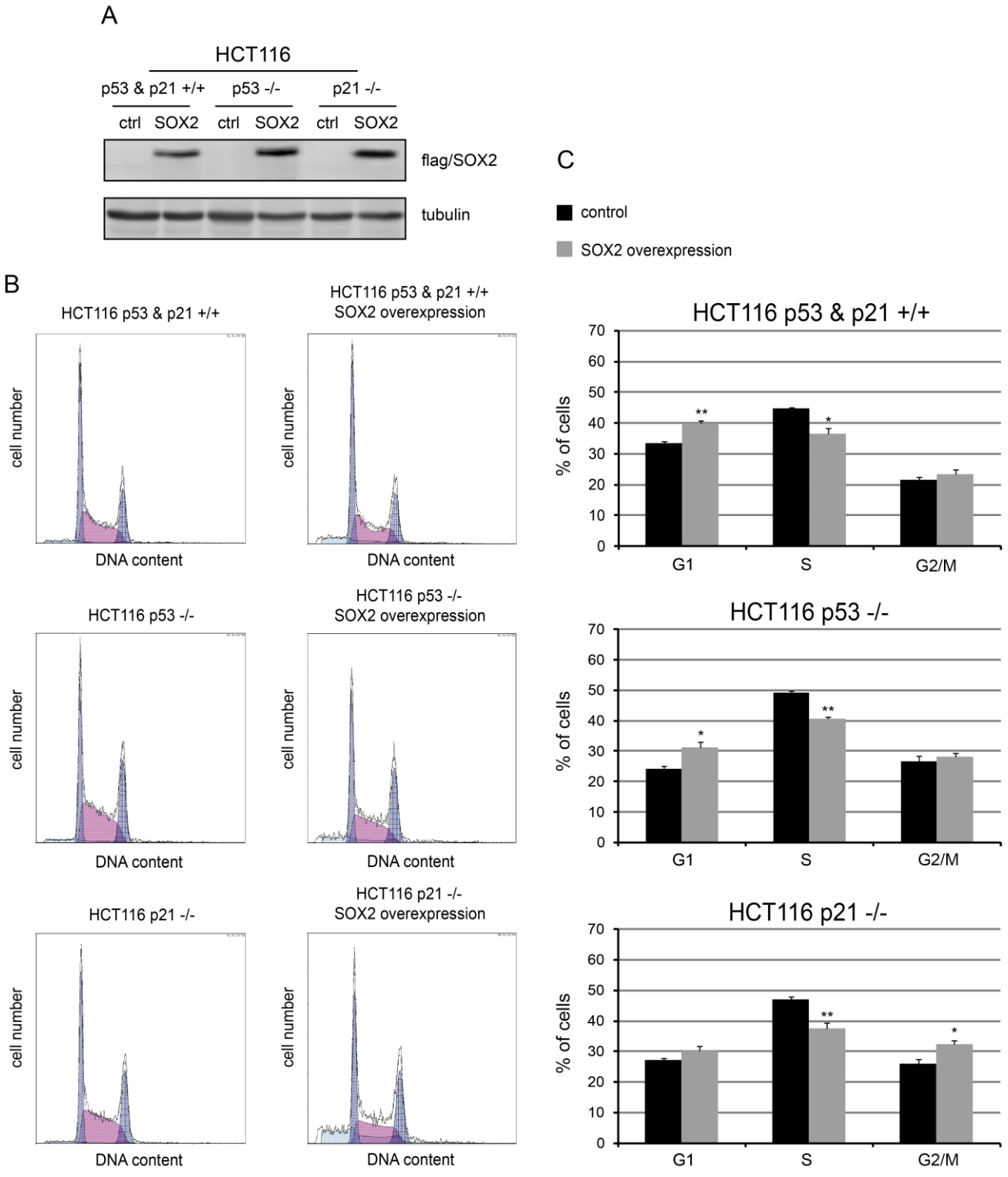

Figure 15. *Role of p53 and p21 in cell cycle blocks due to SOX2 overexpression in HCT116 colorectal cancer cell line variants (I)*. (**A**) Western blot showing SOX2 overexpression in parental, p53 KO or p21 KO clones of the HCT116 cell line. (**B**) Cell cycle profiles in these variants in control or SOX2-transduced conditions. (**C**) Graphical representation of the distribution of cells in different phases of the cell cycle.

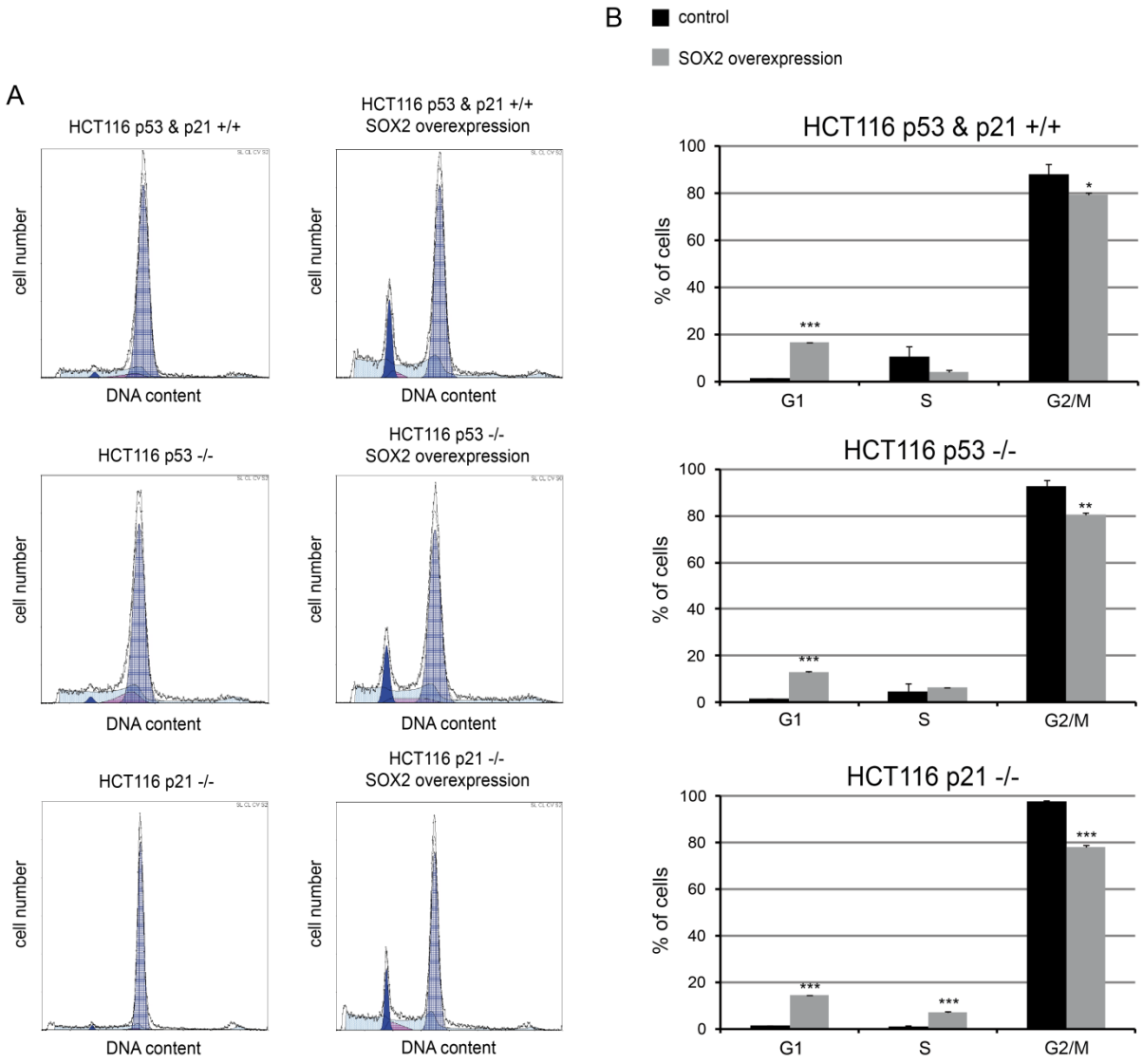

Figure 16. *Role of p53 and p21 in cell cycle blocks due to SOX2 overexpression in HCT116 colorectal cancer cell line variants (II)*. (**A**) Flow cytometry histograms of DNA content in HCT116 variants after G2/M blockade with nocodazole in control *vs* SOX2-transduced conditions, and (**E**) graphical representation of cell distribution in different phases of the cell cycle.

2.3 Assessing DNA damage response (DDR) upon SOX2 overexpression

The evidence provided above indicates that the cell cycle effects induced by overexpression of SOX2 in SW620 and HCT116 cells do not involve p53-mediated responses. Reprogramming factors, including SOX2, induce DNA damage leading to cell cycle arrest and senescence during the generation of induced pluripotent cells [462]. Therefore, we next assessed whether overexpression of SOX2 in SW480 and SW620 cells caused DNA damage to an extent that might help to explain the increase in apoptosis preferentially observed in SW480 cells and the G1/S arrest observed in SW620 cells. DNA

damage was evaluated by means of immunofluorescent staining for two established DDR markers, phospho-H2AX and 53BP1.

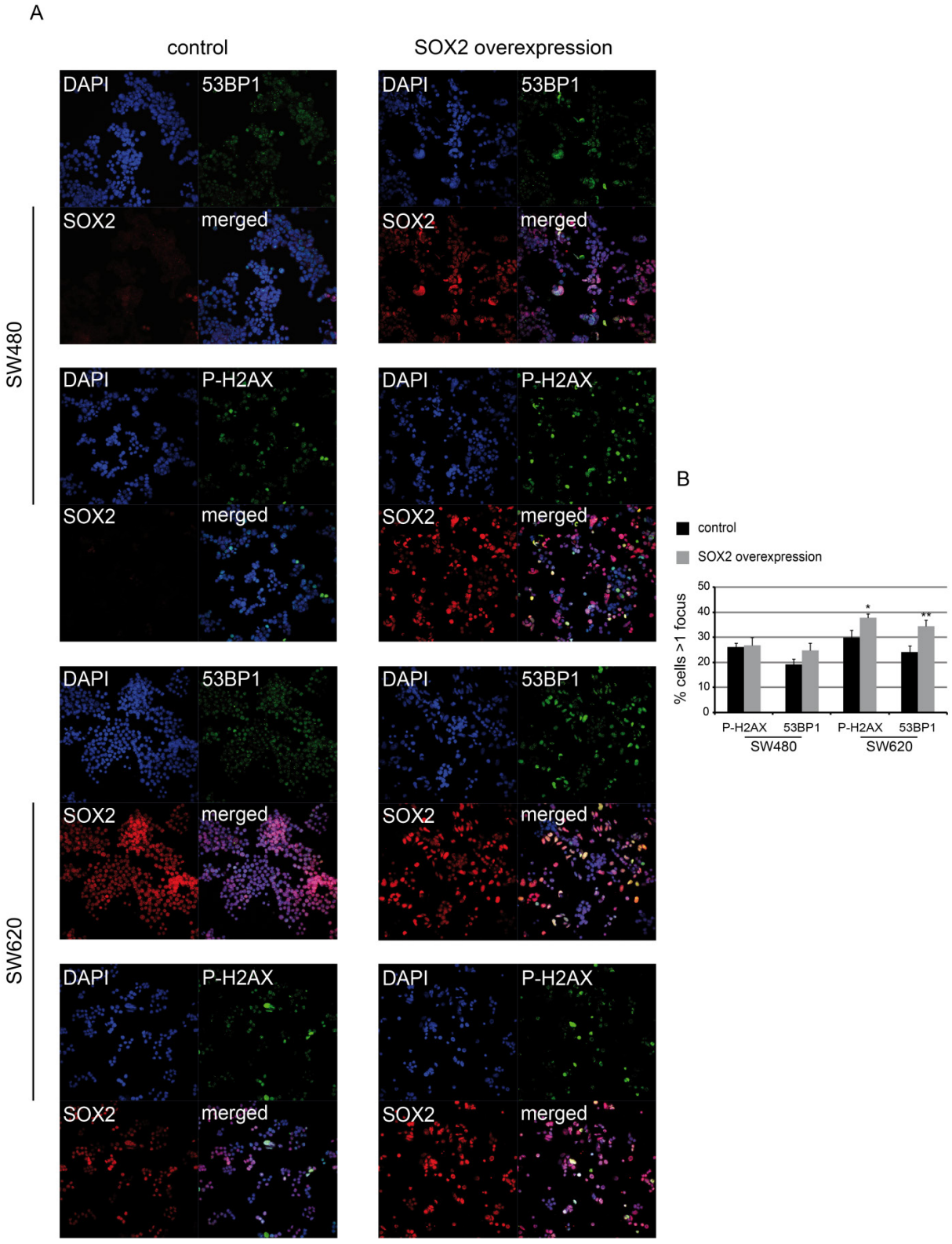

Figure 17. *Immunocytochemical assessment of DNA damage induced by SOX2 overexpression in SW480 and SW620 cells (I)*. (**A**) Immunocytochemistry for the detection of P-H2AX, 53BP1 and SOX2 in control and SOX2-transduced SW480 and SW620 cells, and (**B**) graph showing quantification of percentage of cells with more than one 53BP1 or P-H2AX focus.

Both cell lines showed a significant proportion of cells with P-H2AX and 53BP1 staining (≥ 2 fluorescent foci/nucleus) under basal conditions, which might be a reflection of continued replicative and oncogenic stresses in these cells, as frequently observed in malignant cells [463]. Interestingly, SW620 cells, but not SW480 cells, responded to exogenous SOX2 with a significant increase in the proportion of cells positive for P-H2AX and 53BP1 foci (Figure 17B), thereby suggesting a link between DDR and the cell cycle phenotype observed in this cell line.

Attempting to discriminate whether the observed foci are related to replicative stress, we assessed the colocalization of P-H2AX or 53BP1 with nuclei positive for cyclin A, which marks mainly S and G2 phases of the cell cycle (Figure 18). Overexpression of SOX2 in SW620 cells was not associated with significant changes in the proportion of cyclin A-positive nuclei containing P-H2AX foci, which may argue against replicative stress being induced by SOX2 in these cells. On the other hand, overexpression of SOX2 in SW620 cells resulted in diminished numbers of cyclin A-positive nuclei with 53BP1 foci (Figure 18B). Given that the recruitment of 53BP1 and downstream components of the repair machinery at DNA damage sites tends to occur outside of mitosis [464], we infer that the majority of the newly induced 53PB1 foci observed after SOX2 overexpression in SW620 cells occur in cells that are in the G1 phase of the cell cycle, which is consistent with the G1/S block described above. Together, these observations suggest that the expression of high levels of exogenous SOX2 in SW620 cells induces DNA damage outside of the S phase of the cell cycle, and thus it is unlikely to be related to replicative stress.

As described above, the overexpression of SOX2 in SW480 cells did not prompt an overall modulation of P-H2AX or 53BP1 foci (Figure 17). However, we observed that it caused a decrease in cyclin A-positive nuclei containing P-H2AX foci and an increase in cyclin A-positive nuclei containing 53BP1 foci (Figure 18B). The interpretation of these observations is not straightforward, since P-H2AX participates in DDR cascades upstream of 53BP1 [465].

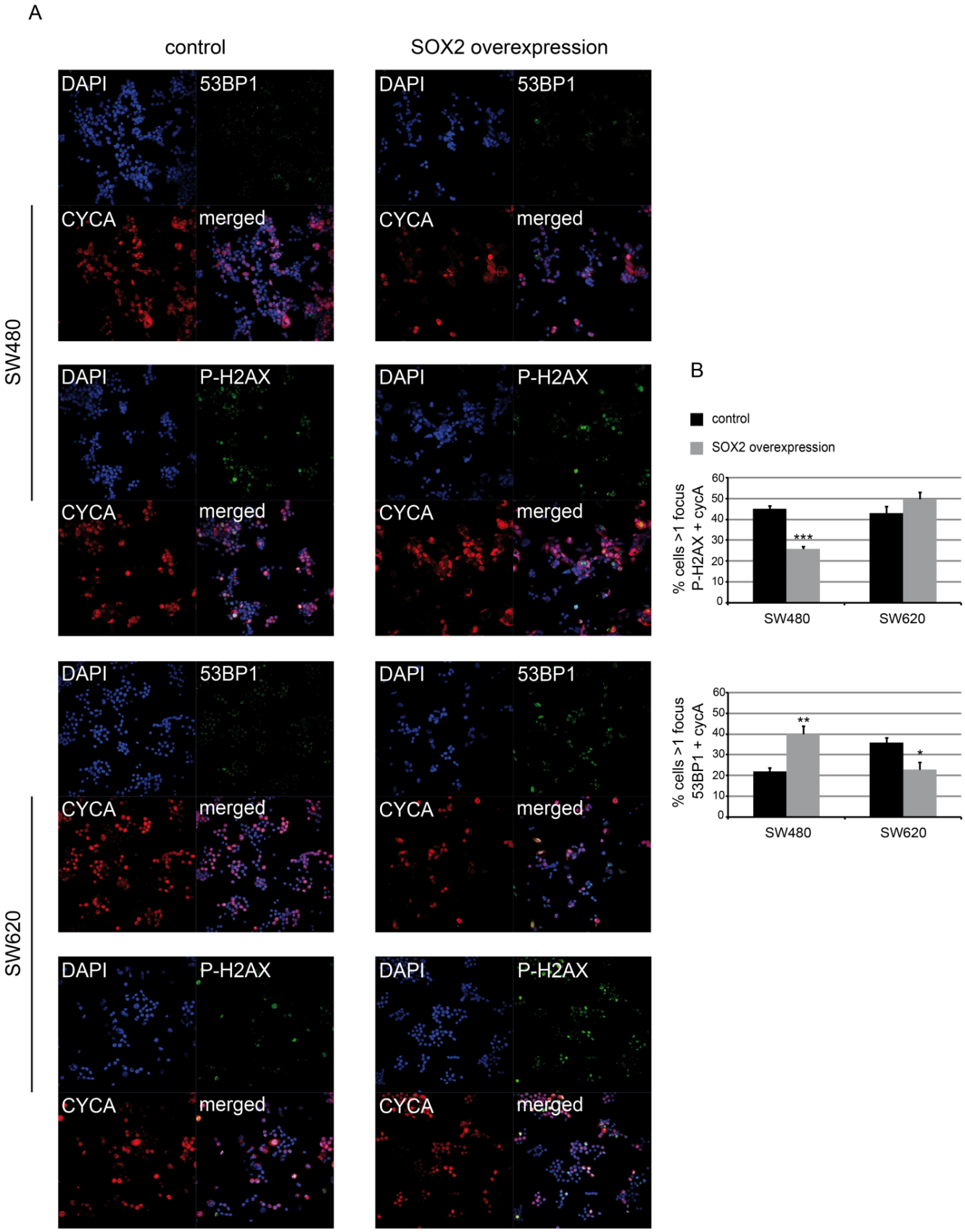

Figure 18. *Immunocytochemical assessment of DNA damage induced by SOX2 overexpression in SW480 and SW620 cells (II)*. (**A**) Immunocytochemical analysis to study the colocalization of cyclin A and P-H2AX or 53BP1 in control or SOX2-transduced SW480 and SW620 cells, and (**B**) graphs showing quantification of the signal colocalization observed in (**A**).

2.4 SOX2 overexpression and induction of reactive oxygen species (ROS)

The above results indicated the occurrence of DNA damage as a result of exogenous SOX2 overexpression in SW620 cells, albeit possibly unrelated to replicative stress. We thus explored the induction of reactive oxygen species (ROS) as another potential mechanism that might help to explain the observed DNA damage and related phenotypes. It is well known that exacerbated oxidative stress can cause damage to lipids, proteins or DNA, and may lead to cell death. Although malignant cells can display higher rates of ROS generation than their normal counterparts, they are also endowed with compensatory mechanisms, including the upregulation of ROS scavenging molecules, which permit their survival against ROS insults [466]. Importantly, inducing oxidative stress and targeting antioxidant systems have been explored as therapeutic approaches in cancer.

Figure 19 illustrates ROS levels detected in SW480 and SW620 cells as the intracellular oxidation of the H_2DCFDA fluorescent reporter quantified by flow cytometry. Interestingly, we observed that SW480 cells had higher basal

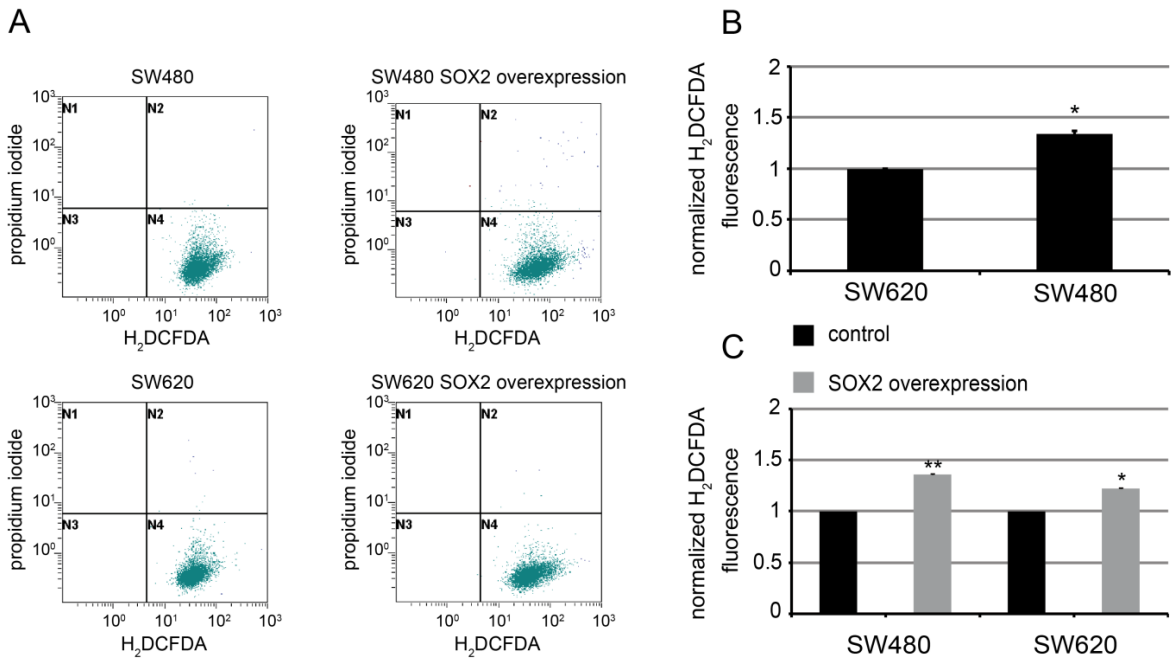

Figure 19. *Assessment of ROS generation induced by SOX2 overexpression in SW480 and SW620.* (**A**) Two parameter histogram displaying ROS generation (H_2DCFDA-oxidized fluorescence) in viable cells (no propidium iodide staining) in control SW480 and SW620 in comparison with SOX2 overexpressing cells, obtained by flow cytometry. (**B**) Normalization of ROS levels in viable cells comparing basal levels in SW620 and SW480 control cells, and (**C**) comparison of ROS levels upon overexpression of SOX2 in both cells lines referred to control levels.

levels of ROS than SW620 cells (increase of 34%, Figure 19B), perhaps reflecting their different metabolic adaptations. Importantly, overexpression of SOX2 caused an increase in ROS levels in both cell lines, with a 36% of induction in SW480 cells and a 22% of induction in SW620 cells over cells transduced with control retroviruses (Figure 19).

These observations may account for, at least partially, the induction of DNA damage in SW620 cells upon overexpression of SOX2. On the other hand, the link between increased ROS levels and apoptosis in SW480 cells in response to SOX2 overexpression is not immediately apparent. ROS induction in SW480 cells caused by high levels of SOX2 would not involve increased DNA damage, which is not observed in these cells, and thus other mechanisms (e.g. mitochondrial) should be invoked to explain the increased levels in apoptosis.

2.5 Involvement of the CDK inhibitors p21 and p27 in the cell cycle phenotype induced by the overexpression of SOX2 in SW620 cells

In preceding sections, we have described the long-lasting G1/S arrest of a significant proportion of SW620 cells caused by the overexpression of exogenous SOX2, which is accompanied with the upregulation of the CDK inhibitors p21 and p27, and the possible involvement of ROS accumulation and DNA damage as potential mechanisms that may underlie the observed phenotype. We next focused our study on further assessing the involvement of p21 and p27 in the G1/S arrest and reduction of self-renewal exerted by the overexpression of SOX2 in SW620 cells.

Our preceding experiments with HCT116 cell variants had suggested a partial p21 dependence of the G1/S arrest induced by SOX2 overexpression, possibly limited to transient but not long-lasting accumulation of cells in G1. In order to determine more directly the role of p21 in the observed phenotypes in SW620 cells, we resorted to its knock down through the expression of a specific shRNA transduced by lentiviral particles (Figure 20).

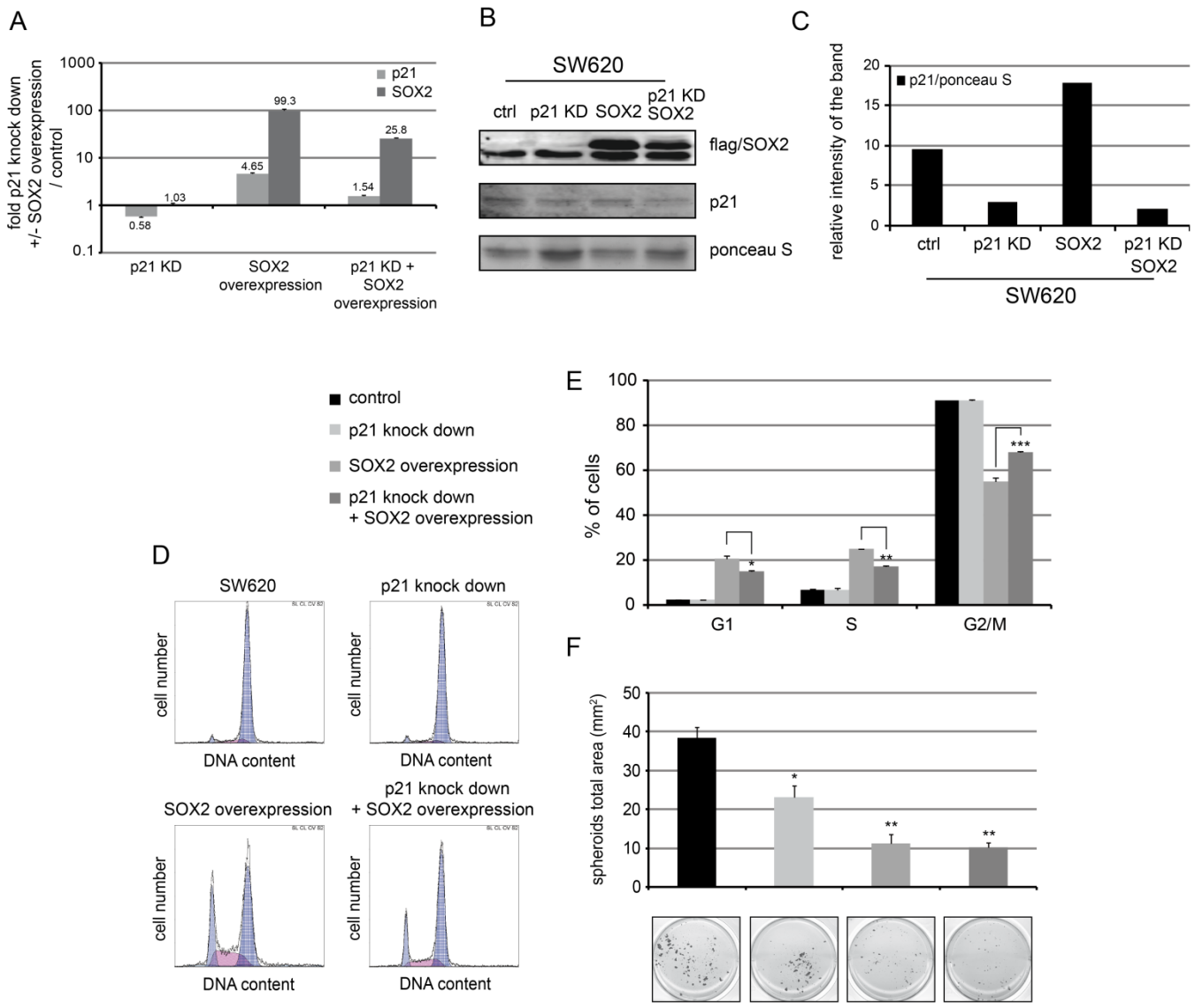

Figure 20. *Exploring the role of p21 in the G1/S arrest and inhibition of self-renewal induced by SOX2 overexpression in SW620 cells.* (**A**) RT-qPCR showing gene expression levels of p21 and SOX2 in SW620 cells knocked down for p21 (p21 KD) and/or transduced with SOX2 (SOX2 overexpression). (**B**) Western blot to assess p21 and flag/SOX2 protein levels in the generated cell lines. (**C**) Quantification of p21 protein levels, corresponding to (**B**). (**D**) Flow cytometry histograms showing DNA content profiles in the generated cell lines after cell cycle synchronization in G2/M with nocodazole. (**E**) Quantification and distribution in each phase of cell cycle, corresponding to (**D**). (**F**) Spheroid formation assay in control or p21 KD and/or SOX2-overexpressing SW620 cells.

The shRNA used in these experiments caused a relatively modest knock down of p21 at the transcript level (decrease of 40% relative to control cells), but it demonstrated its efficiency in diminishing the observed upregulation induced by SOX2 overxpression (Figure 20A), as also confirmed by Western blotting (Figure 20C). Of interest, although both p21 knock down and control cells were transduced in parallel with SOX2 retroviral particles, SOX2 was expressed at consistently lower levels in p21 knock down cells (Figure 20B),

possibly reflecting one or more levels of regulation of SOX2 by p21 [467]. After documenting concomitant p21 repression and SOX2 overexpression in SW620 cells, we performed cell cycle analysis following cell synchronization with nocodazole in order to assess the induction of long-term G1/S arrest. We observed that overexpression of SOX2, but not knock down of p21 alone, caused a long-term G1/S arrest in a significant proportion of cells (Figure 20D). Knock down of p21 led to a decrease (approximately 15% of cells) in the G1/S arrest imposed by SOX2 overexpression (Figure 20D & E). Simultaneously, p21 knock down was accompanied with an increase in cells blocked in G2/M (Figure 20D & E). This suggests that knock down of p21 partially relieves the SOX2-induced long-term G1/S arrest, thus improving this cell cycle transition in SW620 cells.

We next tested the effects of p21 knock down on the anchorage-independent growth of SW620. Contrary to the lack of observable cell cycle effects in comparison with unmanipulated SW620 cells, and the partial recovery from the SOX2-induced arrest observed above, knock down of p21 alone inhibited the formation of spheroids and was unable to revert the strong suppression of spheroid growth caused by SOX2 overexpression (Figure 21F). Hence, these results suggest a dichotomous role for p21 in the phenotypes induced by the overexpression of exogenous SOX2 in SW620 cells: it is partially responsible for the G1/S cell cycle arrest but not for the inhibition of self-renewal.

The same approach was used to study the role of p27 in the phenotypes induced in SW620 cells by SOX2 overexpresion, with the addition of double knock down experiments for p21 and p27 (Figure 21A). As observed above for p21 knock down, single p27 or double p21 and p27 knock down did not alter the basal cell cycle profiles as compared to control cells (not shown) or in their arrest in G2/M upon nocodazole treatment (Figure 21B & C). A double p21 and p27 knock down partially relieved the G1/S arrest induced by SOX2 overexpression, to the same extent, but not greater than, the relief exerted by knocking down p21 alone as observed above (Figure 20D & E). This suggests that p21, but not p27, plays a role in the long-term G1/S arrest induced by overexpression of SOX2 in SW620 cells.

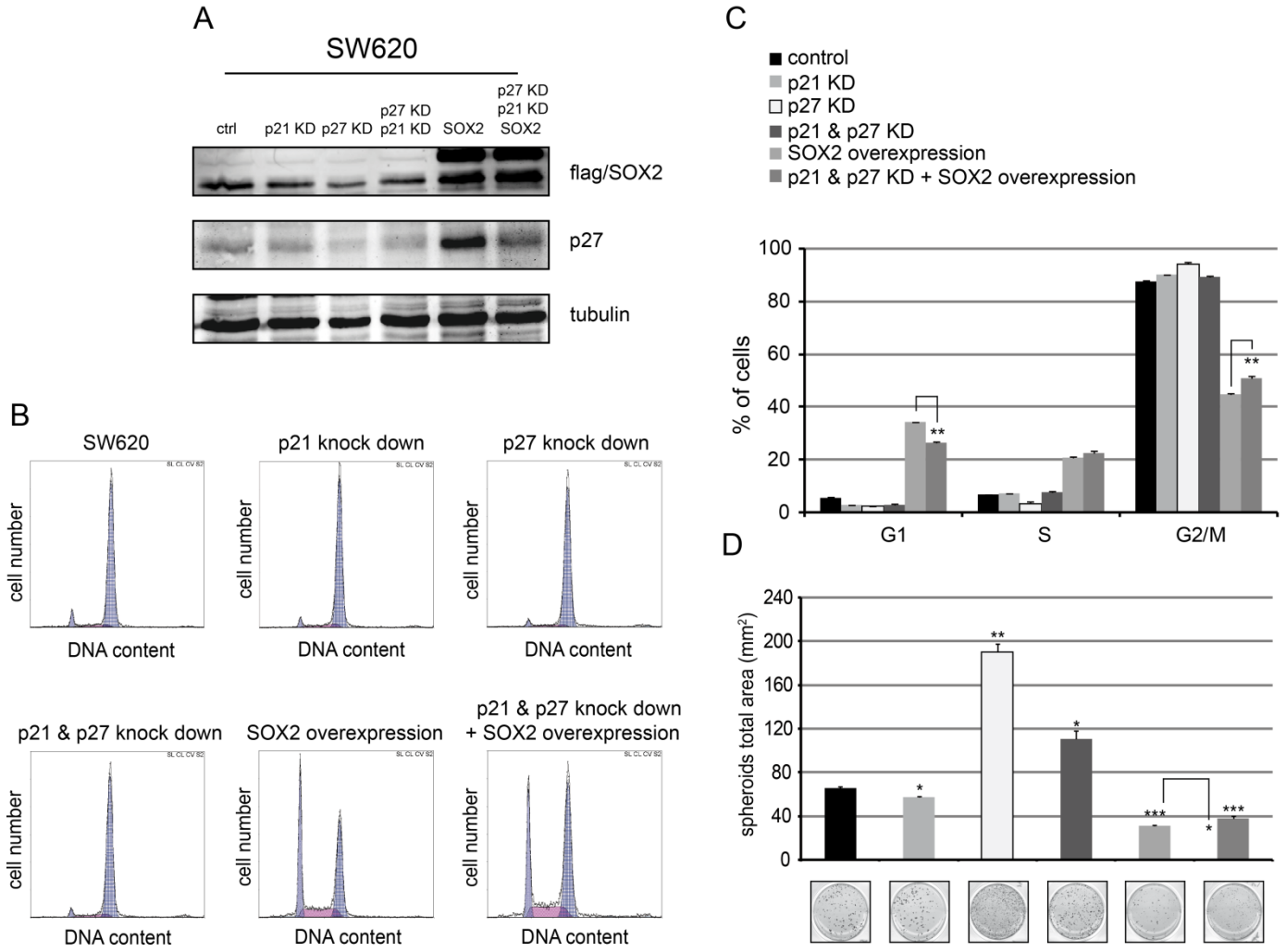

Figure 21. *Exploring the role of p21 and p27 in G1/S block and inhibition of self-renewal induced by SOX2 overexpression in SW620 cells*. (**A**) Western blot showing p27 and flag/SOX2 levels in control cells, p21 and/or p27 repressed with or without SOX2 overexpression. (**B**) DNA content histograms of the generated cell lines obtained by flow cytometry, and (**C**) quantification and distribution in each phase of cell cycle. (**D**) Effect in spheroid formation in control and SW620 cells with p21 and/or p27 knock down, with or without SOX2 overexpression.

When these cells were tested for spheroid formation under anchorage-independent growth conditions, we observed that knock down of p27 caused a remarkable increase in the number of colonies as compared to control cells, although these spheroids were smaller in size. A double p21 and p27 knock down partially rescued the inhibition of spheroid formation caused by SOX2 overexpression (Figure 21D). Therefore, these results suggest yet another dichotomous function for p27 in the phenotypes induced by the overexpression of SOX2 in SW620 cells, but in opposite roles observed for p21: p27 does not appear to be involved in the long-term G1/S arrest caused by SOX2

overexpression, but it is partially responsible for the observed loss of self-renewal. We would like to note that these two complementary roles of p21 and p27 in two phenotypic traits induced by SOX2 overexpression in SW620 cells, cell cycle arrest and inhibition of anchorage-independent growth, appear to only partially explain such effects and thus additional mechanisms are likely to exist that may help to provide a full mechanistic explanation of the observed effects.

2.6 Effects of SOX2 silencing on cell cycle and self-renewal in SW620 cells

We showed above (Objective 1) that silencing of SOX2 expression in cell lines with relative high endogenous levels also impaired cell proliferation. We extend below our study to the effects of SOX2 silencing on relevant growth properties of the metastatic cell line SW620 (Figure 22).

Knock down of SOX2 in SW620 cells did not elicit major changes in cell morphology, which continued to show the typical rounded shape displayed in control cells, although cells tended to grow scattered without forming the compact clusters observed in control cells (Figure 22A). Interestingly, cell cycle profiles showed an accumulation of cells in G1 and G2/M in detriment of cells in S phase as compared to controls (Figure 22B & C). Moreover, cell cycle profiling after nocodazole treatment indicated the long-lasting nature of the G1 arrest (Figure 22D & E). In addition, in both cell cycle profile determinations, a small sub G1 subpopulation was observed upon SOX2 silencing.

Consistent with the observed G1/S arrest, an upregulation of p21 and p27 transcripts, being particularly strong in the case of the latter, was observed in SW620 cells knocked down for SOX2 (Figure 22F & G), with an increased nuclear localization of p27 as visualized by immunofluorescence (Figure 22H). In addition, and also in agreement with the cell cycle profiles, cyclin D1 and B1 were downregulated upon SOX2 knock down (Figure 22H). Finally, the ability of SW620 cells to form spheroids was almost completely abrogated when SOX2 was silenced (Figure 22I).

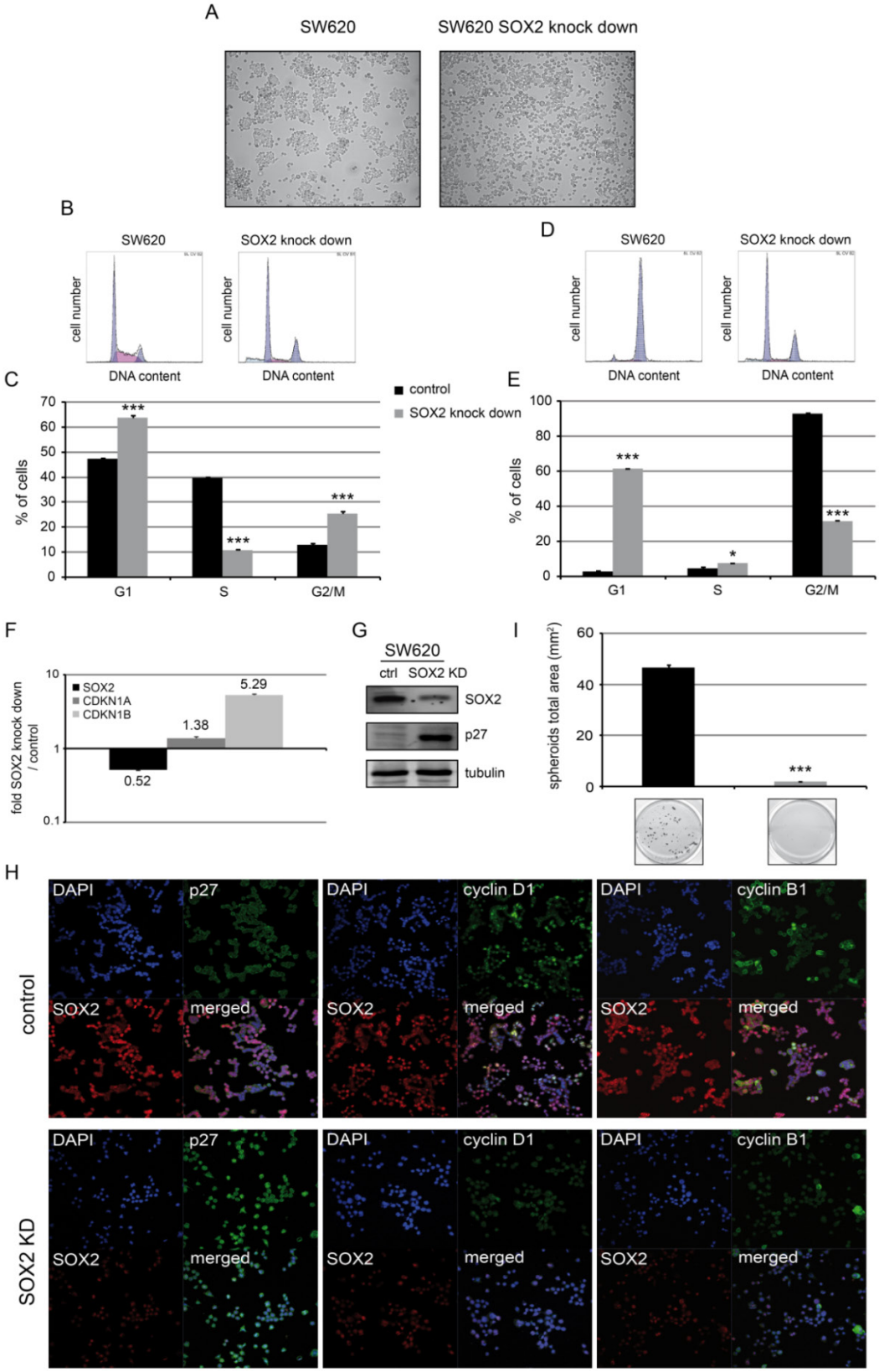

Figure 22. *Characterization of growth effects of SOX2 knock down in SW620 cells.* (**A**) Bright field images displaying control and knock down cells. (**B**) Flow cytometry histograms showing DNA content profiles of control and SOX2 knock down (SOX2 KD) SW620 cells, and (**C**) quantification and distribution in each phase of cell cycle of these cell lines. (**D**) Flow cytometry histograms showing DNA content profiles of control and SOX2 KD SW620 cells after G2/M synchronization with nocodazole, and (**E**) quantification and distribution in each phase of the cell cycle. (**F**) RT-qPCR showing SOX2, p21 and p27 gene expression levels in control and SOX2 KD SW620 cells. (**G**) Western blot comparing SOX2 and p27 protein levels in control *vs*. SOX2 KD cells. (**H**) Immunocytochemistry for p27, cyclin D1 and cyclin B1 in control and knock down cells. (**I**) Effect in spheroid formation of the SOX2 knock down in SW620 cells.

2.7 Role of p27 in SW620 cell cycle and growth phenotypes caused by SOX2 knock down

We next followed a similar approach to that used above in order to address the possible involvement of p27 in the G1 arrest and inhibition of self-renewal caused in SW620 cells by SOX2 knock down (Figure 23). To this end, we generated single and double knock down cells for p27 and SOX2 (Figure 23A) and monitored relevant functional readouts. First, when cell cycle profiles were analyzed after G2/M nocodazole synchronization, we observed that up to 15% of the cells that were arrested in G1 upon SOX2 knock down, were released from the arrest upon concomitant knock down of p27 (Figure 23B & C).

Consistent with the emergence of sub G1 subpopulations upon SOX2 knock down, a 20% decrease in cell viability was observed (Figure 23D & E), which was not reverted by a double p27 and SOX2 knock down. Similarly, p27 knock down did not rescue the abrogation of self-renewal due to silencing of SOX2 in SW620 cells (Figure 23F).

We offer the following unifying interpretation for these apparently divergent sets of observations: On the one hand, SOX2 is absolutely required for the self-renewal properties of SW620 cells, as evidenced by the almost complete inhibition of spheroid growth as a consequence of SOX2 knock down, which is not rescued by p27 knock down. SOX2 is also required for a normal G1/S cell cycle transition through putative repression of p27 and p21, suggested by the upregulation of these two CDK inhibitors elicited by SOX2 silencing. The G1/S block that follows SOX2 knock down is partially reverted by knock down of p27, which indicates that this arrest is partially mediated by this CDK inhibitor. Other laboratories have demonstrated a transcriptional repression of SOX2 by p21 and p27 [467], [468], which, together with our observations, may suggest the existence of a mutually repressive transcriptional loop between SOX2 and p21, and SOX2 and p27.

On the other hand, as shown above, the expression of high levels of exogenous SOX2 in SW620 cells leads to DNA damage and oxidative stress, known inducers of cell cycle arrest and apoptosis [469], [470]. Our evidences suggest that the observed G1/S arrest is mediated, at least in part, through p21,

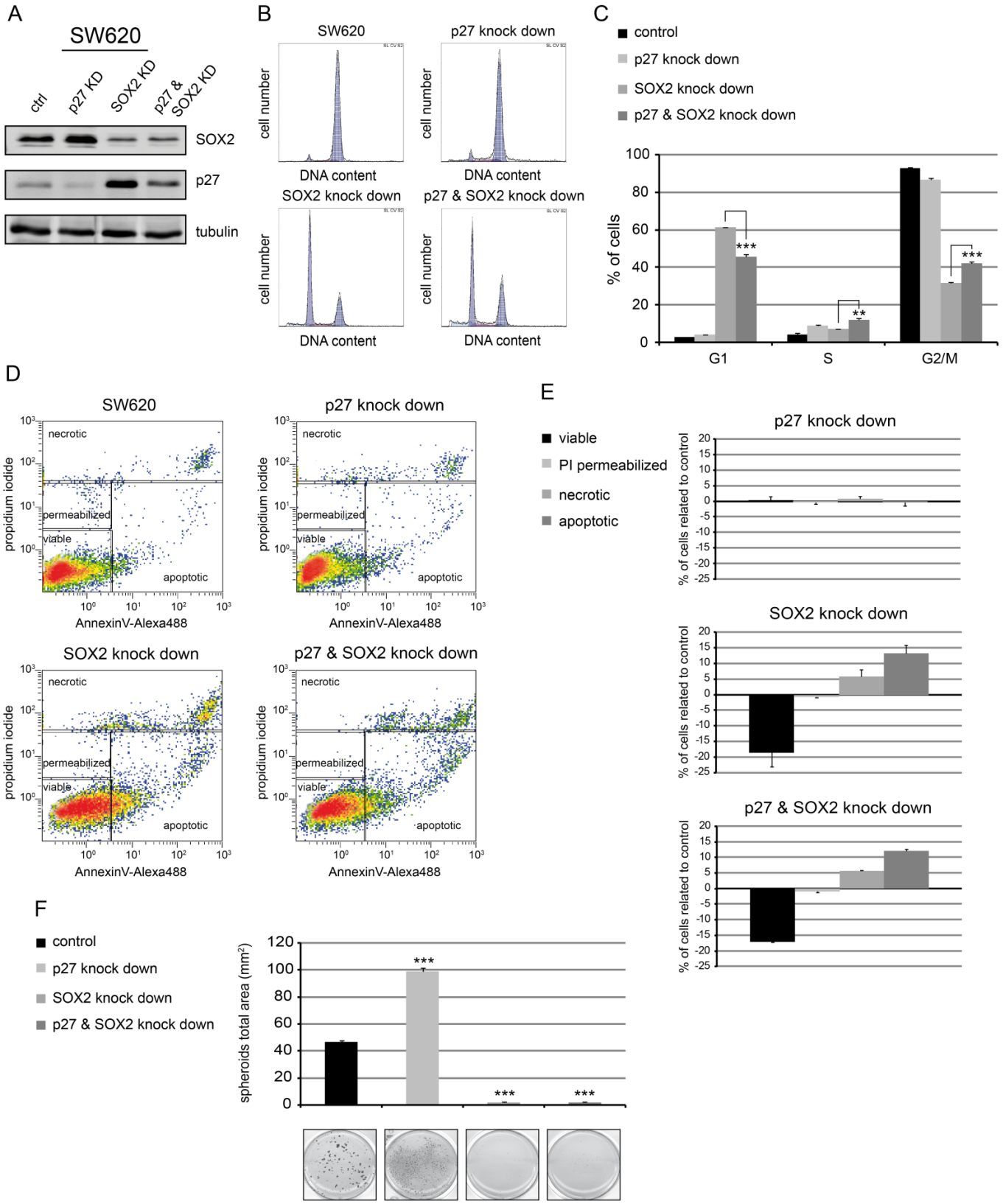

Figure 23. *Exploring the role of the CDK inhibitor p27 in the growth phenotypes induced in SW620 by SOX2 knock down.* (**A**) Western blot comparing SOX2 and p27 protein levels in control SW620, p27 knock down, SOX2 knock down and double p27 & SOX2 knock down. (**B**) Flow cytometry histograms showing DNA content profiles of control, p27 and/or SOX2 knock down SW620 cells after G2/M synchronization with nocodazole, and (**C**) quantification and distribution in each phase of the cell cycle of these cell lines. (**D**) Flow cytometry determination of viable, apoptotic and necrotic cells, and (**E**) normalization referred to control cells of viable, permeabilized for propidium iodide, necrotic and apoptotic subpopulations. (**F**) Effect on spheroid formation in SW620 cells with p27 and/or SOX2 knock down as compared to control cells.

whose upregulation may be a consequence of the engagement of general p53-independent stress-induced pathways [459] rather than a specific transcriptional activation by SOX2. The increased spheroid growth observed after p27 silencing suggests that it functions as an inhibitor of self-renewal in SW620 cells. The inability of its knock down to rescue the spheroid growth inhibition caused by SOX2 knock down may be attributed to the absolute requirement for SOX2 of this growth property in SW620 cells.

2.8 Transcriptional regulation of p27 by SOX2

The foregoing considerations imply a direct or indirect transcriptional regulation of p27 by SOX2, as supported by transcript upregulation. This assumption was substantiated by means of experiments with a p27 promoter-specific luciferase reporter system [441] that showed enhanced p27 transcriptional activity both by SOX2 overexpression and by SOX2 knock down (Figure 24A & B). As control and normalizer of transfection efficiency, we co-transfected a plasmid for the expression of the *Renilla* luciferase gene under a constitutive promoter.

We next reasoned that, if endogenous SOX2 is a p27 transcriptional repressor, the transcriptional upregulation observed upon SOX2 knock down could be counteracted by reintroducing a SOX2 mRNA in cells that is not targeted by the shRNA used for knock down. The retroviral construct used for the transduction of exogenous SOX2 throughout this study is adequate for these complementation experiments, since it lacks the endogenous SOX2 3'UTR sequences targeted by the shRNA used. However, because high levels of exogenous SOX2 also caused p27 upregulation, we first performed preliminary titration experiments aimed at finding the appropriate conditions to yield exogenous SOX2 levels sufficient to complement knock down, but below a putative threshold triggering p27 upregulation.

Thus, we knocked down SOX2 in SW620 cells and subsequently transduced them with different dilutions of retrovirus supernatants (ranging from 1/5 to 1/160). SOX2 and p27 transcript levels were assessed by RT-qPCR (Figure 24C), showing that transduction with the highest dilution of retroviral particles (1/160) restored SOX2 levels that approached those of control cells

and were thus considered to provide the desired complementation conditions. Cells were then transfected with the p27 promoter reporter construct, and firefly luciferase activity was measured and normalized to the co-transfected *Renilla* luciferase activity. The results show that the upregulation of p27 transcription induced by SOX2 knock down, was significantly blunted by restoration of SOX2 levels with exogenous shRNA-resistant SOX2 (Figure 24E). This supports the conclusions that SOX2 is a p27 transcriptional repressor. Chromatin immunoprecipitation experiments are underway to determine whether SOX2 directly associates with specific binding sites at regulatory regions of the p27 gene.

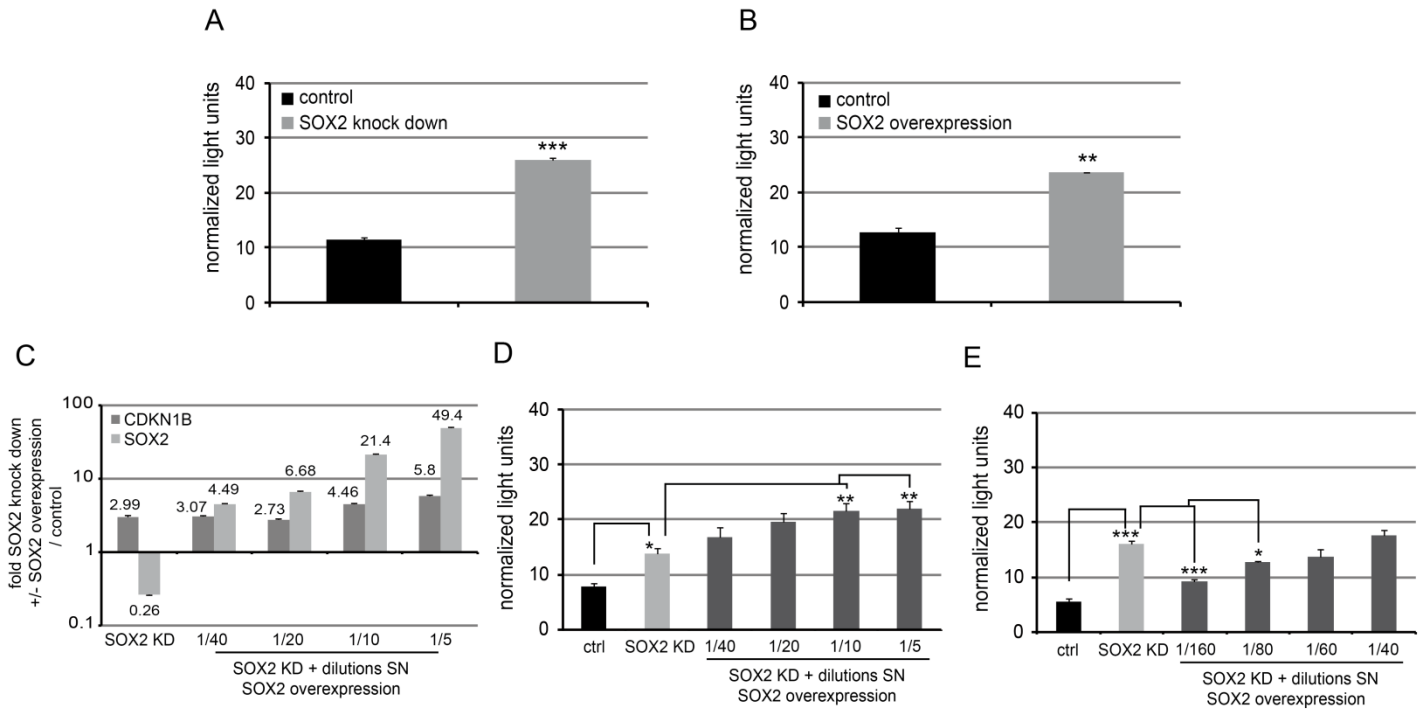

Figure 24. *Exploring the induction of CDK inhibitor p27 in SW620 cells as a function of SOX2 levels.* (**A**) Luminometric measures of p27 firefly luciferase reporter in control *vs*. SOX2 knock down SW620 cells, and (**B**) in control *vs*. SOX2 overexpressing SW620 cells. (**C**) RT-qPCR showing p27 (CDKN1B) and SOX2 gene expression levels normalized to control cells, in SW620 SOX2 knock down with or without overexpression of SOX2 transduced with different dilutions of retrovirus supernatants (SN). (**D** & **E**) Luminometric measures of p27 firefly luciferase reporter in control SW620 and in SOX2 knock down cells with or without overexpression of SOX2 performed with indicated dilutions of retrovirus supernatants.

2.9 Transcriptional profiling of SW620 SOX2 knock down cells

With the aim to extend our study and find candidates that could account for the G1/S arrest and loss of self-renewal in SW620 with SOX2 silenced, the expression levels of a selection of genes of potential interest were quantified by RT-qPCR (Figure 25). Among the genes analyzed, we assessed the levels of genes related to self-renewal, pluripotency, differentiation and stem cell markers (KLF4, NANOG, MYC, OCT3/4, POU2F1, CD24, KLF9 and LGR5), genes involved in Wnt signaling and nuclear pore complex (RNF128, RNF43, ZNRF3, NUP188), mesenchymal and epithelial markers (SPARC, VIM, FN1, DSP, β-catenin [CTNNB1], CDH1 [epithelial cadherin] and EPCAM), as well as transcription factors that function as inducers of epithelial-to-mesenchymal transition (EMT) (TWIST2, SNAI1, SNAI2 and ZEB1).

This analysis corroborated once more the upregulation of p21 and, more significantly, p27, upon SOX2 knock down in SW620 cells (Figure 25). Of additional interest, we found an association of upregulation of EMT inducers (TWIST2 and ZEB1) and mesenchymal markers (SPARC, VIM, FN1) with downregulation of epithelial markers (epithelial cadherin, EPCAM), suggesting that knock down of SOX2 provokes an EMT in SW620 cells. This is in agreement with our own observation in a different cell model [130] in which SOX2 sustains an epithelial gene program. Of the self-renewal genes analyzed, MYC and NANOG were moderately downregulated but KLF4 was strongly upregulated in SW620 SOX2 knock down cells. Remarkably, the intestinal stem cell marker LGR5 was profoundly downregulated in SOX2-silenced cells as compared to control cells. The latter observation caught our attention, because it suggests that SOX2 regulates the expression of LGR5, a seven-transmembrane protein that plays a prominent role in conferring stem cell properties in a variety of epithelial tissues and in particular, colon and intestinal epithelium [20], [177], [471].

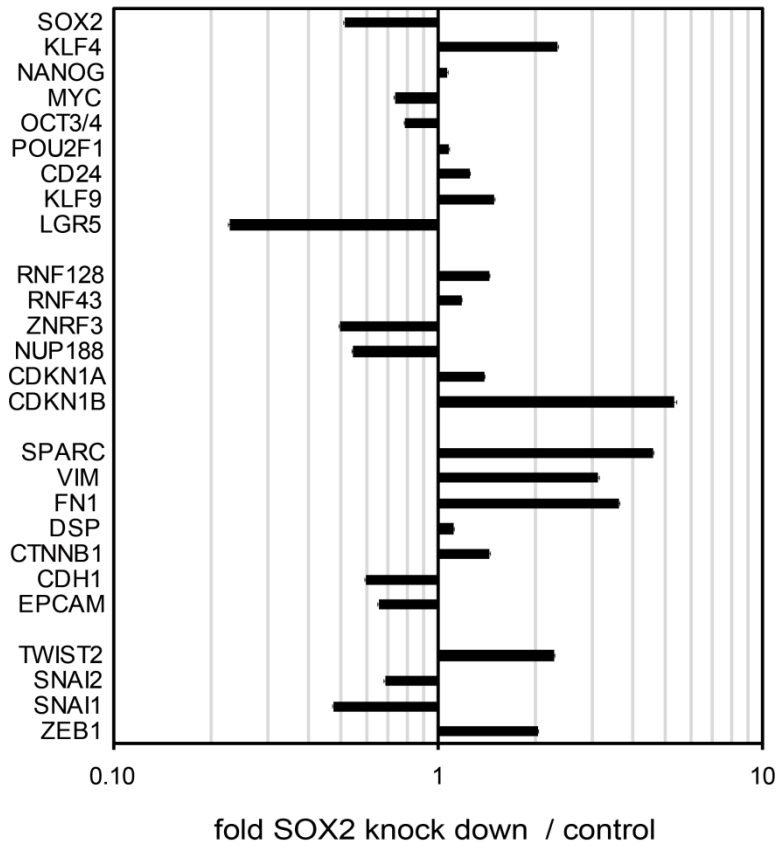

Figure 25. *Transcriptional analysis of selected genes in SOX2 knock down SW620 cells.*

2.10 Assessing the involvement of LGR5 in phenotypic traits induced by SOX2 silencing in SW620 cells

Due to the unexpected strong downregulation of LGR5 observed when SOX2 was silenced in SW620 cells, we next silenced LGR5 expression in order to determine its potential role in the phenotypes observed in SW620 cells upon SOX2 knock down (Figure 26). Morphologically, most LGR5-silenced SW620 cells displayed a polygonal and flattened shape in clear contrast with the typical rounded shape observed in control cells (Figure 26A).

Next, we determined the impact of LGR5 knock down on the spheroid formation potential and cell cycle profile of SW620 cells. Notably, downregulation of LGR5 caused a significant inhibition of spheroid growth of SW620 cells without inducing a G1/S cell arrest (Figure 26B-D). This indicates a dissociation between these two phenotypic traits and a selective role for LGR5 in sustaining the self-renewal potential of these cells.

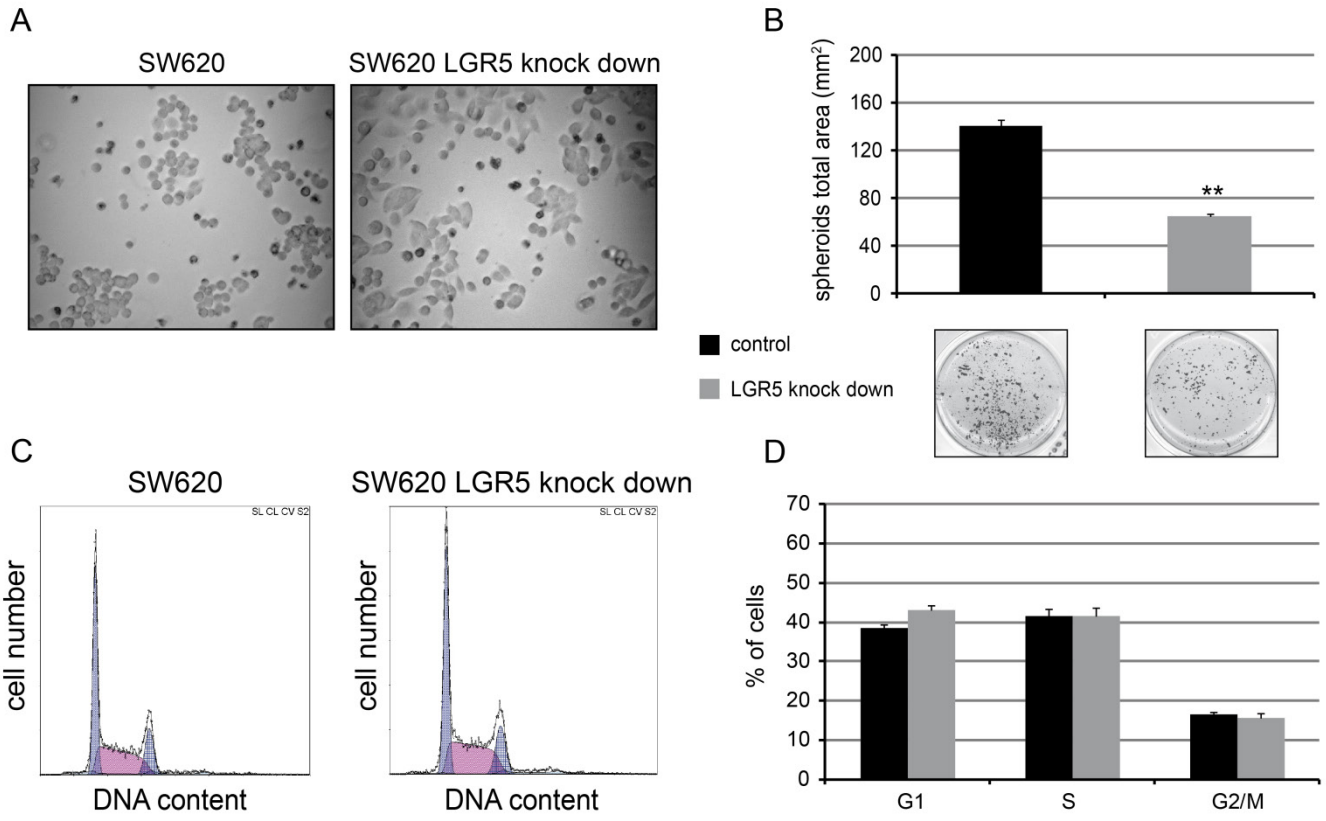

Figure 26. *Studying the potential implication of LGR5 in phenotypic traits observed in SW620 SOX2 knock down cells*. (**A**) Bright field images showing control and LGR5 knock down SW620 cells. (**B**) Effect of LGR5 knock down on spheroid formation of SW620 cells. (**C**) Flow cytometry histograms showing DNA content profiles in control and LGR5 knock down SW620 cells, and (**D**) quantification and distribution in each phase of the cell cycle.

2.11 Transcriptional profiling of SW620 LGR5 knock down cells

To gain further insight into the phenotype observed upon knock down of LGR5 in SW620 cells, we performed a RT-qPCR transcriptional profiling similar to the one described above for SOX2 knock down (Figure 27). Unexpectedly, rather than being downregulated, several of the genes related to pluripotency and self-renewal in stem cells showed an increase of expression levels (KLF4, CD24 and SOX2), thus suggesting that other molecular mechanisms not reflected in this analysis must override these upregulations in order to explain the loss of spheroid growth observed upon LGR5 knock down of SW620 cells. In the case of known or putative regulators of LGR5 and Wnt signaling [419], [472], they were either downregulated (RNF128, RNF43) or upregulated (ZNRF3) upon LGR5 knock down. Finally, as observed for SOX2 knock down, there was a tendency to downregulation of several of the epithelial markers

assessed (DSP, CDH1, EPCAM) concomitant with an upregulation of mesenchymal markers (SPARC, VIM, FN1), which suggests the induction of an EMT. In agreement with this possibility, a decrease in E-cadherin and increase in fibronectin protein levels upon LGR knock down were certified by Western blotting (Figure 27B). However, none of the EMT-inducing transcription factors determined in this validation showed a significant increase in their transcript levels upon LGR5 knock down.

Because of the described regulation exerted by LGR5 of the Wnt signaling [472], levels of β-catenin protein levels were assessed by Western blotting, but no significant changes were detected in LGR5 knock down cells. In contrast, cyclin D1, a known β-catenin transcriptional target, increased its levels relative to control cells (Figure 27B). The latter result is unlikely to be explained by an increased growth rate, because SW620 cells knocked down for LGR5 proliferate at the same rate than control cells (not shown) but are less efficient in growing spheroids.

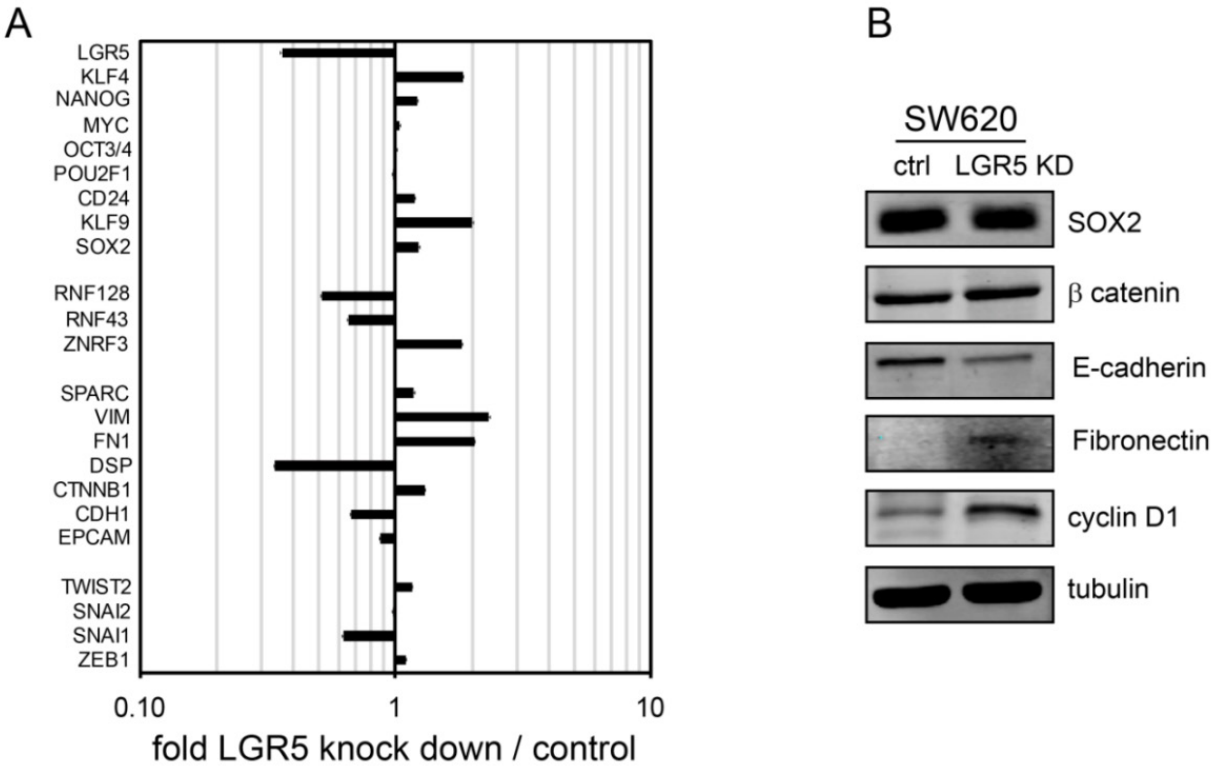

Figure 27. *Transcriptional analysis of selected genes in LGR5 knock down SW620 cells and protein levels of selected proteins.* (**A**) RT-qPCR for determining expression levels of selected genes (the same genes determined in SOX2 knock down SW620 cells) in LGR5 knock down SW620 cells normalized to control levels. (**B**) Western blot comparing SOX2, β-catenin, E-cadherin, fibronectin and cyclin D1 in control and LGR5 knock down SW620 cells.

2.12 Analysis of EMT induction in SW620 cells silenced for LGR5

The above results prompted us to further investigate whether silencing of LGR5 in SW620 cells was indeed engaging an EMT program. To this end, we performed immunofluorescence analysis to determine the localization of E-cadherin together with β-catenin and SOX2 in control and LGR5 knock down cells (Figure 28A). We found that cells knocked down for LGR5 showed a significant loss of membrane localization of E-cadherin, concomitant with a gain in nuclear localization of β-catenin. SOX2 staining did not vary noticeably between control and knock down cells.

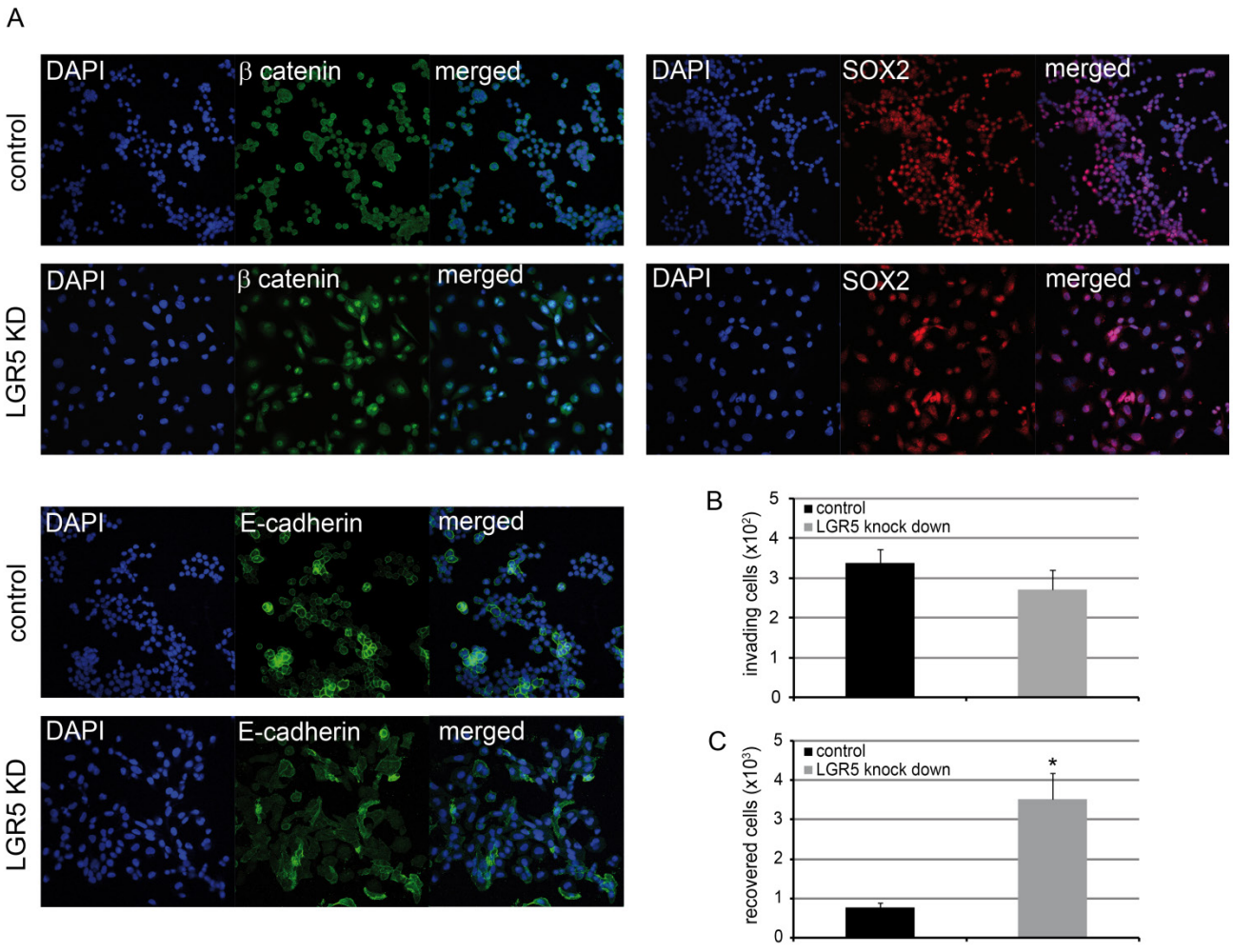

Figure 28. *Assessing epithelial-to-mesenchymal transition (EMT) in SW620 cells knocked down for LGR5.* (**A**) Immunocytochemistry in control and LGR5 knock down SW620 cells for β-catenin, E-cadherin and SOX2. (**B**) Invasiveness assay in control and LGR5 knock down SW620 cells. Cells resuspended in medium containing 0.5% FBS were seeded in the upper chamber of Transwell-Matrigel inserts and allowed to migrate to the lower chamber containing medium with 10% FBS. After 24 h, all cells in the bottom chamber were collected and counted. The assay was performed in triplicate. (**C**) Migration assay in control and LGR5 knock down SW620 cells. Cells resuspended in medium containin 0.5% FBS were seeded in the upper chamber of a Transwell insert (without Matrigel) and allowed to migrate to the lower chamber containing 10% FBS gradient. After 24 h, cells in the bottom chamber were collected and counted. This assay was performed in triplicate.

Since EMT confers to cells a gain of motility and invasion [53], [100], [101], we next assessed these traits in LGR5 knock down cells *in vitro* (Figure 28B & C). Under the assayed conditions (10% FBS gradient), SW620 cells silenced for LGR5 significantly increased their motility in comparison with control cells, although they failed to show a gain of invasiveness through Matrigel. Taken together, these results suggest that repression of LGR5 in these cells may engage a partial EMT program.

2.13 Enhanced β-catenin activity in SW620 cells silenced for LGR5

In striking contrast to other studies that have demonstrated the role of some members of the LGR family as enhancers of the Wnt signaling upon interaction with their ligands (namely R-spondins) [417], [472], [473], the preceding observations in which silencing of LGR5 in SW620 cells promoted the nuclear localization of β-catenin without an increase of protein levels, suggest that LGR5 inhibits Wnt/β-catenin signaling in SW620 cells under standard growth conditions in the absence of cognate ligands. Consequently, we next assessed the functionality of this increased nuclear localization of β-catenin in terms of TCF/LEF transcriptional factor activity.

The β-catenin transcriptional activity was determined by means of the TOPFlash/FOPFlash system [378], in which the transcription of a firefly luciferase reporter gene is driven by tandemly repeated TCF/LEF binding sites (TOPFlash) and background transcription is established by transfection in parallel cultures of a construct in which the same binding sites are mutated to prevent specific β-catenin/TCF/LEF binding (FOPFlash). The resulting transfection efficiencies and firefly luciferase activities were normalized to *Renilla* luciferase activities of cells co-transfected with a reporter construct for the constitutive expression of the *Renilla* luciferase gene, and thus yielding levels of specific β-catenin/TCF/LEF transcriptional activity. These experiments showed that the β-catenin/TCF/LEF transcriptional activity was enhanced 2.5-fold in LGR5-silenced SW620 cells compared to control cells (Figure 29A). In addition, these results are in agreement with the gain of β-catenin nuclear translocation observed above and confirm that silencing of LGR5 induces β-catenin/TCF/LEF transcriptional activity in SW620 cells.

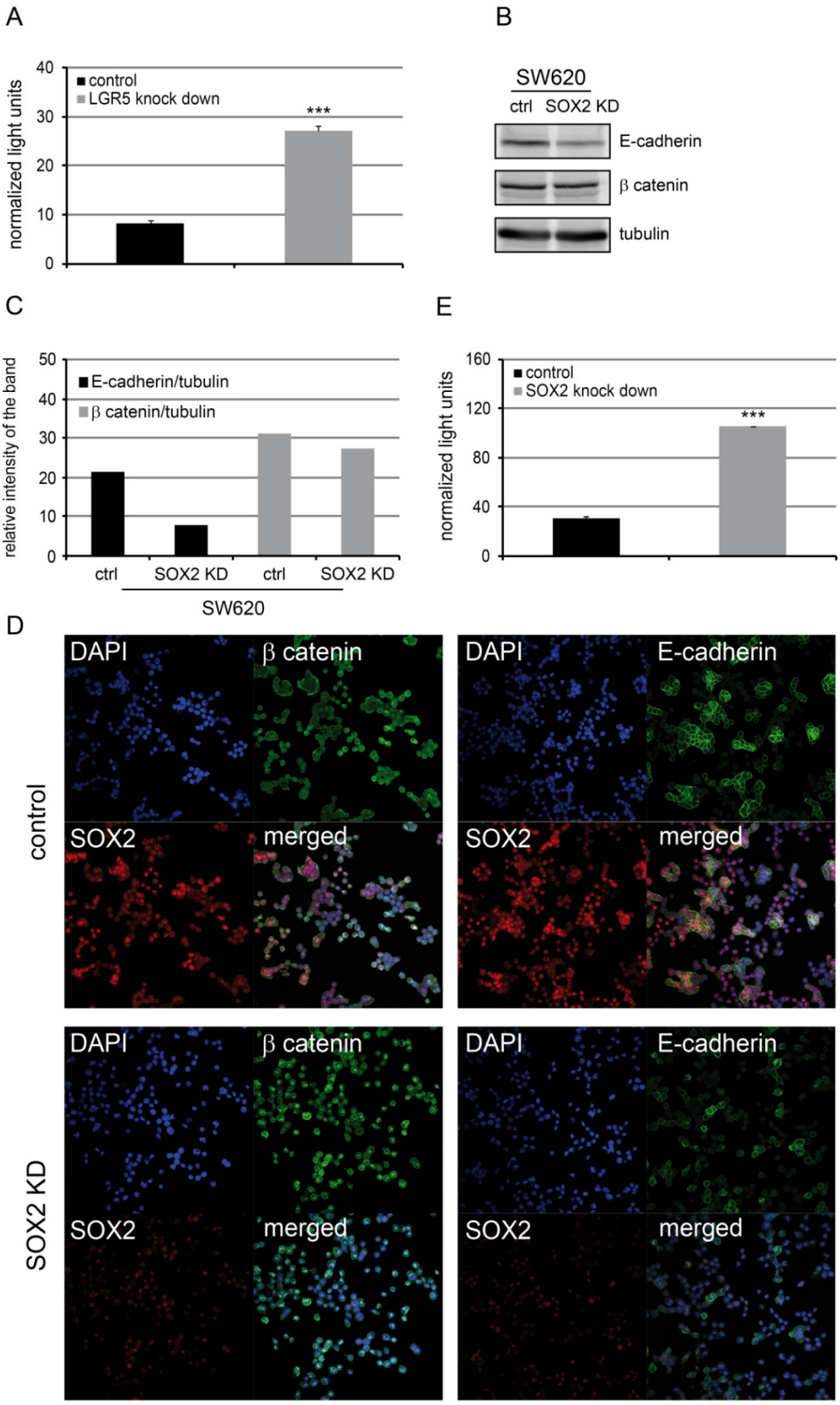

Figure 29. *Assessing EMT phenotype: TCF/LEF transcription factor activity in SW620 cells silenced for LGR5 and SOX2.* (**A**) Luminometric measures reflecting TCF/LEF transcription factor activity (firefly luciferase reporter construct) performed in control and LGR5 knock down SW620 cells. (**B**) Western blot for E-cadherin and β-catenin in control and SOX2 knock down SW620 cells. (**C**) Graphs illustrating normalized protein levels corresponding to (**B**). (**D**) Immunocytochemistry for SOX2, β-catenin and E-cadherin in control and SOX2 knock down SW620 cells and (**E**), luminometric measures reflecting TCF/LEF transcription factor activity in these cells.

Because the preceding results suggested that the expression of LGR5 is regulated by SOX2, we analyzed β-catenin/TCF/LEF transcriptional activity in SW620 cells in which SOX2 had been silenced. Similarly to the LGR5-silenced cells, SOX2-silenced SW620 cells did not show significant changes in β-catenin protein levels compared to control cells, while presenting decreased levels of E-cadherin (Figure 29B & C). In spite of its unchanged total protein levels, immunofluorescence analysis showed a gain in nuclear localization of β-catenin in SOX2 knock down cells while E-cadherin staining was less intense but mainly associated with membrane localization (Figure 29D). Consistent with the observed nuclear translocation of β-catenin, SOX2-silenced SW620 cells showed a significant increase in β-catenin/TCF/LEF transcriptional activity (Figure 29E).

Taken together, these results indicate a relationship between SOX2, LGR5 and the Wnt/β-catenin signaling axis that control the epithelial-mesenchymal phenotypic switches and self-renewal properties of SW620 cells.

2.14 LGR5 as regulator of growth and inhibitor of β–catenin signaling in SW480 cells

As described in preceding sections, the metastatic SW620 cells express SOX2 at significantly higher levels than non-metastatic SW480 cells. SW620 cells also express LGR5 at 5-fold higher levels than SW480, consistent with a positive regulation of LGR5 by SOX2. In spite of this differential expression, SW480 cells expressed significant basal levels of LGR5 and thus we decided to study its relevance for the growth properties of these cells and its relationship with β-catenin/TCF/LEF transcriptional activity (Figure 30).

Upon LGR5 silencing, a significant proportion of SW480 cells displayed a flattened appearance that was not observed in control cells (Figure 30A). Similarly to the results obtained with SW620 cells, silencing of LGR5 in SW480 cells caused a significant reduction in their ability to grow spheroids (Figure 30B), in the absence of significant effects on cell cycle profile (Figure 30C & D). In apparent contrast to the observed reduction of spheroid formation, LGR5 silencing of SW480 cells caused an upregulation of several regulators of stem cell pluripotency and self-renewal genes (KLF4, MYC, NANOG, OCT3/4 and

SOX2) together with increased expression of the differentiation factor KLF9 (Figure 30E). Concomitantly, the mesenchymal markers VIM and FN1 were upregulated, as well as all the EMT inducers TWIST2, SNAI1, SNAI2 and ZEB1. In contrast, E-cadherin was not downregulated.

Interestingly, knock down of LGR5 in SW480 cells was accompanied with a downregulation of β-catenin transcript and protein levels while putative and known negative regulators of Wnt signaling were upregulated (RNF128, RNF43 and ZNRF3) (Figure 30E & F). In contrast, silencing of LGR5 resulted in a clear nuclear translocation of β-catenin (Figure 30G) and a strong increase in β-catenin/TCF/LEF transcriptional activity (Figure 30H).

These results, together with the increased β-catenin transcriptional activity induced by LGR5 knock down in SW620 cells, suggests that LGR5, in the absence of cognate ligands activation, functions as an inhibitor of β-catenin nuclear translocation and transcriptional activity. They also suggest that this activity of LGR5 is independent of modulation of β-catenin stability, e.g. through changes in membrane localization or expression levels of the inhibitory E3 ligases ZNFRF3 or RNF43 [472], [474]. Finally, they show that these colorectal cancer cells are absolutely dependent on LGR5 and SOX2 for anchorage-independent growth even in the presence of high levels of β-catenin activity. An additional unexpected corollary to these observations is that β-catenin nuclear localization and transcriptional activity can be dissociated from protein levels and efficient anchorage-independent growth.

The above observations are in sharp contrast to observations by many laboratories showing a strong correlation between β-catenin activity and/or levels and the ability to form spheroids in anchorage-independent conditions in colorectal cancer cells [475]–[478]. In order to study the β-catenin dependence of the spheroid-forming ability in SW480 and SW620 cells, we proceeded to knock down β-catenin (Figure 31A & B). After confirming the effective knock down of β-catenin at the transcript and protein levels, which did not significantly alter E-cadherin or SOX2 levels (Figure 31A & B), we observed a strong inhibition of the capacity of both cell lines in forming spheroids in anchorage-independent growth conditions (Figure 31C & D). These results indicate that the expression of β-catenin is indeed required for the spheroid forming potential of SW620 and SW480 cells.

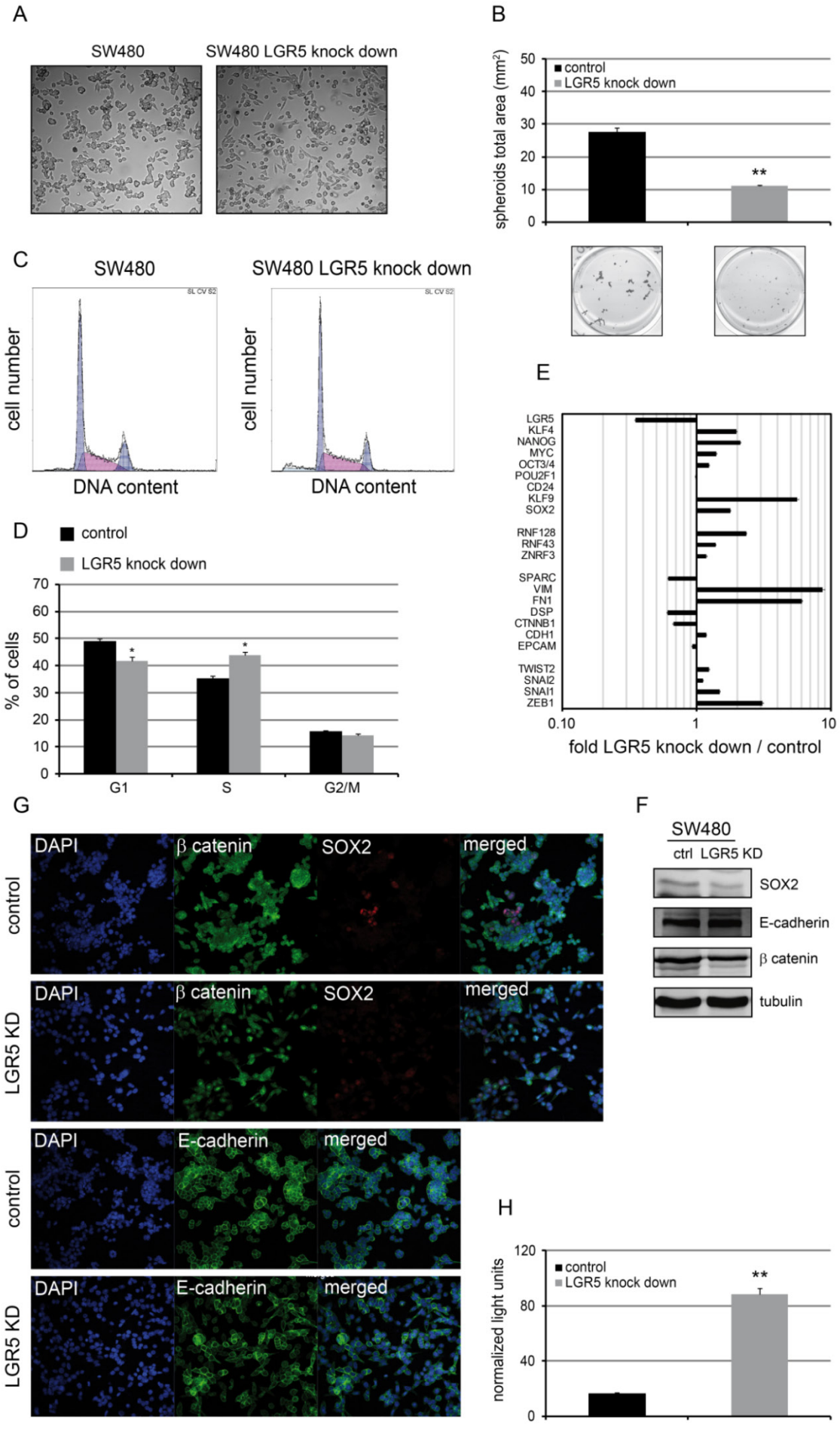
A
SW480
SW480 LGR5 knock down
B
spheroids total area (mm²)
control
LGR5 knock down
**
C
SW480
SW480 LGR5 knock down
cell number
DNA content
D
control
LGR5 knock down
% of cells
G1
S
G2/M
E
LGR5
KLF4
NANOG
MYC
OCT3/4
POU2F1
CD24
KLF9
SOX2
RNF128
RNF43
ZNRF3
SPARC
VIM
FN1
DSP
CTNNB1
CDH1
EPCAM
TWIST2
SNAI2
SNAI1
ZEB1
fold LGR5 knock down / control
F
SW480
ctrl LGR5 KD
SOX2
E-cadherin
β catenin
tubulin
G
DAPI
β catenin
SOX2
merged
control
LGR5 KD
E-cadherin
H
normalized light units

Figure 30. *Phenotypic characterization of LGR5 knock down in SW480 cells: Assessment of EMT and activation of β-catenin signaling.* (**A**) Bright field images of control and LGR5 knock down SW480 cells. (**B**) Spheroid formation in control and LGR5 knock down SW480 cells. (**C**) Flow cytometry histograms showing DNA content profiles of control and LGR5 knock down SW480 cells. (**D**) Quantification and distribution in each phase of cell cycle of the experiment shown in (**C**). (**E**) Quantification by RT-qPCR of the expression of selected genes in control and LGR5 knock down SW480 cells, normalized to control levels. (**F**) Western blot for SOX2, E-cadherin and β-catenin in control and LGR5 knock down SW480 cells. (**G**) Immunocytochemistry for the same proteins as analyzed in (**F**). (**H**) Luminometric measures reflecting TCF/LEF transcription factor activity performed in control and LGR5 knock down SW480 cells.

One possible conclusion from these observations is that the transcriptional β-catenin activity may not be required for spheroid growth potential of SW620 and SW480 cells, and that the maintenance of anchorage-independent growth properties may rely, for instance, on membrane-associated functions of β-catenin, perhaps through the regulation of E-cadherin and the dynamics of cortical cytoskeleton [479], [480]. Alternatively, canonical Wnt

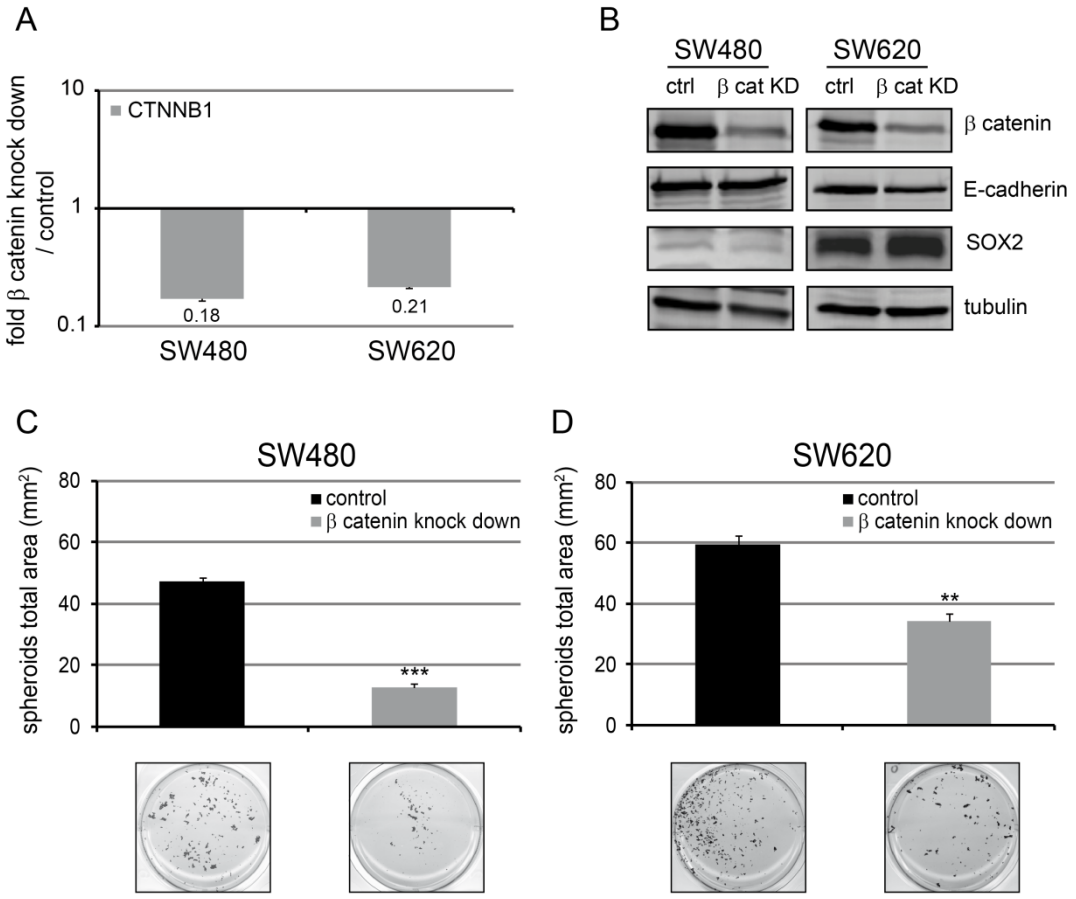

Figure 31. *Role of β catenin in spheroid formation in SW480 and SW620 cells.* (**A**) RT-qPCR assessment of β-catenin (CTNNB1) knock down efficiency in SW480 and SW620 cells, normalized to control levels. (**B**) Western blot for β-catenin, E-cadherin, SOX2 and tubulin in control and β-catenin knock down SW480 and SW620 cells. (**C** & **D**) Effect of β-catenin knock down on spheroid formation in SW480 and SW620 cells.

signaling through β-catenin/TCF/LEF transcriptional activity, may enable these cells to display an optimal self-renewal capacity but only within an appropriate range of expression levels or activity. Expression or activity of β-catenin at levels beyond these limits (upper and lower thresholds) may affect the self-renewal potential of these cells. The latter model would fit with our observations of loss of self-renewal properties (spheroid growth) in SW620 cells both under conditions of low β-catenin levels (through β-catenin knock down) and high β-catenin activity (associated with LGR5 or SOX2 knock down).

2.15 LGR5 and SOX2 are required for the in vivo tumorigenic potential of SW620 cells

The *in vitro* spheroid growth assay is a surrogate test for assessing the self-renewal potential of tumor cells and also a good predictor of the tumorigenic and/or metastatic potentials of these cells in immunodeficient mice [25], [33], [52]. In spite of the strong inhibition of spheroid growth caused by the repression of SOX2 or LGR5 in SW620 cells, which would predict reduced tumor growth *in vivo*, and their associated upregulation of β-catenin/TCF/LEF transcriptional activity, we tested the consequences of these manipulations on the tumorigenic potential of SW620 cells.

Control and SOX2 or LGR5 knock down cells were modified in order to stably integrate in their genomes the firefly luciferase gene under the transcriptional control of a constitutive promoter. Subsequently, these cells were xenografted into SCID-NOD mice (intramuscular injection in their hind legs) and tumor growth was monitored in real time by bioluminescence (Figure 32A & C). Knock down of either SOX2 or LGR5 caused a dramatic reduction in the rate of tumor growth of SW620 cells as compared to control cells (Figure 32B & D, respectively), reflecting a good correlation between loss of self-renewal observed in *in vitro* spheroid formation assays and the *in vivo* tumorigenic assay.

To confirm our observations in functional experiments performed *in vitro*, immunohistochemical staining was performed to determine the intensity and subcellular localization of β-catenin in samples of tumors grown in mice of control and LGR5 knock down SW620 cells (Figure 32E). In agreement with the

results obtained in functional assays, SW620 control cells displayed membrane bound and diffuse cytoplasmic/nucleus β-catenin stain while in LGR5 knock down cells, β-catenin largely lost its membrane localization and was preferentially localized in nucleus and with stronger signal than in control cells.

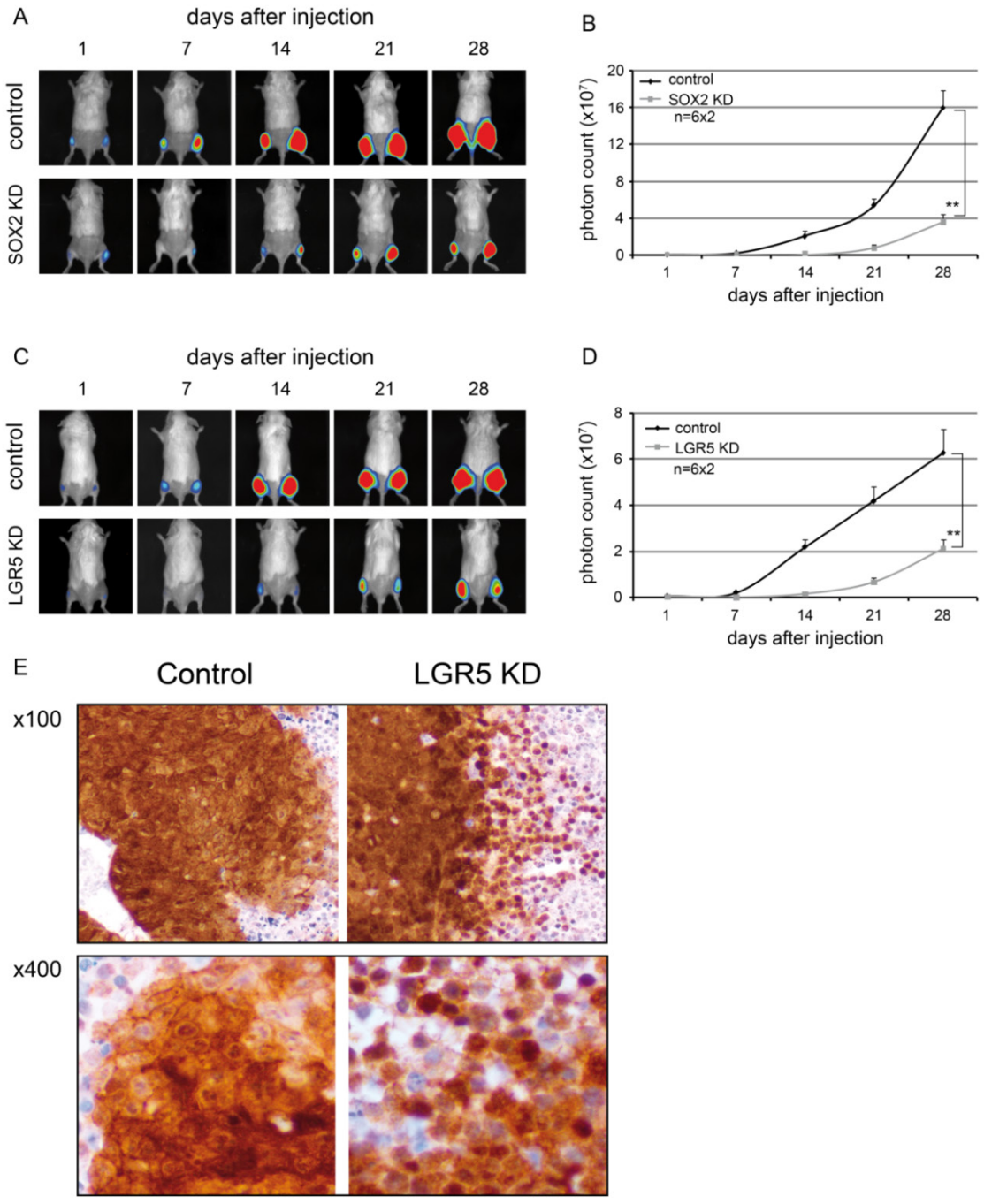

Figure 32. *Strong reduction of tumorigenicity in xenografted SOX2 and LGR5 knock down SW620 cells.* (**A**) Control SW620 and SOX2-repressed cells were transduced for stably express firefly luciferase gene and injected i.m. in hind legs of mice. Monitoring of growing tumors was done after injection of luciferin at indicated days and (**B**) photon counts were quantified. (**C**) Procedure described above was done for assessing tumorigenicity of control SW620 and LGR5-silenced cells, and (**D**) photon counts were quantified. (**E**) β–catenin staining was performed in tumor samples of control and LGR5-repressed SW620 cells (x100 and x400 magnification).


Discussion

Messier object 13, The Great Globular Cluster in Hercules

M13, also designated NGC6205 and known as the Great Globular Cluster in Hercules, is a globular cluster of about 300,000 stars in the constellation named after the Greek mythological hero. M13 was discovered by Edmond Halley in 1714, and catalogued by Charles Messier on June 1st of 1764. This globular cluster is about 145 light-years in diameter. The brightest star is the variable star V11 with an apparent magnitude of 11.95. M13 is 25,100 light-years away from Earth…On November 16th of 1974, at a ceremony to mark the remodeling of the Arecibo radio telescope in Puerto Rico, Carl Sagan and other scientists broadcast a message aimed at the location of this globular cluster containing information about…

Exploration of SOX2 as a determinant of traits of tumor cell aggressiveness: drug resistance

The rationale for studying the relationship between SOX2 expression and drug resistance is supported by previous studies in our lab that have demonstrated that expression of SOX2 is tightly associated with an epithelial-CSC phenotype in prostate and bladder cancer cell models [130], by other recent works that have showed in mice models that a quiescent or slow proliferative subpopulation of tumor cells that express Sox2 is responsible for tumor initiation in SCC [309], and responsible for relapse after chemotherapy in a subtype of medulloblastoma [308], as well as by other studies that have found that repression of SOX2 in breast cancer models can restore sensitivity to chemotherapeutic agents [337], or that upregulation of SOX2 is associated in turn, with drug resistance by upregulation of members of the ABC family of transporters in glioma cell lines [338].

In the first part of this work, we have intended to demonstrate a hypothetical relationship between SOX2 expression and drug resistance carrying out a survey on a panel of 22 cancer cell lines from 8 different tumor types, with the aim to identify pairs of cell lines derived from the same tumor type and displaying differential aggressiveness traits (based on the literature or our own previous observations), such as metastatic *vs.* nonmetastatic phenotype or by histological traits such as tumor differentiation grade, and correlation with SOX2 expression. Eventually, we chose the prostate cancer pair PC-3/Mc *vs.* PC-3/S (metastatic with relatively high transcriptional activity of SOX2/OCT3/4 *vs.* nonmetastatic and with relatively low SOX2/OCT3/4 transcriptional activity, respectively), the colorectal cancer pair SW620 *vs.* SW480 (same pattern as the prostate cancer pair), and the pancreatic cancer pair PANC-1 *vs.* CAPAN-1 (both metastatic; PANC-1 generating poorly differentiated tumors and displaying relatively high SOX2/OCT3/4 transcriptional activity than CAPAN-1, which forms well-differentiated tumors).

For the initial screening, we transduced all cell lines with enhanced-GFP (eGFP) reporter plasmids for SOX2/OCT3/4 transcriptional activity, generated by others for improving the efficiency of detection and isolation of iPS, and used flow cytometry as readout of transcriptional activity. It is important to remark

here that in all cases, the cells presented a Gaussian distribution comprising negative, low, mid and a tail of high intensity of GFP-positive cells, with no peaks revealing subpopulations for the latter (illustrated in Figure 1A for SW620). Likewise, since the reporter plasmid had no selectable markers, the cells were transduced for the reporters under conditions intended to achieve 100% of efficiency on the basis of extrapolation of results in parallel transduction experiments with the same backbone vectors carrying a GFP reporter plasmid for the transcriptional activity of the constitutive expressed gene EF1α. Because this methodology can introduce some bias (although all viruses were produced in parallel), the results obtained in this first screening were validated by other complementary means (e.g. transcript or protein levels of SOX2 and/or OCT3/4). In this regard, the higher percentages of GFP-positive cells for SOX2/OCT3/4 transcriptional activity (81% in PC-3/Mc or 77% in PANC-1 cells) did not show a linear correlation with SOX2 protein levels (whose levels were significantly higher in SW620 [results figure 1D]), perhaps reflecting some of the complex post-translational modifications to which SOX2 is subjected (including acetylation, methylation, phosphorylation or sumoylation of key residues) that regulate its functionality [481]–[484]. One more example of lack of correlation of relatively high SOX2/OCT3/4 transcriptional activity and SOX2 protein level is the case of colorectal cancer cell lines HCT116 40.16 and variant 379.2, whose percentages of GFP-positive cells were 65% and 57%, respectively, and showed undetectable SOX2 protein levels (results figure 15A). It is known that some pluripotency factors such as NANOG show fluctuations in their expression in ESC or neuronal progenitors while others, such as SOX2 or OCT3/4 show a more steady expression pattern [485]–[487]. Although it is unknown to what extent these expression patterns are applicable to cancer cell models, one possible explanation for these discordant results in HCT116 clones may be the existence of certain post-translational modifications in SOX2 in these cell lines that may impair its detection by Western blot with the antibody used in this study, and that presumably would not reduce its binding and transcriptional activity together with OCT3/4.

In order to assess a hypothetical relationship between SOX2 expression and drug resistance, we stably repressed the expression of this transcription factor by means of transduction of lentiviral particles for the expression of

shRNAs specifically targeting SOX2 mRNA in cell lines with relatively high endogenous levels (PC-3/Mc, PANC-1 and SW620), and overexpressed SOX2 in cell lines with relatively low endogenous levels by means of transduction of retroviral particles carrying the mature mRNA of the human SOX2 gene tagged with Flag. Next, and within the same week of transduction, cells were seeded and end-point cytotoxicity assays at 72 h were performed with drugs belonging to different families of chemotherapeutic agents, and cell proliferation/viability was determined by the MTT method.

Several points merit discussion in these experiments. First, a factor that may distort the values obtained by this procedure is the dependence of the MTT method in the capacity of NADPH-dependent cellular oxidoreductase enzymes to reduce the MTT dye. This may be considered as a potential confounding factor, since experiments performed as part of objective 2 show, that, at least in CRC cells, overexpression of SOX2 increases the production of ROS, known activators of NADPH oxidases [488]. This effect may also explain why PC-3/S control cells show higher proliferation ratios than PC-3/Mc control cells at 72 h, since we know from previous studies that PC-3/Mc proliferate significantly more rapidly than PC-3/S cells *in vitro* (evaluations by means of luciferase reporter activity) but metabolic studies carried out by collaborators have demonstrated that PC-3/S cells produce more NADPH than PC-3/Mc cells (unpublished data). To what extent this fact may affect MTT values for the rest of cell lines and in the case of SOX2 knock down conditions is unknown, but perhaps determinations of cell proliferation/viability by other means could have reduced this possible source of bias (e.g. luminometric measures of crystal violet staining and solubilization or by constitutive luciferase reporter activity). Assuming this source of bias, MTT determinations do not show a general pattern of enhanced resistance in control cells with relatively high endogenous SOX2 expressing cells *vs.* their low relative endogenous SOX2 expression counterparts, since similar values of loss of viability to the different compounds and concentrations were observed.

A number of studies have demonstrated that SOX2 silencing significantly reduces the proliferative potential *in vitro* in a number of cell lines, including breast, pancreas, lung, gastric and colorectal cancer cells [318], [319], [321], [325], [326], while evidence of enhanced proliferation upon SOX2

overexpression (4-fold increase in SOX2 protein level in respect of control cells) has been shown in the DU145 prostate cancer cell line [320]. However, *in vitro* studies linking downregulation or overexpression of SOX2 with loss or gain of drug resistance do not abound. One recent work that used SW480 cells has demonstrated that resistance to 5-FU is acquired when cells are simultaneously transduced for the expression of OCT3/4, KLF4 and SOX2 but not for each of these factors separately [489]. A second study has related these processes in breast cancer cell models [337]. In this paper, tamoxifen-resistant MCF-7 cells were obtained after culturing cells in the presence of low micromolar doses of tamoxifen during 6 months under standard culturing conditions. After phenotypic characterization, it was found that resistant cells proliferated at the same rate as parental cells but displayed traits of breast CSCs (enriched proportion of breast CSC markers $CD44^{high}/CD24^{-/low}$, diminished expression of estrogen receptor, enhanced spheroid formation and tumorigenic potential), and 30-fold increased expression of SOX2 relative to parental cells. Upon knock down of SOX2 in these tamoxifen resistant cells, the authors showed that sensitivity to the drug was restored. Conversely, overexpression of SOX2 in MCF-7 parental cells provided resistance to tamoxifen. However, neither experiment showed how these manipulations of SOX2 levels affected cell proliferation or viability *per se*. Rather, cell viability was expressed in terms of *relative cell viability*; namely, normalizing the values of cells after treatment with different concentrations of the drug to their respective untreated controls in end-point experiments. Had we represented our data using this approach, the apparent result would have been that SOX2 knock down or overexpression in most cases leads to a gain in drug resistance for all compounds and concentrations relative to control cells. Instead, we have chosen to represent our data in terms of ratios of cell numbers referred to cells seeded at time 0 for each condition, thus highlighting the fact that manipulation of SOX2 levels impairs the cell viability/proliferation in the cell lines tested. Furthermore, we have found in the SW480 cell line that increasing levels of SOX2 correlates with a reduction in cell viability, even at protein levels similar to those displayed endogenously by their counterpart cell line SW620 (Results Figures 8 & 9). Taken together, we conclude that rather than conferring drug resistance or sensitivity, manipulations of SOX2 levels in these cells lines

have profound effects in cell viability/proliferation at least in these short-term experiments.

Exploration of SOX2 as a determinant of traits of tumor cell aggressiveness: Focus on the SW620 colorectal cancer cell model

In view of the results and conclusions of Objective 1, we decided to further explore some of the molecular mechanisms that may lead to the marked loss of proliferation/viability upon knock down of SOX2 in cells with relatively high endogenous levels or upon overexpression in cells with relatively low endogenous levels of the transcription factor. For this purpose, we focused the study in the SW620-SW480 CRC cell pair because of their shared origin and the good correlation between aggressiveness and SOX2 expression.

The first question that we addressed was the study of the mechanisms that allow SW620 cells to express and *tolerate* high levels of endogenous SOX2 in comparison to SW480, in which cell growth is inhibited upon expression of exogenous SOX2 even at relative low levels. For this approach, we characterized the phenotype of both CRC cell lines upon overexpression of SOX2 in relatively short-term experiments. First, we observed that, similarly to what we had observed for SW480 cells, SW620 cells were inhibited in their proliferation as a function of the levels of exogenous SOX2 expression. One possible interpretation that may account for these unexpected results is that SOX2 is already expressed in these cells at levels that may represent a near-maximally tolerated dose that, if surpassed by expressing exogenous SOX2, it results in adverse phenotypic effects. Consistent with this notion, subsequent transduction experiments were standardized in order to achieve exogenous SOX2 expression levels above of this hypothetical threshold of tolerance, in an attempt to observe unequivocal phenotypic effects.

The phenotypic characterization of these cells revealed common traits in both cell lines after exogenous SOX2 expression, such as dramatic reduction of self-renewal potential *in vitro* (diminished spheroid formation), but also remarkable differential phenotypic traits between them. The most relevant findings are that transduction of SOX2 leads to a significantly higher loss of viable cells (necrotic and apoptotic) in SW480 cells than in SW620 cells, and

that the latter present a significant percentage of cells with a long-term G1/S arrest, as shown by flow cytometry analysis of cells blocked in G2/M with nocodazole. The latter effect was accompanied with a significant upregulation of the cyclin-dependent kinase inhibitors p21 and p27 that was not observed in SOX2-transduced SW480 cells.

To better understand to what extent these cell cycle regulators are involved in phenotypic traits induced by the transduction of SOX2 in SW620 cells, experiments combining SOX2 overexpression and p21 or double p21 and p27 knock down, were performed. The results of these experiments suggest the existence of dissociated functions of these proteins and their roles in phenotypic traits associated with SOX2 transduction. Thus, knock down of p21 but not p27 partially relieved the lasting G1/S arrest in SOX2-transduced SW620 cells, while repression of p27 in double knock down in these cells (but not in p21 knock down), partially restored the ability of SW620 cells to form spheres under anchorage independent conditions. These results indicate that additional mechanisms other than p21 and p27-mediated cell cycle arrest and inhibition of self-renewal must participate and account for the observed phenotypic effects of SOX2 transduction in these cells.

In additional set of experiments, we attempted to determine whether these CRC cell lines were subjected to different forms of stress upon SOX2 transduction, such as induction of ROS or DNA damage (reflecting oncogenic and/or replicative stress), may account for the observed different responses of these cells to SOX2 transduction. A summary of these experiments is that SW620, but not SW480 cells, respond to SOX2 transduction with an induction of ROS and DNA damage response. The latter may not be related to replicative stress (no increase of colocalization of DDR markers with cyclin A) in SW620 cells. These differential responses may partially explain the lasting cell arrest in G1 observed in SW620 cells, given the known effects of increased ROS levels and DNA damage on triggering cell cycle checkpoints [469], [490]. In the case of SW480 cells, SOX2 transduction induced increased ROS levels without evidence of increased DDR, although we have observed an increased colocalization of 53BP1 foci with cyclin A, suggesting that, in these cells, SOX2 transduction may cause replicative stress. Why increased levels of ROS would lead to DNA damage in SW620 cells but not in SW480 cells, may be explained

by differential activity of antioxidant systems (e.g. superoxide dismutase, catalase, thioredoxin or glutathione) [466]. Nevertheless, this still leaves unexplained the mechanisms by which SOX2 overexpression induces higher mortality in SW480 cells than in SW620 cells.

Our results stand in apparent contrast to other studies [319] in which overexpression of SOX2 enhances the ability of HeLa and pancreatic cancer cells to form spheroids under anchorage-independent conditions and, particularly in HeLa cells, drives a faster progression through the S phase [319]. In contrast, other studies have highlighted that SOX2 overexpression can promote cellular senescence (with upregulation of p53, p21 and p16 and increased senescence-associated β-galactosidase activity) and autophagy in CRC cancer cells through upregulation of ATG10 [491]. The latter study shows that SOX2 overexpression in HCT116 cells and other cell lines is associated with vacuolization and lysosomal activation. In addition, and supporting our observations, the same study shows that SOX2 overexpression in HCT116 cells causes an accumulation of cells in the G1 phase of the cell cycle and of a sub G1 subpopulation, together with a reduction in the proliferation potential and in the ability to grow spheroids.

Although we have not addressed autophagy and cellular senescence in the CRC cell model used in our study upon SOX2 overexpression, we did observe the induction of a marked vacuolization in SW480 cells caused by SOX2 transduction. It might be worth exploring whether transduction of SOX2 in SW480 cells (but not SW620 cells) may induce autophagy and thus account for the observed loss of viability and increased apoptosis, since these pathways can be linked depending on the cellular context [492]. Additionally it may explain why in our experiments, the increased proportion of apoptotic and necrotic cells occurs without increased levels of cleaved caspase 3 [493]. Conversely, we do not have a mechanistic explanation for the decreased levels of cleaved caspase 3 observed in association with SOX2 transduction in SW620 cells, although this may reflect protective anti-apoptotic mechanisms differentially expressed in these cells. In this regard, a similar pattern has been reported in ovarian cancer cells overexpressing SOX2 under treatments known to trigger the intrinsic and extrinsic apoptosis pathways (e.g. staurosporine, chemotherapeutic agents or death ligand TRAIL treatment) [334].

We have also addressed the mechanistic basis underlying the loss of proliferation/viability upon SOX2 knock down, as well as other growth properties in the metastatic cell line SW620. We have found that knock down of SOX2 causes a dramatic reduction in their *in vitro* self-renewal capacity and tumorigenicity *in vivo*, as well as a lasting cell cycle arrest in G1, with downregulation of cyclin D1 and cyclin B1, and upregulation of p21 and p27. These observations are in agreement with other studies in cells from other tumor types. In breast cancer cell models, knock down of SOX2 led to a decrease of spheroid formation and cell cycle arrest, with downregulation of cyclin D1 [494] and loss of tumorigenicity in xenografts models [318]. Similar results have been observed in gastric and melanoma cancer cells lines, in which in addition, loss of viability and proliferation was related to cells undergoing apoptosis upon SOX2 knock down [321], with upregulation of pro-apoptotic or cell cycle-related proteins such as NOXA or GADD45A [335]. Interestingly, another study in pancreatic cancer cell models reported that growth inhibition and cell cycle arrest following SOX2 knock down was mediated through the upregulation of p21 and p27; moreover, chromatin immunoprecipitation (ChIP) experiments in that model showed that SOX2 was associated with the promoter regions of these genes where it may function as a negative transcriptional regulator [319]. Furthermore, given that other studies in ESC and adult neural stem cells have demonstrated that both p21 and p27 can exert a negative transcriptional regulation of SOX2 [467], [468], it is possible that these proteins may act in a mutually repressive transcriptional loop. In our study, we show evidence that SOX2 may function as a negative transcriptional regulator of p27 in SW620 cells, as indicated by complementation experiments combining SOX2 knock down with transduction of different levels of siRNA-resistant SOX2 and luciferase reporters for p27 transcriptional activity. We are currently carrying out chromatin immunoprecipitation experiments to validate whether SOX2 is indeed associated with the promoter regions of the p21 and p27 genes in SW620 cells.

In contrast to SOX2 overexpression experiments, we have demonstrated that the cell cycle arrest observed in these cells upon SOX2 repression (but not loss of viability or spheroid formation) is partially dependent on p27, as indicated in double knock down of p27 and SOX2 experiments. These divergent

observations may be interpreted, on one hand, by the tight dependence on SOX2 for the self-renewal potential in SW620 cells, which is almost completely abolished upon SOX repression, and in a putative SOX2-mediated repression of p27 (and likely p21) required for normal G1/S cell cycle transition. On the other hand, increased DNA damage and ROS production by SOX2 overexpression may lead remarkably to cell cycle arrest in SW620 cells; in this scenario, upregulation of p21 (and other unknown mechanisms) would be mediating the G1/S cell cycle arrest observed through p53-independent stress-induced pathways rather than by specific transcriptional activation by SOX2. Finally, the increase of spheroid formation upon p27 knock down indicates that it acts as an inhibitor of self-renewal; its inability to restore the self-renewal caused by SOX2 knock down may reflect the absolute dependence on SOX2 for this growth property in SW620 cells.

Evidence for a SOX2-LGR5-β-catenin axis

Because of the strong downregulation of transcript levels of the colon stem cell marker LGR5 upon SOX2 knock down, we investigated a putative role of this protein in the phenotype observed in SOX2 knock down cells and whether SOX2 acts in this system as a positive transcriptional regulator of LGR5 (analysis to be complemented by ChIP). For this, we knocked down LGR5 in SW620 cells and analyzed several resulting growth properties. We have found that LGR5 knock down did not affect the cell cycle profile, proliferation rate or cell viability of SW620 cells. However, and resembling some phenotypic traits observed in SOX2 knock down cells, both self-renewal potential *in vitro* and ability to grow tumors in xenograft experiments was significantly reduced, indicating a selective role of LGR5 in these properties. This implies that the regulation of cell cycle progression and survival in SW620 cells are distinct properties under the control of SOX2, but not LGR5. Similar effects on phenotypic traits have been reported upon LGR5 knock down in glioma cells expressing high levels of LGR5 (U87-MG), with the difference that cell cycle progression and proliferation were also impaired [495].

Because of the acquisition of a more mesenchymal-like morphology in a subset of cells, we also studied whether LGR5 knock down was promoting an

EMT program in SW620 cells. Functionally, we observed an increase in the motility of these cells upon LGR5 knock down, but not of invasive properties *in vitro*. Moreover, although some of the EMT inducers analyzed by RT-qPCR were not significantly upregulated, decreased levels of epithelial markers (desmoplakin, E-cadherin) concomitant with an upregulation of mesenchymal markers (fibronectin, vimentin) were observed. In the case of E-cadherin and fibronectin, these results were further validated by Western blotting and/or immunocytochemistry. Taken together, these results suggest that knock down of LGR5 in these cells may engage a partial EMT program.

Unexpectedly, we observed an increased nuclear localization of β-catenin in SW620 cells upon LGR5 knock down in the absence of altered protein levels, suggesting an activation of the Wnt/β-catenin signaling pathway. The latter possibility was confirmed by the finding of a 2.5-fold increase of the β-catenin/TCF/LEF luciferase reporter activity induced by LGR5 knock down. In addition, we have found that in tumors grown in mice, β-catenin staining was more intense and was preferentially localized in the nucleus of LGR5 knock down tumor cells than in control tumor cells. As a result of these observations, we conclude that in the absence of LGR5 cognate ligands, namely R-spondins, LGR5 attenuates Wnt/β-catenin signaling in SW620 cells. Likewise, although SW480 cells express SOX2 and LGR5 at significantly lower levels than SW620 cells, similar results were obtained upon knock down of LGR5 in SW480 cell line: namely, significant reduction in spheroid formation (despite upregulation of most of the genes analyzed involved in self-renewal in ES cells) without affecting proliferation or cell viability, acquisition of a flatter morphology (without loss of E-cadherin), and remarkably, gain in nuclear localization of β-catenin (with downregulation of β-catenin transcript and protein levels) coupled to a significant (5.5-fold) increase of β-catenin/TCF/LEF transcriptional activity.

In spite of the fact that the proposed initial function of LGR5 (and its homologs LGR4 and LGR6) upon binding to its cognate ligands R-spondins, is to enhance canonical (β-catenin) Wnt signaling by arresting and mediating the clearance in cytoplasmic membrane of RNF43 and ZNFR3, known negative regulators of the Frizzled/LRP receptors [472], recent studies have highlighted that this model may be too simplistic. Particularly, it has been proposed that R-

spondin 2 (RSPO2), frequently downregulated in CRC cells, may function as a tumor suppressor by negatively regulating Wnt/β-catenin signaling through an LGR5-dependent feedback mechanism [496]; in the model proposed in this study and in CRC cells that do not express LGR5, RSPO2 could directly bind to the Frizzled/LRP receptors and stimulate canonical Wnt pathway and in turn, induce the expression of LGR5 (a Wnt target gene). RSPO2 may selectively bind to LGR5 in the cell membrane (or in cells that already display high levels of expression). This interaction would promote the membrane stabilization and function of ZNFR3, which leads to polyubiquitination of Frizzled receptor and internalization of Frizzled/LRP receptor complex and subsequent attenuation of canonical Wnt signaling. This model opens new insights into the regulation of LGR5 and Wnt signaling; for instance, as we have observed in our model, LGR5 (or other members of this family of receptors) could interact with and promote, the negative regulatory function of RNF43 and/or ZNFR3 in the absence of R-spondins, thus acting as default attenuators of canonical Wnt signaling.

Other studies in which LGR5 levels have been manipulated in CRC cell models, have obtained results that are partially discordant with ours. For instance, Burgess and colleagues, using two LIM colorectal cancer variants (β-catenin mutated), have reported that LGR5 knock down does not affect cell proliferation but promotes invasiveness and motility *in vitro*, together with increase in spheroid and colony formation that correlates in turn with a gain of capacity to form tumors *in vivo*. The opposite behavior is found upon LGR5 overexpression, and in consequence they conclude that LGR5 acts as a negative regulator of tumorigenesis in CRC cells [497]. However, this conclusion does not fit with other evidence that demonstrate that the fraction of CRC cells (derived from mouse and human samples or human CRC cells) that are capable to grow spheroids are enriched in CSC traits (e.g. increase tumorigenicity and metastatic potential) and expression of colon CSC such as Musashi-1, CD44, EpCAM or CD133, and importantly, LGR5 [88], [477], [498], [499]. In contrast, the cell lines in the Burgess study are *per se* barely capable of growing spheroids or forming tumors *in vivo* (at least one of the cell lines used). The intrinsic differences in the model selected may explain the discordant results between their results and those obtained in our cell model

(e.g. β-catenin *vs*. APC mutated, respectively). In spite of these differences, and in agreement with our study, the transcriptomic profiles of the cells studied by Burgess and colleagues upon LGR5 silencing are consistent with an enhanced canonical Wnt signaling (while overexpression of LGR5 has the reverse effect), and engagement of an EMT program. Other recent studies in colorectal cancer cells (HT29 and DLD1) have shown that downregulation of miR-363 promotes the upregulation of GATA6 that, in turn, acts as a direct positive transcriptional regulator of LGR5 [500]. In these models, and in agreement with our results, both knock down of GATA6 (with subsequent downregulation of LGR5) or LGR5, suppresses the *in vitro* self-renewal and *in vivo* tumorigenic potential of these cells, without affecting their *in vitro* proliferation rates.

Next, we explored the consequences of SOX2 knock down in SW620 cells that may phenocopy, at least partially, LGR5 knock down. First, we assessed EMT markers, and found a transcriptional upregulation of several EMT inducers (TWIST1, ZEB1) and mesenchymal markers (SPARC, vimentin and fibronectin), concomitant with a downregulation of epithelial markers such as E-cadherin and EpCAM. In the case of E-cadherin, the downregulation was confirmed by decreased protein levels and membrane-associated staining by immunocytochemistry. Importantly, and mirroring the results obtained in LGR5 knock down cells, we observed a significant gain in nuclear localization of β-catenin that was translated into a 3.5-fold increase in β-catenin/TCF/LEF transcriptional activity, in the absence of alterations in β-catenin protein levels.

Taken together, these results suggest the existence of a functional relationship between SOX2, LGR5 and the Wnt/β-catenin signaling axis that controls the epithelial-mesenchymal phenotypic switches and self-renewal properties of SW620 cells. However, we do not rule out that this relationship may be specific to our cell model and tightly related to LGR5 expression levels. In other cancer cell models (ovarian and glioblastoma), SOX2 has been inferred to be an inducer of EMT phenotypes (e.g. enhanced motility, invasiveness, expression of MMPs and mesenchymal markers) in cells with low or undetectable endogenous SOX2 levels [324][501]. Likewise, it has been shown that SOX2 binds and promotes the transcription of the EMT master regulator

SNAI1 in pancreatic cells [319]. Additional studies have found that overexpression of SOX2 leads to upregulation of Wnt signaling (prostate and breast cancer models) [323], [337], with the demonstration of a direct positive transcriptional regulation of the β-catenin gene exerted by SOX2 (MCF-7 cells) [323]. Thus, it is possible that in our model, loss of LGR5 (by direct knock down or indirectly by SOX2 knock down) engages an EMT program (partial EMT program), as other aforementioned studies in LGR5 knock down CRC cells have demonstrated [497].

Nevertheless, the reciprocal regulation between SOX2 and β-catenin seems to be complex and dependent on cellular context. For instance, in a subset of MCF-7 breast cancer cells, it has been reported that β-catenin binds to SOX2 and reduces its DNA binding affinity, which results in an inhibition of SOX2 transcriptional activity and expression of target genes [502]; interestingly, the authors reasoned that this interaction would be dependent on post-transcriptional modifications in β-catenin and possibly also in SOX2, on the basis of preliminary and unpublished data. In another study, Sox2 was found to inhibit the Wnt/β-catenin pathway in mouse osteoblasts [503], while in two other studies, β-catenin was reported to suppress the expression of Sox2 in mouse osteosarcoma cells and in early distal lung endoderm development [329], [504]. Remarkably, in our study we have found that knock down of LGR5 caused a 2.5-fold increase of β-catenin/TCF/LEF transcriptional activity in SW620 cells and a 5.5-fold increase in SW480 cells. On the other hand, knock down of SOX2 in SW620 cells induced a 3.5-fold increase in β-catenin/TCF/LEF transcriptional activity, supporting a negative regulation of β-catenin by SOX2 in these cells. We speculate that the significant higher levels of endogenous SOX2 expressed by SW620 cells as compared to SW480 cells may partially explain the more subdued increment of β-catenin/TCF/LEF activity observed in the former cells in response to LGR5 knock down.

CRC is generally characterized by a *constitutively* activated Wnt-β-catenin pathway mediated in the most cases, by mutations in β-catenin (CTNNB1) or APC genes. Therefore, the observation of increased activation of this pathway in cells bearing such mutations may seem to be contradictory. However, rather than a constitutive pathway activation to its maximal levels, it

appears that CRC cells present a lower threshold to Wnt signaling activation. Recent studies have demonstrated that, in the case of CRC cells with truncated APC (which applies for SW620 and SW480 cells), this regulatory protein is still capable of binding to β-catenin (with an efficiency that is inversely proportional to the length of deletion) and form a less effective but still active, β-catenin destruction complex [505]. This leaves sufficient room for further Wnt/β-catenin activation, and indeed CRC cells respond to exogenous Wnt ligands and actively produce them to stimulate Wnt signaling in an autocrine fashion, dependent on the expression of the Wnt-secretion regulatory protein GPR177 [505]. As a matter of fact, immunohistochemical studies have revealed that colon carcinomas harboring APC mutations do not express nuclear β-catenin homogeneously [110], [111]. Likewise, the aforementioned studies that characterize the fraction of CRC cells that form spheroids and conclude that are enriched in colon CSCs, also show that these cells display higher β-catenin/TCF/LEF transcriptional activity. This finding may seem contradictory with our results that higher canonical Wnt signaling is linked with loss of self-renewal potential. However, in these studies, LGR5 is also highly expressed in putative isolated colon CSCs, while in our study, genetic manipulations lead to dramatic reduction of its levels. Therefore, this may also indicate that loss of LGR5 engages other unknown mechanisms that impair the self-renewal potential of our cells independently of the activation of canonical Wnt pathway.

Wnt/β-catenin signaling has been implicated in the maintenance of both mouse and human ESCs *in vitro* [285], [506]–[512]. Wnt signaling has also been reported to promote the acquisition of a pluripotent state during reprogramming of somatic cells to induced pluripotent stem cells [513], [514]. Many studies have shown that activating Wnt/β-catenin signaling promotes self-renewal of mouse ESCs [285], [506], [509]–[512], whereas reciprocal loss-of-function studies indicate that β-catenin is required for multilineage differentiation but is dispensable for self-renewal [512], [515], [516]. The role of Wnt/β-catenin signaling in hESCs is less clear due to contradictory results among published studies. Sato *et al*. have found that activation of the Wnt/β-catenin pathway with either Wnt3A or a GSK3β inhibitor, preserves the self-renewal of hESCs under feeder-free conditions [285]. Conversely, others have reported that presence of

Wnt3A or GSK3β inhibitors leads to differentiation of hESCs towards primitive streak and definitive endoderm lineages [517], [518]. Another study has found that another GSK3β inhibitor promotes undifferentiated cellular morphology and maintains expression of pluripotency markers in short-term assays, but is not sufficient to expand undifferentiated hESCs over multiple passages [519]. It has also been shown that Wnt3A and Wnt1 transiently stimulate proliferation and/or increased clonal survival of hESCs, but fail to maintain other functional attributes of pluripotency over several passages [520]–[522]. In addition, a recent work has found that Wnt/β-catenin signaling is not active during hESC self-renewal by using a sensitive reporter system [523]; moreover, inhibition of the pathway over several passages did not impair hESC maintenance while activation led to loss of self-renewal and induction of mesoderm lineage genes. The authors concluded that Wnt/β-catenin signaling is linked to differentiation rather than self-renewal in hESCs.

Therefore, whether Wnt/β-catenin signaling maintains hESCs in an undifferentiated and self-renewing state, or whether it promotes differentiation, remains controversial. One possible explanation is that Wnt/β-catenin may function specifically in asymmetric cell divisions rather than in self-renewal *per se*. In order to maintain a balance of dividing and differentiating cells within a tissue, progenitor cells divide asymmetrically, giving rise to one progenitor and one cell committed to differentiation [524], [525]. *C. elegans* embryos show early signs of Wnt/β-catenin-dependent asymmetric cell divisions, which distinguish and specify the fates of early progenitors [526]–[528]. More recently, it has been shown that if Wnt3a is added to one side of a murine ES cell, β-catenin will asymmetrically distribute to its two daughter nuclei [529]. These findings suggest that polarized canonical Wnt signaling might be important in promoting asymmetric cell divisions, providing a possible explanation for how Wnts may function in both stem cells´ self-renewal and promoting differentiation. Furthermore, since many stem and progenitor cells can divide both asymmetrically and symmetrically [530], [531] and because this can shift to primarily symmetric divisions in cancers [188], [532], it is likely that when Wnt signaling is unpolarized or too high, symmetrical divisions can arise, which may include driving both daughters to differentiate.

The signaling that governs the multipotency of stem cells that reside within the intestinal crypt has been extensively studied. These intestinal stem cells (ISCs) are responsible for generating the villus, enteroendocrine, goblet and Paneth cells; the latter are considered as niche cells for ISCs and are the main source of Wnt signaling in the crypt [533], [534]. The importance of Wnt/β-catenin signaling in the maintenance of the adult murine intestine was first demonstrated by the loss of intestinal crypts that arises from either β-catenin deficiency or ectopic expression of the Wnt inhibitor DKK1 [535], [536]. This corroborated earlier studies showing that failure to express TCF4 also led to a failure to maintain ISCs and intestinal crypts [537]. Moreover, ISCs can generate minigut organoid cultures that can be long-term maintained *in vitro* as long as R-spondin 1 is present to stimulate canonical Wnt signaling [538]. In contrast, BMP signaling antagonizes Wnt signaling through the PTEN tumor-suppressor protein in the mouse small intestine and, therefore, restricts proliferation [539], [540]. As a matter of fact, high levels of Wnt receptors expression are observed at the top of the human colonic crypt [541]. Optimal maintenance of ISCs *in vitro* is also achieved by inhibiting BMP signaling [538], [542]. In addition, the Notch receptor, its ligand Delta1 and associated Hes transcription factors, are all expressed mainly at the base of small intestinal crypts [543]. Notch signaling seems to be relevant in maintaining the proliferative compartment of intestinal crypts and in determining lineage commitment. The proliferative small intestinal crypt cells of mice injected intraperitoneally with γ-secretase (which inhibits the activated Notch receptor) rapidly transform into postmitotic goblet cells [544]. All these observations indicate that these pathways may represent opposing forces in the maintenance of active stem cells and are subjected to a particular tight regulation in ISCs.

Additionally, ISCs exist in two distinct states based in part on their sensitivity to Wnt signaling; the more quiescent stem cells (the so-called crypt +4 ISCs) are in a more Wnt-restricted microenvironment, while the active stem cells (0 to +3 ISCs) display a reduced threshold for activation to canonical Wnt stimulation [172], [175], [410], [545], [546]. In both cases, Wnt/β-catenin activity is associated with proliferation and cell fate determination and, as discussed above, these two features might be inseparable if Wnt/β-catenin signaling turns

out to function in these tissues at least in part to promote asymmetric cell divisions. Moreover, very high levels of Wnt signaling in the intestine are associated with terminal differentiation, represented by the Paneth cell [547], [548].

The above examples illustrate that it is plausible that activation of canonical Wnt signaling as a result of SOX2 and LGR5 repression in SW620 cells, and LGR5 knock down in SW480 cell line, may lead to such imbalance in the pathways regulating their self-renewal potential and differentiation (e.g. Notch or BMP signaling) that this property is compromised. Genome-wide transcriptomic profiles of SOX2 and LGR5 knock down SW620 cells may shed some light on this matter (ongoing work).

We have also demonstrated by β-catenin knock down in both SW480 and SW620 cells, that presumable reduction of Wnt/β-catenin signaling and/or loss of a structural function of β-catenin also leads to the loss of self-renewal potential of these cells. Following the same reasoning, one possible interpretation may be that these cells require certain levels of canonical Wnt signaling and β-catenin activity for optimal self-renewal; once the threshold of tolerance are surpassed (upper and lower thresholds), this property is affected. Therefore, it is likely that this may be related to promotion by Wnt signaling of symmetrical divisions in putative CSCs contained in SW620 and SW480 cells that preferentially give rise to two daughter cells fated to differentiation rather than two CSCs, with the consequent overall loss of self-renewal. However, in the case of SOX2, SW620 cells may be so dependent on its transcriptional program that its repression directly causes the loss of self-renewal properties among other growth capabilities.


Conclusions

Messier object 33, The Triangulum Galaxy

The Triangulum Galaxy is a spiral galaxy located approximately 3 million light-years away from our galaxy in the constellation Triangulum. With a diameter of about 50,000 light-years, is the third-largest member of the Local Group of galaxies, which includes the Milky Way, the Andromeda Galaxy and about 44 other smaller galaxies. Triangulum may be home to 40 billion stars, compared to 400 billion for the Milky Way, and 1 trillion (1,000 billion) stars for Andromeda…

1. End-point experiments with short-term (72 h) exposure to drugs and MTT assays, show that differential SOX2 expression is not associated with the intrinsic drug resistance capacity displayed by cancer cell lines of prostate (PC-3/Mc and PC-3/S), pancreas (PANC-1 and CAPAN-1) and colorectal (SW620 and SW480) origins.

2. Modulation of SOX2 levels, either through shRNA-mediated knock down or through overexpression by exogenous transduction impairs, *per se*, the cell proliferation and/or viability of prostate, pancreas and colorectal cancer cell lines.

3. The colorectal cancer cell lines SW620 and SW480 display differential growth and viability responses to exogenous SOX2 overexpression. The major phenotypes observed in SW480 cells are a significant increase in apoptosis and necrotic cells with reduction of their self-renewal capacity, concomitant to a significant increase in ROS levels. The major phenotypes observed in SW620 cells are a reduction in cell proliferation with relatively lasting G1 arrest, elevation of cyclin-dependent kinase inhibitors p21 and p27, loss of self-renewal potential and increase in ROS levels and DNA damage response. The cell cycle arrest induced by overexpression of exogenous SOX2 in SW620 cells is partially mediated by p21 while loss of self-renewal is partially mediated by p27.

4. SW620 cells are highly dependent on SOX2 for the maintenance of their growth properties. Silencing of SOX2 in SW620 cells induces apoptosis and a lasting cell cycle arrest in G1 with upregulation of p21 and p27. The cell cycle arrest induced by SOX2 repression in SW620 cells is partially mediated by p27. SOX2 knock down in this cell line also causes a dramatic loss of self-renewal *in vitro* and a significant reduction in the ability to grow tumors *in vivo*.

5. Silencing of SOX2 in SW620 cells leads to a strong downregulation of the colon stem cell marker LGR5, gain in nuclear localization of β-catenin and increase of β-catenin/TCF/LEF transcriptional activity. Knock down of SOX2 in SW620 cells seems to engage a partial epithelial-to-mesenchymal transition program. Similar effects are observed in SW620 and SW480 cells upon knock

down of LGR5. In these cell lines, LGR5 seems to act as a negative regulator of the canonical Wnt signaling in the absence of their cognate ligands (R-spondins). In addition, repression of LGR5 in SW620 and SW480 cells also impairs their self-renewal ability, and in the case of SW620 cells, it also significantly diminishes their tumorigenic potential *in vivo*.

6. Silencing of β-catenin inhibits the self-renewal potential of SW620 and SW480 cells, as measured by anchorage-independent spheroid formation assays. As a result of our previous finding that upregulation of β-catenin activity induced by knock down of LGR5 (and SOX2 in the case of SW620 cells) is associated with loss of their self-renewal rate, we propose that Wnt/β-catenin signaling enable these cells to display an optimal self-renewal capacity but only within an appropriate range of activity. Expression or activity of β-catenin at levels beyond this range (upper and lower thresholds) may impair the self-renewal potential of these cells.


Bibliography

Messier object 51, The Whirlpool Galaxy

The Whirlpool Galaxy is an interacting grand-design spiral galaxy with 2 active galactic nucleus located at the constellation Canes Venatici. It is about 23 million light-years away from the Milky Way. The very pronounced spiral structure of the Whirlpool Galaxy is believed to be the result of the close interaction with its companion galaxy NGC5195; the last collision of these two gravitationally bound galaxies, has been estimated to occur about 500 to 600 million years ago…

[1] D. Hanahan and R. Weinberg, “The hallmarks of cancer,” *Cell*, vol. 100, pp. 57–70, 2000.
[2] D. Hanahan and R. A. Weinberg, “Hallmarks of Cancer: The Next Generation,” *Cell*, vol. 144, no. 5, pp. 646–674, Mar. 2011.
[3] D. Hanahan and L. M. Coussens, “Accessories to the crime: functions of cells recruited to the tumor microenvironment.,” *Cancer Cell*, vol. 21, no. 3, pp. 309–22, Mar. 2012.
[4] M. R. Junttila and F. J. de Sauvage, “Influence of tumour micro-environment heterogeneity on therapeutic response.,” *Nature*, vol. 501, no. 7467, pp. 346–54, Sep. 2013.
[5] C. Greaves, M Maley, “Clonal evolution in cancer,” *Nature*, vol. 481, no. 7381, pp. 306–313, 2012.
[6] R. A Burrell *et al.*, “The causes and consequences of genetic heterogeneity in cancer evolution.,” *Nature*, vol. 501, no. 7467, pp. 338–45, Sep. 2013.
[7] J. Dick, “Stem cell concepts renew cancer research,” *Blood*, vol. 112, no. 13, pp. 4793–4807, 2008.
[8] C. E. Meacham and S. J. Morrison, “Tumour heterogeneity and cancer cell plasticity.,” *Nature*, vol. 501, no. 7467, pp. 328–37, Sep. 2013.
[9] L. V Nguyen *et al.*, “Cancer stem cells: an evolving concept.,” *Nat. Rev. Cancer*, vol. 12, no. 2, pp. 133–43, Jan. 2012.
[10] P. C. Nowell, “The clonal evolution of tumor cell populations.,” *Science*, vol. 194, no. 4260, pp. 23–8, Oct. 1976.
[11] B. Vogelstein *et al.*, “Genetic alterations during colorectal-tumor development,” *N. Engl. J. Med.*, vol. 319, pp. 525–532, 1988.
[12] M. Gerlinger and A. Rowan, “Intratumor heterogeneity and branched evolution revealed by multiregion sequencing,” *N. Engl. J. Med.*, vol. 366, no. 10, pp. 883–892, 2012.
[13] L. Melchor *et al.*, “Single-cell genetic analysis reveals the composition of initiating clones and phylogenetic patterns of branching and parallel evolution in myeloma.,” *Leukemia*, vol. 28, no. 8, pp. 1705–15, Aug. 2014.
[14] N. Navin *et al.*, “Tumour evolution inferred by single-cell sequencing.,” *Nature*, vol. 472, no. 7341, pp. 90–4, Apr. 2011.
[15] N. Potter and L. Ermini, “Single-cell mutational profiling and clonal phylogeny in cancer,” *Genome Res.*, no. 23, pp. 2115–2125, 2013.
[16] L. Shlush, N. Chapal-Ilani, and R. Adar, “Cell lineage analysis of acute leukemia relapse uncovers the role of replication-rate heterogeneity and microsatellite instability,” *Blood*, vol. 120, no. 3, pp. 603–612, 2012.
[17] L. Alonso and E. Fuchs, “Stem cells of the skin epithelium,” *Proc. Natl. Acad. Sci.*, vol. 100, no. suppl. 1, pp. 11830–11835, 2003.
[18] A. P. Beltrami *et al.*, “Adult cardiac stem cells are multipotent and support myocardial regeneration.,” *Cell*, vol. 114, no. 6, pp. 763–76, Sep. 2003.
[19] S. Bonner-Weir and A. Sharma, “Pancreatic stem cells.,” *J. Pathol.*, vol. 197, no. 4, pp. 519–26, Jul. 2002.
[20] N. Barker *et al.*, “Identification of stem cells in small intestine and colon by marker gene Lgr5.,” *Nature*, vol. 449, no. 7165, pp. 1003–7, Oct. 2007.
[21] M. F. Clarke *et al.*, “Cancer stem cells--perspectives on current status and future directions: AACR Workshop on cancer stem cells.,” *Cancer Res.*, vol. 66, no. 19, pp. 9339–44, Oct. 2006.
[22] T. Reya *et al.*, “Stem cells, cancer, and cancer stem cells.,” *Nature*, vol. 414, no. 6859, pp. 105–11, Nov. 2001.
[23] J. E. Visvader and G. J. Lindeman, “Cancer stem cells in solid tumours: accumulating evidence and unresolved questions.,” *Nat. Rev. Cancer*, vol. 8, no. 10, pp. 755–68, Oct. 2008.
[24] D. Bonnet and J. Dick, “Human acute myeloid leukemia is organized as a hierarchy that originates from a primitive hematopoeietic cell,” *Nat. Med.*, vol. 3, no. 7, pp. 730–737, 1997.
[25] S. Singh *et al.*, “Identification of human brain tumour initiating cells,” *Nature*, vol. 432, no. November, 2004.
[26] M. E. Prince *et al.*, “Identification of a subpopulation of cells with cancer stem cell properties in head and neck squamous cell carcinoma.,” *Proc. Natl. Acad. Sci. U. S. A.*, vol. 104, no. 3, pp. 973–8, Jan. 2007.

[27] P. C. Hermann *et al.*, “Distinct populations of cancer stem cells determine tumor growth and metastatic activity in human pancreatic cancer.,” *Cell Stem Cell*, vol. 1, no. 3, pp. 313–23, Sep. 2007.
[28] C. Li *et al.*, “Identification of pancreatic cancer stem cells.,” *Cancer Res.*, vol. 67, no. 3, pp. 1030–7, Feb. 2007.
[29] A. Eramo *et al.*, “Identification and expansion of the tumorigenic lung cancer stem cell population.,” *Cell Death Differ.*, vol. 15, no. 3, pp. 504–14, Mar. 2008.
[30] A. T. Collins *et al.*, “Prospective identification of tumorigenic prostate cancer stem cells.,” *Cancer Res.*, vol. 65, no. 23, pp. 10946–51, Dec. 2005.
[31] L. Patrawala *et al.*, “Highly purified CD44+ prostate cancer cells from xenograft human tumors are enriched in tumorigenic and metastatic progenitor cells.,” *Oncogene*, vol. 25, no. 12, pp. 1696–708, Mar. 2006.
[32] C. A. O’Brien *et al.*, “A human colon cancer cell capable of initiating tumour growth in immunodeficient mice.,” *Nature*, vol. 445, no. 7123, pp. 106–10, Jan. 2007.
[33] L. Ricci-Vitiani *et al.*, “Identification and expansion of human colon-cancer-initiating cells.,” *Nature*, vol. 445, no. 7123, pp. 111–5, Jan. 2007.
[34] C. Wu *et al.*, “Side population cells isolated from mesenchymal neoplasms have tumor initiating potential.,” *Cancer Res.*, vol. 67, no. 17, pp. 8216–22, Sep. 2007.
[35] G. P. Gupta and J. Massagué, “Cancer metastasis: building a framework.,” *Cell*, vol. 127, no. 4, pp. 679–95, Nov. 2006.
[36] M. Al-Hajj *et al.*, “Prospective identification of tumorigenic breast cancer cells.,” *Proc. Natl. Acad. Sci. U. S. A.*, vol. 100, no. 7, pp. 3983–8, Apr. 2003.
[37] H. Liu *et al.*, “Cancer stem cells from human breast tumors are involved in spontaneous metastases in orthotopic mouse models.,” *Proc. Natl. Acad. Sci. U. S. A.*, vol. 107, no. 42, pp. 18115–20, Oct. 2010.
[38] X. Li *et al.*, “Intrinsic resistance of tumorigenic breast cancer cells to chemotherapy.,” *J. Natl. Cancer Inst.*, vol. 100, no. 9, pp. 672–9, May 2008.
[39] J. M. Goldman *et al.*, “Chronic myeloproliferative diseases with and without the Ph chromosome: some unresolved issues.,” *Leukemia*, vol. 23, no. 10, pp. 1708–15, Oct. 2009.
[40] K. I. Oravecz-Wilson *et al.*, “Persistence of leukemia-initiating cells in a conditional knockin model of an imatinib-responsive myeloproliferative disorder.,” *Cancer Cell*, vol. 16, no. 2, pp. 137–48, Aug. 2009.
[41] D. Perrotti *et al.*, “Chronic myeloid leukemia : mechanisms of blastic transformation,” *J. Clin. Invest.*, vol. 120, no. 7, pp. 2254–2264, 2010.
[42] F. Watt and B. Hogan, “Out of Eden: stem cells and their niches,” *Science* , vol. 287, pp. 1427–1430, 2000.
[43] R. Pardal, M. F. Clarke, and S. J. Morrison, “Applying the principles of stem-cell biology to cancer.,” *Nat. Rev. Cancer*, vol. 3, no. 12, pp. 895–902, Dec. 2003.
[44] S. A. Bapat, “Evolution of cancer stem cells.,” *Semin. Cancer Biol.*, vol. 17, no. 3, pp. 204–13, Jun. 2007.
[45] A. Merlos-Suárez *et al.*, “The intestinal stem cell signature identifies colorectal cancer stem cells and predicts disease relapse.,” *Cell Stem Cell*, vol. 8, no. 5, pp. 511–24, May 2011.
[46] S. Pece *et al.*, “Biological and molecular heterogeneity of breast cancers correlates with their cancer stem cell content.,” *Cell*, vol. 140, no. 1, pp. 62–73, Jan. 2010.
[47] P. J. Campbell *et al.*, “The patterns and dynamics of genomic instability in metastatic pancreatic cancer.,” *Nature*, vol. 467, no. 7319, pp. 1109–13, Oct. 2010.
[48] S. Yachida *et al.*, “Distant metastasis occurs late during the genetic evolution of pancreatic cancer.,” *Nature*, vol. 467, no. 7319, pp. 1114–7, Oct. 2010.
[49] C. Odoux *et al.*, “A stochastic model for cancer stem cell origin in metastatic colon cancer.,” *Cancer Res.*, vol. 68, no. 17, pp. 6932–41, Sep. 2008.
[50] P. B. Gupta *et al.*, “Stochastic state transitions give rise to phenotypic equilibrium in populations of cancer cells.,” *Cell*, vol. 146, no. 4, pp. 633–44, Aug. 2011.
[51] J. Zhou and Y. Zhang, “Cancer stem cells. Models, mechanisms and implications for improved treatment,” *Cell cycle*, vol. 7, no. 10, pp. 1360–1370, 2008.
[52] S. A. Mani *et al.*, “The epithelial-mesenchymal transition generates cells with properties of stem cells,” *Cell*, vol. 133, no. 4, pp. 704–15, May 2008.
[53] J. P. Thiery *et al.*, “Epithelial-mesenchymal transitions in development and disease.,” *Cell*, vol. 139, no. 5, pp. 871–90, Nov. 2009.

[54] U. Wellner *et al.*, “The EMT-activator ZEB1 promotes tumorigenicity by repressing stemness-inhibiting microRNAs.,” *Nat. Cell Biol.*, vol. 11, no. 12, pp. 1487–95, Dec. 2009.
[55] M. Cordenonsi *et al.*, “The Hippo transducer TAZ confers cancer stem cell-related traits on breast cancer cells.,” *Cell*, vol. 147, no. 4, pp. 759–72, Nov. 2011.
[56] A. D. Rhim *et al.*, “EMT and dissemination precede pancreatic tumor formation.,” *Cell*, vol. 148, no. 1–2, pp. 349–61, Jan. 2012.
[57] H. Clevers, “The intestinal crypt, a prototype stem cell compartment.,” *Cell*, vol. 154, no. 2, pp. 274–84, Jul. 2013.
[58] Y.-C. Hsu and E. Fuchs, “A family business: stem cell progeny join the niche to regulate homeostasis.,” *Nat. Rev. Mol. Cell Biol.*, vol. 13, no. 2, pp. 103–14, Feb. 2012.
[59] K. a Moore and I. R. Lemischka, “Stem cells and their niches.,” *Science*, vol. 311, no. 5769, pp. 1880–5, Mar. 2006.
[60] S. J. Morrison and A. C. Spradling, “Stem cells and niches: mechanisms that promote stem cell maintenance throughout life.,” *Cell*, vol. 132, no. 4, pp. 598–611, Feb. 2008.
[61] H. Iwasaki and T. Suda, “Cancer stem cells and their niche.,” *Cancer Sci.*, vol. 100, no. 7, pp. 1166–72, Jul. 2009.
[62] Y. Soda *et al.*, “Transdifferentiation of glioblastoma cells into vascular endothelial cells.,” *Proc. Natl. Acad. Sci. U. S. A.*, vol. 108, no. 11, pp. 4274–80, Mar. 2011.
[63] C. Calabrese *et al.*, “A perivascular niche for brain tumor stem cells.,” *Cancer Cell*, vol. 11, no. 1, pp. 69–82, Jan. 2007.
[64] S. Bao *et al.*, “Stem cell-like glioma cells promote tumor angiogenesis through vascular endothelial growth factor.,” *Cancer Res.*, vol. 66, no. 16, pp. 7843–8, Aug. 2006.
[65] C. Folkins *et al.*, “Glioma tumor stem-like cells promote tumor angiogenesis and vasculogenesis via vascular endothelial growth factor and stromal-derived factor 1,” *Cancer Res.*, vol. 69, no. 18, pp. 7243–7251, 2009.
[66] R. Gilbertson and J. Rich, “Making a tumour’s bed: glioblastoma stem cells and the vascular niche,” *Nat. Rev. Cancer*, vol. 7, no. october, pp. 733–736, 2007.
[67] J. D. Lathia *et al.*, “Integrin alpha 6 regulates glioblastoma stem cells.,” *Cell Stem Cell*, vol. 6, no. 5, pp. 421–32, May 2010.
[68] N. Charles *et al.*, “Perivascular nitric oxide activates notch signaling and promotes stem-like character in PDGF-induced glioma cells.,” *Cell Stem Cell*, vol. 6, no. 2, pp. 141–52, Feb. 2010.
[69] X. Yao, Y. Ping, and J. Chen, “Glioblastoma stem cells produce vascular endothelial growth factor by activation of a G-protein coupled formylpeptide receptor FPR,” *J. Pathol.*, vol. 8, no. 215, pp. 369–376, 2008.
[70] R. Ezhilarasan *et al.*, “Glioma cells suppress hypoxia-induced endothelial cell apoptosis and promote the angiogenic process.,” *Int. J. Oncol.*, vol. 30, no. 3, pp. 701–7, Mar. 2007.
[71] C. K. Brown *et al.*, “Glioblastoma cells block radiation-induced programmed cell death of endothelial cells.,” *FEBS Lett.*, vol. 565, no. 1–3, pp. 167–70, May 2004.
[72] B. Beck *et al.*, “A vascular niche and a VEGF-Nrp1 loop regulate the initiation and stemness of skin tumours.,” *Nature*, vol. 478, no. 7369, pp. 399–403, Oct. 2011.
[73] E. C. Finger and A. J. Giaccia, “Hypoxia, inflammation, and the tumor microenvironment in metastatic disease.,” *Cancer Metastasis Rev.*, vol. 29, no. 2, pp. 285–93, Jun. 2010.
[74] S. Grivennikov *et al.*, “IL-6 and Stat3 are required for survival of intestinal epithelial cells and development of colitis-associated cancer.,” *Cancer Cell*, vol. 15, no. 2, pp. 103–13, Feb. 2009.
[75] D. Iliopoulos, H. A. Hirsch, and K. Struhl, “An epigenetic switch involving NF-kappaB, Lin28, Let-7 MicroRNA, and IL6 links inflammation to cell transformation.,” *Cell*, vol. 139, no. 4, pp. 693–706, Nov. 2009.
[76] M. Jinushi *et al.*, “Tumor-associated macrophages regulate tumorigenicity and anticancer drug responses of cancer stem/initiating cells.,” *Proc. Natl. Acad. Sci. U. S. A.*, vol. 108, no. 30, pp. 12425–30, Jul. 2011.
[77] S. Carmans *et al.*, “The inhibitory neurotransmitter glycine modulates macrophage activity by activation of neutral amino acid transporters.,” *J. Neurosci. Res.*, vol. 88, no. 11, pp. 2420–30, Aug. 2010.
[78] S. Muramatsu *et al.*, “Visualization of stem cell features in human hepatocellular carcinoma reveals in vivo significance of tumor-host interaction and clinical course.,” *Hepatology*, vol. 58, no. 1, pp. 218–28, Jul. 2013.

[79] X. Ye *et al.*, “Tumor-associated microglia/macrophages enhance the invasion of glioma stem-like cells via TGF-β1 signaling pathway.,” *J. Immunol.*, vol. 189, no. 1, pp. 444–53, Jul. 2012.
[80] J. Wei *et al.*, “Hypoxia potentiates glioma-mediated immunosuppression.,” *PLoS One*, vol. 6, no. 1, p. e16195, Jan. 2011.
[81] L. M. Coussens, L. Zitvogel, and A. K. Palucka, “Neutralizing tumor-promoting chronic inflammation: a magic bullet?,” *Science*, vol. 339, no. 6117, pp. 286–91, Jan. 2013.
[82] R. A. Flavell *et al.*, “The polarization of immune cells in the tumour environment by TGFbeta.,” *Nat. Rev. Immunol.*, vol. 10, no. 8, pp. 554–67, Aug. 2010.
[83] C. Dierks *et al.*, “Expansion of Bcr-Abl-positive leukemic stem cells is dependent on Hedgehog pathway activation.,” *Cancer Cell*, vol. 14, no. 3, pp. 238–49, Sep. 2008.
[84] C. Zhao *et al.*, “Hedgehog signalling is essential for maintenance of cancer stem cells in myeloid leukaemia.,” *Nature*, vol. 458, no. 7239, pp. 776–9, Apr. 2009.
[85] M. Kobune *et al.*, “Stromal cells expressing hedgehog-interacting protein regulate the proliferation of myeloid neoplasms.,” *Blood Cancer J.*, vol. 2, no. 9, p. e87, Jan. 2012.
[86] R. Kalluri and M. Zeisberg, “Fibroblasts in cancer.,” *Nat. Rev. Cancer*, vol. 6, no. 5, pp. 392–401, May 2006.
[87] A. Orimo *et al.*, “Stromal fibroblasts present in invasive human breast carcinomas promote tumor growth and angiogenesis through elevated SDF-1/CXCL12 secretion.,” *Cell*, vol. 121, no. 3, pp. 335–48, May 2005.
[88] L. Vermeulen *et al.*, “Wnt activity defines colon cancer stem cells and is regulated by the microenvironment.,” *Nat. Cell Biol.*, vol. 12, no. 5, pp. 468–76, May 2010.
[89] I. Malanchi *et al.*, “Cutaneous cancer stem cell maintenance is dependent on beta-catenin signalling.,” *Nature*, vol. 452, no. 7187, pp. 650–3, Apr. 2008.
[90] W. K. Chau *et al.*, “c-Kit mediates chemoresistance and tumor-initiating capacity of ovarian cancer cells through activation of Wnt/β-catenin-ATP-binding cassette G2 signaling.,” *Oncogene*, vol. 32, no. 22, pp. 2767–81, May 2013.
[91] F. De Bacco *et al.*, “The MET oncogene is a functional marker of a glioblastoma stem cell subtype.,” *Cancer Res.*, vol. 72, no. 17, pp. 4537–50, Sep. 2012.
[92] D. C. Radisky, “Leading the charge,” *Nat. Cell Biol.*, vol. 9, no. 12, pp. 1341–1342, 2007.
[93] P. Barcellos-de-Souza *et al.*, “Tumor microenvironment: bone marrow-mesenchymal stem cells as key players.,” *Biochim. Biophys. Acta*, vol. 1836, no. 2, pp. 321–35, Dec. 2013.
[94] J. Yang and R. A. Weinberg, “Epithelial-mesenchymal transition: at the crossroads of development and tumor metastasis.,” *Dev. Cell*, vol. 14, no. 6, pp. 818–29, Jun. 2008.
[95] K. McLean, Y. Gong, and Y. Choi, “Human ovarian carcinoma–associated mesenchymal stem cells regulate cancer stem cells and tumorigenesis via altered BMP production,” *J. Clin. Invest.*, vol. 121, no. 8, pp. 3206–3219, 2011.
[96] E. Lonardo *et al.*, “Pancreatic stellate cells form a niche for cancer stem cells and promote their self-renewal and invasiveness.,” *Cell cycle*, vol. 11, no. 7, pp. 1282–90, Apr. 2012.
[97] A. Tsuyada *et al.*, “CCL2 mediates cross-talk between cancer cells and stromal fibroblasts that regulates breast cancer stem cells.,” *Cancer Res.*, vol. 72, no. 11, pp. 2768–79, Jun. 2012.
[98] S. Liu *et al.*, “Breast cancer stem cells are regulated by mesenchymal stem cells through cytokine networks.,” *Cancer Res.*, vol. 71, no. 2, pp. 614–24, Jan. 2011.
[99] M. W. Klymkowsky and P. Savagner, “Epithelial-mesenchymal transition: a cancer researcher’s conceptual friend and foe.,” *Am. J. Pathol.*, vol. 174, no. 5, pp. 1588–93, May 2009.
[100] K. Polyak and R. A. Weinberg, “Transitions between epithelial and mesenchymal states: acquisition of malignant and stem cell traits.,” *Nat. Rev. Cancer*, vol. 9, no. 4, pp. 265–73, Apr. 2009.
[101] M. Yilmaz and G. Christofori, “EMT, the cytoskeleton, and cancer cell invasion.,” *Cancer Metastasis Rev.*, vol. 28, no. 1–2, pp. 15–33, Jun. 2009.
[102] S. Park and A. Gaur, “The miR-200 family determines the epithelial phenotype of cancer cells by targeting the E-cadherin repressors ZEB1 and ZEB2,” *Genes Dev.*, no. 22, pp. 894–907, 2008.
[103] P. A. Gregory *et al.*, “The miR-200 family and miR-205 regulate epithelial to mesenchymal transition by targeting ZEB1 and SIP1.,” *Nat. Cell Biol.*, vol. 10, no. 5, pp. 593–601, May 2008.

[104] S. Lamouille, J. Xu, and R. Derynck, “Molecular mechanisms of epithelial-mesenchymal transition.,” *Nat. Rev. Mol. Cell Biol.*, vol. 15, no. 3, pp. 178–96, Mar. 2014.
[105] J. H. Taube *et al.*, “Core epithelial-to-mesenchymal transition interactome gene-expression signature is associated with claudin-low and metaplastic breast cancer subtypes.,” *Proc. Natl. Acad. Sci. U. S. A.*, vol. 107, no. 35, pp. 15449–54, Aug. 2010.
[106] O. Schmalhofer, S. Brabletz, and T. Brabletz, “E-cadherin, beta-catenin, and ZEB1 in malignant progression of cancer.,” *Cancer Metastasis Rev.*, vol. 28, no. 1–2, pp. 151–66, Jun. 2009.
[107] H. Peinado *et al.*, “Snail and E47 repressors of E-cadherin induce distinct invasive and angiogenic properties in vivo.,” *J. Cell Sci.*, vol. 117, no. Pt 13, pp. 2827–39, Jun. 2004.
[108] D. S. Micalizzi, S. M. Farabaugh, and H. L. Ford, “Epithelial-mesenchymal transition in cancer: parallels between normal development and tumor progression.,” *J. Mammary Gland Biol. Neoplasia*, vol. 15, no. 2, pp. 117–34, Jun. 2010.
[109] A. E. Karnoub and R. A. Weinberg, “Chemokine networks and breast cancer metastasis.,” *Breast Dis.*, vol. 26, pp. 75–85, 2007.
[110] T. Brabletz *et al.*, “Variable beta-catenin expression in colorectal cancers indicates tumor progression driven by the tumor environment.,” *Proc. Natl. Acad. Sci. U. S. A.*, vol. 98, no. 18, pp. 10356–61, Aug. 2001.
[111] F. Hlubek *et al.*, “Heterogeneous expression of Wnt/beta-catenin target genes within colorectal cancer.,” *Int. J. Cancer*, vol. 121, no. 9, pp. 1941–8, Nov. 2007.
[112] H. Hugo *et al.*, “Epithelial-Mesenchymal and Mesenchymal-Epithelial Transitions in Carcinoma Progression,” *J. Cell. Physiol.*, no. June, pp. 374–383, 2007.
[113] P. Friedl and K. Wolf, “Tube travel: the role of proteases in individual and collective cancer cell invasion.,” *Cancer Res.*, vol. 68, no. 18, pp. 7247–9, Sep. 2008.
[114] P. Friedl and K. Wolf, “Plasticity of cell migration: a multiscale tuning model.,” *J. Cell Biol.*, vol. 188, no. 1, pp. 11–9, Jan. 2010.
[115] C. D. Madsen and E. Sahai, “Cancer dissemination-lessons from leukocytes.,” *Dev. Cell*, vol. 19, no. 1, pp. 13–26, Jul. 2010.
[116] F. Sabeh, R. Shimizu-Hirota, and S. J. Weiss, “Protease-dependent versus -independent cancer cell invasion programs: three-dimensional amoeboid movement revisited.,” *J. Cell Biol.*, vol. 185, no. 1, pp. 11–9, Apr. 2009.
[117] K. Kessenbrock, V. Plaks, and Z. Werb, “Matrix metalloproteinases: regulators of the tumor microenvironment.,” *Cell*, vol. 141, no. 1, pp. 52–67, Apr. 2010.
[118] B. Z. Qian and J. W. Pollard, “Macrophage diversity enhances tumor progression and metastasis.,” *Cell*, vol. 141, no. 1, pp. 39–51, Apr. 2010.
[119] J. A. Joyce and J. W. Pollard, “Microenvironmental regulation of metastasis.,” *Nat. Rev. Cancer*, vol. 9, no. 4, pp. 239–52, Apr. 2009.
[120] M. Egeblad, E. Nakasone, and Z. Werb, “Tumors as organs: complex tissues that interface with the entire organism,” *Dev. Cell*, vol. 18, no. 6, pp. 884–901, 2010.
[121] A. E. Karnoub *et al.*, “Mesenchymal stem cells within tumour stroma promote breast cancer metastasis.,” *Nature*, vol. 449, no. 7162, pp. 557–63, Oct. 2007.
[122] C. Palermo and J. A. Joyce, “Cysteine cathepsin proteases as pharmacological targets in cancer.,” *Trends Pharmacol. Sci.*, vol. 29, no. 1, pp. 22–8, Jan. 2008.
[123] M. M. Mohamed and B. F. Sloane, “Cysteine cathepsins: multifunctional enzymes in cancer.,” *Nat. Rev. Cancer*, vol. 6, no. 10, pp. 764–75, Oct. 2006.
[124] V. Gocheva *et al.*, “IL-4 induces cathepsin protease activity in tumor-associated macrophages to promote cancer growth and invasion.,” *Genes Dev.*, vol. 24, no. 3, pp. 241–55, Feb. 2010.
[125] J. B. Wyckoff *et al.*, “Direct visualization of macrophage-assisted tumor cell intravasation in mammary tumors.,” *Cancer Res.*, vol. 67, no. 6, pp. 2649–56, Mar. 2007.
[126] A. J. Evans *et al.*, “VHL promotes E2 box-dependent E-cadherin transcription by HIF-mediated regulation of SIP1 and snail.,” *Mol. Cell. Biol.*, vol. 27, no. 1, pp. 157–69, Jan. 2007.
[127] B. Krishnamachary *et al.*, “Hypoxia-inducible factor-1-dependent repression of E-cadherin in von Hippel-Lindau tumor suppressor-null renal cell carcinoma mediated by TCF3, ZFHX1A, and ZFHX1B.,” *Cancer Res.*, vol. 66, no. 5, pp. 2725–31, Mar. 2006.
[128] G. Semenza, “Hypoxia-inducible factors: mediators of cancer progression and targets for cancer therapy,” *Trends Pharmacol. Sci.*, vol. 33, no. 4, pp. 207–214, 2012.
[129] X. Lu and Y. Kang, “Hypoxia and hypoxia-inducible factors: master regulators of metastasis.,” *Clin. cancer Res.*, vol. 16, no. 24, pp. 5928–35, Dec. 2010.

[130] T. Celià-Terrassa *et al.*, *Epithelial-mesenchymal transition can suppress major attributes of human epithelial tumor-initiating cells.*, vol. 122, no. 5. 2012, pp. 1849–68.
[131] T. Tsuji, S. Ibaragi, and G. Hu, "Epithelial-mesenchymal transition and cell cooperativity in metastasis.," *Cancer Res.*, vol. 69, no. 18, pp. 7135–9, Sep. 2009.
[132] S. Floor *et al.*, "Cancer cells in epithelial-to-mesenchymal transition and tumor-propagating-cancer stem cells: distinct, overlapping or same populations.," *Oncogene*, pp. 1–13, Jun. 2011.
[133] M. R. Stratton, "Exploring the genomes of cancer cells: progress and promise.," *Science*, vol. 331, no. 6024, pp. 1553–8, Mar. 2011.
[134] A. Van Keymeulen and C. Blanpain, "Tracing epithelial stem cells during development, homeostasis, and repair," *J. Cell Biol.*, vol. 197, no. 5, pp. 575–584, 2012.
[135] J. Ferlay *et al.*, "Estimates of worldwide burden of cancer in 2008: GLOBOCAN 2008.," *Int. J. Cancer*, vol. 127, no. 12, pp. 2893–917, Dec. 2010.
[136] C. J. Kemp, "Multistep skin cancer in mice as a model to study the evolution of cancer cells.," *Semin. Cancer Biol.*, vol. 15, no. 6, pp. 460–73, Dec. 2005.
[137] E. L. Abel *et al.*, "Multi-stage chemical carcinogenesis in mouse skin: fundamentals and applications.," *Nat. Protoc.*, vol. 4, no. 9, pp. 1350–62, Jan. 2009.
[138] J. Perez-Losada and A. Balmain, "Stem-cell hierarchy in skin cancer.," *Nat. Rev. Cancer*, vol. 3, no. 6, pp. 434–43, Jun. 2003.
[139] D. M. Owens and F. M. Watt, "Contribution of stem cells and differentiated cells to epidermal tumours.," *Nat. Rev. Cancer*, vol. 3, no. 6, pp. 444–51, Jun. 2003.
[140] T. S. Argyris, T. J. Slaga, and S. Argyris, "Promotion of Carcinomas by Repeated Abrasion in Initiated Skin of Mice.," *Cancer Res.*, vol. 41, pp. 5193–5195, 1981.
[141] K. Brown *et al.*, "The malignant capacity of skin tumours induced by expression of a mutant H-ras transgene depends on the cell type targeted.," *Curr. Biol.*, vol. 8, no. 9, pp. 516–24, Apr. 1998.
[142] A. C. White *et al.*, "Defining the origins of Ras/p53-mediated squamous cell carcinoma.," *Proc. Natl. Acad. Sci. U. S. A.*, vol. 108, no. 18, pp. 7425–30, May 2011.
[143] G. Lapouge *et al.*, "Identifying the cellular origin of squamous skin tumors.," *Proc. Natl. Acad. Sci. U. S. A.*, vol. 108, no. 18, pp. 7431–6, May 2011.
[144] S. Li *et al.*, "A keratin 15 containing stem cell population from the hair follicle contributes to squamous papilloma development in the mouse.," *Mol. Carcinog.*, vol. 52, no. 10, pp. 751–9, Oct. 2013.
[145] M. D. Taylor *et al.*, "Molecular subgroups of medulloblastoma: the current consensus.," *Acta Neuropathol.*, vol. 123, no. 4, pp. 465–72, Apr. 2012.
[146] Z.-J. Yang *et al.*, "Medulloblastoma can be initiated by deletion of Patched in lineage-restricted progenitors or stem cells.," *Cancer Cell*, vol. 14, no. 2, pp. 135–45, Aug. 2008.
[147] U. Schüller *et al.*, "Acquisition of granule neuron precursor identity is a critical determinant of progenitor cell competence to form Shh-induced medulloblastoma.," *Cancer Cell*, vol. 14, no. 2, pp. 123–34, Aug. 2008.
[148] P. Gibson *et al.*, "Subtypes of medulloblastoma have distinct developmental origins.," *Nature*, vol. 468, no. 7327, pp. 1095–9, Dec. 2010.
[149] D. Kawauchi *et al.*, "A mouse model of the most aggressive subgroup of human medulloblastoma.," *Cancer Cell*, vol. 21, no. 2, pp. 168–80, Feb. 2012.
[150] Y. Pei *et al.*, "An animal model of MYC-driven medulloblastoma.," *Cancer Cell*, vol. 21, no. 2, pp. 155–67, Feb. 2012.
[151] F. J. Swartling *et al.*, "Distinct neural stem cell populations give rise to disparate brain tumors in response to N-MYC.," *Cancer Cell*, vol. 21, no. 5, pp. 601–13, May 2012.
[152] C. Sotiriou and M. J. Piccart, "Taking gene-expression profiling to the clinic: when will molecular signatures become relevant to patient care?," *Nat. Rev. Cancer*, vol. 7, no. 7, pp. 545–53, Jul. 2007.
[153] J. Visvader, "Keeping abreast of the mammary epithelial hierarchy and breast tumorigenesis," *Genes Dev.*, no. 23, pp. 2563–2577, 2009.
[154] A. Van Keymeulen *et al.*, "Distinct stem cells contribute to mammary gland development and maintenance.," *Nature*, vol. 479, no. 7372, pp. 189–93, Nov. 2011.
[155] J. Palacios *et al.*, "Phenotypic characterization of BRCA1 and BRCA2 tumors based in a tissue microarray study with 37 immunohistochemical markers.," *Breast Cancer Res. Treat.*, vol. 90, no. 1, pp. 5–14, Mar. 2005.

[156] X. Liu *et al.*, “Somatic loss of BRCA1 and p53 in mice induces mammary tumors with features of human BRCA1-mutated basal-like breast cancer.,” *Proc. Natl. Acad. Sci. U. S. A.*, vol. 104, no. 29, pp. 12111–6, Jul. 2007.
[157] G. Molyneux *et al.*, “BRCA1 basal-like breast cancers originate from luminal epithelial progenitors and not from basal stem cells.,” *Cell Stem Cell*, vol. 7, no. 3, pp. 403–17, Sep. 2010.
[158] T. A. Proia *et al.*, “Genetic predisposition directs breast cancer phenotype by dictating progenitor cell fate.,” *Cell Stem Cell*, vol. 8, no. 2, pp. 149–63, Feb. 2011.
[159] E. Lim *et al.*, “Aberrant luminal progenitors as the candidate target population for basal tumor development in BRCA1 mutation carriers.,” *Nat. Med.*, vol. 15, no. 8, pp. 907–13, Aug. 2009.
[160] K. K. Youssef *et al.*, “Identification of the cell lineage at the origin of basal cell carcinoma.,” *Nat. Cell Biol.*, vol. 12, no. 3, pp. 299–305, Mar. 2010.
[161] M. Shen and C. Abate-Shen, “Molecular genetics of prostate cancer: new prospects for old challenges,” *Genes Dev.*, no. 212, pp. 1967–2000, 2010.
[162] X. Wang *et al.*, “A luminal epithelial stem cell that is a cell of origin for prostate cancer.,” *Nature*, vol. 461, no. 7263, pp. 495–500, Sep. 2009.
[163] J. Liu *et al.*, “Regenerated luminal epithelial cells are derived from preexisting luminal epithelial cells in adult mouse prostate.,” *Mol. Endocrinol.*, vol. 25, no. 11, pp. 1849–57, Nov. 2011.
[164] N. Choi *et al.*, “Adult murine prostate basal and luminal cells are self-sustained lineages that can both serve as targets for prostate cancer initiation.,” *Cancer Cell*, vol. 21, no. 2, pp. 253–65, Feb. 2012.
[165] A. S. Goldstein *et al.*, “Identification of a cell of origin for human prostate cancer.,” *Science*, vol. 329, no. 5991, pp. 568–71, Jul. 2010.
[166] D. J. Mulholland *et al.*, “Lin-Sca-1+CD49fhigh stem/progenitors are tumor-initiating cells in the Pten-null prostate cancer model.,” *Cancer Res.*, vol. 69, no. 22, pp. 8555–62, Nov. 2009.
[167] D. A. Lawson *et al.*, “Basal epithelial stem cells are efficient targets for prostate cancer initiation.,” *Proc. Natl. Acad. Sci. U. S. A.*, vol. 107, no. 6, pp. 2610–5, Feb. 2010.
[168] C. K. Ratnacaram *et al.*, “Temporally controlled ablation of PTEN in adult mouse prostate epithelium generates a model of invasive prostatic adenocarcinoma.,” *Proc. Natl. Acad. Sci. U. S. A.*, vol. 105, no. 7, pp. 2521–6, Feb. 2008.
[169] L. C. Trotman *et al.*, “Pten dose dictates cancer progression in the prostate.,” *PLoS Biol.*, vol. 1, no. 3, p. E59, Dec. 2003.
[170] S. Wang *et al.*, “Prostate-specific deletion of the murine Pten tumor suppressor gene leads to metastatic prostate cancer.,” *Cancer Cell*, vol. 4, no. 3, pp. 209–21, Sep. 2003.
[171] N. Barker, S. Bartfeld, and H. Clevers, “Tissue-resident adult stem cell populations of rapidly self-renewing organs.,” *Cell Stem Cell*, vol. 7, no. 6, pp. 656–70, Dec. 2010.
[172] E. Sangiorgi and M. R. Capecchi, “Bmi1 is expressed in vivo in intestinal stem cells.,” *Nat. Genet.*, vol. 40, no. 7, pp. 915–20, Jul. 2008.
[173] R. K. Montgomery *et al.*, “Mouse telomerase reverse transcriptase (mTert) expression marks slowly cycling intestinal stem cells.,” *Proc. Natl. Acad. Sci. U. S. A.*, vol. 108, no. 1, pp. 179–84, Jan. 2011.
[174] N. Takeda *et al.*, “Interconversion between intestinal stem cell populations in distinct niches.,” *Science*, vol. 334, no. 6061, pp. 1420–4, Dec. 2011.
[175] H. Tian *et al.*, “A reserve stem cell population in small intestine renders Lgr5-positive cells dispensable.,” *Nature*, vol. 478, no. 7368, pp. 255–9, Oct. 2011.
[176] J. Muñoz *et al.*, “The Lgr5 intestinal stem cell signature: robust expression of proposed quiescent ‘+4’ cell markers.,” *EMBO J.*, vol. 31, no. 14, pp. 3079–91, Jul. 2012.
[177] S. Itzkovitz *et al.*, “Single-molecule transcript counting of stem-cell markers in the mouse intestine.,” *Nat. Cell Biol.*, vol. 14, no. 1, pp. 106–14, Jan. 2012.
[178] “http://globocan.iarc.fr/Pages/fact_sheets_ cancer.aspx.”
[179] K. W. Kinzler and B. Vogelstein, “Lessons from hereditary colorectal cancer.,” *Cell*, vol. 87, no. 2, pp. 159–70, Oct. 1996.
[180] P. J. Morin, “Activation of beta -Catenin-Tcf Signaling in Colon Cancer by Mutations in beta -Catenin or APC,” *Science*, vol. 275, no. 5307, pp. 1787–1790, Mar. 1997.
[181] N. Barker *et al.*, “Crypt stem cells as the cells-of-origin of intestinal cancer.,” *Nature*, vol. 457, no. 7229, pp. 608–11, Jan. 2009.

[182] L. Zhu *et al.*, “Prominin 1 marks intestinal stem cells that are susceptible to neoplastic transformation.,” *Nature*, vol. 457, no. 7229, pp. 603–7, Jan. 2009.
[183] G. Y. Wang *et al.*, “Basal cell carcinomas arise from hair follicle stem cells in Ptch1(+/-) mice.,” *Cancer Cell*, vol. 19, no. 1, pp. 114–24, Jan. 2011.
[184] M. Ito *et al.*, “Wnt-dependent de novo hair follicle regeneration in adult mouse skin after wounding.,” *Nature*, vol. 447, no. 7142, pp. 316–20, May 2007.
[185] X. Xu *et al.*, “Evidence for type II cells as cells of origin of K-Ras-induced distal lung adenocarcinoma.,” *Proc. Natl. Acad. Sci. U. S. A.*, vol. 109, no. 13, pp. 4910–5, Mar. 2012.
[186] K. Shin *et al.*, “Cellular origin of bladder neoplasia and tissue dynamics of its progression to invasive carcinoma.,” *Nat. Cell Biol.*, vol. 16, no. 5, pp. 469–78, May 2014.
[187] Z. Zhu *et al.*, “Targeting Self-Renewal in High-Grade Brain Tumors Leads to Loss of Brain Tumor Stem Cells and Prolonged Survival.,” *Cell Stem Cell*, pp. 1–14, May 2014.
[188] G. Driessens *et al.*, “Defining the mode of tumour growth by clonal analysis.,” *Nature*, vol. 488, no. 7412, pp. 527–30, Aug. 2012.
[189] A. G. Schepers *et al.*, “Lineage tracing reveals Lgr5+ stem cell activity in mouse intestinal adenomas.,” *Science*, vol. 337, no. 6095, pp. 730–5, Aug. 2012.
[190] J. Chen *et al.*, “A restricted cell population propagates glioblastoma growth after chemotherapy,” *Nature*, pp. 1–6, Aug. 2012.
[191] T. Oskarsson, E. Batlle, and J. Massagué, “Metastatic stem cells: sources, niches, and vital pathways.,” *Cell Stem Cell*, vol. 14, no. 3, pp. 306–21, Mar. 2014.
[192] P. Dalerba *et al.*, “Single-cell dissection of transcriptional heterogeneity in human colon tumors.,” *Nat. Biotechnol.*, vol. 29, no. 12, pp. 1120–7, Dec. 2011.
[193] I. Baccelli *et al.*, “Identification of a population of blood circulating tumor cells from breast cancer patients that initiates metastasis in a xenograft assay.,” *Nat. Biotechnol.*, vol. 31, no. 6, pp. 539–44, Jun. 2013.
[194] S. M. Dieter *et al.*, “Distinct types of tumor-initiating cells form human colon cancer tumors and metastases.,” *Cell Stem Cell*, vol. 9, no. 4, pp. 357–65, Oct. 2011.
[195] A. Kreso *et al.*, “Variable clonal repopulation dynamics influence chemotherapy response in colorectal cancer.,” *Science*, vol. 339, no. 6119, pp. 543–8, Feb. 2013.
[196] O. H. Ocaña *et al.*, “Metastatic Colonization Requires the Repression of the Epithelial-Mesenchymal Transition Inducer Prrx1,” *Cancer Cell*, vol. 22, pp. 1–16, Nov. 2012.
[197] M. Stankic *et al.*, “TGF-β-Id1 signaling opposes Twist1 and promotes metastatic colonization via a mesenchymal-to-epithelial transition.,” *Cell Rep.*, vol. 5, no. 5, pp. 1228–42, Dec. 2013.
[198] J. H. Tsai *et al.*, “Spatiotemporal Regulation of Epithelial-Mesenchymal Transition Is Essential for Squamous Cell Carcinoma Metastasis,” *Cancer Cell*, vol. 22, pp. 1–12, Nov. 2012.
[199] M. A. Nieto, “Epithelial plasticity: a common theme in embryonic and cancer cells.,” *Science*, vol. 342, no. 6159, p. 1234850, Nov. 2013.
[200] S. Valastyan and R. A. Weinberg, “Tumor metastasis: molecular insights and evolving paradigms.,” *Cell*, vol. 147, no. 2, pp. 275–92, Oct. 2011.
[201] S. Liu *et al.*, “Breast Cancer Stem Cells Transition between Epithelial and Mesenchymal States Reflective of their Normal Counterparts.,” *Stem cell reports*, vol. 2, no. 1, pp. 78–91, Jan. 2014.
[202] B. Vogelstein *et al.*, “Cancer genome landscapes.,” *Science*, vol. 339, no. 6127, pp. 1546–58, Mar. 2013.
[203] I. Bozic *et al.*k, “Accumulation of driver and passenger mutations during tumor progression.,” *Proc. Natl. Acad. Sci. U. S. A.*, vol. 107, no. 43, pp. 18545–50, Oct. 2010.
[204] S. Vanharanta and J. Massagué, “Origins of metastatic traits.,” *Cancer Cell*, vol. 24, no. 4, pp. 410–21, Oct. 2013.
[205] S. Vanharanta *et al.*, “Epigenetic expansion of VHL-HIF signal output drives multiorgan metastasis in renal cancer.,” *Nat. Med.*, vol. 19, no. 1, pp. 50–6, Jan. 2013.
[206] W. K. C. Cheung *et al.*, “Control of alveolar differentiation by the lineage transcription factors GATA6 and HOPX inhibits lung adenocarcinoma metastasis.,” *Cancer Cell*, vol. 23, no. 6, pp. 725–38, Jun. 2013.
[207] M. M. Winslow *et al.*, “Suppression of lung adenocarcinoma progression by Nkx2-1.,” *Nature*, vol. 473, no. 7345, pp. 101–4, May 2011.
[208] G. Di Leva, M. Garofalo, and C. M. Croce, “MicroRNAs in cancer.,” *Annu. Rev. Pathol.*, vol. 9, pp. 287–314, Jan. 2014.

[209] W. Guo *et al.*, “Slug and Sox9 cooperatively determine the mammary stem cell state.,” *Cell*, vol. 148, no. 5, pp. 1015–28, Mar. 2012.
[210] M. J. Moore and N. J. Proudfoot, “Pre-mRNA processing reaches back to transcription and ahead to translation.,” *Cell*, vol. 136, no. 4, pp. 688–700, Feb. 2009.
[211] N. Pencheva and S. F. Tavazoie, “Control of metastatic progression by microRNA regulatory networks.,” *Nat. Cell Biol.*, vol. 15, no. 6, pp. 546–54, Jun. 2013.
[212] S. Valastyan and A. Chang, “Activation of miR-31 function in already-established metastases elicits metastatic regression,” *Genes …*, vol. 25, pp. 646–659, 2011.
[213] P. D. Bos *et al.*, “Genes that mediate breast cancer metastasis to the brain.,” *Nature*, vol. 459, no. 7249, pp. 1005–9, Jun. 2009.
[214] A. Calon *et al.*, “Dependency of colorectal cancer on a TGF-β-driven program in stromal cells for metastasis initiation.,” *Cancer Cell*, vol. 22, no. 5, pp. 571–84, Nov. 2012.
[215] G. Hu *et al.*, “MTDH activation by 8q22 genomic gain promotes chemoresistance and metastasis of poor-prognosis breast cancer.,” *Cancer Cell*, vol. 15, no. 1, pp. 9–20, Jan. 2009.
[216] A. J. Minn *et al.*, “Genes that mediate breast cancer metastasis to lung.,” *Nature*, vol. 436, no. 7050, pp. 518–24, Jul. 2005.
[217] D. X. Nguyen *et al.*, “WNT/TCF signaling through LEF1 and HOXB9 mediates lung adenocarcinoma metastasis.,” *Cell*, vol. 138, no. 1, pp. 51–62, Jul. 2009.
[218] S. F. Tavazoie *et al.*, “Endogenous human microRNAs that suppress breast cancer metastasis.,” *Nature*, vol. 451, no. 7175, pp. 147–52, Jan. 2008.
[219] W. Zhang *et al.*, “A NIK-IKKα module expands ErbB2-induced tumor-initiating cells by stimulating nuclear export of p27/Kip1.,” *Cancer Cell*, vol. 23, no. 5, pp. 647–59, May 2013.
[220] X. H. F. Zhang *et al.*, “Selection of bone metastasis seeds by mesenchymal signals in the primary tumor stroma.,” *Cell*, vol. 154, no. 5, pp. 1060–73, Aug. 2013.
[221] C. A. Klein, “Parallel progression of primary tumours and metastases.,” *Nat. Rev. Cancer*, vol. 9, no. 4, pp. 302–12, Apr. 2009.
[222] K. R. Hess *et al.*, “Metastatic patterns in adenocarcinoma.,” *Cancer*, vol. 106, no. 7, pp. 1624–33, Apr. 2006.
[223] S. Jones *et al.*, “Comparative lesion sequencing provides insights into tumor evolution.,” *Proc. Natl. Acad. Sci. U. S. A.*, vol. 105, no. 11, pp. 4283–8, Mar. 2008.
[224] A. F. Chambers, A. C. Groom, and I. C. MacDonald, “Dissemination and growth of cancer cells in metastatic sites.,” *Nat. Rev. Cancer*, vol. 2, no. 8, pp. 563–72, Aug. 2002.
[225] I. Fidler, “The pathogenesis of cancer metastasis: the’seed and soil'hypothesis revisited,” *Nat. Rev. Cancer*, vol. 3, no. June, pp. 1–6, 2003.
[226] D. X. Nguyen, P. D. Bos, and J. Massagué, “Metastasis: from dissemination to organ-specific colonization.,” *Nat. Rev. Cancer*, vol. 9, no. 4, pp. 274–84, Apr. 2009.
[227] C. W. Wong *et al.*, “Apoptosis: an early event in metastatic inefficiency,” *Cancer Res.*, no. 61, pp. 333–338, 2001.
[228] M. D. Cameron *et al.*, “Temporal Progression of Metastasis in Lung : Cell Survival , Dormancy , and Location Dependence of Metastatic Inefficiency,” *Cancer Res.*, no. 60, pp. 2541–2546, 2000.
[229] K. J. Luzzi *et al.*, “Multistep nature of metastatic inefficiency: dormancy of solitary cells after successful extravasation and limited survival of early micrometastases.,” *Am. J. Pathol.*, vol. 153, no. 3, pp. 865–73, Sep. 1998.
[230] M. Y. Kim *et al.*, “Tumor self-seeding by circulating cancer cells.,” *Cell*, vol. 139, no. 7, pp. 1315–26, Dec. 2009.
[231] R. D. Schreiber, L. J. Old, and M. J. Smyth, “Cancer immunoediting: integrating immunity’s roles in cancer suppression and promotion.,” *Science*, vol. 331, no. 6024, pp. 1565–70, Mar. 2011.
[232] Y. Kienast *et al.*, “Real-time imaging reveals the single steps of brain metastasis formation.,” *Nat. Med.*, vol. 16, no. 1, pp. 116–22, Jan. 2010.
[233] M. Perera *et al.*, “In Vivo Magnetic Resonance Imaging for Investigating the Development and Distribution of Experimental Brain Metastases due to Breast Cancer,” *Transl. Oncol.*, vol. 5, no. 3, pp. 217–225, Jun. 2012.
[234] P. S. Steeg, K. A. Camphausen, and Q. R. Smith, “Brain metastases as preventive and therapeutic targets.,” *Nat. Rev. Cancer*, vol. 11, no. 5, pp. 352–63, May 2011.
[235] M. Valiente *et al.*, “Serpins promote cancer cell survival and vascular co-option in brain metastasis.,” *Cell*, vol. 156, no. 5, pp. 1002–16, Feb. 2014.

[236] N. Takebe *et al.*, “Targeting cancer stem cells by inhibiting Wnt, Notch, and Hedgehog pathways.,” *Nat. Rev. Clin. Oncol.*, vol. 8, no. 2, pp. 97–106, Feb. 2011.
[237] A. Müller *et al.*, “Involvement of chemokine receptors in breast cancer metastasis.,” *Nature*, vol. 410, no. 6824, pp. 50–6, Mar. 2001.
[238] A. Zlotnik, A. M. Burkhardt, and B. Homey, “Homeostatic chemokine receptors and organ-specific metastasis.,” *Nat. Rev. Immunol.*, vol. 11, no. 9, pp. 597–606, Sep. 2011.
[239] S. Acharyya *et al.*, “A CXCL1 paracrine network links cancer chemoresistance and metastasis.,” *Cell*, vol. 150, no. 1, pp. 165–78, Jul. 2012.
[240] N. Charles and E. C. Holland, “The perivascular niche microenvironment in brain tumor progression.,” *Cell Cycle*, vol. 9, no. 15, pp. 3012–21, Aug. 2010.
[241] D. Hambardzumyan, O. Becher, and E. Holland, “Cancer stem cells and survival pathways,” *Cell Cycle*, vol. 7, no. 10, pp. 1371–1378, 2008.
[242] W. S. Carbonell *et al.*, “The vascular basement membrane as ‘soil’ in brain metastasis.,” *PLoS One*, vol. 4, no. 6, p. e5857, Jan. 2009.
[243] K. Doberstein *et al.*, “L1-CAM expression in ccRCC correlates with shorter patients survival times and confers chemoresistance in renal cell carcinoma cells.,” *Carcinogenesis*, vol. 32, no. 3, pp. 262–70, Mar. 2011.
[244] C. Schroder and U. Schumacher, “Expression and prognostic value of L1-CAM in breast cancer.,” *Oncol. Rep.*, vol. 22, pp. 1109–1117, 2009.
[245] J. M. Butler, H. Kobayashi, and S. Rafii, “Instructive role of the vascular niche in promoting tumour growth and tissue repair by angiocrine factors.,” *Nat. Rev. Cancer*, vol. 10, no. 2, pp. 138–46, Feb. 2010.
[246] J. Lu *et al.*, “Endothelial cells promote the colorectal cancer stem cell phenotype through a soluble form of Jagged-1.,” *Cancer Cell*, vol. 23, no. 2, pp. 171–85, Feb. 2013.
[247] C. M. Ghajar *et al.*, “The perivascular niche regulates breast tumour dormancy.,” *Nat. Cell Biol.*, vol. 15, no. 7, pp. 807–17, Jul. 2013.
[248] R. N. Kaplan *et al.*, “VEGFR1-positive haematopoietic bone marrow progenitors initiate the pre-metastatic niche.,” *Nature*, vol. 438, no. 7069, pp. 820–7, Dec. 2005.
[249] M. Yamamoto *et al.*, “TSU68 prevents liver metastasis of colon cancer xenografts by modulating the premetastatic niche.,” *Cancer Res.*, vol. 68, no. 23, pp. 9754–62, Dec. 2008.
[250] T. Oskarsson *et al.*, “Breast cancer cells produce tenascin C as a metastatic niche component to colonize the lungs.,” *Nat. Med.*, vol. 17, no. 7, pp. 867–74, Jul. 2011.
[251] I. Malanchi *et al.*, “Interactions between cancer stem cells and their niche govern metastatic colonization.,” *Nature*, vol. 481, no. 7379, pp. 85–9, Jan. 2012.
[252] I. Kii *et al.*, “Incorporation of tenascin-C into the extracellular matrix by periostin underlies an extracellular meshwork architecture.,” *J. Biol. Chem.*, vol. 285, no. 3, pp. 2028–39, Jan. 2010.
[253] A. Pietras *et al.*, “Osteopontin-CD44 signaling in the glioma perivascular niche enhances cancer stem cell phenotypes and promotes aggressive tumor growth.,” *Cell Stem Cell*, vol. 14, no. 3, pp. 357–69, Mar. 2014.
[254] Y. Li *et al.*, “Silencing of hyaluronan synthase 2 suppresses the malignant phenotype of invasive breast cancer cells.,” *Int. J. Cancer*, vol. 120, no. 12, pp. 2557–67, Jun. 2007.
[255] H. Okuda *et al.*, “Hyaluronan synthase HAS2 promotes tumor progression in bone by stimulating the interaction of breast cancer stem-like cells with macrophages and stromal cells.,” *Cancer Res.*, vol. 72, no. 2, pp. 537–47, Jan. 2012.
[256] X. H. F. Zhang *et al.*, “Latent bone metastasis in breast cancer tied to Src-dependent survival signals.,” *Cancer Cell*, vol. 16, no. 1, pp. 67–78, Jul. 2009.
[257] Q. Chen, X. H. F. Zhang, and J. Massagué, “Macrophage binding to receptor VCAM-1 transmits survival signals in breast cancer cells that invade the lungs.,” *Cancer Cell*, vol. 20, no. 4, pp. 538–49, Oct. 2011.
[258] J. S. Desgrosellier and D. A. Cheresh, “Integrins in cancer: biological implications and therapeutic opportunities.,” *Nat. Rev. Cancer*, vol. 10, no. 1, pp. 9–22, Jan. 2010.
[259] J. L. Luo *et al.*, “Inhibition of NF-kappaB in cancer cells converts inflammation- induced tumor growth mediated by TNFalpha to TRAIL-mediated tumor regression.,” *Cancer Cell*, vol. 6, no. 3, pp. 297–305, Sep. 2004.
[260] S. Maeda *et al.*, “Ikappa B kinasebeta/nuclear factor-kappaB activation controls the development of liver metastasis by way of interleukin-6 expression.,” *Hepatology*, vol. 50, no. 6, pp. 1851–60, Dec. 2009.

[261] B. K. Park *et al.*, “NF-kappaB in breast cancer cells promotes osteolytic bone metastasis by inducing osteoclastogenesis via GM-CSF.,” *Nat. Med.*, vol. 13, no. 1, pp. 62–9, Jan. 2007.
[262] J. Abdulghani *et al.*, “Stat3 promotes metastatic progression of prostate cancer.,” *Am. J. Pathol.*, vol. 172, no. 6, pp. 1717–28, Jun. 2008.
[263] I. Barbieri *et al.*, “Stat3 is required for anchorage-independent growth and metastasis but not for mammary tumor development downstream of the ErbB-2 oncogene.,” *Mol. Carcinog.*, vol. 49, no. 2, pp. 114–20, Feb. 2010.
[264] D. Wei *et al.*, “Stat3 activation regulates the expression of vascular endothelial growth factor and human pancreatic cancer angiogenesis and metastasis.,” *Oncogene*, vol. 22, no. 3, pp. 319–29, Jan. 2003.
[265] T. Xie *et al.*, “Activation of stat3 in human melanoma promotes brain metastasis.,” *Cancer Res.*, vol. 66, no. 6, pp. 3188–96, Mar. 2006.
[266] G. P. Gupta *et al.*, “Mediators of vascular remodelling co-opted for sequential steps in lung metastasis.,” *Nature*, vol. 446, no. 7137, pp. 765–70, Apr. 2007.
[267] M. Labelle, S. Begum, and R. O. Hynes, “Direct signaling between platelets and cancer cells induces an epithelial-mesenchymal-like transition and promotes metastasis.,” *Cancer Cell*, vol. 20, no. 5, pp. 576–90, Nov. 2011.
[268] V. Müller *et al.*, “Circulating Tumor Cells in Breast Cancer : Correlation to Bone Marrow Micrometastases , Heterogeneous Response to Systemic Therapy and Low Proliferative Activity umor Cells in Breast Cancer : Correlation to Bone Marrow Micrometastases , Heterogeneous Resp,” *Cancer Res.*, no. 11, pp. 3678–3685, 2005.
[269] P. E. Goss and A. F. Chambers, “Does tumour dormancy offer a therapeutic target?,” *Nat. Rev. Cancer*, vol. 10, no. 12, pp. 871–7, Dec. 2010.
[270] C. A. Klein, “Framework models of tumor dormancy from patient-derived observations.,” *Curr. Opin. Genet. Dev.*, vol. 21, no. 1, pp. 42–9, Feb. 2011.
[271] J. Aguirre-Ghiso, L. Ossowski, and S. Rosenbaum, “fluorescent protein tagging of extracellular signal-regulated kinase and p38 pathways reveals novel dynamics of pathway activation during primary and metastatic,” *Cancer Res.*, pp. 7336–7345, 2004.
[272] H. Gao *et al.*, “The BMP inhibitor Coco reactivates breast cancer cells at lung metastatic sites.,” *Cell*, vol. 150, no. 4, pp. 764–79, Aug. 2012.
[273] K. N. Weilbaecher, T. a Guise, and L. K. McCauley, “Cancer to bone: a fatal attraction.,” *Nat. Rev. Cancer*, vol. 11, no. 6, pp. 411–25, Jun. 2011.
[274] X. Lu, E. Mu *et al.*, “VCAM-1 promotes osteolytic expansion of indolent bone micrometastasis of breast cancer by engaging α4β1-positive osteoclast progenitors.,” *Cancer Cell*, vol. 20, no. 6, pp. 701–14, Dec. 2011.
[275] J. Wang *et al.*, “A protein interaction network for pluripotency of embryonic stem cells.,” *Nature*, vol. 444, no. 7117, pp. 364–8, Nov. 2006.
[276] H. Niwa, J. Miyazaki, and A. G. Smith, “Quantitative expression of Oct-3/4 defines differentiation, dedifferentiation or self-renewal of ES cells.,” *Nat. Genet.*, vol. 24, no. 4, pp. 372–6, Apr. 2000.
[277] S. Masui *et al.*, “Pluripotency governed by Sox2 via regulation of Oct3/4 expression in mouse embryonic stem cells.,” *Nat. Cell Biol.*, vol. 9, no. 6, pp. 625–35, Jun. 2007.
[278] I. Chambers *et al.*, “Nanog safeguards pluripotency and mediates germline development.,” *Nature*, vol. 450, no. 7173, pp. 1230–4, Dec. 2007.
[279] J. Jiang *et al.*, “A core Klf circuitry regulates self-renewal of embryonic stem cells.,” *Nat. Cell Biol.*, vol. 10, no. 3, pp. 353–60, Mar. 2008.
[280] J. Kim *et al.*, “An extended transcriptional network for pluripotency of embryonic stem cells.,” *Cell*, vol. 132, no. 6, pp. 1049–61, Mar. 2008.
[281] X. Chen *et al.*, “Integration of external signaling pathways with the core transcriptional network in embryonic stem cells.,” *Cell*, vol. 133, no. 6, pp. 1106–17, Jun. 2008.
[282] H. Niwa *et al.*, “A parallel circuit of LIF signalling pathways maintains pluripotency of mouse ES cells.,” *Nature*, vol. 460, no. 7251, pp. 118–22, Jul. 2009.
[283] T. Miki, S. Yasuda, and M. Kahn, “Wnt/β-catenin signaling in embryonic stem cell self-renewal and somatic cell reprogramming.,” *Stem Cell Rev.*, vol. 7, no. 4, pp. 836–46, Nov. 2011.
[284] A. Suzuki *et al.*, “Nanog binds to Smad1 and blocks bone morphogenetic protein-induced differentiation of embryonic stem cells.,” *Proc. Natl. Acad. Sci. U. S. A.*, vol. 103, no. 27, pp. 10294–9, Jul. 2006.

[285] N. Sato *et al.*, “Maintenance of pluripotency in human and mouse embryonic stem cells through activation of Wnt signaling by a pharmacological GSK-3-specific inhibitor.,” *Nat. Med.*, vol. 10, no. 1, pp. 55–63, Jan. 2004.
[286] L. Pereira, F. Yi, and B. J. Merrill, “Repression of Nanog gene transcription by Tcf3 limits embryonic stem cell self-renewal.,” *Mol. Cell. Biol.*, vol. 26, no. 20, pp. 7479–91, Oct. 2006.
[287] M. Cole and S. Johnstone, “Tcf3 is an integral component of the core regulatory circuitry of embryonic stem cells,” *Genes Dev.*, no. 22, pp. 746–755, 2008.
[288] K. Takahashi *et al.*, “Induction of pluripotent stem cells from adult human fibroblasts by defined factors.,” *Cell*, vol. 131, no. 5, pp. 861–72, Nov. 2007.
[289] J. Yu *et al.*, “Induced pluripotent stem cell lines derived from human somatic cells.,” *Science*, vol. 318, no. 5858, pp. 1917–20, Dec. 2007.
[290] M. Nakagawa *et al.*, “Generation of induced pluripotent stem cells without Myc from mouse and human fibroblasts.,” *Nat. Biotechnol.*, vol. 26, no. 1, pp. 101–6, Jan. 2008.
[291] T. Redmer *et al.*, “E-cadherin is crucial for embryonic stem cell pluripotency and can replace OCT4 during somatic cell reprogramming.,” *EMBO Rep.*, vol. 12, no. 7, pp. 720–6, Jul. 2011.
[292] D. J. Wong *et al.*, “Module map of stem cell genes guides creation of epithelial cancer stem cells.,” *Cell Stem Cell*, vol. 2, no. 4, pp. 333–44, Apr. 2008.
[293] S. Sinha *et al.*, “Systematic functional characterization of cis -regulatory motifs in human core promoters,” *Genome Res.*, no. 18, pp. 477–488, 2008.
[294] I. Ben-Porath *et al.*, “An embryonic stem cell-like gene expression signature in poorly differentiated aggressive human tumors.,” *Nat. Genet.*, vol. 40, no. 5, pp. 499–507, May 2008.
[295] S. Bao *et al.*, “Glioma stem cells promote radioresistance by preferential activation of the DNA damage response.,” *Nature*, vol. 444, no. 7120, pp. 756–60, Dec. 2006.
[296] M. Diehn *et al.*, “Association of reactive oxygen species levels and radioresistance in cancer stem cells.,” *Nature*, vol. 458, no. 7239, pp. 780–3, Apr. 2009.
[297] F. Ishikawa *et al.*, “Chemotherapy-resistant human AML stem cells home to and engraft within the bone-marrow endosteal region.,” *Nat. Biotechnol.*, vol. 25, no. 11, pp. 1315–21, Nov. 2007.
[298] Y. Saito *et al.*, “Induction of cell cycle entry eliminates human leukemia stem cells in a mouse model of AML.,” *Nat. Biotechnol.*, vol. 28, no. 3, pp. 275–80, Mar. 2010.
[299] A. Viale *et al.*, “Cell-cycle restriction limits DNA damage and maintains self-renewal of leukaemia stem cells.,” *Nature*, vol. 457, no. 7225, pp. 51–6, Jan. 2009.
[300] M. Zhang, R. L. Atkinson, and J. M. Rosen, “Selective targeting of radiation-resistant tumor-initiating cells.,” *Proc. Natl. Acad. Sci. U. S. A.*, vol. 107, no. 8, pp. 3522–7, Feb. 2010.
[301] R. Tehranchi *et al.*, “Persistent malignant stem cells in del(5q) myelodysplasia in remission.,” *N. Engl. J. Med.*, vol. 363, no. 11, pp. 1025–37, Sep. 2010.
[302] R. Majeti *et al.*, “CD47 is an adverse prognostic factor and therapeutic antibody target on human acute myeloid leukemia stem cells.,” *Cell*, vol. 138, no. 2, pp. 286–99, Jul. 2009.
[303] M. Todaro *et al.*, “Colon cancer stem cells dictate tumor growth and resist cell death by production of interleukin-4.,” *Cell Stem Cell*, vol. 1, no. 4, pp. 389–402, Oct. 2007.
[304] J. Lessard and G. Sauvageau, “Bmi-1 determines the proliferative capacity of normal and leukaemic stem cells.,” *Nature*, vol. 423, no. 6937, pp. 255–60, May 2003.
[305] A. Molofsky *et al.*, “Bmi-1 dependence distinguishes neural stem cell self-renewal from progenitor proliferation,” *Nature*, vol. 425, no. October, pp. 1–6, 2003.
[306] I. Park *et al.*, “Bmi-1 is required for maintenance of adult self-renewing haematopoietic stem cells.,” *Nature*, vol. 423, no. 6937, pp. 302–5, May 2003.
[307] A. Kreso *et al.*, “Self-renewal as a therapeutic target in human colorectal cancer.,” *Nat. Med.*, vol. 20, no. 1, pp. 29–36, Jan. 2014.
[308] R. J. Vanner *et al.*, “Quiescent Sox2(+) Cells Drive Hierarchical Growth and Relapse in Sonic Hedgehog Subgroup Medulloblastoma.,” *Cancer Cell*, vol. 26, no. 1, pp. 33–47, Jun. 2014.
[309] S. Boumahdi *et al.*, “SOX2 controls tumour initiation and cancer stem-cell functions in squamous-cell carcinoma.,” *Nature*, vol. 511, pp. 246–253, Jun. 2014.
[310] T. Hussenet *et al.*, “SOX2 is an oncogene activated by recurrent 3q26. 3 amplifications in human lung squamous cell carcinomas,” *PLoS One*, vol. 5, no. 1, 2010.

[311] M. M. Alonso *et al.*, “Genetic and epigenetic modifications of Sox2 contribute to the invasive phenotype of malignant gliomas.,” *PLoS One*, vol. 6, no. 11, p. e26740, Jan. 2011.
[312] T. Hussenet and S. du Manoir, “SOX2 in squamous cell carcinoma,” *Cell Cycle*, vol. 9, no. 8, pp. 1480–1486, 2010.
[313] A. J. Bass *et al.*, “SOX2 is an amplified lineage-survival oncogene in lung and esophageal squamous cell carcinomas.,” *Nat. Genet.*, vol. 41, no. 11, pp. 1238–42, Nov. 2009.
[314] C. M. Rudin *et al.*, “Comprehensive genomic analysis identifies SOX2 as a frequently amplified gene in small-cell lung cancer.,” *Nat. Genet.*, vol. 44, no. 10, pp. 1111–6, Oct. 2012.
[315] K. Freier and K. Knoepfle, “Recurrent copy number gain of transcription factor SOX2 and corresponding high protein expression in oral squamous cell carcinoma,” *Genes, Chromosones and Cancer*, vol. 16, no. August 2009, pp. 9–16, 2010.
[316] V. Justilien *et al.*, “The PRKCI and SOX2 oncogenes are coamplified and cooperate to activate Hedgehog signaling in lung squamous cell carcinoma.,” *Cancer Cell*, vol. 25, no. 2, pp. 139–51, Feb. 2014.
[317] L. Toschi, G. Finocchiaro, and T. Nguyen, “Gene Copy Number Is Associated with FGFR1 and PIK3CA Gene Gain in Non-Small Cell Lung Cancer and Predicts Improved Survival in Early Stage Disease,” *PLoS One*, vol. 9, no. 4, pp. 1–7, 2014.
[318] S. Stolzenburg *et al.*, “Targeted silencing of the oncogenic transcription factor SOX2 in breast cancer.,” *Nucleic Acids Res.*, vol. 40, no. 14, pp. 6725–40, Aug. 2012.
[319] M. Herreros-Villanueva, J. Zhang, and A. Koenig, “SOX2 promotes dedifferentiation and imparts stem cell-like features to pancreatic cancer cells,” *Oncogenesis*, vol. 2, no. 8, pp. e61–12, 2013.
[320] X. Jia *et al.*, “SOX 2 promotes tumorigenesis and increases the anti-apoptotic property of human prostate cancer cell,” *J. Mol. Cell Biol.*, vol. 3, pp. 230–238, 2011.
[321] K. Hütz *et al.*, “The stem cell factor SOX2 regulates the tumorigenic potential in human gastric cancer cells.,” *Carcinogenesis*, vol. 35, no. 4, pp. 942–50, Apr. 2014.
[322] S. Chen *et al.*, “SOX2 regulates apoptosis through MAP4K4-survivin signaling pathway in human lung cancer cells.,” *Carcinogenesis*, vol. 35, no. 3, pp. 613–23, Mar. 2014.
[323] X. Li *et al.*, “SOX2 promotes tumor metastasis by stimulating epithelial-to-mesenchymal transition via regulation of WNT/β-catenin signal network.,” *Cancer Lett.*, vol. 336, no. 2, pp. 379–89, Aug. 2013.
[324] X. Lou *et al.*, “SOX2 targets fibronectin 1 to promote cell migration and invasion in ovarian cancer: new molecular leads for therapeutic intervention,” *Omi. a J. …*, vol. 17, no. 10, pp. 510–518, 2013.
[325] W. T. Fang *et al.*, “Downregulation of a putative tumor suppressor BMP4 by SOX2 promotes growth of lung squamous cell carcinoma.,” *Int. J. Cancer*, vol. 135, no. 4, pp. 809–19, Aug. 2014.
[326] X. Fang *et al.*, “ChIP-seq and Functional Analysis of the SOX2 Gene in Colorectal Cancers.,” *OMICS*, vol. 14, no. 0, Aug. 2010.
[327] X. Han *et al.*, “Silencing SOX2 induced mesenchymal-epithelial transition and its expression predicts liver and lymph node metastasis of CRC patients.,” *PLoS One*, vol. 7, no. 8, p. e41335, Jan. 2012.
[328] R. M. R. Gangemi *et al.*, “SOX2 silencing in glioblastoma tumor-initiating cells causes stop of proliferation and loss of tumorigenicity.,” *Stem Cells*, vol. 27, no. 1, pp. 40–8, Jan. 2009.
[329] U. Basu-Roy, E. Seo, and L. Ramanathapuram, “Sox2 maintains self renewal of tumor-initiating cells in osteosarcomas,” *Oncogene*, vol. 31, no. 18, pp. 2270–2282, 2011.
[330] A. P. Rybak and D. Tang, “SOX2 plays a critical role in EGFR-mediated self-renewal of human prostate cancer stem-like cells.,” *Cell. Signal.*, vol. 25, no. 12, pp. 2734–42, Dec. 2013.
[331] S. Singh *et al.*, “EGFR/Src/Akt signaling modulates Sox2 expression and self-renewal of stem-like side-population cells in non-small cell lung cancer.,” *Mol. Cancer*, vol. 11, no. 1, p. 73, Jan. 2012.
[332] C. Xu *et al.*, “β-Catenin/POU5F1/SOX2 transcription factor complex mediates IGF-I receptor signaling and predicts poor prognosis in lung adenocarcinoma.,” *Cancer Res.*, vol. 73, no. 10, pp. 3181–9, May 2013.

[333] O. Leis *et al.*, “Sox2 expression in breast tumours and activation in breast cancer stem cells.,” *Oncogene*, pp. 1–12, Aug. 2011.
[334] P. M. Bareiss *et al.*, “SOX2 expression associates with stem cell state in human ovarian carcinoma.,” *Cancer Res.*, vol. 73, no. 17, pp. 5544–55, Sep. 2013.
[335] R. Santini, S. Pietrobono, and S. Pandolfi, “SOX2 regulates self-renewal and tumorigenicity of human melanoma-initiating cells,” *Oncogene*, pp. 1–12, 2014.
[336] A. Shervington and C. Lu, “Expression of multidrug resistance genes in normal and cancer stem cells.,” *Cancer Invest.*, vol. 26, no. 5, pp. 535–42, Jun. 2008.
[337] M. Piva *et al.*, “Sox2 promotes tamoxifen resistance in breast cancer cells.,” *EMBO Mol. Med.*, vol. 6, no. 1, pp. 66–79, Jan. 2013.
[338] H. M. Jeon *et al.*, “ID4 imparts chemoresistance and cancer stemness to glioma cells by derepressing miR-9*-mediated suppression of SOX2.,” *Cancer Res.*, vol. 71, no. 9, pp. 3410–21, May 2011.
[339] R. R. Huxley *et al.*, “The impact of dietary and lifestyle risk factors on risk of colorectal cancer: a quantitative overview of the epidemiological evidence.,” *Int. J. cancer.*, vol. 125, no. 1, pp. 171–80, Jul. 2009.
[340] E. T. Hawk and B. Levin, “Colorectal cancer prevention.,” *J. Clin. Oncol.*, vol. 23, no. 2, pp. 378–91, Jan. 2005.
[341] D. P. Taylor *et al.*, “Population-based family history-specific risks for colorectal cancer: a constellation approach.,” *Gastroenterology*, vol. 138, no. 3, pp. 877–85, Mar. 2010.
[342] S. D. Markowitz *et al.*, “Focus on colon cancer.,” *Cancer Cell*, vol. 1, no. 3, pp. 233–6, Apr. 2002.
[343] T. André *et al.*, “Oxaliplatin, fluorouracil, and leucovorin as adjuvant treatment for colon cancer.,” *N. Engl. J. Med.*, vol. 350, no. 23, pp. 2343–51, Jun. 2004.
[344] C. Lengauer, K. Kinzler, and B. Vogelstein, “Genetic instability in colorectal cancers,” *Nature*, vol. 368, pp. 623–627, 1997.
[345] T. D. Barber *et al.*, “Chromatid cohesion defects may underlie chromosome instability in human colorectal cancers.,” *Proc. Natl. Acad. Sci. U. S. A.*, vol. 105, no. 9, pp. 3443–8, Mar. 2008.
[346] R. J. Leary *et al.*, “Integrated analysis of homozygous deletions, focal amplifications, and sequence alterations in breast and colorectal cancers.,” *Proc. Natl. Acad. Sci. U. S. A.*, vol. 105, no. 42, pp. 16224–9, Oct. 2008.
[347] The Cancer Genome Atlas Network, “Comprehensive molecular characterization of human colon and rectal cancer.,” *Nature*, vol. 487, no. 7407, pp. 330–7, Jul. 2012.
[348] F. S. Leach *et al.*, “Mutations of a mutS homolog in hereditary nonpolyposis colorectal cancer.,” *Cell*, vol. 75, no. 6, pp. 1215–25, Dec. 1993.
[349] N. Papadopoulos *et al.*, “Mutation of a mutL homolog in hereditary colon cancer.,” *Science*, vol. 263, no. 5153, pp. 1625–9, Mar. 1994.
[350] R. Fishel *et al.*, “The human mutator gene homolog MSH2 and its association with hereditary nonpolyposis colon cancer.,” *Cell*, vol. 77, no. 1, p. 1 p following 166, Apr. 1994.
[351] M. Miyaki, M. Konishi, and K. Tanaka, “Germline mutation of MSH6 as the cause of hereditary nonpolyposis colorectal cancer,” *Nat. Genet.*, vol. 17, pp. 271–272, 1997.
[352] F. Kastrinos and S. Syngal, “Recently Identified Colon Cancer Predispositions: MYH and MSH6 Mutations,” *Semin. Oncol.*, vol. 34, no. 5, pp. 418–424, 2007.
[353] R. Kolodner, J. Tytell, and J. Schmeits, “Germ-line msh6 mutations in colorectal cancer families,” *Cancer Res.*, vol. 50, pp. 5068–5074, 1999.
[354] M. F. Kane *et al.*, “Methylation of the hMLH1 Promoter Correlates with Lack of Expression of hMLH1 in Sporadic Colon Tumors and Mismatch hMLH1 in Sporadic Colon Tumors and Mismatch Repair-defective Human Tumor Cell Lines,” *Cancer Res.*, vol. 57, pp. 808–811, 1997.
[355] J. G. Herman *et al.*, “Incidence and functional consequences of hMLH1 promoter hypermethylation in colorectal carcinoma.,” *Proc. Natl. Acad. Sci. U. S. A.*, vol. 95, no. 12, pp. 6870–5, Jun. 1998.
[356] M. L. Veigl *et al.*, “Biallelic inactivation of hMLH1 by epigenetic gene silencing, a novel mechanism causing human MSI cancers.,” *Proc. Natl. Acad. Sci. U. S. A.*, vol. 95, no. 15, pp. 8698–702, Jul. 1998.
[357] H. T. Lynch *et al.*, “Hereditary colorectal cancer syndromes: molecular genetics, genetic counseling, diagnosis and management.,” *Fam. Cancer*, vol. 7, no. 1, pp. 27–39, Jan. 2008.

[358] N. Al-Tassan *et al.*, “Inherited variants of MYH associated with somatic G:C-->T:A mutations in colorectal tumors.,” *Nat. Genet.*, vol. 30, no. 2, pp. 227–32, Feb. 2002.
[359] J. Issa, “CpG island methylator phenotype in cancer,” *Nat. Rev. Cancer*, vol. 4, no. December, pp. 988–993, 2004.
[360] K. Nosho *et al.*, “Comprehensive biostatistical analysis of CpG island methylator phenotype in colorectal cancer using a large population-based sample,” *PLoS One*, vol. 3, no. 11, pp. 1–12, 2008.
[361] D. Weisenberger and K. Siegmund, “CpG island methylator phenotype underlies sporadic microsatellite instability and is tightly associated with BRAF mutation in colorectal cancer,” *Nat. Genet.*, vol. 38, no. 7, pp. 787–793, 2006.
[362] L. Shen, M. Toyota, and Y. Kondo, “Integrated genetic and epigenetic analysis identifies three different subclasses of colon cancer,” *Proc. Natl. Acad. Sci.*, vol. 104, no. 47, pp. 18654–18659, 2007.
[363] L. Barault, C. Charon-Barra, and V. Jooste, “Hypermethylator phenotype in sporadic colon cancer: study on a population-based series of 582 cases,” *Cancer Res.*, vol. 68, pp. 8541–8546, 2008.
[364] K. Tamai *et al.*, “LDL-receptor-related proteins in Wnt signal transduction.,” *Nature*, vol. 407, no. 6803, pp. 530–5, Sep. 2000.
[365] Y. Liu *et al.*, “Wnt5a induces homodimerization and activation of Ror2 receptor tyrosine kinase.,” *J. Cell. Biochem.*, vol. 105, no. 2, pp. 497–502, Oct. 2008.
[366] H. Clevers and R. Nusse, “Wnt/β-catenin signaling and disease.,” *Cell*, vol. 149, no. 6, pp. 1192–205, Jun. 2012.
[367] M. Kühl *et al.*, “The Wnt/Ca 2+ pathway: a new vertebrate Wnt signaling pathway takes shape,” *Trends Genet.*, vol. 9525, no. 00, pp. 279–283, 2000.
[368] I. Oishi *et al.*, “The receptor tyrosine kinase Ror2 is involved in non-canonical Wnt5a/JNK signalling pathway.,” *Genes to cells*, vol. 8, no. 7, pp. 645–54, Jul. 2003.
[369] A. Schambony and D. Wedlich, “Wnt-5A/Ror2 regulate expression of XPAPC through an alternative noncanonical signaling pathway.,” *Dev. Cell*, vol. 12, no. 5, pp. 779–92, May 2007.
[370] M. Hart *et al.*, “The F-box protein beta-TrCP associates with phosphorylated beta-catenin and regulates its activity in the cell.,” *Curr. Biol.*, vol. 9, no. 4, pp. 207–10, Feb. 1999.
[371] C. Liu *et al.*, “beta-Trcp couples beta-catenin phosphorylation-degradation and regulates Xenopus axis formation.,” *Proc. Natl. Acad. Sci. U. S. A.*, vol. 96, no. 11, pp. 6273–8, May 1999.
[372] C. Liu *et al.*, “Control of beta-catenin phosphorylation/degradation by a dual-kinase mechanism.,” *Cell*, vol. 108, no. 6, pp. 837–47, Mar. 2002.
[373] E. Lee *et al.*, “The roles of APC and Axin derived from experimental and theoretical analysis of the Wnt pathway.,” *PLoS Biol.*, vol. 1, no. 1, p. E10, Oct. 2003.
[374] L. Azzolin *et al.*, “Role of TAZ as mediator of Wnt signaling.,” *Cell*, vol. 151, no. 7, pp. 1443–56, Dec. 2012.
[375] J. Klingensmith, R. Nusse, and N. Perrimon, “The Drosophila segment polarity gene dishevelled encodes a novel protein required for response to the wingless signal.,” *Genes Dev.*, vol. 8, no. 1, pp. 118–130, Jan. 1994.
[376] J. D. Axelrod *et al.*, “Differential recruitment of Dishevelled provides signaling specificity in the planar cell polarity and Wingless signaling pathways,” *Genes Dev.*, vol. 12, no. 16, pp. 2610–2622, Aug. 1998.
[377] K. Goss and J. Groden, “Biology of the adenomatous polyposis coli tumor suppressor,” *J. Clin. Oncol.*, vol. 18, no. 9, pp. 1967–1979, 2000.
[378] J. Morin *et al.*, “Constitutive Transcriptional Activation by a beta -Catenin-Tcf Complex in APC-/- Colon Carcinoma,” *Science*, vol. 275, no. 5307, pp. 1784–1787, Mar. 1997.
[379] B. Zhao *et al.*, “The Hippo-YAP pathway in organ size control and tumorigenesis: an updated version.,” *Genes Dev.*, vol. 24, no. 9, pp. 862–74, May 2010.
[380] X. Varelas *et al.*, “The Hippo pathway regulates Wnt/beta-catenin signaling.,” *Dev. Cell*, vol. 18, no. 4, pp. 579–91, Apr. 2010.
[381] T. Heallen *et al.*, “Hippo pathway inhibits Wnt signaling to restrain cardiomyocyte proliferation and heart size.,” *Science*, vol. 332, no. 6028, pp. 458–61, Apr. 2011.
[382] M. Imajo *et al.*, “A molecular mechanism that links Hippo signalling to the inhibition of Wnt/β-catenin signalling.,” *EMBO J.*, pp. 1–14, Jan. 2012.

[383] M. Aragona *et al.*, “A mechanical checkpoint controls multicellular growth through YAP/TAZ regulation by actin-processing factors.,” *Cell*, vol. 154, no. 5, pp. 1047–59, Aug. 2013.
[384] L. Azzolin *et al.*, “YAP/TAZ Incorporation in the β-Catenin Destruction Complex Orchestrates the Wnt Response.,” *Cell*, vol. 158, no. 1, pp. 157–70, Jul. 2014.
[385] J. Behrens *et al.*, “Functional interaction of β-catenin with the transcription factor LEF-1,” *Nature*, vol. 382, pp. 638–642, 1996.
[386] A. Rattner *et al.*, “A family of secreted proteins contains homology to the cysteine-rich ligand-binding domain of frizzled receptors.,” *Proc. Natl. Acad. Sci. U. S. A.*, vol. 94, no. 7, pp. 2859–63, Apr. 1997.
[387] A. Glinka *et al.*, “Dickkopf-1 is a member of a new family of secreted proteins and functions in head induction.,” *Nature*, vol. 391, no. 6665, pp. 357–62, Jan. 1998.
[388] J. Hsieh, L. Kodjabachian, and M. Rebbert, “A new secreted protein that binds to Wnt proteins and inhibits their activites,” *Nature*, vol. 398, no. April, pp. 431–436, 1999.
[389] C. Blanpain and E. Fuchs, “Epidermal homeostasis: a balancing act of stem cells in the skin.,” *Nat. Rev. Mol. Cell Biol.*, vol. 10, no. 3, pp. 207–17, Mar. 2009.
[390] J. Hülsken, W. Birchmeier, and J. Behrens, “E-cadherin and APC compete for the interaction with beta-catenin and the cytoskeleton.,” *J. Cell Biol.*, vol. 127, no. 6 Pt 2, pp. 2061–9, Dec. 1994.
[391] W. Nelson and R. Nusse, “Convergence of Wnt, ß-catenin, and cadherin pathways,” *Science*, vol. 303, no. 5663, pp. 1483–1487, 2004.
[392] O. Huber *et al.*, “Nuclear localization of beta-catenin by interaction with transcription factor LEF-1.,” *Mech. Dev.*, vol. 59, no. 1, pp. 3–10, Sep. 1996.
[393] M. Molenaar *et al.*, “XTcf-3 transcription factor mediates beta-catenin-induced axis formation in Xenopus embryos.,” *Cell*, vol. 86, no. 3, pp. 391–9, Aug. 1996.
[394] V. Korinek *et al.*, “Constitutive Transcriptional Activation by a b-Catenin- Tcf Complex in APC -/- Colon Carcinoma,” *Science*, vol. 275, no. 1997, pp. 1784–1787, 1997.
[395] M. van de Wetering *et al.*, “Armadillo coactivates transcription driven by the product of the Drosophila segment polarity gene dTCF.,” *Cell*, vol. 88, no. 6, pp. 789–99, Mar. 1997.
[396] S. C. Hsu, J. Galceran, and R. Grosschedl, “Modulation of transcriptional regulation by LEF-1 in response to Wnt-1 signaling and association with beta-catenin.,” *Mol. Cell. Biol.*, vol. 18, no. 8, pp. 4807–18, Aug. 1998.
[397] K. Giese, A. Amsterdam, and R. Grosschedl, “DNA-binding properties of the HMG domain of the lymphoid-specific transcriptional regulator LEF-1.,” *Genes Dev.*, vol. 5, pp. 2567–2578, 1991.
[398] A. Hurlstone and H. Clevers, “T-cell factors: turn-ons and turn-offs,” *EMBO J.*, vol. 21, no. 10, pp. 2303–2311, 2002.
[399] A. Hecht *et al.*, “The p300/CBP acetyltransferases function as transcriptional coactivators of beta-catenin in vertebrates.,” *EMBO J.*, vol. 19, no. 8, pp. 1839–50, Apr. 2000.
[400] N. Barker *et al.*, “The chromatin remodelling factor Brg-1 interacts with beta-catenin to promote target gene activation.,” *EMBO J.*, vol. 20, no. 17, pp. 4935–43, Sep. 2001.
[401] K. I. Takemaru and R. T. Moon, “The transcriptional coactivator CBP interacts with beta-catenin to activate gene expression.,” *J. Cell Biol.*, vol. 149, no. 2, pp. 249–54, Apr. 2000.
[402] F. M. Townsley, A. Cliffe, and M. Bienz, “Pygopus and Legless target Armadillo/beta-catenin to the nucleus to enable its transcriptional co-activator function.,” *Nat. Cell Biol.*, vol. 6, no. 7, pp. 626–33, Jul. 2004.
[403] J. Roose *et al.*, “The Xenopus Wnt effector XTcf-3 interacts with Groucho-related transcriptional repressors.,” *Nature*, vol. 395, no. 6702, pp. 608–12, Oct. 1998.
[404] R. A. Cavallo *et al.*, “Drosophila Tcf and Groucho interact to repress Wingless signalling activity.,” *Nature*, vol. 395, no. 6702, pp. 604–8, Oct. 1998.
[405] H. Brantjes and J. Roose, “All Tcf HMG box transcription factors interact with Groucho-related co-repressors,” *Nucleic Acids Res.*, vol. 29, no. 7, pp. 1410–1419, 2001.
[406] L. Arce, K. T. Pate, and M. L. Waterman, “Groucho binds two conserved regions of LEF-1 for HDAC-dependent repression.,” *BMC Cancer*, vol. 9, p. 159, Jan. 2009.
[407] G. Chen and J. Fernandez, “A functional interaction between the histone deacetylase Rpd3 and the corepressor groucho in Drosophila development,” *Genes Dev.*, vol. 13, pp. 2218–2230, 1999.

[408] B. Rubinfeld *et al.*, “Association of the APC gene product with beta-catenin.,” *Science*, vol. 262, no. 5140, pp. 1731–4, Dec. 1993.
[409] M. van de Wetering *et al.*, “The beta-catenin/TCF-4 complex imposes a crypt progenitor phenotype on colorectal cancer cells.,” *Cell*, vol. 111, no. 2, pp. 241–50, Oct. 2002.
[410] S. J. A. Buczacki *et al.*, “Intestinal label-retaining cells are secretory precursors expressing Lgr5.,” *Nature*, vol. 495, no. 7439, pp. 65–9, Mar. 2013.
[411] N. Barker *et al.*, “Lgr5(+ve) stem cells drive self-renewal in the stomach and build long-lived gastric units in vitro.,” *Cell Stem Cell*, vol. 6, no. 1, pp. 25–36, Jan. 2010.
[412] M. Huch *et al.*, “In vitro expansion of single Lgr5+ liver stem cells induced by Wnt-driven regeneration.,” *Nature*, vol. 494, no. 7436, pp. 247–50, Feb. 2013.
[413] M. Huch *et al.*, “Unlimited in vitro expansion of adult bi-potent pancreas progenitors through the Lgr5/R-spondin axis.,” *EMBO J.*, vol. 32, no. 20, pp. 2708–21, Oct. 2013.
[414] N. Barker *et al.*, “Lgr5(+ve) stem/progenitor cells contribute to nephron formation during kidney development.,” *Cell Rep.*, vol. 2, no. 3, pp. 540–52, Sep. 2012.
[415] K. E. de Visser *et al.*, “Developmental stage-specific contribution of LGR5(+) cells to basal and luminal epithelial lineages in the postnatal mammary gland.,” *J. Pathol.*, vol. 228, no. 3, pp. 300–9, Nov. 2012.
[416] V. Plaks *et al.*, “Lgr5-expressing cells are sufficient and necessary for postnatal mammary gland organogenesis.,” *Cell Rep.*, vol. 3, no. 1, pp. 70–8, Jan. 2013.
[417] W. de Lau *et al.*, “Lgr5 homologues associate with Wnt receptors and mediate R-spondin signalling.,” *Nature*, vol. 476, no. 7360, pp. 293–7, Aug. 2011.
[418] K. S. Carmon *et al.*, “R-spondins function as ligands of the orphan receptors LGR4 and LGR5 to regulate Wnt/beta-catenin signaling.,” *Proc. Natl. Acad. Sci. U. S. A.*, vol. 108, no. 28, pp. 11452–7, Jul. 2011.
[419] B. K. Koo *et al.*, “Tumour suppressor RNF43 is a stem-cell E3 ligase that induces endocytosis of Wnt receptors.,” *Nature*, vol. 488, no. 7413, pp. 665–9, Aug. 2012.
[420] H. X. Hao *et al.*, “ZNRF3 promotes Wnt receptor turnover in an R-spondin-sensitive manner.,” *Nature*, vol. 485, no. 7397, pp. 195–200, May 2012.
[421] A. Ahumada *et al.*, “Signaling of rat Frizzled-2 through phosphodiesterase and cyclic GMP.,” *Science*, vol. 298, no. 5600, pp. 2006–10, Dec. 2002.
[422] L. C. Sheldahl *et al.*, “Dishevelled activates Ca2+ flux, PKC, and CamKII in vertebrate embryos.,” *J. Cell Biol.*, vol. 161, no. 4, pp. 769–77, May 2003.
[423] A. D. Kohn and R. T. Moon, “Wnt and calcium signaling: beta-catenin-independent pathways.,” *Cell Calcium*, vol. 38, no. 3–4, pp. 439–46, 2005.
[424] L. M. A. and H. Wang, “Mitogen-activated protein kinase p38 regulates the Wnt/cyclic GMP/Ca2+ non-canonical pathway.,” *J. Biol. Chem.*, vol. 282, no. 39, pp. 28980–90, Sep. 2007.
[425] T. Ishitani *et al.*, “The TAK1-NLK mitogen-activated protein kinase cascade functions in the Wnt-5a/Ca(2+) pathway to antagonize Wnt/beta-catenin signaling.,” *Mol. Cell. Biol.*, vol. 23, no. 1, pp. 131–9, Jan. 2003.
[426] L. L. S. Murphy and C. C. W. Hughes, “Endothelial Cells Stimulate T Cell NFAT Nuclear Translocation in the Presence of Cyclosporin A: Involvement of the wnt/Glycogen Synthase Kinase-3 Pathway,” *J. Immunol.*, vol. 169, no. 7, pp. 3717–3725, Oct. 2002.
[427] A. J. Mikels and R. Nusse, “Purified Wnt5a Protein Activates or Inhibits beta-catenin-TCF Signaling Depending on Receptor Context,” vol. 4, no. 4, 2006.
[428] A. S. Nateri, B. Spencer-Dene, and A. Behrens, “Interaction of phosphorylated c-Jun with TCF4 regulates intestinal cancer development,” vol. 437, no. September, pp. 281–285, 2005.
[429] D. Bottomly *et al.*, “Identification of beta-catenin binding regions in colon cancer cells using ChIP-Seq,” vol. 38, no. 17, pp. 5735–5745, 2010.
[430] W. M. Grady *et al.*, “Mutational inactivation of transforming growth factor β receptor type II in microsatellite stable colon cancers,” *Cancer Res.*, vol. 29, pp. 320–324, 1999.
[431] L. D. Wood *et al.*, “The genomic landscapes of human breast and colorectal cancers.,” *Science*, vol. 318, no. 5853, pp. 1108–13, Nov. 2007.
[432] S. Markowitz *et al.*, “Inactivation of the type II TGF-beta receptor in colon cancer cells with microsatellite instability,” *Science*, vol. 268, no. December 1994, pp. 1336–1338, 1995.
[433] K. Eppert *et al.*, “MADR2 maps to 18q21 and encodes a TGFbeta-regulated MAD-related protein that is functionally mutated in colorectal carcinoma.,” *Cell*, vol. 86, no. 4, pp. 543–52, Aug. 1996.

[434] W. M. Grady *et al.*, “Mutation of the Type II Transforming Growth Factor- β Receptor Is Coincident with the Transformation of Human Colon Adenomas to Malignant Carcinomas,” *Cancer Res.*, vol. 58, pp. 3101–3104, 1998.
[435] M. Malumbres and M. Barbacid, “RAS oncogenes: the first 30 years.,” *Nat. Rev. Cancer*, vol. 3, no. 6, pp. 459–65, Jun. 2003.
[436] H. Davies *et al.*, “Mutations of the BRAF gene in human cancer.,” *Nature*, vol. 417, no. 6892, pp. 949–54, Jun. 2002.
[437] H. Rajagopalan *et al.*, “RAF/ RAS oncogenes and mismatch-repair status,” *Nature*, vol. 418, no. August, p. 934, 2002.
[438] L. Zhao and P. K. Vogt, “Class I PI3K in oncogenic cellular transformation.,” *Oncogene*, vol. 27, no. 41, pp. 5486–96, Sep. 2008.
[439] Y. Samuels *et al.*, “High frequency of mutations of the PIK3CA gene in human cancers.,” *Science*, vol. 304, no. 5670, p. 554, Apr. 2004.
[440] D. W. Parsons *et al.*, “Colorectal cancer: mutations in a signalling pathway.,” *Nature*, vol. 436, no. 7052, p. 792, Aug. 2005.
[441] S. Minami *et al.*, “Molecular cloning and characterization of the human p27Kip1 gene promoter,” *FEBS Lett.*, vol. 411, no. 1, pp. 1–6, Jul. 1997.
[442] B. Nicke *et al.*, “Involvement of MINK, a Ste20 family kinase, in Ras oncogene-induced growth arrest in human ovarian surface epithelial cells.,” *Mol. Cell*, vol. 20, no. 5, pp. 673–85, Dec. 2005.
[443] A. Hotta *et al.*, “Isolation of human iPS cells using EOS lentiviral vectors to select for pluripotency,” *Nat. Methods*, vol. 6, no. 5, 2009.
[444] M. Kaighn, K. Narayan, and Y. Ohnuki, “Establishment and characterization of a human prostatic carcinoma cell line (PC-3).,” *Invest. Urol.*, vol. 17, no. 1, pp. 16–23, 1979.
[445] A. Leibovitz, J. Stinson, and W. McCombs, “Classification of human colorectal adenocarcinoma cell lines,” *Cancer Res.*, vol. 36, no. 12, pp. 4562–4569, 1976.
[446] A. Kyriazis and A. Kyriazis, “Human pancreatic adenocarcinoma line Capan-1 in tissue culture and the nude mouse: morphologic, biologic, and biochemical characteristics.,” *Am. J. Pathol.*, vol. 106, no. 2, pp. 250–260, 1982.
[447] M. Lieber and J. Mazzetta, “Establishment of a continuous tumor cell line (PANC1) from a human carcinoma of the exocrine pancreas,” *Int. J. cancer.*, vol. 15, no. 5, pp. 741–6, 1975.
[448] R. E. Hewitt *et al.*, “Validation of a model of colon cancer progression.,” *J. Pathol.*, vol. 192, no. 4, pp. 446–54, Dec. 2000.
[449] B. Feng *et al.*, “Colorectal cancer migration and invasion initiated by microRNA-106a.,” *PLoS One*, vol. 7, no. 8, p. e43452, Jan. 2012.
[450] E. Deer, J. González-Hernández, and J. Coursen, “Phenotype and genotype of pancreatic cancer cell lines,” *Pancreas*, vol. 39, no. 4, pp. 425–435, 2010.
[451] P. Loukopoulos *et al.*, “Orthotopic transplantation models of pancreatic adenocarcinoma derived from cell lines and primary tumors and displaying varying metastatic activity.,” *Pancreas*, vol. 29, no. 3, pp. 193–203, Oct. 2004.
[452] T. Aasen *et al.*, “Efficient and rapid generation of induced pluripotent stem cells from human keratinocytes.,” *Nat. Biotechnol.*, vol. 26, no. 11, pp. 1276–84, Nov. 2008.
[453] L. Hengst and S. I. Reed, “Translational control of p27Kip1 accumulation during the cell cycle.,” *Science*, vol. 271, no. 5257, pp. 1861–4, Mar. 1996.
[454] W. Yang *et al.*, “Repression of transcription of the p27(Kip1) cyclin-dependent kinase inhibitor gene by c-Myc.,” *Oncogene*, vol. 20, no. 14, pp. 1688–702, Mar. 2001.
[455] R. H. Medema *et al.*, “AFX-like Forkhead transcription factors mediate cell-cycle regulation by Ras and PKB through p27kip1.,” *Nature*, vol. 404, no. 6779, pp. 782–7, Apr. 2000.
[456] I. M. Chu, L. Hengst, and J. M. Slingerland, “The Cdk inhibitor p27 in human cancer: prognostic potential and relevance to anticancer therapy.,” *Nat. Rev. Cancer*, vol. 8, no. 4, pp. 253–67, Apr. 2008.
[457] W. Miskimins, G. Wang, and M. Hawkinson, “Control of cyclin-dependent kinase inhibitor p27 expression by cap-independent translation,” *Mol. Cell. Biol.*, vol. 21, no. 15, pp. 4960–4967, 2001.
[458] A. Gartel and A. Tyner, “Transcriptional Regulation of the p21(WAF1/CIP1) Gene,” *Exp. Cell Res.*, vol. 246, pp. 280–289, 1999.
[459] T. Abbas and A. Dutta, “p21 in Cancer: Intricate Networks and Multiple Activities.,” *Nat. Rev. Cancer*, vol. 9, no. 6, pp. 400–14, Jun. 2009.

[460] D. Ahmed *et al.*, “Epigenetic and genetic features of 24 colon cancer cell lines.,” *Oncogenesis*, vol. 2, p. e71, Jan. 2013.
[461] F. Bunz *et al.*, “Requirement for p53 and p21 to Sustain G2 Arrest After DNA Damage,” *Science*, vol. 282, no. 5393, pp. 1497–1501, Nov. 1998.
[462] A. Banito *et al.*, “Senescence impairs successful reprogramming to pluripotent stem cells.,” *Genes Dev.*, vol. 23, no. 18, pp. 2134–9, Sep. 2009.
[463] T. D. Halazonetis, V. G. Gorgoulis, and J. Bartek, “An oncogene-induced DNA damage model for cancer development.,” *Science*, vol. 319, no. 5868, pp. 1352–5, Mar. 2008.
[464] C. Lukas *et al.*, “53BP1 nuclear bodies form around DNA lesions generated by mitotic transmission of chromosomes under replication stress.,” *Nat. Cell Biol.*, vol. 13, no. 3, pp. 243–53, Mar. 2011.
[465] S. Panier and S. J. Boulton, “Double-strand break repair: 53BP1 comes into focus.,” *Nat. Rev. Mol. Cell Biol.*, vol. 15, no. 1, pp. 7–18, Jan. 2014.
[466] D. Trachootham, J. Alexandre, and P. Huang, “Targeting cancer cells by ROS-mediated mechanisms: a radical therapeutic approach?,” *Nat. Rev. Drug Discov.*, vol. 8, no. 7, pp. 579–91, Jul. 2009.
[467] M. A. Marqués-Torrejón *et al.*, “Cyclin-dependent kinase inhibitor p21 controls adult neural stem cell expansion by regulating Sox2 gene expression.,” *Cell Stem Cell*, vol. 12, no. 1, pp. 88–100, Jan. 2013.
[468] H. Li *et al.*, “p27(Kip1) directly represses Sox2 during embryonic stem cell differentiation.,” *Cell Stem Cell*, vol. 11, no. 6, pp. 845–52, Dec. 2012.
[469] C. J. Norbury and B. Zhivotovsky, “DNA damage-induced apoptosis.,” *Oncogene*, vol. 23, no. 16, pp. 2797–808, Apr. 2004.
[470] H. U. Simon, A. Haj-Yehia, and F. Levi-Schaffer, “Role of reactive oxygen species (ROS) in apoptosis induction.,” *Apoptosis*, vol. 5, no. 5, pp. 415–8, Nov. 2000.
[471] H. J. Snippert *et al.*, “Intestinal crypt homeostasis results from neutral competition between symmetrically dividing Lgr5 stem cells.,” *Cell*, vol. 143, no. 1, pp. 134–44, Oct. 2010.
[472] W. de Lau *et al.*, “The R-spondin/Lgr5/Rnf43 module: regulator of Wnt signal strength.,” *Genes Dev.*, vol. 28, no. 4, pp. 305–16, Feb. 2014.
[473] K. A. Kim *et al.*, “Mitogenic influence of human R-spondin1 on the intestinal epithelium.,” *Science*, vol. 309, no. 5738, pp. 1256–9, Aug. 2005.
[474] N. Takahashi *et al.*, “Identification of two Wnt-responsive elements in the intron of RING finger protein 43 (RNF43) gene.,” *PLoS One*, vol. 9, no. 1, p. e86582, Jan. 2014.
[475] K. Kemper *et al.*, “Monoclonal antibodies against Lgr5 identify human colorectal cancer stem cells.,” *Stem Cells*, vol. 30, no. 11, pp. 2378–86, Nov. 2012.
[476] S. S. Kanwar *et al.*, “The Wnt/beta-catenin pathway regulates growth and maintenance of colonospheres.,” *Mol. Cancer*, vol. 9, p. 212, Jan. 2010.
[477] X. Y. Han *et al.*, “Epithelial-mesenchymal transition associates with maintenance of stemness in spheroid-derived stem-like colon cancer cells.,” *PLoS One*, vol. 8, no. 9, p. e73341, Jan. 2013.
[478] H. Ohata *et al.*, “Induction of the stem-like cell regulator CD44 by Rho kinase inhibition contributes to the maintenance of colon cancer-initiating cells.,” *Cancer Res.*, vol. 72, no. 19, pp. 5101–10, Oct. 2012.
[479] D. G. Drubin and W. J. Nelson, “Origins of Cell Polarity,” *Cell*, vol. 84, pp. 335–344, 1996.
[480] A. Ratheesh and A. S. Yap, “A bigger picture: classical cadherins and the dynamic actin cytoskeleton.,” *Nat. Rev. Mol. Cell Biol.*, vol. 13, no. 10, pp. 673–9, Oct. 2012.
[481] G. Baltus, M. Kowalski, and H. Zhai, “Acetylation of sox2 induces its nuclear export in embryonic stem cells,” *Stem Cells*, vol. 29, pp. 2175–2184, 2009.
[482] H. Zhao *et al.*, “CARM1 mediates modulation of Sox2.,” *PLoS One*, vol. 6, no. 10, p. e27026, Jan. 2011.
[483] D. Van Hoof *et al.*, “Phosphorylation dynamics during early differentiation of human embryonic stem cells.,” *Cell Stem Cell*, vol. 5, no. 2, pp. 214–26, Aug. 2009.
[484] C. H. Jeong *et al.*, “Phosphorylation of Sox2 cooperates in reprogramming to pluripotent stem cells.,” *Stem Cells*, vol. 28, no. 12, pp. 2141–50, Dec. 2010.
[485] T. Kalmar *et al.*, “Regulated fluctuations in nanog expression mediate cell fate decisions in embryonic stem cells.,” *PLoS Biol.*, vol. 7, no. 7, p. e1000149, Jul. 2009.

[486] I. Glauche, M. Herberg, and I. Roeder, “Nanog variability and pluripotency regulation of embryonic stem cells--insights from a mathematical model analysis.,” *PLoS One*, vol. 5, no. 6, p. e11238, Jan. 2010.
[487] I. Imayoshi *et al.*, “Oscillatory control of factors determining multipotency and fate in mouse neural progenitors.,” *Science*, vol. 342, no. 6163, pp. 1203–8, Dec. 2013.
[488] S. Chanock and J. El Benna, “The respiratory burst oxidase,” *J. Biol. Chem.*, vol. 40, no. 15, pp. 24519–22, 1994.
[489] N. Oshima *et al.*, “Induction of Cancer Stem Cell Properties in Colon Cancer Cells by Defined Factors,” *PLoS One*, vol. 9, no. 7, p. e101735, Jul. 2014.
[490] J. Boonstra and J. A. Post, “Molecular events associated with reactive oxygen species and cell cycle progression in mammalian cells.,” *Gene*, vol. 337, pp. 1–13, Aug. 2004.
[491] Y. Y. Cho *et al.*, “Autophagy and cellular senescence mediated by sox2 suppress malignancy of cancer cells.,” *PLoS One*, vol. 8, no. 2, p. e57172, Jan. 2013.
[492] M. C. Maiuri *et al.*, “Self-eating and self-killing: crosstalk between autophagy and apoptosis.,” *Nat. Rev. Mol. Cell Biol.*, vol. 8, no. 9, pp. 741–52, Sep. 2007.
[493] G. Kroemer and S. J. Martin, “Caspase-independent cell death.,” *Nat. Med.*, vol. 11, no. 7, pp. 725–30, Jul. 2005.
[494] Y. Chen *et al.*, “The molecular mechanism governing the oncogenic potential of SOX2 in breast cancer.,” *J. Biol. Chem.*, vol. 283, no. 26, pp. 17969–78, Jun. 2008.
[495] D. Wang *et al.*, “Knockdown of LGR5 suppresses the proliferation of glioma cells in vitro and in vivo.,” *Oncol. Rep.*, vol. 31, no. 1, pp. 41–9, Jan. 2014.
[496] C. Wu *et al.*, “RSPO2-LGR5 signaling has tumour-suppressive activity in colorectal cancer.,” *Nat. Commun.*, vol. 5, p. 3149, Jan. 2014.
[497] F. Walker *et al.*, “LGR5 is a negative regulator of tumourigenicity, antagonizes Wnt signalling and regulates cell adhesion in colorectal cancer cell lines.,” *PLoS One*, vol. 6, no. 7, p. e22733, Jan. 2011.
[498] P. R. Prasetyanti *et al.*, “Regulation of stem cell self-renewal and differentiation by Wnt and Notch are conserved throughout the adenoma-carcinoma sequence in the colon.,” *Mol. Cancer*, vol. 12, no. 1, p. 126, Jan. 2013.
[499] S. S. Kanwar *et al.*, “The Wnt/beta-catenin pathway regulates growth and maintenance of colonospheres.,” *Mol. Cancer*, vol. 9, p. 212, Jan. 2010.
[500] S. Tsuji *et al.*, “The miR-363-GATA6-Lgr5 pathway is critical for colorectal tumourigenesis.,” *Nat. Commun.*, vol. 5, p. 3150, Jan. 2014.
[501] M. Alonso, *et al.*, “Genetic and epigenetic modifications of Sox2 contribute to the invasive phenotype of malignant gliomas,” *PLoS One*, vol. 6, no. 11, 2011.
[502] X. Ye *et al.*, “β-Catenin, a Sox2 binding partner, regulates the DNA binding and transcriptional activity of Sox2 in breast cancer cells.,” *Cell. Signal.*, vol. 26, no. 3, pp. 492–501, Mar. 2014.
[503] E. Seo *et al.*, “Distinct functions of Sox2 control self-renewal and differentiation in the osteoblast lineage.,” *Mol. Cell. Biol.*, vol. 31, no. 22, pp. 4593–608, Nov. 2011.
[504] S. Hashimoto *et al.*, “β-Catenin-SOX2 signaling regulates the fate of developing airway epithelium.,” *J. Cell Sci.*, vol. 125, no. Pt 4, pp. 932–42, Feb. 2012.
[505] O. Voloshanenko *et al.*, “Wnt secretion is required to maintain high levels of Wnt activity in colon cancer cells.,” *Nat. Commun.*, vol. 4, no. May, p. 2610, Jan. 2013.
[506] J. Hao *et al.*, “WNT/beta-catenin pathway up-regulates Stat3 and converges on LIF to prevent differentiation of mouse embryonic stem cells.,” *Dev. Biol.*, vol. 290, no. 1, pp. 81–91, Feb. 2006.
[507] T. Miyabayashi *et al.*, “Wnt/beta-catenin/CBP signaling maintains long-term murine embryonic stem cell pluripotency.,” *Proc. Natl. Acad. Sci. U. S. A.*, vol. 104, no. 13, pp. 5668–73, Mar. 2007.
[508] D. K. Singla *et al.*, “Wnt3a But Not Wnt11 Supports Self-Renewal of Embryonic Stem Cells.,” *Biochem. Biophys. Res. Commun.*, vol. 345, no. 2, pp. 789–95, Jun. 2006.
[509] D. ten Berge *et al.*, “Embryonic stem cells require Wnt proteins to prevent differentiation to epiblast stem cells.,” *Nat. Cell Biol.*, vol. 13, no. 9, pp. 1070–5, Sep. 2011.
[510] K. Ogawa *et al.*, “Synergistic action of Wnt and LIF in maintaining pluripotency of mouse ES cells.,” *Biochem. Biophys. Res. Commun.*, vol. 343, no. 1, pp. 159–66, Apr. 2006.
[511] Y. Takao, T. Yokota, and H. Koide, “Beta-catenin up-regulates Nanog expression through interaction with Oct-3/4 in embryonic stem cells.,” *Biochem. Biophys. Res. Commun.*, vol. 353, no. 3, pp. 699–705, Feb. 2007.

[512] R. T. Wagner *et al.*, “Canonical Wnt/β-catenin regulation of liver receptor homolog-1 mediates pluripotency gene expression.,” *Stem Cells*, vol. 28, no. 10, pp. 1794–804, Oct. 2010.
[513] A. Marson *et al.*, “Wnt signaling promotes reprogramming of somatic cells to pluripotency.,” *Cell Stem Cell*, vol. 3, no. 2, pp. 132–5, Aug. 2008.
[514] F. Lluis *et al.*, “Periodic activation of Wnt/beta-catenin signaling enhances somatic cell reprogramming mediated by cell fusion.,” *Cell Stem Cell*, vol. 3, no. 5, pp. 493–507, Nov. 2008.
[515] N. Lyashenko *et al.*, “Differential requirement for the dual functions of β-catenin in embryonic stem cell self-renewal and germ layer formation.,” *Nat. Cell Biol.*, vol. 13, no. 7, pp. 753–61, Jul. 2011.
[516] F. Soncin *et al.*, “Abrogation of E-cadherin-mediated cell-cell contact in mouse embryonic stem cells results in reversible LIF-independent self-renewal.,” *Stem Cells*, vol. 27, no. 9, pp. 2069–80, Sep. 2009.
[517] H. K. Bone *et al.*, “A novel chemically directed route for the generation of definitive endoderm from human embryonic stem cells based on inhibition of GSK-3.,” *J. Cell Sci.*, vol. 124, no. Pt 12, pp. 1992–2000, Jun. 2011.
[518] M. Nakanishi *et al.*, “Directed induction of anterior and posterior primitive streak by Wnt from embryonic stem cells cultured in a chemically defined serum-free medium.,” *FASEB J.*, vol. 23, no. 1, pp. 114–22, Jan. 2009.
[519] U. Ullmann *et al.*, “GSK-3-specific inhibitor-supplemented hESC medium prevents the epithelial-mesenchymal transition process and the up-regulation of matrix metalloproteinases in hESCs cultured in feeder-free conditions.,” *Mol. Hum. Reprod.*, vol. 14, no. 3, pp. 169–79, Mar. 2008.
[520] K. Hasegawa, T. Fujioka, and Y. Nakamura, “A Method for the Selection of Human Embryonic Stem Cell Sublines with High Replating Efficiency After Single-Cell Dissociation,” *Stem Cells*, vol. 24, pp. 2649–2660, 2006.
[521] G. Dravid *et al.*, “Defining the Role of Wnt/β-Catenin Signaling in the Survival, Proliferation, and Self-Renewal of Human Embryonic Stem Cells,” *Stem Cells*, vol. 23, pp. 1489–1501, 2005.
[522] L. Cai *et al.*, “Promoting human embryonic stem cell renewal or differentiation by modulating Wnt signal and culture conditions,” *Cell Res.*, vol. 17, pp. 62–72, 2007.
[523] K. C. Davidson *et al.*, “Wnt/β-catenin signaling promotes differentiation, not self-renewal, of human embryonic stem cells and is repressed by Oct4.,” *Proc. Natl. Acad. Sci. U. S. A.*, vol. 109, no. 12, pp. 4485–90, Mar. 2012.
[524] R. A. Neumüller and J. a Knoblich, “Dividing cellular asymmetry: asymmetric cell division and its implications for stem cells and cancer.,” *Genes Dev.*, vol. 23, no. 23, pp. 2675–99, Dec. 2009.
[525] Y. M. Yamashita *et al.*, “Polarity in stem cell division: asymmetric stem cell division in tissue homeostasis.,” *Cold Spring Harb. Perspect. Biol.*, vol. 2, no. 1, pp. 1-14, Jan. 2010.
[526] K. Mizumoto and H. Sawa, “Cortical beta-catenin and APC regulate asymmetric nuclear beta-catenin localization during asymmetric cell division in C. elegans.,” *Dev. Cell*, vol. 12, no. 2, pp. 287–99, Feb. 2007.
[527] M. Owraghi *et al.*, “Roles of the Wnt effector POP-1/TCF in the C. elegans endomesoderm specification gene network.,” *Dev. Biol.*, vol. 340, no. 2, pp. 209–21, Apr. 2010.
[528] H. Ren and H. Zhang, “Wnt signaling controls temporal identities of seam cells in Caenorhabditis elegans.,” *Dev. Biol.*, vol. 345, no. 2, pp. 144–55, Sep. 2010.
[529] S. J. Habib *et al.*, “A localized Wnt signal orients asymmetric stem cell division in vitro.,” *Science*, vol. 339, no. 6126, pp. 1445–8, Mar. 2013.
[530] T. Lechler and E. Fuchs, “Asymmetric cell divisions promote stratification and differentiation of mammalian skin.,” *Nature*, vol. 437, no. 7056, pp. 275–80, Sep. 2005.
[531] N. D. Poulson and T. Lechler, “Robust control of mitotic spindle orientation in the developing epidermis.,” *J. Cell Biol.*, vol. 191, no. 5, pp. 915–22, Dec. 2010.
[532] G. Mascré *et al.*, “Distinct contribution of stem and progenitor cells to epidermal maintenance.,” *Nature*, vol. 489, no. 7415, pp. 257–62, Sep. 2012.
[533] T. Sato *et al.*, “Paneth cells constitute the niche for Lgr5 stem cells in intestinal crypts.,” *Nature*, vol. 469, no. 7330, pp. 415–8, Jan. 2011.

[534] K. S. Yan *et al.*, “The intestinal stem cell markers Bmi1 and Lgr5 identify two functionally distinct populations.,” *Proc. Natl. Acad. Sci. U. S. A.*, vol. 109, no. 2, pp. 466–71, Jan. 2012.
[535] D. Pinto *et al.*, “Canonical Wnt signals are essential for homeostasis of the intestinal epithelium.,” *Genes Dev.*, vol. 17, no. 14, pp. 1709–13, Jul. 2003.
[536] H. Ireland *et al.*, “Inducible cre-mediated control of gene expression in the murine gastrointestinal tract: effect of loss of β-catenin,” *Gastroenterology*, vol. 126, no. 5, pp. 1236–1246, May 2004.
[537] V. Korinek *et al.*, “Depletion of epithelial stem-cell compartments in the small intestine of mice lacking Tcf-4.,” *Nat. Genet.*, vol. 19, no. 4, pp. 379–83, Aug. 1998.
[538] T. Sato *et al.*, “Single Lgr5 stem cells build crypt-villus structures in vitro without a mesenchymal niche.,” *Nature*, vol. 459, no. 7244, pp. 262–5, May 2009.
[539] C. Crosnier, D. Stamataki, and J. Lewis, “Organizing cell renewal in the intestine: stem cells, signals and combinatorial control.,” *Nat. Rev. Genet.*, vol. 7, no. 5, pp. 349–59, May 2006.
[540] X. C. He *et al.*, “PTEN-deficient intestinal stem cells initiate intestinal polyposis.,” *Nat. Genet.*, vol. 39, no. 2, pp. 189–98, Feb. 2007.
[541] C. Kosinski *et al.*, “Gene expression patterns of human colon tops and basal crypts and BMP antagonists as intestinal stem cell niche factors.,” *Proc. Natl. Acad. Sci. U. S. A.*, vol. 104, no. 39, pp. 15418–23, Sep. 2007.
[542] X. C. He *et al.*, “BMP signaling inhibits intestinal stem cell self-renewal through suppression of Wnt-beta-catenin signaling.,” *Nat. Genet.*, vol. 36, no. 10, pp. 1117–21, Oct. 2004.
[543] J. Jensen *et al.*, “Control of endodermal endocrine development by Hes-1.,” *Nat. Genet.*, vol. 24, no. 1, pp. 36–44, Jan. 2000.
[544] J. H. van Es *et al.*, “Notch/gamma-secretase inhibition turns proliferative cells in intestinal crypts and adenomas into goblet cells.,” *Nature*, vol. 435, no. 7044, pp. 959–63, Jun. 2005.
[545] V. Greco *et al.*, “A two-step mechanism for stem cell activation during hair regeneration.,” *Cell Stem Cell*, vol. 4, no. 2, pp. 155–69, Feb. 2009.
[546] L. Ritsma *et al.*, “Intestinal crypt homeostasis revealed at single-stem-cell level by in vivo live imaging.,” *Nature*, vol. 507, no. 7492, pp. 362–5, Mar. 2014.
[547] P. Andreu *et al.*, “Crypt-restricted proliferation and commitment to the Paneth cell lineage following Apc loss in the mouse intestine.,” *Development*, vol. 132, no. 6, pp. 1443–51, Mar. 2005.
[548] P. Andreu *et al.*, “A genetic study of the role of the Wnt/beta-catenin signalling in Paneth cell differentiation.,” *Dev. Biol.*, vol. 324, no. 2, pp. 288–96, Dec. 2008.

Appendix: Publications

Messier object 104, The Sombrero Galaxy

The Sombrero Galaxy belongs to our Local Group of galaxies. This neighboring giant elliptical galaxy in the constellation of Virgo is located 28 million light-years away from our galaxy. It has a bright nucleus, an unusually large central bulge, and a prominent dust lane in its inclined disk. Sombrero is the closest galaxy to the Milky Way that presents an active galactic nucleus or quasar, or in other words, presents an active central supermassive black hole that emits vast amounts of radiation in the whole range of the electromagnetic spectrum…

1) TITLE: *SPARC mediates metastatic cooperation between CSC and non-CSC prostate cancer cell subpopulations*

AUTHORS & JOURNAL: Mateo F, **Meca-Cortés O**, Celià-Terrassa T, Fernández Y, Abasolo I, Sánchez-Cid L, Bermudo R, Sagasta A, Rodríguez-Carunchio L, Pons M, Cánovas V, Marín-Aguilera M, Mengual L, Alcaraz A, Schwartz Jr S, Mellado B, Aguilera K.Y., Brekken R, Fernández P.L., Paciucci R & Thomson TM *(Molecular Cancer, 2014, Vol 13(237), epub)*

2) TITLE: *Acid ceramidase as a therapeutic target in metastatic prostate cancer*

AUTHORS & JOURNAL: Camacho L, **Meca-Cortés O**, Abad JL, García S, Rubio N, Díaz A, Celià-Terrassa T, Bermudo R, Fernández PL, Blanco J, Delgado A, Casas J, Fabriàs G & Thomson TM *(Journal of Lipid Research, 2013, Vol 54, 1207-1220)*

3) TITLE: *Epithelial-mesenchymal transition can suppress major attributes of human epithelial tumor-initiating cells*

AUTHORS & JOURNAL: Celià-Terrassa T, **Meca-Cortés O**, Mateo F, Martínez de Paz A, Rubio N, Arnal-Estapé A, Ell BJ, Bermudo R, Díaz A, Guerra-Rebollo M, Lozano JJ, Estarás C, Ulloa C, Álvarez-Simón D, Milà J, Vilella R, Paciucci R, Martínez-Balbás M, García de Herreros A, Gomis RR, Kang Y, Blanco J, Fernández PL & Thomson TM *(Journal of Clinical Investigation, 2012, Vol 122(5), 1849-68)*

4) TITLE: *Protein-protein interaction antagonist as novel inhibitors of non-canonical polyubiquitylation*

AUTHORS & JOURNAL: Scheper J, Guerra-Rebollo M, Sanclimens G, Moure A, Masip I, González-Ruiz D, Rubio N, **Meca-Cortés O**, Crosas B, Loukili N, Plans V, Morreale A, Blanco J, Ortiz AR, Messeguer A & Thomson TM *(PLoS One, 2009, Vol 5(6), e11403)*

5) TITLE*: HER3 is required for the maintenance of neuregulin–dependent and -independent attributes of malignant progression in prostate and breast cancer cells*

AUTHORS & JOURNAL: Soler M, Mancini F, Rubio N, López-Fernández S, Sánchez-Cid L, **Meca-Cortés O**, Lozano JJ, Blanco J, Fernández PL & Thomson TM *(International journal of cancer, 2009, Vol 125(11), 2565-75)*